NUMERICAL INVESTIGATION OF RIVER DISCHARGE AND TIDAL VARIATIONS IMPACT ON THE SALINITY IN DELTAIC SYSTEMS

Thesis submitted in accordance with the requirements of the University of Liverpool for the degree of Doctor in Philosophy by

Konstantinos Matsoukis

FEBRUARY 2022

THE UNIVERSITY OF LIVERPOOL
SCHOOL OF ENVIRONMENTAL SCIENCES
DEPARTMENT OF GEOGRAPHY AND PLANNING

UNIVERSITY OF LIVERPOOL

ABSTRACT

Thesis title: Numerical Investigation of river discharge and tidal variations impact on the salinity in deltaic systems

Author: Konstantinos Matsoukis

The present project is an effort to identify key parameters and controlling factors of salinity variations in deltaic systems. The salinity's driving mechanisms and response to hydrodynamic changes are under investigation. This is demanded because of the risks that these ecosystems are subject to by increases of salinity due to sea level rise and human activities. Numerical modelling is implemented to study the salinity distribution in idealized deltas configuration under various hydrodynamic conditions. In particular, variations of the river discharge and tidal levels are considered.

The results indicate that salinity undergoes significant seasonal changes due to dynamic flow variability. Sustained drought periods could result in critical conditions with salt intrusion in the delta's trunk (fluvial) channel. On the contrary, high river discharges during wet periods could mix completely the vertical column with freshwater for at least some distance from the river mouth. Tides could contribute further in mixing improving the conditions in the delta by decreasing the salinity in the downstream delta areas. Hence, many tidally influenced deltas could contain higher freshwater volumes than river dominated systems. Nevertheless, tidal level increases could limit significantly the deltas freshwater availability in mesotidal or macrotidal regimes. Results analysis and implementation of simple and innovative techniques uncovered the existence of certain correlations that could be useful as prognostic tools of salinity. Channels classification by their class or number of links provides a correlation that shows the salinity to increase with the decrease of either the channels order or delta's cross-section width. In addition, radial and depth averages of salinity are negatively and exponentially correlated with the river discharge. The extracted exponential equation summarizes successfully the complex 3D delta dynamics into a 1D analytical solution. The equation resembles theoretical solutions of the 1D advection-diffusion equations under certain theoretical assumptions of which many are satisfied in the present idealized models setup. The above correlations incur modifications when external (e.g. hydrodynamic forcing) or intrinsic (e.g. bathymetry) parameters cause changes to the spatial salinity distribution. Bathymetric effects affect the salinity distribution in both horizontal and vertical directions especially at low flow periods when the bottom friction becomes stronger. Increases of the river discharge and/or tidal level override these effects.

This study aspires to provide knowledge that could be useful for the development of technical or non-technical solutions for the aversion of salinization issues in deltas. With the goal of contributing to the efforts for the development of environmentally friendlier solutions, the last part of this work investigates the effect of different shape but equal volume hydrographs on the salinity. The results show that it is possible to alleviate the consequences of increased salinity by better management of existing water resources instead of seeking for additional ones.

ACKNOWLEDGMENTS

This dissertation is the product of a laborious research work that was conducted during the last 4 years. The challenges during the last four years have been tremendous on a personal and not only level. Despite the obstacles and difficulties through this long process, I consider the outcome to be successful, valuable and the founding stone for my future research goals. This would have not been possible without the support and guidance of my supervisors, Dr Nicoletta Leonardi, Dr Laurent Amoudry and Dr Lucy Bricheno. I would like to cordially thank them all first for the opportunity they gave me to pursue my research interests, their thoughtful and insightful instructions and of course their moral support and patience with me. I strongly believe that I was considerably benefited by their knowledge, research experience and status and I have improved my personal and professional skills under their supervision. Their support and guidance from the initial to the final level enabled me to develop a better understanding on the subject and research methods.

This PhD study was funded and supported by the Natural Environment Research Council (NERC) EAO Doctoral Training Partnership whose support is gratefully acknowledged. Grant ref NE/L002469/1. Funding support from the School of Environmental Sciences, University of Liverpool is also gratefully acknowledged. I wish to thank all the students in my DTP cohort for the time and experiences we shared together.

I owe many thanks to all students and scientists with whom I came in contact at the National Oceanography Centre but also all the fellow students, officemates, lecturers and professors that I met all these years at the Department of Geography and Planning. The time that I spent with them and the meaningful discussions we had, made this experience more pleasant and entertaining.

Finally, I want to express my gratitude to my family for their moral support and patience while I was carrying out my PhD project.

Table of Contents

LIST OF TABLES

LIST OF FIGURES

PREFACE

The need for the present PhD project derives from the tremendous consequences of climate change and global warming on deltaic systems. These complex and environmentally sensitive coastal ecosystems face the hazard of serious degradation because of sea level rise. One of the main threats for them is the increase of salinity levels which is detrimental for a number of activities including soil cultivation, irrigation and drinking water consumption. Sea level rise in combination with human interferences such as dam construction, river diversions and groundwater extraction exacerbate the problem by limiting the freshwater availability. This puts further pressure on the deltas' sustainability. It is imperative for the deltas to remain sustainable as they accommodate large populations and constitute an important source of economy because many anthropogenic activities take place there. The physical processes taking place in a delta and its complex dynamics is an ongoing research topic. Even though much of this research discusses salinity related issues, most studies are surficial and site-specific. Basic knowledge in this field derives mainly from estuarine studies because of their similarities with deltas. This project is an independent non-site specific modelling study on the salinity distribution in river deltas. It is an attempt to identify the effect of certain parameters (i.e. river discharge, tides, and bathymetry) on the salinity's seasonal, spatial and temporal variation in both horizontal and vertical directions. This is done through 3D idealized numerical modelling. The models' output is further analysed to detect correlations of salinity with physical parameters and delta's topography. This can be achieved by the implementation of innovative methods and techniques that are proposed. The goal is to 1): increase our understanding of salinity's response into external forcing in channelized networks, 2): achieve parameterizations to be used as predictive tools of salinity and 3) provide knowledge for better management of freshwater resources instead of resorting to expensive and harmful for the environment technical solutions.

The thesis starts with an introduction chapter that presents basic information on river deltas and articulates the problem of salinization. The second chapter is a literature review that contains basic theoretical knowledge on concepts related to this research and a review on previous works on salinity in river deltas. The third chapter provides information on the building process and setup of the two idealized models that were used for the purposes of this project. The next part of the thesis is written in the form of research papers. The three papers included comprise the core of this work and present the results, analysis and outcome of this research. The papers are structured in the traditional way with different sections for Introduction, Methods, Results, Discussion and Conclusions. An overall discussion chapter comes next that tries to connect and unify the research outcomes from the three different papers. It also elaborates further on some of the findings. The thesis ends by summarizing the conclusions and suggestions for future work. The list of tables and figures includes only those outside of the three paper chapters that follow their own numbering independently from the other chapters. On the contrary, the bibliography includes references from every chapter.

1. INTRODUCTION

1.1. Scope of the project

River deltas are delicate and valuable ecosystems. They are rich in aquaculture, have fertile regions and accommodate large populations that perform many anthropogenic activities there (e.g. land cultivation, irrigation, agriculture, fish farming and drinking water consumption). Their importance in economy, ecology and their role in environmental balance renders them a subject of continuous research that has intensified in recent years. These complex morphological formations are subject currently in many changes due to natural and/or anthropogenic climate change and human activities. A better understanding of the physical mechanisms and processes taking place in deltas is required in order to predict future changes and propose measures to alleviate their impact. Scientists endeavour to shed light on the physics controlling deltas' distributary network. The effect of river discharge, tides, waves and sediment properties on mouth bar deposits, channels bifurcation, avulsion and distribution in deltas has been the topic of many papers (Dalrymple & Choi, 2007; D. A. Edmonds & Slingerland, 2007; D. Edmonds et al. 2010; Edmonds & Slingerland, 2010; Fagherazzi, 2008; Fagherazzi et al., 2015; Geleynse et al. 2010; Geleynse et al., 2011; Hoitink et al.2017; Jerolmack, 2009; Jerolmack & Swenson, 2007; Leonardi et al. 2013; Leonardi et al. 2015; Nardin et al. 2013;Nardin & Fagherazzi, 2012; Nienhuis et al., 2020;Nienhuis et al. 2018; Caldwell and Edmonds, 2014; Zhang et al. 2018). Many site-specific studies focused on the morphological changes occurring in deltas influenced by climate change and human constructions such as diking, river diversions and dam construction (Allison, 1998; Allison et al.2017; Brunier et al. 2014; Kravtsova et al.2009; Maloney et al., 2018; Nittrouer et al.2011; Passalacqua et al.2013; Sassi et al. 2012; Shaw et al. 2013; Zhang et al., 2018). Land loss and subsidence, sediment load deficiency, channels erosion and migration are all issues that pose great concern and with which the scientific community is occupied seeking appropriate solutions. Such problems combined with sea level rise result in another important issue that is the increase of salinity in deltaic systems. This causes many problems because salinity can be detrimental for the water quality, some marine and vegetation species and can indirectly affect human health. The direct and indirect consequences from an increase in salinity can be catastrophic for the delta's sustainability. Therefore, the issue of salinization in deltas attains great interest in recent years. Research on this topic develops in parallel with the aforementioned topics and has progressed significantly in late decades.

The majority of related studies concerns the investigation of salinity's response to changes in hydrodynamic forcing (e.g. river discharge, tides) and their impact on the salt intrusion length (see section 2.2). So far, our understanding on this topic is largely based on our knowledge from estuaries where density changes due to variations in the hydrodynamic forcing have been extensively studied. However, this has not been tested adequately in the case of channelized networks such as deltas. The present study attempts to fill this gap and detect any differences on the spatiotemporal salinity distribution and evolution in the presence of a multichannel system. This is done through idealized numerical modelling. The choice for idealized modelling is done with the consideration that existing literature is mainly site-specific and inhibits conclusions with some generality and universality. It is further supported by the fact that idealization allows to isolate the effects of different parameters (e.g. river discharge, tides) on certain variables (e.g. salinity). This is necessary in order to increase our understanding of the controlling factors of salinity distribution in deltas. This project goes beyond a simple monitoring and illustration of the salt intrusion zone and investigates the linkage between salinity and the complex features of a river delta (e.g. multichannel system, irregular bathymetry and topography). Simple techniques and methods were implemented for this purpose and with the aspiration to derive correlations of salinity with intrinsic delta features (e.g. bifurcation order) and

relationships between external and internal system variables (e.g. river discharge and salinity respectively). Such parameterizations could act as prognostic tools that will allow to predict future changes in salinity under various hydrodynamic conditions. The aim is to provide in the end results and conclusions that could be used for the development of solutions to alleviate the impact of salinization. Lately, the need for the development of friendlier environmental solutions instead of technical ones has been identified. In that sense, adaptions to the water management policy might be an alternative. These, should also take into account possible changes to catchments' hydrographs and limitations in freshwater supply as a result of climate change and human interferences. With the ambition to provide meaningful results for better water management, the last chapter of this study is an investigation of the effect of various annual hydrographs on salinity. The work aimed to identify the optimum shape for establishing long-lasting freshwater conditions. This kind of information is crucial because it indicates possible changes to the flow distribution that could act against salinization. In addition, it gives an insight on the salinity's response to changes of the hydrograph's shape from natural or anthropogenic causes.

1.2. River Deltas definition and main features

River deltas are sedimentary deposits developed after cliff or rock erosion from stream flow and consequent transferring of the associated sediments into the ocean. Nemec (2009) defines deltas as 'a deposit built by a terrestrial feeder system, typically alluvial, into or against a body of standing water, either lake or a sea'. Sediment loads start to deposit as soon as they enter into the receiving water body forming a complex channels system of a dendritic shape usually. Elliott (1986) describes deltas as 'discrete shoreline protuberances formed where river enter oceans, semi-enclosed seas, lakes or lagoons and supply sediments more rapidly than they can be redistributed'. Deltas occur in all latitudes and climatic zones except for the poles. They are found in sections linked to drainage basins that carry sufficient sediments to produce a delta. A major concentration of deltas occurs globally in two regions, the circum-Arctic as a result of seasonal melt-water delivering high amount of sediments and the South East Asia. Rock weathering because of the warm tropic climate in combination with enhanced rainfall due to monsoonal periods contribute to the delta building in South East Asia (Roberts et al. 2012). Deltas consist of a subaerial delta plain with rather coarser material deposited and a subaqueous delta front and pro delta where finer sediments are transported (Wright, 1977). The delta plain is further subdivided in an upper and a lower part. The upper plain is beyond the tidal influence and has usually large flood basins with freshwater peats and lacustrine deposits. The lower part of the delta plain is under tidal influence and contains brackish to saline interdistributary areas such as lagoons, salt marshes and tidal flats. The subaqueous delta area lies below the low tide and so it remains completely underwater. Mouth bars form at the delta front and at the mouth of distributaries where sand bodies are built. The pro delta lies further seaward and is the most distal part composed of fine silt to clay deposits (Hori & Saito 2007). Figure 1 displays the basic delta features as discussed.

1.3. Deltas Classification

Delta's high variability in geomorphology, sedimentology and stratigraphy leads to various configurations around the world. Several classification schemes have been proposed by many authors depending on the source of variability (Roberts et al. 2012). A first approach is to categorize deltas based on their plan morphology. Based on their shape, deltas can be classified as arcuate, digitate or cuspate (Hasslet, 2000). An arcuate delta, meaning that it forms an arc-shape is the commonest type of all. These deltas are composed by relatively coarse material with well-defined distributaries and equal balance between wave and river activity. Digitate (or bird's foot) deltas are developed under strong river action when the wave energy is weak and progradation occurs transporting the sediment

supply further beyond the shoreline. Cuspate deltas form in regions where strong wave currents act spreading the sediments in various directions. As a result, their shape resembles the arcuate type but with less distributaries. However, in recent years, deltas are most commonly classified based on the ratio between marine and fluvial processes in a deltaic environment.

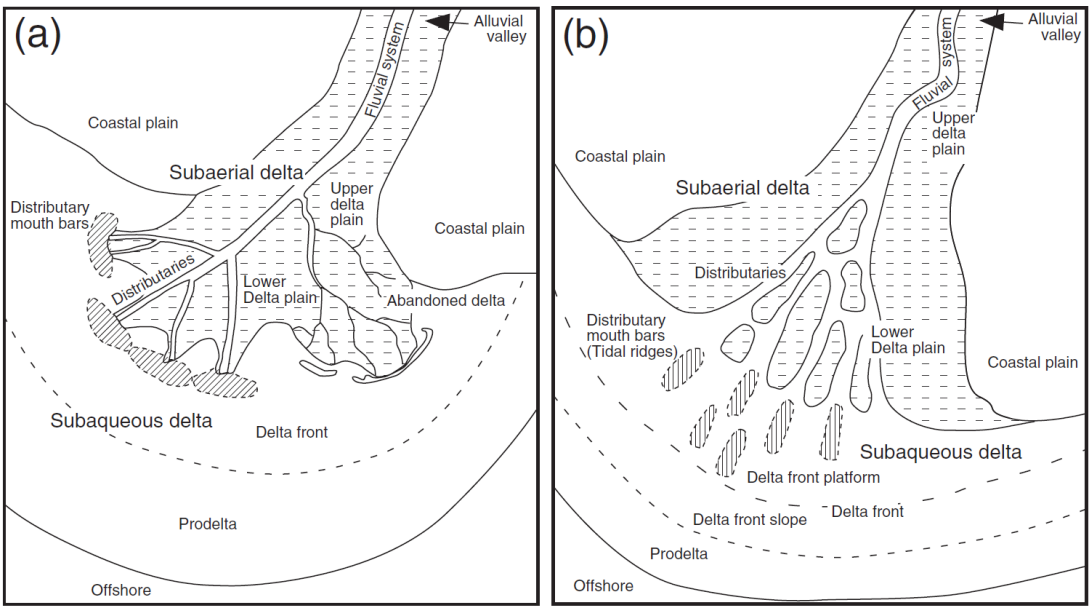

Figure 1 Basic delta features in a) fluvial dominated and b) tide-dominated deltas (taken from Saito & Hori 2007)

Fischer et al. (1969) emphasized on the main role that flow sources, wave energy and tidal currents have on determining the deltas geomorphology and subdivided them in high-constructive and high-destructive deltas. Basin processes dominate in the latter while fluvial processes dominate in the former case. Focusing on the fluvial and marine intensities, Galloway (1975) classified deltas in three main categories: river-dominated, tide-dominated and wave-dominated (Figure 2). River dominated deltas occur in micro-tidal regimes with limited wave energy. The sediment input from the river exceeds the capability of waves and tides to redistribute it and so these deltas are typically elongated acquiring a shape that is commonly referred to as a bird's foot. Examples are the Mississippi, Atchafalaya and Wax Lake deltas in the Gulf of Mexico (USA) (Figure 3A). Wave dominated deltas (e.g. San Francisco, Nile and Niger deltas, Figure 3B) form when the strong wave currents control the sediments distribution and determine the size and shape of the delta. They exhibit mouth bars under the influence of longshore currents and transgressive processes which lead to shore-parallel sand bodies. Tide-dominated deltas display usually more estuarine-like geometry with many tidal flats and mouth bars present developed perpendicular to the shore (Fagherazzi, 2008). Tide-dominated deltas are observed in regions of large tidal ranges where the tide currents are stronger than the river outflows. Such examples are the Ganges-Brahmaputra (Bangladesh, Figure 3C) and the Mekong (Vietnam) deltas (Roberts et al. 2012). Galloway's classification scheme was further revised by Coleman & Wright (1975) who added a sand body geometry classification and Orton and Reading (1993) who added the grain size of the sediments delivered to the delta as another parameter in the classification scheme. For the purposes of this study which does not focus necessarily on sediment properties, the classic Galloway's scheme will be adopted.

The density difference between the inflowing water and the receiving standing water body affects the flow jet and sedimentation processes at the river mouth (Chorley et al.1984) and thus is identified as another parameter that can influence a delta's geomorphology. Bates (1953) established the following

three conditions in relevance to the water density: 1) Homopycnal where there is no density contrast. In this case there is no vertical gradient and three-dimensional mixing occurs. 2) Hyperpycnal where the river discharge is denser than and plunges beneath the water of receiving basin. 3) Hypopycnal where the river is less dense than the standing water and spreading of the sediments occurs through the expansion of a buoyant plume.

Wright (1977) identified the river mouth forms (as a result of sedimentation) for the homopycnal and hypopycnal conditions when the tidal range and wave power of the receiving basin are negligible to the river outflows. In such cases, the effluent processes are classified as 1) inertia dominated, 2) friction dominated or 3) buoyancy dominated (Figure 4). Fully turbulent jet diffusion develops in the case of inertia effluents with low lateral spreading angles. The plume decelerates progressively and narrow river mouth bars are formed.

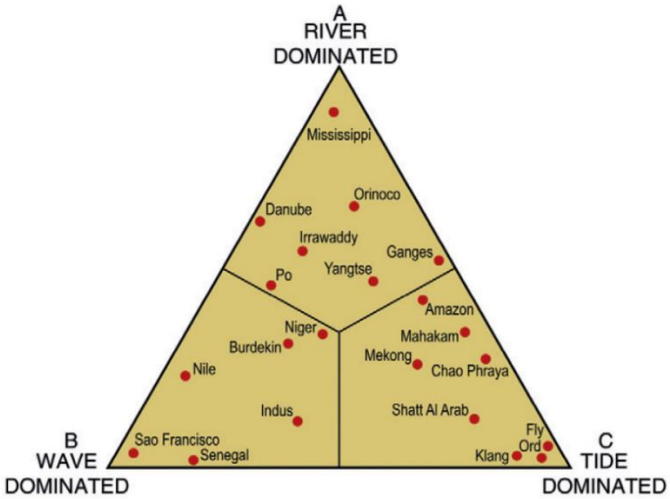

Figure 2 Galloway's (1975) river deltas classification according to river, wave and tide influence (taken from Roberts et al. 2012)

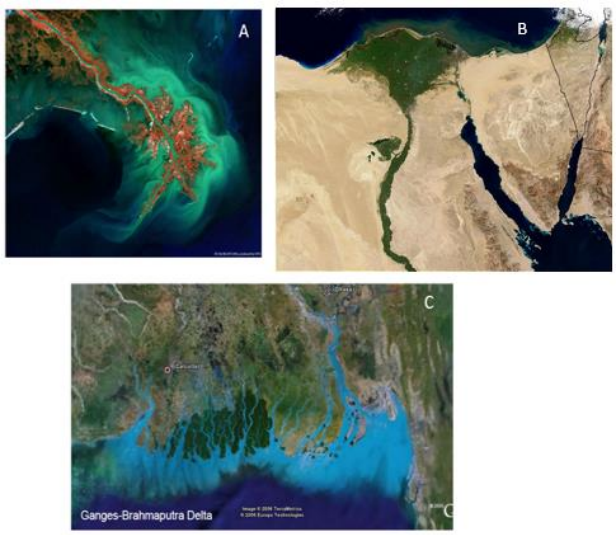

Figure 3 A) River Dominated Delta (Mississippi, available at www.earth.esa.int) B) Wave Dominated Delta (Nile, available at www.esa.int) C) Tide-Dominated Delta (Ganges Brahmaputra, Google Earth photo)

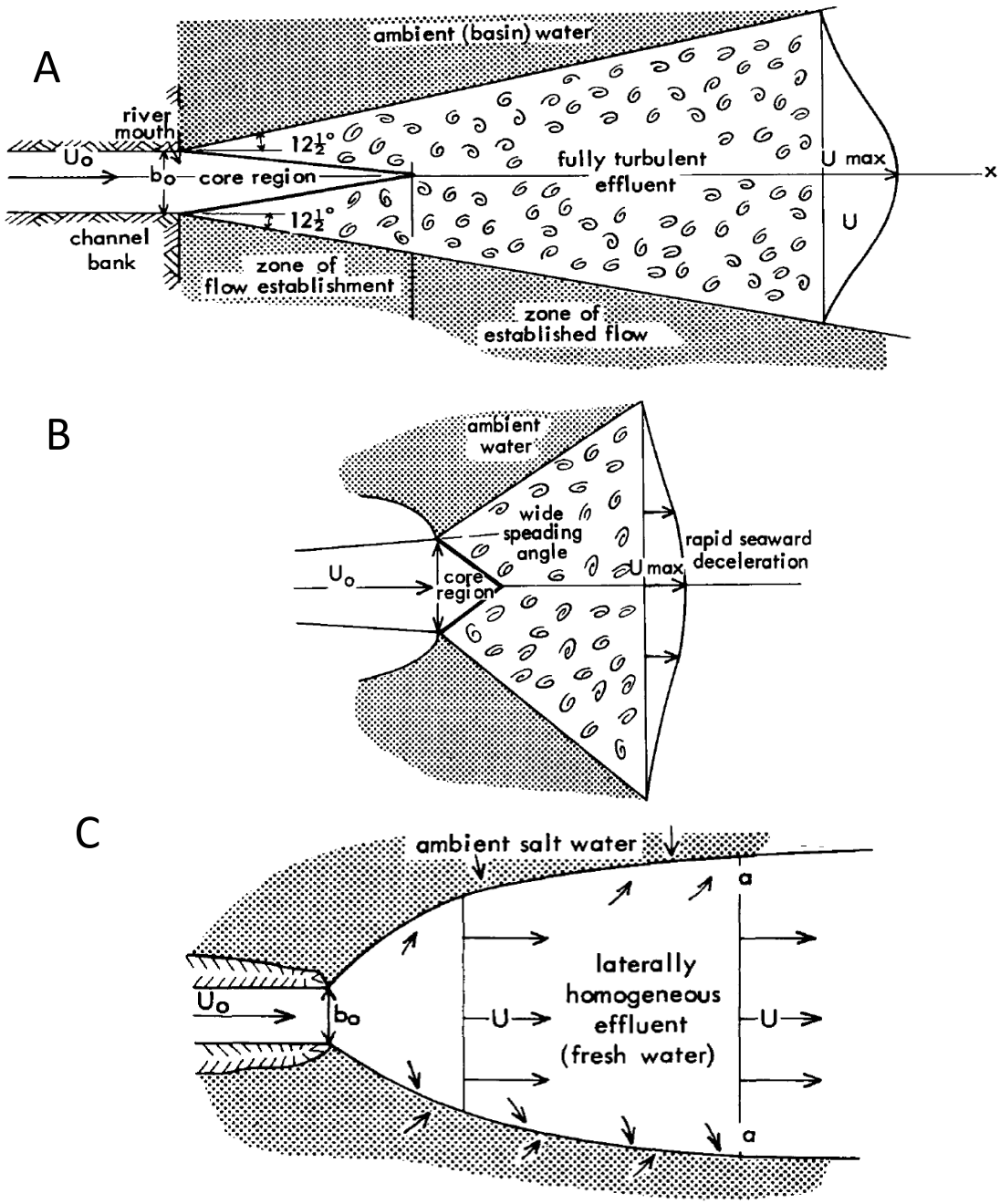

Figure 4 Plan views of A) Inertia-dominated B) Friction Dominated and C) Buoyancy Dominated effluents (modified from Wright 1977).

Friction dominates where there is a depth shallowing seaward of the river mouth causing more rapid deceleration and lateral expansion. Frequent channels bifurcation is observed in this case. Finally, buoyant effluents develop in the absence of mixing factors (e.g. low tidal range) and in high depths favouring stratification. Much less bifurcation occurs in such cases.

1.4. Channels Classification

As common in every river network, river deltas consist of a trunk channel and several distributary and terminal distributary channels. The trunk channel derives from a coalescing of a drainage basin's rivers and it is the main delta channel that feeds the distributive system (Olariu and Bhattacharya, 2006). This main channel ends at the delta apex which is the point where distributary channels start to form. This happens when the flow in the trunk channel reaches an open area and other channels start to

develop due to topographic differences (Olariu and Bhattacharya, 2006). The distributary channels present relatively low gradients to the trunk and are further bifurcated when a single channel (referred to as a parent channel) branches into two or more channels referred to as daughter channels (Coffey, 2017). With each bifurcation, the discharge is split into the new formed channels. The channels become smaller in the downstream direction. Yalin (1992) developed empirical relationships that showed that both the depth and width of a channel decrease downstream as the river discharge does too even though these may be subject to changes due to human activities. Distributary channels that extend between the last subaerial bifurcation and the last subaqueous channelization, usually located at the very end of the delta are defined as terminal distributary channels (Olariu and Bhattacharya, 2006). The terminal channels differ from the distributary network because they develop steeper angles normal to the main river channel and are usually shallower and narrower. Both distributary and terminal channels are important features as they control water, sediment and nutrient routing (Coffey, 2017). The areas between the distributary channels (referred to as inter-distributary areas) change downstream from fresh water through brackish to saline environments. In the case that distributary channels enter lagoons or lakes, new minor deltas may be formed.

1.5. Role significance of river deltas in global society and economy

Deltas are productive aquatic and coastal ecosystems that have highly fertile soils, diverse landscapes and are easily navigable. These areas have also high concentration of freshwater, nutrients and sediment inputs in their coastal zone. This makes them attractive places for living and working and creates perfect conditions for dense population and high economic activity (Bianchi 2016). It is estimated that half a billion people worldwide are dependent on deltaic ecosystems (Ericson et al., 2006;Nicholls et al., 2018). Thus, deltas are extremely important from an environmental and economic point of view. Since antiquity, deltas played a key role for the civilization. For example, the Yangtze deltaic plain in China has always been a very fertile region. Built in the centre of it, the city of Shanghai developed quickly in time and became one of the most important industrial and economic centres in the world (Chen and Zong, 1999). Some other examples of deltas with critical role for both society and economy are: the Mekong Delta that constitutes 50% of Vietnam's cultivation-mainly rice and shrimp-(Dun, 2011), the densely populated Ganges-Brahmaputra Delta in Bangladesh where rapid agricultural development, urbanization and industrialization took place in recent years through the use of water for irrigation, industry and public supply (Whitehead, Sarkar, *et al.*, 2015) and the Mississippi Delta which is a source of freshwater in the Gulf of Mexico and provides food, habitat and nursery ground for a number of ecologically important species (Kolker et al., 2018). Moreover, many deltas host reservoirs of oil and natural gas making them even more important for the global economy (Roberts et al. 2012). Significant hydrocarbons have been discovered in at least eighteen deltaic provinces worldwide (Wescott 1992).For example, the Niger Delta oil and gas resources rank as the twelfth largest in the world (Tuttle et al.1999). Rich in oil and gas basins have also been found in the Mahakam, Pearl River and Nile deltas (Deng 2016). In addition, deltas can provide a coastal defence buffer against storms (Nicholls et al.2018, Loucks 2019) if their aggradation rate remains in balance or exceeds land subsidence and relative sea level rise (Syvitski et al.2009). This is the case in some deltas as for example the Amazon and Mahakam that provide a level of ongoing protection from storm-surge landward penetration (Syvitski et al.2009). However, this may change in the future due to climate change and human activities as it is explained in the next paragraph.

1.6. River Deltas Sustainability

River deltas belong to a complex natural system and are directly influenced by the physical processes taking place in it (Figure 5). Human activities in the river catchment can have a severe impact on delta's maintenance and sustainability by modifying water flows and sedimentary processes (Syvitski et al., 2009; Nicholls et al.2018). The sediment supply in the delta is limited by activities such as intensification of agriculture, including deforestation, and dam construction that cause erosion increasing flooding risk (Hasslet, 2000). Global warming and climate change exacerbate this risk through sea level rise (IPCC 2007). The total volume of sediments delivered to deltas reflects conditions in the drainage basin and indicates climate change impact. Changes of the sea level are important in a depositional context because they can indicate channels extension and shortening in periods of falling and rising sea level respectively (Blum & Tornqvist, 2000). The issue becomes even more acute when compounded by land subsidence. This usually results from natural sediment compaction, often occurring in deltas, but is now further accelerated by urban construction, groundwater extraction and rivers channelization. Consequently, the rate of relative sea level rise (RSLR), which is the combination of land subsidence and sea level rise increases further (Tessler *et al.*, 2015). Overall, deltas' submergence and erosion can be the outcome of the combination of human interferences in the ecosystem with climate-driven processes such as precipitation, sea level rise and storm frequency and intension (Ericson *et al.*, 2006) .

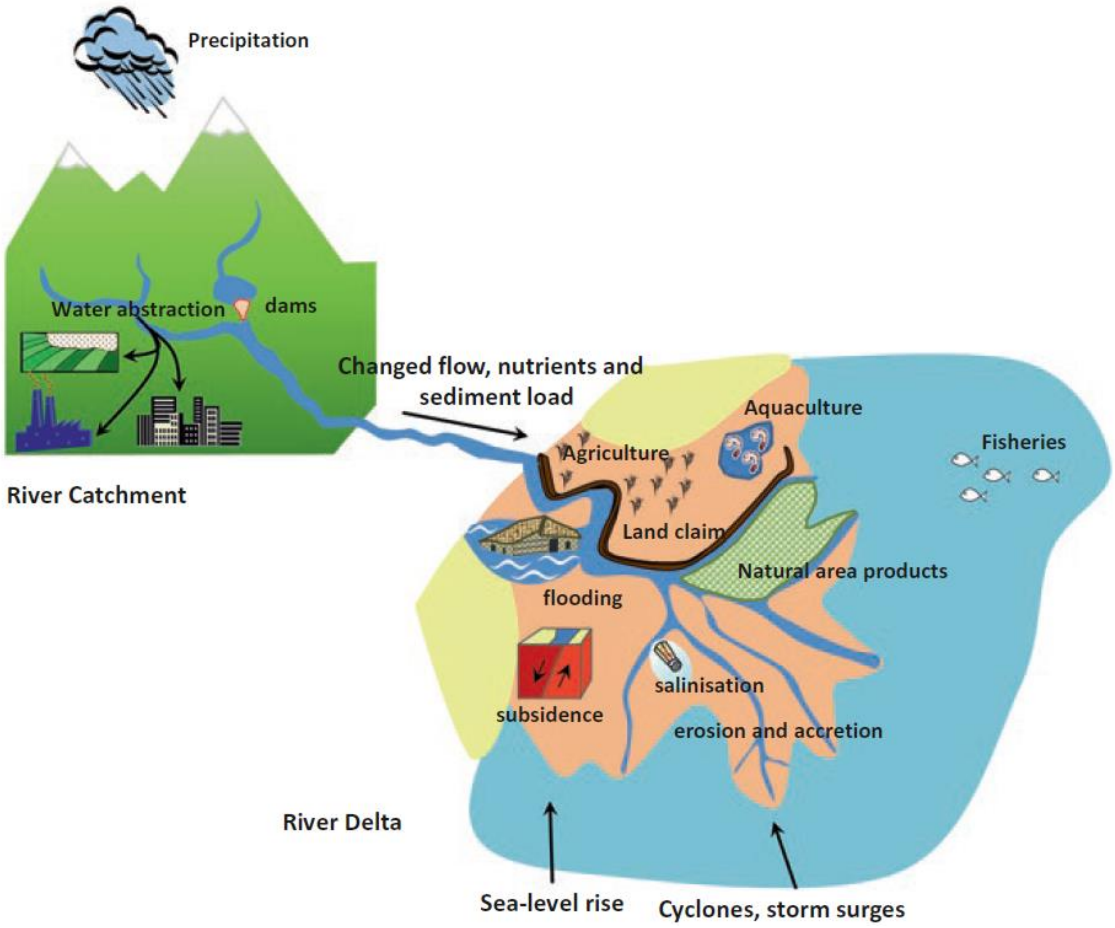

Figure 5 Natural Processes in a deltaic ecosystem (from Nicholls et al. 2018)

Many deltas around the world face similar challenges. For instance, the Mississippi Delta has seen a total loss of 2551 km^2 in a period of 50 years which is attributed to RSLR increase and decrease of sediment capacity due to dam construction upstream (Kesel 1989; Penland et al. 1988; Visser et al.2012). Land subsidence in rates overwhelming that of SLR in the Ganges-Brahmaputra and Mekong deltas puts in danger millions of people that may have to be displaced (Syvitski *et al.*, 2009) while the sediment capacity in the Yangtze delta has been significantly reduced in recent decades due to dams construction (Hu and Ding, 2009; Zhang *et al.*, 2018). Finally, the Nile delta is subject to erosion and possible flooding threat because of changes in the wave activity after the construction of the Aswan dam (El-Raey et al. 1999). Flooding of the delta plain as a consequence of erosion will lead to a rise of the water table and incursion of sea water especially during sustained dry season periods decreasing the fresh water availability. Considering that the agricultural activity is significantly high in the majority of the deltas, salinization could be a serious damage for these regions. The issue of salinization is discussed in more detail in the next paragraph.

1.7.Salinization of Deltas

A direct impact of the sea level rise is the increased salinity levels inside deltas (Hull and Titus 1986; Bhuiyan and Dutta, 2012; Hong and Shen, 2012; Bricheno et al. 2021) . This could have several adverse effects. High salinity in soil and water is detrimental for the anthropogenic activities taking place in river deltas and causes ecological degradation. Increased salinity levels damage soil cultivation and crop production (Clarke et al.2015; Kashefipour et al. 2012; Su et al.2005) and decrease the water quality for irrigation, agriculture and drinking (Allison, 1964; Smedema & Shiati, 2002; Rosen et al., 2018). For example, severe reduction of rice and wheat production is reported in the Bangladesh delta where many freshwater rice paddies have been converted to brackish water shrimp farms (Sarwar, 2005; Bricheno and Wolf, 2018). Conversion of freshwater to brackish or saltwater habitats has also occurred in the Mississippi Delta where serious ecological degradation is taking place because of frequent flooding (Holm and Sasser, 2001; Kaplan *et al.*, 2010). Nevertheless, salinity can have an indirect impact on society by threatening livelihood, income generation and compromise food security (Khanom, 2016). Consumption of saline waters is known to increase health risks and be responsible for stroke and hypertension (Khan et al., 2011; Rahman et al., 2019; Vineis et al. 2011). Many cholera outbreaks in Bangladesh occurred after flooding episodes because the water supply was contaminated (Sarwar, 2005). Saline water has been also reported as a leading cause for hypertension (Rahman *et al.*, 2019). Environmental consequences extend to vegetation and aquatic life as well. Many vegetation (e.g. Sagittaria Latifolia, Sagittaria Lancifolia, phragmites australis) and marine species (e.g. benthic animals,larvae fish,shrimps) cannot survive in saline environments (Day et al. 1989; LaSalle & Bishop 1990; Chen 2004,White et al.2019) while high salinity may be responsible also for plant stress and mortality and hampering of tree production (Kaplan *et al.*, 2010; Bhuiyan and Dutta, 2012). In addition, high vertical salinity gradients can develop anoxic conditions detrimental for fisheries, recreation and tourism (Chant, 2012).

The issue of salinization has raised serious concerns in recent years since many deltas face already its implications. For example, the Mekong River Delta in Vietnam saw an increase of the salinity levels by 8.6% in the 1980s which rose to 13.1% by the first decade of the 21st century (CGIAR, 2016) and is expected to increase even further after a dam construction in the lower delta. Low rainfall due to the El Nino phenomenon prolongs drought periods with freshwater shortage which is harmful for farming. The Ganges-Brahmaputra delta in Bangladesh also faces sustained drought periods because of changes in the monsoon rainfall. Combined with sea level rise after enhanced cyclones activity, it increases dramatically the salinity in the area (Whitehead, Barbour, *et al.*, 2015). As a result, the crop production is hampered due to lack of good quality irrigation water and farmers experience a

significant yield loss. This is devastating for the country's economy since 30% of its cultivatable land lies in the delta area and 53% of this is affected by salinity in various degrees (Rahman, 2012; Seal & Baten, 2012; Whitehead et al., 2015; Zaman et al., 2017). Furthermore, a water diversion project in the Yangtze Delta in China has enhanced salt intrusion in the delta and it is expected to become worse during dry seasons (Hu & Ding, 2009). As a result, freshwater demand for 50 million people has been frequently interrupted in recent years (Wu *et al.*, 2016). The deltas of the Louisiana, USA (Mississippi, Atchafalaya, and Wax Lake) also face ecological degradation caused by salinity intrusion. The present status of primary plant succession, wildlife, and vegetation and fisheries dynamics is endangered (Holm et al, 2001). More examples on salinization issues in deltas around the globe are included in chapters 4,5 and 6.

2. LITTERATURE REVIEW

The study of the salt intrusion in deltas requires knowledge of estuarine processes because the same dynamics apply. The two systems have many similarities. In fact, river deltas can be considered as estuaries affected by morphodynamic processes of sedimentation (de Miranda et al.2017). Sedimentation processes influence the distribution of fine-grained sediment that are prone to be located in the inner half of estuaries while deltas export mud to the delta front and pro-delta (Sutherland et al. 2015). Usually estuaries evolve to deltas under stable sea level conditions when there is sufficient time for continuous sediment supply (Dalrymple et al.1992; Heap 2004). The result is a complex multi-channel system that distinguishes deltas from estuaries. It is this channelized network that makes the study of salt intrusion more challenging in deltas than estuaries. The deltas' complex morphology introduces more degrees of uncertainty due to the variable depths and cross-sections that interfere and may cause deviations to simple predictive models and/or analytical solutions that have been developed for estuaries when implemented for deltas (Nguyen and Savenije 2006). For example, the freshwater discharge distribution over a multi-channel estuary with many branches such as the Mekong Delta is very difficult to compute and cannot be measured directly (Nguyen et al.2008). More importantly, river deltas are more vulnerable to human activities and in some cases the anthropic control on the natural environment can override the climatic signal, forcing deltas toward a man-made river-dominated system (Maselli & Trincardi, 2013; Bellafiore et al.2021). The rapid response of these natural habitats to human perturbation should be seriously considered in any management attempt because of the extra challenges it poses on such endeavours (Maselli & Trincardi 2013). The present work aspires to fill the gap into our knowledge of the effect that braided networks may have on what is already known about salinity response to hydrodynamic changes and salt intrusion.

The first part of this chapter presents succinctly fundamental theoretical concepts related to the content of this research. Definitions are provided and the topics are further discussed based on the existing literature. The second part cites earlier studies that focused exclusively on salinity in river deltas and not estuaries.

2.1. MAIN CONCEPTS

2.1.1. Estuarine Circulation

Estuaries connect the coast with the sea and act as a transition state from low to high salinity. The horizontal salinity gradient that develops has a key role on the estuarine physics because it induces a vertically varying pressure gradient (Geyer 2010) and thus is usually associated with densimetric differences and stratification. The horizontal gradient induces a seaward flux that balances the landward salt transport controlled by tidal dispersion and estuarine circulation (Hansen & Rattray, 1965). The estuarine circulation expresses the tidally averaged along-channel velocity through an

estuarine cross-section (Geyer and MacCready, 2014). This circulation is a density contrast between ocean and river water (MacCready et al., 2021) which results in a bidirectional flow that transports fresh water offshore at the surface and denser water onshore at the bottom (Figure 6). The pressure gradient induced by the horizontal salinity gradient ϑS⁄ϑx can be related to the estuarine circulation through the simplified tidally averaged one dimensional momentum equation (Geyer 2010):

$$g\frac{\vartheta\eta}{\vartheta x} + \beta g\frac{\vartheta S}{\vartheta x}(h-z) = A_z\frac{\vartheta^2 u}{\vartheta z^2} \qquad (1)$$

g, η, β, h, u and z are the gravity acceleration, water free surface, saline contraction, water depth, horizontal velocity and the vertical coordinate measured upward from the bottom. A_z is the vertical eddy viscosity that represents the turbulent stress. Its magnitude is determined by tidal flow and stratification.

The landward flow (inflow) gradually rises and joins the river outflow in the upper half of the estuary resulting in an overall pattern called exchange flow (Geyer and MacCready 2014). The importance of the exchange flow lies on trapping of sinking particles such as sediments and organic matter because of the strong vertical density gradients that develop. This could lead to high sediment accumulation, excess nutrient recycling and anoxic conditions at the bed (Feely et al., 2010; Traykovski et al. 2004). In addition, the volume flux of the exchange flow is much greater than that of the river alone (MacCready and Geyer 2010). The scale of the exchange flow can derive from the analytical solution of equation 1 with respect to the horizontal velocity expressing the estuarine circulation and is equal to (MacCready and Geyer 2010):

$$u = \frac{1}{48}\frac{\beta g\frac{\vartheta S}{\vartheta x}h^3}{A_z} \qquad (2)$$

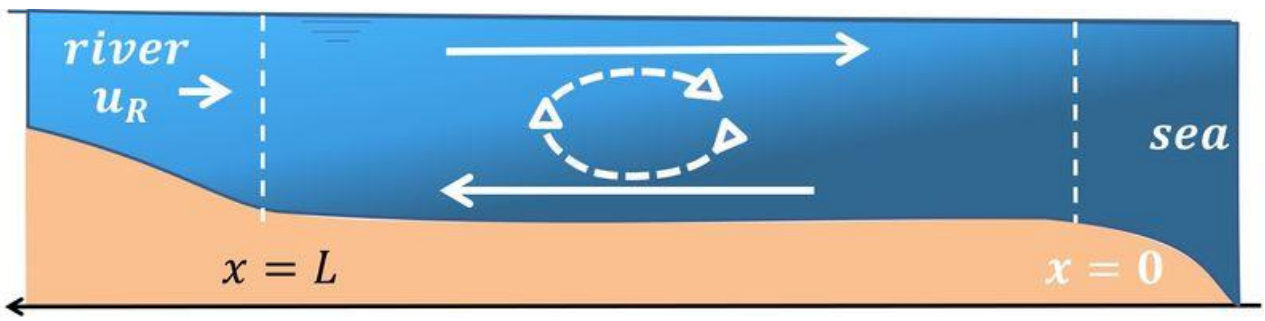

Figure 6 Schematic representation of the intrusion of seawater (dark blue) in a longitudinal section of a prismatic estuary. (taken from CoastalWiki)

Revisions on the estuarine circulation

The role of tides

Tidal effects and nonlinearities in early estuarine studies (Chatwin, 1976; Pritchard, 1956; Hansen & Rattray, 1965) were parameterised through the mixing coefficients while tidal motion and processes were removed by averaging. In that sense, estuarine circulation can be referred to as gravitational circulation because it is assumed that the primary driving force is the baroclinic pressure gradient (Geyer and MacCready 2014). However, this downgrades significantly the role of tides in the estuarine circulation. It has been demonstrated that tidal variations in estuaries with strong tidal forcing may

affect significantly the stratification in a much larger amount than the gravitational circulation does (Geyer and MacCready, 2014). The phenomenon of the strain-induced periodic stratification (SIPS) has been introduced by Simpson et al. (1990). According to this, vertical mixing decreases at the ebb and increases at the flood tide causing the landward flow at the bottom layer to be higher during the flood than the ebb tide (Jay and Musiak, 1994). This tidal asymmetry (referred as tidal straining according to Burchard & Hetland (2010)) results in a circulation similar to the gravitational one (landward flow at the deep and seaward at the surface water) that enhances the estuarine circulation. Based on a series of 1D modelling experiments, Burchard & Hetland (2010) identified that the velocity components due to tidal straining and gravitational circulation have the same vertical shape but the former could be twice the latter. If the longitudinal salinity gradient intensifies further, the salt field follows a transition from a SIPS state to runaway stratification (Monismith et al.2002; Simpson et al., 1990) that refers to an increased stratification when straining overtakes mixing (Geyer and MacCready, 2014).

Secondary estuarine circulation

In previous considerations of the estuarine circulation, the focus is given only on the along-estuary and vertical structure of velocity and salinity (Geyer et al.2020). Nevertheless, the lateral dimension has important effects on the estuarine circulation (Geyer and MacCready 2014). This topic has been addressed in a number of remarkable studies (Burchard et al. 2011; Geyer et al.2008; Lerczak & Geyer, 2004; Nunes & Simpson, 1985; Scully et al. 2009; Smith, 1977). Cross-estuary gradients of velocity and salinity are often larger than their along-estuary gradients and so the magnitude of the cross-estuary advective terms in the momentum equation can be larger than their along-estuary ones (Chant 2010). In addition, secondary flows – defined as the flow that is normal to the along-estuary flow- play an important role on the mixing of tracers and they can determine the fate and transport of material along an estuary (Chant 2010). Interestingly, many studies on this topic identified that lateral straining might be more important than along estuary resulting in maximum stratification during the flood rather than the ebb tide (Lacy et al.2003; Ralston and Stacey 2005; Scully and Geyer 2012; Becherer et al.2015; Schulz et al.2015). This is the result of a lateral circulation induced by a cross-estuary density gradient and carries surface water at the centre of the channel during flood tide with the reverse occurring at the ebb tide. The development of cross-estuary gradients setup by lateral shears in the along-estuary flow is also defined as differential advection (Chant 2010). In particular, Schulz et al. (2015) emphasized on the coupling between lateral circulation induced by differential advection and restratification at the end of the flood tide. Building on this work for a more complex geometry case, Geyer et al. (2020) identified that lateral salinity gradients generated by differential advection at the edge of the channel drive a tidally oscillating cross-channel flow that strongly influences the stratification, along-estuary salt balance and momentum balance.

The effect of secondary flows on the estuarine circulation can be important in deltaic systems where their complex morphology presents significant lateral variations of the depth.

Total exchange flow

Finally, the most recent advance on the topic considers the Total Exchange Flow (TEF), a method in which the subtidal transport is calculated as a function of salinity instead of spatial position (Geyer and MacCready 2014). Results from related studies (Chen et al., 2012; MacCready, 2011; Wang et al., 2017; MacCready et al.2018; Lorenz et al.2019) suggest that TEF can provide a more robust and kinematically accurate quantification of estuarine exchange flow (MacCready and Geyer 2014;Geyer et al.2020). However, this goes beyond the scope of this project and will not be further discussed.

2.1.2. Transport time scales

Exchange flow increases the longitudinal dispersion of passive tracers in an estuary with low buoyancy but causes trapping of sinking waterborne material (Geyer & MacCready, 2014). It is imperative then to know the transport time of substances through an aquatic system because if this is shorter than the scale of their biochemical processes then the latter cannot be exerted (Wang et al. 2004; Yuan et al. 2007). The transport time is expressed through flushing and residence time. These two magnitudes have different definitions and physical meaning.

Flushing times

Flushing time (FT) is defined as the time required for the cumulative freshwater inflow to equal the amount of freshwater originally present in the region (Dyer 1973; Sheldon and Alber, 2002). In a river dominated system, the flushing time could be simply calculated just by dividing the estuary volume over the total flow rate. However, in the case of gravitational circulation this neglects the flushing due to tidal dispersion. Sheldon and Alber (2002) define the flushing time t for an estuary as the ratio of an initial freshwater volume Vol over the freshwater inflowQ_f:

$$t = \frac{Vol\left(\frac{S_o - S_e}{S_o}\right)}{Q_f} \qquad (3)$$

with S_o and S_e the ocean and the average estuarine salinity respectively. Equation 3 represents the 'freshwater fraction method' for flushing time calculation (Lauff 1967; Dyer 1973; Fischer et al. 1979; Williams, 1986). Sheldon and Alber (2006) showed that tidal effects are implicitly included in the calculation with the freshwater fraction method which is more appropriate for estuaries with high freshwater inflow (i.e. large salinity difference between the estuary and the ocean). In such cases, the freshwater fraction provides very similar results to other methods that consider explicitly the tide as a flushing agent such as the tidal prism models method (Lucas 2010). On the contrary, equation 3 is not deemed successful in the case of well-mixed systems with low freshwater inflow (i.e. negligible salinity difference between ocean and estuary) (Lucas 2010). Equation 3 applies either to the whole estuary or to different estuarine segments so that the total transit time is taken as the sum of the specific segment times (Sheldon and Alber, 2002). The determination of the freshwater inflow Q_f to be introduced in the equation can be a difficult task since the river discharge in real estuaries is barely at steady state (Alber and Sheldon, 1999). To overcome this issue, many researchers implemented the method by taking monthly or seasonal discharge averages or averages over a user-defined period (Pilson 1985;Christian et al.1991;Asselin & Spaulding 1993;Balls, 1994; Lebo et al. 1994; Swanson & Mendelson 1996;Eyre and Twigg, 1997;Chan Hilton et al. 1998; Alber and Sheldon, 1999; Hagy, Boynton and Sanford, 2000; Huang and Spaulding, 2002; Sheldon and Alber, 2002; Huang, 2007). Alber and Sheldon(1999) proposed a specific technique to determine the appropriate averaging period of the river discharge by assuming that this should be equal or very close to the flushing time itself. They found that their so called Date Specific Method (DSM) was successful for the calculation of flushing times in Georgia Estuaries. Becker et al. (2010) implemented DSM to determine the appropriate means of incorporating flow history into a discharge value when investigating the discharge-salt intrusion relationship in the Cape Fear River. Using the same method, Paerl et al. (2014) developed relationships between flushing times and pigment concentrations indicative of total phytoplankton biomass in two lagoonal ecosystems. The DSM has been implemented in this project as well (see chapter 4 and 6).

Residence times

The residence time is defined as the remaining time that a particle will spend in a certain region after first arriving at some starting location (Zimmerman, 1976; Sheldon and Alber, 2002). Therefore, it is a site-specific time applied within a restricted geographical area such as an estuary, a water basin or a box model (Hagy et al. 2000; Sheldon and Alber, 2002; Sámano *et al.*, 2012). It depends on the location of a water particle within the embayment and whether it is close to the open boundaries or not (Lucas 2010). Its estimation usually requires numerical modelling (Sheldon and Alber, 2002). If the constituent is a reactive scalar with a growth or loss rate (e.g. phytoplankton) the previous definition of the residence time may not be appropriate to describe its variability (Lucas 2010). The tide can have an impact on this because a constituent may enter, leave and enter again in the domain. However, this is not a concern for the present study that does not deal with reactive scalars.

In this study, only flushing and residence times were considered. Flushing time was determined through the freshwater fraction equation in order to compare the time for freshwater replenishment between dry and wet seasons. Annual flow distributions were considered in an effort to detect the most efficient shape for faster water renewal. The residence time was determined spatially through model results by counting the time that the salinity remains below a threshold value in various locations.

However, it is worthy for completeness to introduce two other additional transport time scales. These are the water age and trapping due to stratification time. In addition to flushing and residence times, these are also important to know in a deltaic system where the complex morphology adds one more factor of influence to the transport time scales.

Age and trapping time

The age of a fluid element within an embayment is the time that has elapsed since the element entered the embayment (Bolin and Rodhe, 1973; Zimmerman, 1976; Dronkers and Zimmerman, 1982; Lucas 2010). Therefore, age and residence time are complementary and together they constitute the transit time of a fluid element (Sheldon and Alber 2002). Earlier modelling studies (Monsen et al.2002; Banas and Hickey 2005) indicated that particle ages can vary significantly in both space and time.

The time scale of stratification can have a direct or indirect effect on transport time scales. In particular, tidally periodic instead of persistent stratification may cause particle trapping in flood-dominated estuaries by allowing particles to sink during stratified ebb tides. On the other hand, particles can be resuspended during destratified floods when up-estuary transport occurs (Chant and Stoner, 2001). Therefore, high-frequency variations of stratification and mixing can yield long-term effects different from a persistent condition and so knowledge of stratification time scales are important to understand the physics of a certain estuary (Lucas 2010).

2.1.3. Buoyant plumes

Freshwater debouches into the ocean from a river mouth and mixes with deeper and denser water forming a buoyant plume. These are distinct regions with dynamics influenced significantly by the freshwater and are found in various sizes and scales. They are subject to wind, tidal and riverine forcing (O'Donnel 2010; Horner-Devine et al. 2015). The fate of the river-borne material in the ocean depends largely on the plume's physical processes and transport (Horner-Devine, Hetland and MacDonald, 2015). Garvine (1995) classified the plumes into small and large scale based on the Kelvin number. According to this definition, small-scale plumes are characterized by strong advection, Froude numbers close to unity and small Coriolis effects. On the contrary, small advection and Froude numbers together with order one Coriolis effects correspond to large scale plumes. A plume's classification may be simplified by comparing only the two length scales, alongshore and across-shore

(L and γL respectively, see Figure 7). Large-scale plumes are usually elongated along the coast and exhibit $\gamma \leq 1$ values.

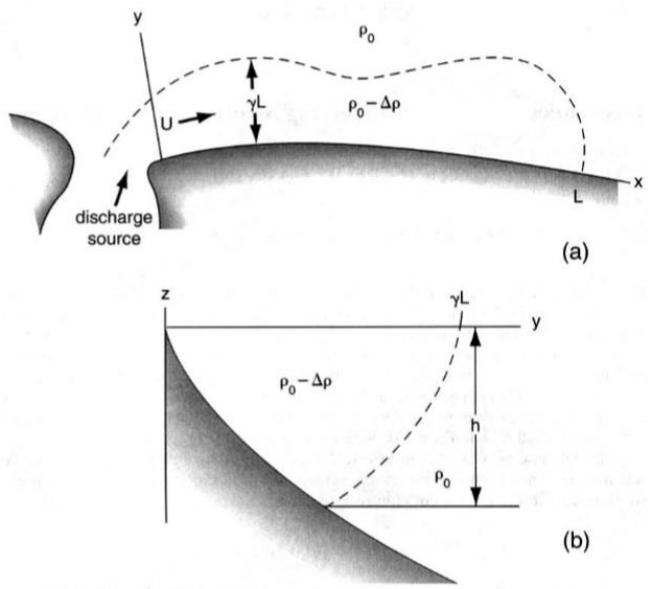

Figure 7 A sketch of an idealized buoyant plume whose limit is bounded by the dashed line, a) the along-shore (x) and across-shore (y) plume development and its length (L in x and γL in y). U is the alongshore velocity. The ambient water has a ρ_o density while the plume's density is $\rho_o - \Delta\rho$. b) the plume's vertical structure in the z direction with an h depth.(taken from Garvine 1995).

Vertical structure

Buoyant plumes could also been classified based on their vertical structure. In a fundamental work, Yankovsky & Chapman (1997) investigated the vertical structure of the plumes and identified two main conditions. The first is when the plume occupies the entire water column and the density front extends from the surface to the bottom. This is called a bottom-advected plume (Figure 8A, B) since it is mainly controlled by advection at the bottom boundary layer. The second type refers to a case when the offshore buoyant flow is limited within a thin layer having no contact with the bottom layer. This constitutes the surface advected plume (Figure 8C,D). However, many plumes may belong into an intermediate stage. In this case, the buoyant flow is transported offshore through the whole vertical column until some distance where the upper part of the plume detaches and spreads seaward with a thin layer close to the surface. Poggioli & Horner-Devine (2018) define the location where the plume is detached from the bottom as the liftoff point. Its location is important for the system's dynamics since it separates the areas with supercritical from the areas with subcritical flow because the Froude number at the liftoff point equals 1. Horner-Devine et al. (2015) name the region beyond the liftoff point as near-field where it is considered that the riverine momentum exceeds the plume's buoyancy.

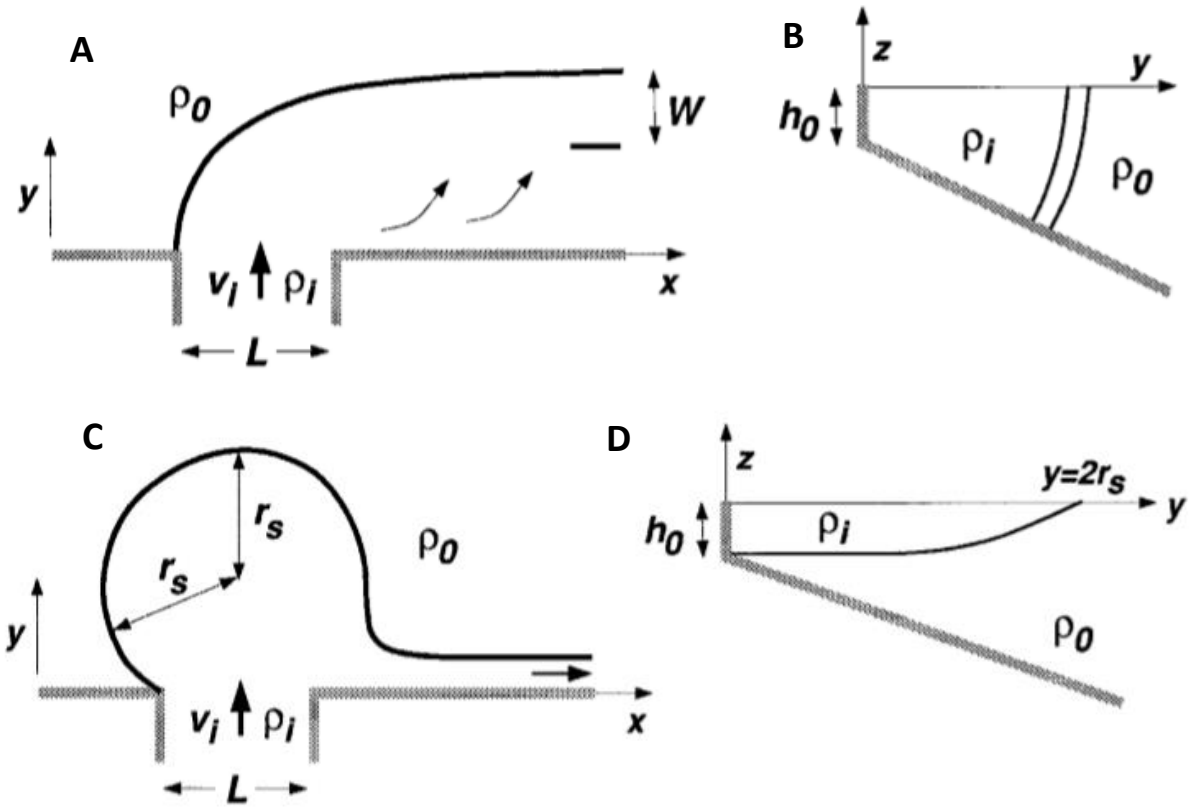

Figure 8 Plan view of a bottom A) and surface C) advected plume. Vertical cross-section of a bottom B) and surface D) advected plume. For the notations we refer to Yankovsky and Chapman (1997) where this sketch is taken from.

The complex dynamics and nonlinear flows that develop within the surface to bottom density front had been already identified in earlier studies (Csanady, 1984; D. G. Wright, 1989; Chapman & Lentz, 1994). More attention though has been given to surface advected plumes (Chao & Boicourt, 1986; Chao, 1988; O'Donnell, 1990; Oye & Mellor 1992; Kourafalou et al.1996; 1996b;1999, 2001; Yankovsky et al. 2001; Schiller & Kourafalou2010; Schiller et al.2011). These studies show that the plume develops two distinct regimes: a bulge region near the river mouth and a downstream coastal current (Chao & Boicourt, 1986; Fong & Geyer, 2002). The majority of the research concerns the downstream current. A common feature in all plume studies is the deflection of this coastal current to the right under the influence of the Coriolis force (Chao & Boicourt, 1986) or ambient crossflows (O'Donnell, 1990). This occurs when inflow momentum is lost so that lateral spreading is arrested and thus the plume dynamics are dominated by Earth's rotation (Horner-Devine, Hetland and MacDonald, 2015).

Tidal influence

Tidal influence is also important in a plume's structure since tidal currents in the inner-shelf might be larger than buoyancy-driven ones (O'Donnel 2010). Chao (1990) was the first to examine the tidal modulation of the river-forced estuarine plumes and stated that the tidal residual circulation enhances the plume growth and limits the coastal jet. Isobe (2005) indicated the development of more symmetric plumes with the tide enhancement. In a study on the effect of tides on mouth bar morphology and hydrodynamics, Leonardi et al. (2013) found that the flow jet spreading was much larger in cases including tides than those that did not. Similar conclusions derived from other studies that included tidal effects on their investigation of buoyant plume evolution (Chao, 1990; Isobe, 2005; Guo and Valle-Levinson, 2007; Lee and Valle-Levinson, 2013). Tidally-driven mixing competes

stratification induced by tidal straining. Garvine (1999) noticed a decrease of upshelf and downshelf buoyant plume penetration with the increase of tidal amplitude in a series of experiments.

Vertical Mixing

The plume structure is subject to changes not only from tidally-driven but also from vertical mixing due to inertial shear. Vertical turbulence and density gradients in the field determine the impact of mixing in a plume (Horner-Devine, Hetland and MacDonald, 2015). Hetland (2005) studied an idealized plume with results indicating that the influence of inertia shear mixing is larger in the near-field region characterized by low salinity areas. The high intensity of turbulence and mixing in the near-field region is reported in other studies too (MacDonald & Geyer, 2004; MacDonald et al. 2007; McCabe et al.2008). The mixing enhancement is caused by shear increase as the plume spreads offshore due to the high density differences between the plume and ambient waters. In its turn, the increase of mixing results in deceleration of the offshore plume transport (Yuan and Horner-Devine, 2013; Horner-Devine, Hetland and MacDonald, 2015).

Other parameters

The role of wind and waves mixing in a plume structure is also important but goes beyond the scope of this project and is not discussed.

The shape and morphology of a buoyant plume depend on the coastal geometry and river discharge magnitude. In combination with external forcing different types develop (Horner-Devine, Hetland and MacDonald, 2015). In the case of a river delta in particular, freshwater debouches in the ocean through a multichannel system (Figure 9). Plumes that develop at the end of each channel outlet interact with each other depending on their spacing. Therefore, the nature and spacing of the distributaries can have a crucial role on the plume characterization (Yuan et al. 2011; Horner-Devine et al., 2015). The next paragraph focuses on available methods to classify these distributaries based on common physical characteristics.

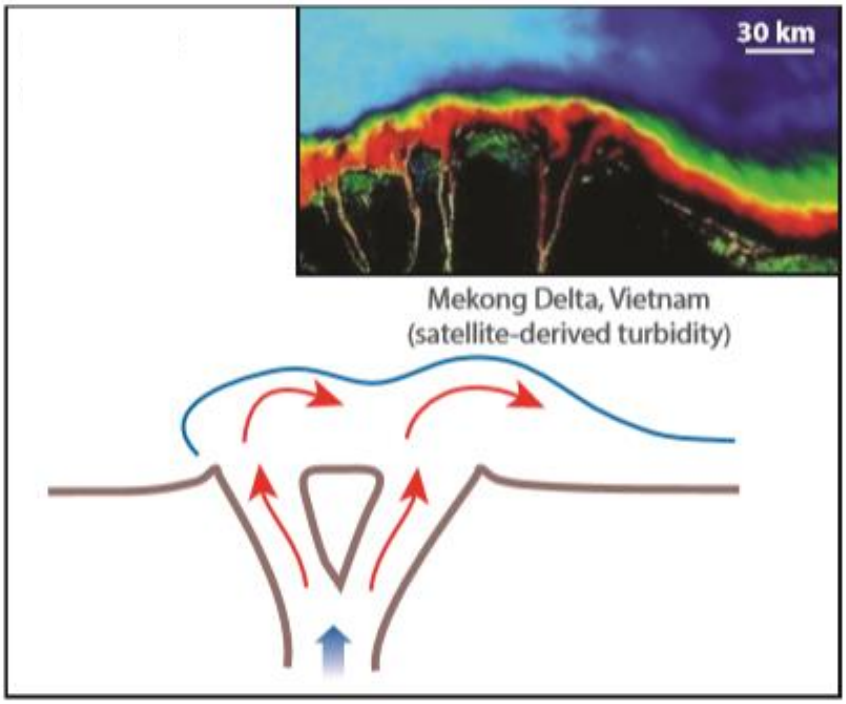

Figure 9 Typical plume morphology for a delta. The coloured image is an example of such a plume in the Mekong Delta (taken from (Horner-Devine, Hetland and MacDonald, 2015)

2.1.4. Bifurcation methods

River deltas are formed in a dendritic shape including many tributaries. This structure resembles riverine networks in drainage basins. In hydrology and geomorphology studies, the geometry of these networks is usually described based on stream labelling and ordering methods (Ranalli & Scheidegger, 1968). Such methods set a hierarchy to the delta tributaries. The most common one is the so called Strahler-Horton scheme. Horton (1945) devised a system of channels classification (or ordering) and introduced the concept of 'stream order' (Smart, 1968). This is a dimensionless parameter that distinguishes different classes (i.e. orders) of streams by assigning at each one of them an integer non-dimensional number. Horton's method applies to complete streams and not nodes or links and so the order remains unchanged along the stream (Figure 10A). This makes it difficult to distinguish branchless channels of first or higher order since the latter can be extensions of longer streams starting from the river source (Ranalli and Scheidegger, 1968). Strahler (1952) revised Horton's method by grouping branchless channels into first order (Figure 10B). If two channels of equal order make a junction, then the order of the parent (upstream) channel increases by one. If the parent channel makes a junction with a lower order channel then its order does not change. The Strahler-Horton order acts a proxy for a stream's physical characteristics such as the length or the basin's area (Kovchegov and Zaliapin, 2019). The number $N$of streams decreases as the Strahler-Horton K order increases according to Horton's law of stream numbers (1945):

$$\frac{N_k}{N_{k+1}} = R_B \quad , \quad R_B \geq 2 \qquad (4)$$

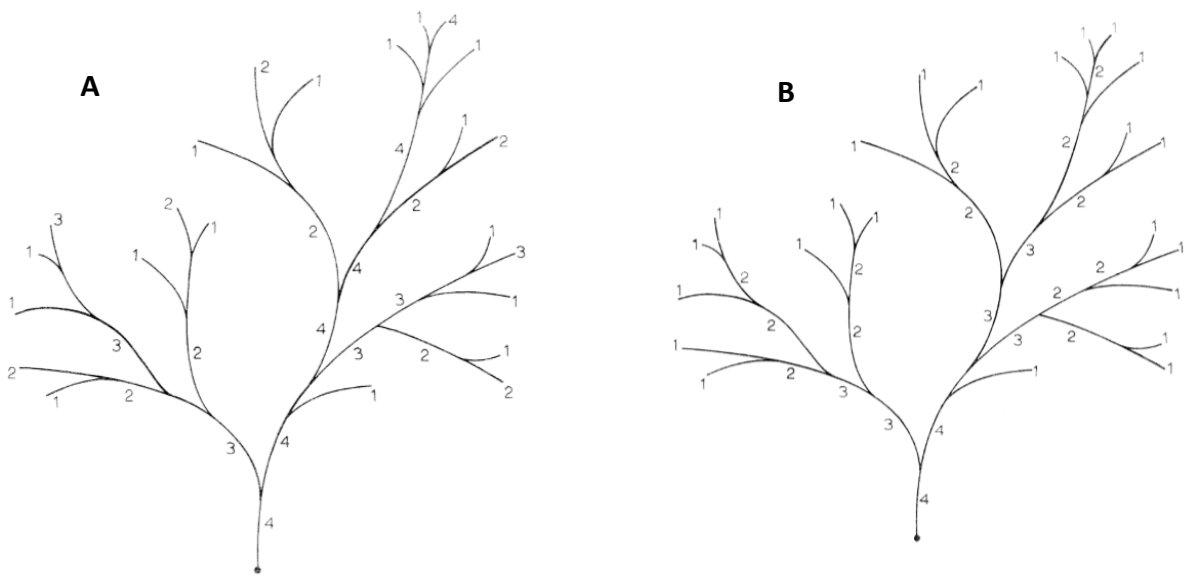

Figure 10 A) Horton's method B) Strahler's method (taken from Ranalli & Scheidegger 1968)

Tree-like structure is ubiquitous in nature allowing for the implementation of the Strahler-Horton method in a wide range of scientific areas (Chunikhina, 2018). These include hydrology (Tarboton et al.1988; Maritan *et al.*, 1996; Tarboton, 1996; Banavarn et al. 1999; Kirchner et al. 2000; Biswal and

Marani, 2010), geomorphology (Dodds and Rothman, 2000, 2001; Heckmann et al. 2015), mathematics and statistics (Kovchegov and Zaliapin, 2017, 2019; Yamamoto, 2017), neuroscience (Pries and Secomb 2008), computer science (Kemp, 1979; Devroye and Kruszewski, 1995;Nebel 2000; Chunikhina 2018), biology (Borchert and Slade 1981; Turcotte et al.1998) and social sciences (Arenas *et al.*, 2004).

It should be noted that other schemes developed in parallel with the Strahler-Horton such as e.g. Scheidegger-Shreve, Milton-Oiller and STORET (Ranalli and Scheidegger, 1968) are less popular. Despite some criticism on the Strahler-Horton method (Ranalli and Scheidegger, 1968; Tokunaga, 1978; Tarboton, 1996; Moussa, 2009) that emphasizes on inaccuracies of the channels delineations in maps, it is preferred because of its simplicity (Smart, 1968; Moussa, 2009). As a result, many authors developed methods to incorporate it to the geomorphologic instantaneous unit hydrograph (GIUH), (Gupta et al.1980; Rosso, 1984; Gupta and Mesa, 1988; Rinaldo *et al.*, 1995; Rodriguez et al. 2005; Kumar et al. 2007; Lee et al. 2008; Moussa, 2009).

In addition to the number and class of streams in a modular network, the set of nodes and links connecting them is another important feature which is termed as connectivity (Passalacqua, 2017). Connectivity is important because it is linked with the transfer of matter, energy or organisms between two different landscape compartments (e.g. streams) (Fryirs, 2013; Wohl et al. 2017). Riverine connectivity in particular, represents the exchange of material (e.g. salinity) longitudinally, laterally and vertically across watersheds and stream channels (Kondolf *et al.*, 2006; Wohl et al. 2017). River deltas are among the systems where such connectivity is high (Fryirs, 2013; Sendrowski and Passalacqua, 2017). Therefore, the research on the process-based connectivity between delta channels and inter-distributary areas has intensified in recent years (Hiat and Passalacqua, 2015; Passalacqua 2017). This deltaic processes connectivity occurs through exchange of information between external forcing (river discharge, tides and winds) and the response of internal variables such as water level, sediment concentrations, nutrients and/or salinity (Passalacqua, 2017; Sendrowski and Passalacqua , 2017).

In that sense, the introduction of the width function method might be sensible since it involves the number of nodes and links between channels. The width function concept was first introduced by Shreve (1969) and gives the number of links in a network at a flow distance x from the outlet. The flow distance is measured along the network and not radially from the outlet (Rodriguez-Iturbe and Rinaldo 1997). Kirkby (1976) implemented the method for a random network model by counting the number of links within a certain space step defining their limits as generations. Kirkby (1976) identified the influence of a catchment's width on a hydrograph's peak. Gupta and Mesa (1988) considered the width function as a planimetric projection of channels network and implemented it to explore physical and analytical connections between channels network and hydrological response. The role and the nature of the width's function influence on the hydrological response of a drainage basin has been investigated by many authors (Gupta and Mesa, 1988; Rinaldo et al. 1991; Snell and Sivapalan, 1994; Rinaldo *et al.*, 1995; Botter and Rinaldo, 2003; Collischonn *et al.*, 2017).

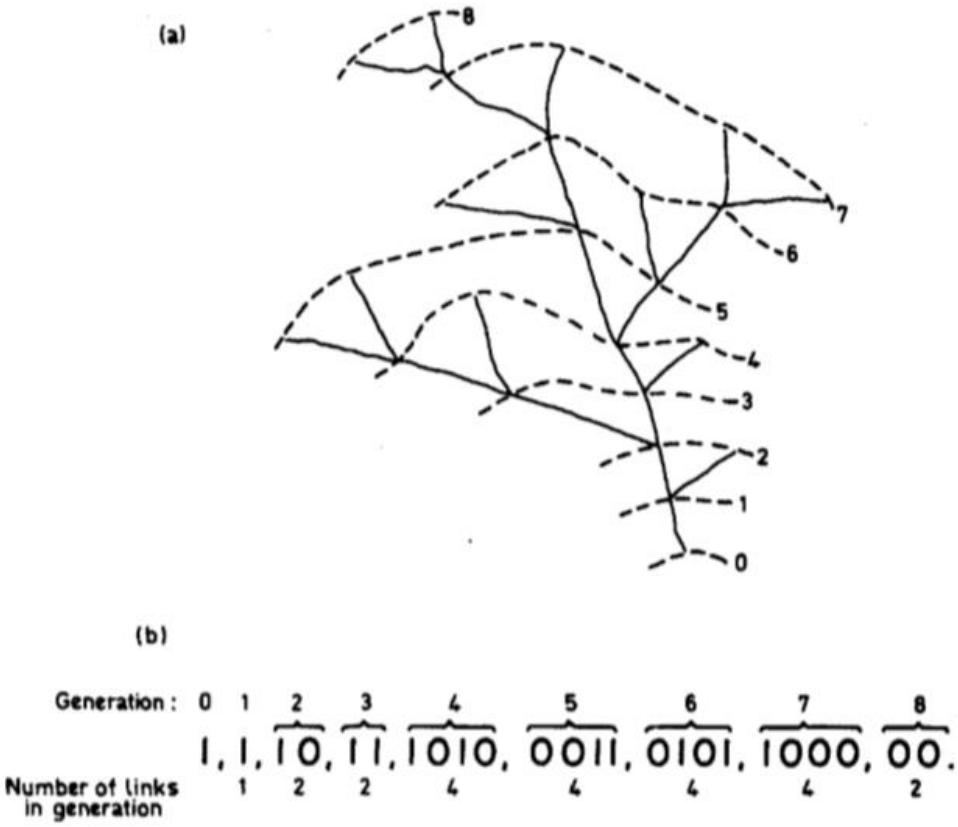

Figure 11 Example of the width function method. a) A channel network delineated by the continuous lines. The dashed lines (named generations) are drawn with an x space step. b) The number of links between each one of the 8 generations. (Taken from Kirkby, 1976).

2.2. PREVIOUS WORK ON RIVER DELTAS SALINITY

Previous works involving salinity in river deltas are mainly site-specific. Most studies focus on the salt intrusion (SI) length and its response to changes in hydrodynamic forcing and human interferences. Some early studies on the salt wedge penetration are available for the Mississippi River Delta (Bates, 1953; Wright and Coleman, 1971, 1974), Danube (Bondar 1968) and Po (Nelson 1970; Dazzi and Tomasino, 1975) deltas. Studying the effects of effluent dynamics on morphological processes in the Mississippi Delta, Wright and Coleman (1974) observed that the salt wedge toe remains seaward of the delta's mouth bars when discharges are high but intrudes into the distributary channels during periods of low discharges. This seasonal effect was observed by Nelson (1970) in the Po delta as well. The salt wedge penetrates the delta during high tide and low river flow but is being flushed out by high flows when the tide is low.

Climate change and sea level rise (SLR) implications lead to an intensification of the research in this field in later decades. Many papers investigate the impact on salt intrusion for a number of potential sea level rise scenarios. This kind of work can be found in the Mekong (Tran and Likitdecharote 2010; Toan, 2014; Anh et al. 2015; Trieu and Phong, 2015; Anh *et al.*, 2018), Bangladesh (Bhuiyan and Dutta, 2012; Dasgupta *et al.*, 2015; Bricheno and Wolf, 2018; Bricheno et al. 2021), Yangtze (W. Chen *et al.*, 2016) Pearl River (Chen *et al.*, 2016) and Po (Bellafiore *et al.*, 2021) deltas. There is a consensus on the SLR negative effect that leads to higher salinity levels and increase of the salt intrusion length. In the Mekong, modelling studies revealed that a landward shift of SI caused by both SLR and upstream flow reduction should be expected in the future (Tran and Likitdecharote 2010; Trieu and Phong 2015). According to Ahn et al. (2018) this will also increase the flushing times in the area. Toan (2014) proposes a number of adaptive measures such as sluice gates and dyke systems to prevent SI. W.Chen

et al. (2016) modelled salinity in the Yangtze and found that the isohalines shift upstream nonlinearly with the SLR and detected a quadratic expression linking SLR and salinity. Bellafiore et al. (2021) used observations and numerical experiments to study SI in the Po Delta. They concluded that river discharge is more important for salinity than SLR unless land subsidence occurs at the same time. In addition, they identified advective and shear dispersive fluxes among the main drivers of salt intrusion. In the delta of Bangladesh, Dasgupta et al. (2015) reported an increase of high salinity areas after implementing a number of climate change scenarios. Bricheno and Wolf (2018) considered a number of SLR and river flow future scenarios in the Bangladesh and noticed a strong seasonal signal in the freshwater distribution due to the discharges high variability between monsoonal and dry periods. In a similar study, Bricheno et al. (2021) state that the impact from SLR is mitigated when it is balanced by stronger discharges. Seasonal variations on the salt intrusion and stratification are reported in the Pearl River delta too by Chen et al. (2016) who did numerical modelling to study the salinity response to potential SLR. Interestingly, their model results indicated a strengthening of the estuarine circulation by SLR.

Many authors have focused on variations of SI between high and low flow seasons and all agree on the fact that it becomes worse during dry periods. Nowacki et al. (2015) did a field study on a tidal river in the Mekong delta. Two campaigns during high and low flow discharges showed a transition of the system from tidal freshwater to partially mixed estuarine system respectively. Gugliotta et al. (2017) took field measurements in the Mekong that show salt intrusion extending further upstream during dry periods. Studying the SI in the Karnafouli Estuary which belongs to the Ganges-Brahmaputra-Meghna delta, Akter and Tanim (2021) saw an increase of salt intrusion in dry seasons too. They attribute it to nonlinear advection, low discharge, spring-neap interactions and tidal asymmetry. Increase of salt intrusion could be the result of other parameters in addition to seasonal flow variations and SLR. For example, Sherin et al. (2020) add depletion of groundwater level as an extra cause of SI increase. Furthermore, Liu et al. (2019) took observations in the Pearl River Delta and attributed increase of salt intrusion to uneven sand dredging, rising tides and changes of wind directions. Rising tides and north-easterly winds strengthen tidal dynamics and push saltwater further upstream. Finally, Hong et al. (2020) found in their modelling work for the Pearl River Delta that SLR will not only increase salinity but also stratification and tidal range. The rate of stratification increase due to SLR in the Pearl River delta is higher during low flow periods.

Other studies investigated the impact of anthropogenic factors on SI. Although not absolute, human structures seem to cause an increase of salinity in most cases. For instance, the field study of Wolanski et al. (1998) in the Mekong suggests that the planned construction of 100 hydroelectric dams and water diversions would increase salt intrusion. Using large data sets from the Mekong, Eslami et al. (2019) found that upstream hydro-infrastructure development increases both tidal amplitude and salinity due to reduced sediment supply and downstream sand mining. Sand dredging and excavations in the Pearl River Delta result in a decrease of the upstream width-depth channels ratio, a decrease of river discharge and increase of salt intrusion. Hu and Ping (2009) modelled the impact of jetties and groines constructed in the Yangtze and found that these result in an enhancement of salt intrusion. For the same delta, Dai et al. (2011) discovered that the abnormal salinity conditions during an extreme dry year occurred in partial coincidence with the second impoundment phase of the Three Gorges Dam (TGD). Xie et al. (2020) conducted a field experiment in the Yangtze and also detected an increase of salinity because of river discharge decrease caused by the TGD. However, the operation of the TGD allows water storage which can be released during the dry seasons shortening significantly the periods with undrinkable water in this region (Chen et al; 2016). In the Mississippi delta, a number of river diversions have been made for wetland restoration. Lane et al. (2007) studied the impact of

river diversions and suggested that salt water intrusion could be controlled with a proper management of discharge structures. They found that discharges from the river diversion greatly affected salinity, with the large spring pulses often causing the entire estuary to become fresh for a short period of time. Das et al. (2012) saw that the effect on salinity differs locally. For example, areas closer to coastal sections don't present significant changes of salinity due to the stronger marine influence. With the Mississippi delta as an example, White et al. (2019) simulated multi-decadal changes in estuarine hydrodynamics under assumed sea-level rise scenarios. Their conclusion was that the negative effect of SLR on salinity could be offset by appropriate river diversions.

Some studies look on the salinity intrusion in mega deltas such as the Ganges-Brahmaputra-Megna or the Pearl River delta. Very often, authors follow a common approach which is to focus into a part only and not the entire delta. This may include a number of the delta's branches. Therefore, the limits between an estuarine and a delta study might be obscure sometimes. Gong and Shen (2011) investigated the response of salinity intrusion to changes in river discharge and tidal mixing in the Modaomen Estuary which includes a number of the more downstream branches in the Pearl River Delta. Using a numerical modelling system with nested grids, the authors observed asymmetries of the salt intrusion response to changes in river discharge and tidal mixing which are developed because the time rate of salt intrusion increase during decreasing flows is smaller than that of salt intrusion decrease during increasing flows. Through a field survey for the Modaomen Estuary, Gong et al. (2014) discovered differences between advective and tidal salt fluxes along the estuary. The authors found that both kind of fluxes are important during neap while the advective flux is more important during the spring tides. Liu et al. (2017) also investigated salt intrusion in the Modaomen by coupling 1D-3D modelling. Their results suggest that the effects of tides and river discharge on the salt intrusion length can be expressed through a regression function. Gong et al. (2013) looked at the salinity intrusion in another Estuary (Huangmaohai) included in the Pearl River Delta. In this case, differences in the salt transport pattern between diurnal and semi-diurnal tides were observed with the latter ones resulting in weaker salt intrusion. More recently, Gong et al. (2018) investigated the effects of winds and waves on salt intrusion in the Pearl River. Local and remote winds strengthen SI while the waves decrease it by increasing mixing. In addition, Shen et al. (2018) simulated the impact of coastal reclamation in the Pearl River delta and found that this causes an increase of salinity because of impeded flow and decreased wave heights in the area.

Akter and Tanim (2021) studied the Karnafouli Estuary that belongs to the Ganges-Brahmaputra-Meghna deltaic system. They found that the salt intrusion length is related with river discharges through a power law equation with an exponent equal to -0.64. Likewise, Nguyen and Tanaka (2007) investigated the effect of morphology on the salinity distribution in the Dihn An estuary which is a very large branch in the Mekong delta. Implementing a three-dimensional model they discovered that changes in estuarine morphology can affect salinity intrusion. River mouth width is found to be directly proportional to the averaged salinity concentration. Nguyen and Savenije (2006) tested the applicability in multichannel systems such as the Mekong delta of analytical equations developed by Savenije (2005) that predicts salt intrusion based on channel topography, river discharge and tidal data. Later, Nguyen et al. (2008) proved that it is possible to estimate the freshwater distribution over branches of a multi-channel estuary using the theoretical model by Savenije (2005) in combination with salinity measurements.

Finally, notable is the work that has been done in the Po delta which is a complex system of interconnected bodies such as river branches, lagoons and salt marshes. It reveals the effect on salinity due to water exchange between different water bodies. Maicu et al. (2018) investigated the salinity levels in the various lagoons of the Po delta. They found that the salinity can be low in lagoons that

have multiple connections with the river branches or have little exchange with sea water. On the contrary, the salinity is high in lagoons with little connection with the river network and have stronger marine influence. Bellafiore et al. (2021) analysed data acquired from stations in the Po delta and confirmed these conclusions by adding that the tide modulates the variability in the lagoons.

2.3 REASONING FOR IDEALIZATION

The majority of the cited papers in the previous section is quite interesting and enlightening and offers useful knowledge on the salt intrusion response to changes of the hydrodynamic forcing and human interventions. Some general conclusions can be extracted such as the negative effect of SLR, the strengthening of SI during dry seasons or the asymmetric response to increasing and decreasing flows. However, these papers concern studies that are site-specific. Therefore, their results have mainly a local interest and may lack universality. The focus of each paper depends on the local characteristics. For example, studies in the Yangtze delta focus inevitably on the TGD impact as those for the Mississippi delta take into consideration a number of river diversions present in the area. Similarly, the work on the Bangladesh delta concentrates on the high seasonality due to the monsoons and SLR effects because of frequent inundation. In addition, the relationship and interactions between forcing factors in each system and their per se effect on salinity is difficult to identify in a real complex system where all these parameters are intertwined to each other. There is a need to work in a more simplified approach to detect this effect. This should be possible through idealization. So far, there is a lack of idealized studies in the bibliography. These are needed for two reasons. First to derive conclusions with some universality that could refer to deltas of similar hydrodynamic conditions and secondly to investigate deeper the effect of certain parameters isolated from other influences. The present project endeavours to fill this gap and go beyond a simple illustration of salinity fields under various hydrodynamic forcing.

The reasoning for the need of idealized studies lies on the difficulty to distinguish the interconnection between the many physical variables involved in a complex real system and isolate their effect on the physical phenomenon. The analysis of complex real cases is done usually through numerical modelling. The focus is mostly on the calibration and validation of these models based on field data and measurements in order to be used as predictive tools of external variables effects. These may include natural impact (e.g. climate change) or human interventions (e.g. engineering works). However, this sets limitations on the level of understanding that these models can safely provide to us on the fundamental mechanisms of the under study natural phenomenon.

In view of that, an alternative approach is necessary that eases the complexity of a real case. This can be done by studying the effect of an internal variable in the same system isolated from other parameters that are usually entangled with it. Therefore, idealization offers the opportunity of a better physical insight because it reduces the level of complexity. The use of idealized models aims to reveal the direct impact of external forcing factors in a system's variable separately for each one of them. This is very useful to know for the design of solutions to avert this impact per case which is to what this study aspires to contribute. However, an idealized approach can have several limitations if it is used to interpret conditions in a real system. These are further discussed in section 7.1.

2.4 AIMS/OBJECTIVE

This project studies the topic of salt intrusion in deltaic systems. It is a topic that has been addressed adequately enough already for estuaries where a vast literature is available. However, it is not certain yet how previous research findings and conclusions for estuaries relate to channelized networks and how the differences in topography and geometry between the two systems affect these conclusions. This project investigates the salinity response to changes in hydrodynamic forcing in river deltas and compares results with what is known from estuaries. The approach of idealization is adapted and its efficiency on studying river deltas is tested. The appropriateness and adequacy of idealized models to provide plausible explanations on the effect of a parameter in salinity distribution when this cannot be distinguished in real models is investigated. The lack of idealized studies has been identified in the literature with the majority of studies having a site-specific focus and interest. Idealized modelling is chosen here to fill this gap and provide if possible 1) conclusions with some universality, 2) a better understanding of the physical processes and 3) the effect of various parameters on salinity isolated from other influences. In addition, it is attempted to correlate salinity with delta's network and extract simple parameterizations and solutions. The ultimate goal is to come up with conclusions from which the society may benefit through the development of prognostic/diagnostic tools that could help for the design of a policy and solutions (technical or not) against salinization. With this in mind, the possibility of establishing longer-lasting fresher water conditions in deltas by better management of existing water resources than seeking for additional ones is investigated.

Overall, the modelling results analysis aims to 1) Increase our understanding on salinity's response to external forcing in channelized networks, 2) achieve qualitative and quantitative salinity parameterizations that could act as predictive tools and 3) investigate the effect of hydrographs shape on salinity while seeking better water management policy.

3. METHODS

Numerical modelling was carried out using the Delft3D modelling suite (Deltares, 2013). Delft3D comprises modules designed to carry out simulations for flows, sediment transport, waves, water quality and morphological processes. In particular, the Delft3D-FLOW module -implemented in this case- solves the Navier-Stokes equations for an incompressible fluid under the shallow water and Boussinesq assumptions. A detailed description of the Delft3D-FLOW governing equations is provided in Lesser et al. 2004, Van der Wegen and Roelvink (2008) and the user manual by Deltares (2013). Delft3D is selected in this study because it is a widely used and well-established software that has been implemented successfully in similar applications like the modelling of river deltas, fresh water discharges in bays, stratified density flows and salt intrusion problems (de Nijs and Pietrzak , 2012; Hu & Ding, 2009; Elhakeem &Elshorbagy, 2013; Martyr-Koller et al., 2017). It has several advantages being an open-source software easily accessible with the option of both structured and unstructured meshes and is capable of 3D simulations of ocean basins, coastal seas and rivers, etc. (Lesser, 2004). The model variables are arranged in a staggered grid (Arakawa C-grid) as indicated in Figure 12A and B. Water level (ζ) and density (ρ) are defined in the centre of the cell. The flow velocity components (u,v,w) are perpendicular to the grid cell face. Figure 12C shows a schematic diagram with the setup of the x, y and z coordinates in the Delft3D model.

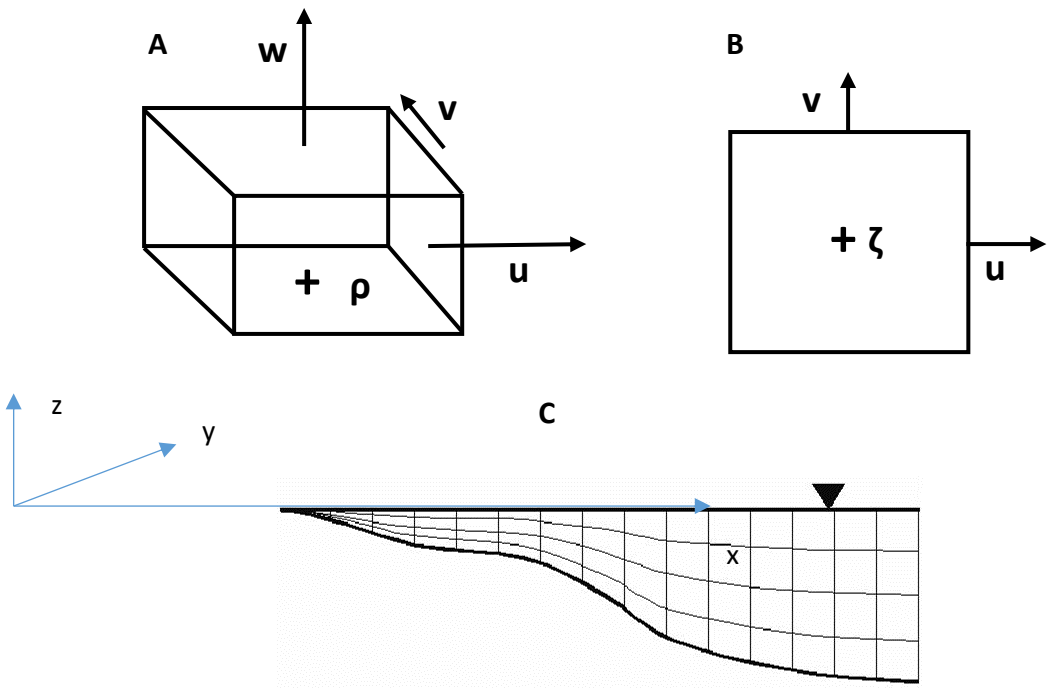

Figure 12 Variable arrangement in a staggered grid in Delft3D, 3D (A) and plan (B) view. C) The orientation of the x, y ,z coordinates in Delft3D

In this project, it is decided to simulate the changes of spatiotemporal salinity distribution in a delta with similar and realistic physical features to natural systems but with no intention to reproduce any specific real bathymetry. The goal is to avoid any comparison with site-specific cases so that results and conclusions are more generic. Therefore, the first step is to build an idealized delta configuration that will be used for the simulations with salinity. The choice of an idealized approach is further discussed in sections 2.3 and 7.1. The idealized delta is built through a 2D morphological simulation. The setup of the simulation must ensure that the idealized delta morphology is realistic and close to what is found in nature as much as possible.

A real delta morphology is determined by hydrodynamic forcing (Galloway, 1975) and sediment properties (Orton and Reading, 1993). Authors have investigated the effects on morphology from river discharge (Edmonds *et al.*, 2010; Leonardi et al. 2015), tides (Leonardi *et al.*, 2013; 2015; Hoitink and Jay, 2016; Hoitink *et al.*, 2017; Nienhuis et al. 2018;2020) and waves (Jerolmack and Swenson, 2007; Nardin and Fagherazzi, 2012; Nardin *et al.*, 2013;Nienhuis et al. 2020; Liu et al. 2020) while others focused on the factors affecting distributary networks range and patterns (Jerolmack and Swenson, 2007; Syvitski and Saito, 2007; Kleinhans *et al.*, 2008; Geleynse *et al.*, 2010). The role of sediment properties on deltas' morphology is also important and has been assessed in a number of modelling studies (Edmonds and Slingerland 2010; Geleynse *et al.*, 2011; Caldwell and Edmonds, 2014; Burpee *et al.*, 2015; Liu *et al.*, 2020) that managed to identify typical delta configurations for various grain sizes, sediment types and composition and river discharges. Edmonds and Slingerland (2010) carried out a number of experiments in Delft3D to investigate the effect of sediment cohesion on delta morphology. They setup 2D simulations in a rectangular grid and modelled the development of delta morphology under the influence of a constant river discharge flowing in a water basin through a rectangular channel that carries sediments. By modifying each time parameters such as the median grain size and sediment discharges for cohesive and non-cohesive material, they found that highly cohesive sediments tend to form bird's-foot deltas while fan-like deltas are developed with less cohesive material. Following the same concept, Caldwell and Edmonds (2014) investigated the effect on morphology of sediment properties such as median, standard deviation, skewness and percent cohesive sediments. They found that semi-circular delta planforms tend to store coarse-grained while fine-grained sediments usually correspond to more elongated shapes.

These very interesting results have been used to build our delta configurations. Using a rectangular grid, a water basin is considered with a channel of certain length and width. The basin has initially a uniform bathymetry. A constant river discharge is implemented carrying sediments of both cohesive and non-cohesive material. A multi-channel bathymetry is created then through sediments deposition and erosion. Sediment parameters are determined after a sensitivity analysis based on the findings from the experiments of Edmonds and Slingerland (2010) and Caldwell and Edmonds (2014). After this, the model is converted to a 3D version to include salinity. Spin-up simulations are first conducted to develop initial conditions for salinity.

With this method, two idealized models with similar but different delta configurations were built to study the salinity's response to changes in hydrodynamic forcing. The first model was designed to simulate salinity in a river dominated delta (chapter 4). The second model was setup for simulations including tidal forcing (chapter 5) and various river flow distributions (chapter 6).This chapter provides the setup of the morphological and the spin-up simulations for these two idealized models.

3.1. MORPHOLOGICAL SIMULATIONS SETUP

3.1.1. First Model Version Setup

The first model has a structured and rectangular grid that covers an area of 16 km^2 (Figure 13A). The grid resolution is 20 m in both X and Y directions but reduces to 10 m in the middle of the domain in the range of ordinates that include the rectangular river inlet to increase accuracy. The inlet is set at the west boundary and is 400 m long and 200 m wide. The grid cells between the inlet's side lines and the model's lateral boundaries are inactive.

Initial conditions and setting parameters

The model is initiated with no surface elevation throughout the domain. A uniform bathymetry is introduced of 2.5 m depth everywhere. The bed subsurface is erodible and has initially a 5 m sediments layer thickness everywhere. The coast on the west boundary is non-erodible and its width

is equal to the inlet's length (400 m). The grid resolution is such that allows the use of the default Delft3D values for horizontal viscosity/diffusivity equal to 1 m^2/s and 10 m^2/s respectively. A uniform bottom roughness is considered with a Chezy coefficient equal to 45 $m^{1/2}/s$. A numerical scheme denoted as Cyclic method (Stelling and Leendertse 1992) is implemented based on an implicit scheme that does not impose time restrictions. For computational efficiency, the time step is set equal to 30 seconds. To speed up the morphological processes, a morphological factor equal to 70 is introduced in the model.

Boundary conditions

Zero gradient water level (Neumann condition) is prescribed at the lateral boundaries. A constant surface water elevation is imposed at the offshore boundary. No sediment input is considered at the boundaries. The model is forced with a steady river discharge equal to 900 m^3/s. The riverine input carries into the basin equilibrium concentrations of a cohesive and a non-cohesive sediment fraction. Both fractions have a concentration of 0.15 kg/m^3. This value is chosen based on the experiments of Edmonds and Slingerland (2010) in order to obtain a fan-like delta. The 2D model calculates the suspended sediment transport through the depth-averaged version of the advection-diffusion equation:

$$\frac{\vartheta C}{\vartheta t} + \frac{\vartheta u_x C}{\vartheta x} + \frac{\vartheta u_y C}{\vartheta y} + \frac{\vartheta (u_z - w_s) C}{\vartheta z} = D_x \frac{\vartheta^2 C}{\vartheta x^2} + D_y \frac{\vartheta^2 C}{\vartheta y^2} + D_z \frac{\vartheta^2 C}{\vartheta z^2} \quad (6)$$

C is the concentration of each sediment fraction, u_x, u_y, u_z are the x-y and z directed flow velocities, w_s is the settling velocity and D_x, D_y, D_z are the directional eddy diffusivities. During the simulation, bed erosion and sedimentation occurs throughout the domain under the influence of the river discharge. The model is stopped after 30 days of simulation time when a fan-like delta has been developed with the typical meandering and channels curvature (Figure 13B). Table 1 lists collectively all the user-defined parameters and coefficients introduced in the model.

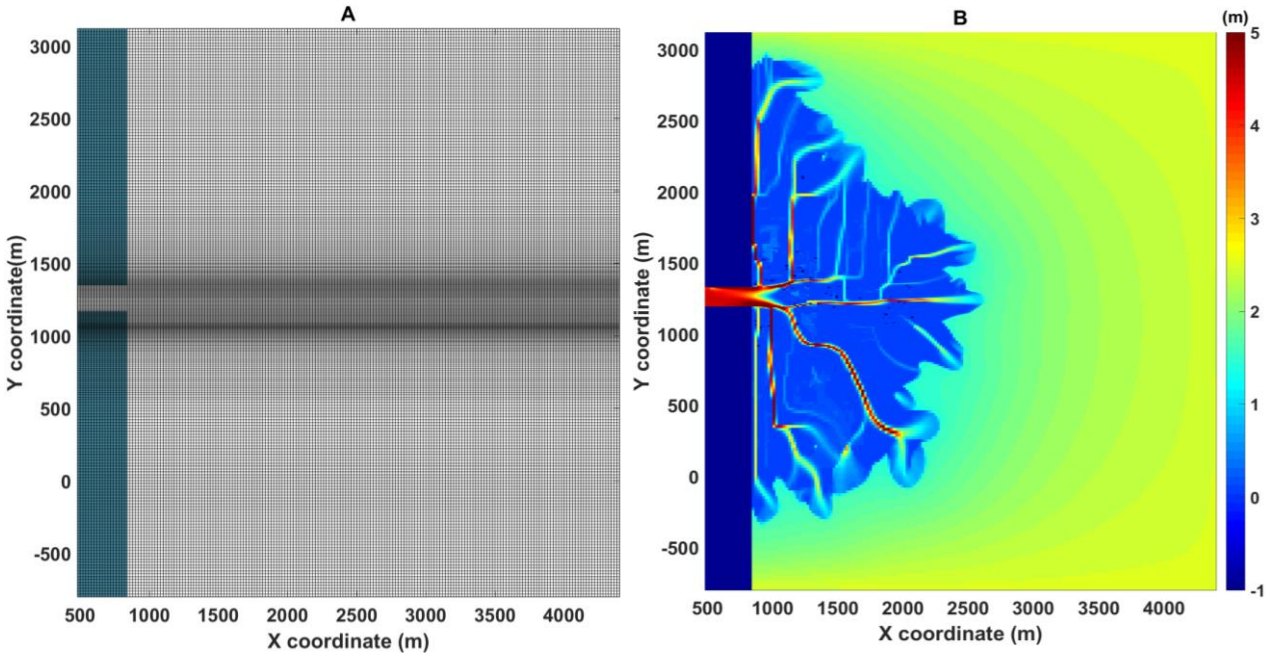

Figure 13 First model A) grid and B) bathymetry. The non-erodible coast is represented by grey colour in A and dark blue in B. Negative values in B indicate areas above the sea level.

Table 1 User-defined physical and sediment parameters introduced in the first model version

Parameter	
D_{50} for sand	500 µm
Density for hindered settling	1600 kg/m^3
Specific density for sediments	2650 kg/m^3
Initial sediment layer thickness at bed	5 m
Critical bed shear stress for erosion	1 N/m^2
Critical bed shear stress for sedimentation	1000 N/m^2
Chezy coefficient	45 m$^{1/2}$/s
Horizontal diffusion	10 m^2/s
Horizontal viscosity	1 m^2/s
Cohesive sediment input	0.15 kg/m^3
Non-cohesive sediment input	0.15 kg/m^3
Morphological factor	70
Time step	30 seconds

3.1.2. Second Model Version Setup

The delta configuration of the first model is used for simulating the salinity in a system with no influence from tides and/or waves. The setup follows closely that of other morphological modelling studies mentioned above. However, the critical difference between the present and those studies is that this model is built to be eventually used for simulating baroclinic flows. In this case, larger dimensions would be preferable for several reasons. The model needs to include other bathymetric features such as a pro-delta area extending beyond the ends of the channels and a much deeper offshore area to represent the sea. The goal is to monitor any bathymetric effects on the salinity distribution knowing that these are usually important. In addition, it is required to allow uninhibited the development of the offshore buoyant plume that is commonly present in studies including buoyancy. Therefore, the model needs to extend beyond the channels and to secure also enough space between the delta and the boundaries to preclude any impact on the salinity distribution. Finally, it is necessary to keep a certain distance between the offshore and the upstream boundary when tides are included so that the tide is attenuated before entering in the river channel.

With this in mind, the second model has a structured and rectangular grid that covers an area of 20 km x 22 km (Figure 14A). This is about 27 times the area of the first model. Larger dimensions force an increase of the grid resolution that in this case varies from 50 m to 200 m in the X direction and between 20 m and 100 m in the Y direction of a Cartesian co-ordinate system. This increase can have an impact on channels meandering because the grid discretization is an important factor when developing a delta morphology but this is discussed in more detail in section 7.1. As in the first model, the resolution is finer close to the river mouth (Figure 14B). The river channel located at the west boundary is 1.3 km long and 380 m wide.

Initial conditions and setting parameters

The rationale behind the two morphological simulations is similar and so many of the setting parameters remain the same in this second version. The model is initiated with no surface elevation throughout the domain. The initial bathymetry is uniform with a depth equal to 3 m up to 10 km from the west (river) boundary. After this point, a bed slope of 0.5° is imposed and the water depth reaches 30 m at the offshore boundary. The horizontal and vertical diffusion/viscosity and the roughness coefficients do not change from the previous case. All the user-defined setting parameters are listed in Table 2. The morphological processes are speeded up by a factor of 175 following the work of Edmonds *et al.*(2010) and Caldwell and Edmonds (2014).

Boundary conditions

The model is forced by an upstream steady river discharge equal to 3000 m^3/s. The bed's subsurface sediment layer thickness remains as before (5 m) but the larger channel dimensions require also a larger river discharge to be able to erode the bed in long distances from the mouth. As a result, the time step decreases to 12 seconds in this case. The lateral and offshore boundary conditions prescribed in the first model version apply in this second case as well.

Sediment settings

The sediment input and many of the sediment parameters are different in this case compared to the previous one. Several changes are required in order to create a larger and elongated delta in this larger model. Critical factors affecting a delta's shape are the median grain size (D_{50}), sediment cohesion and critical shear stress for erosion (Edmonds *et al.*(2010); Caldwell and Edmonds (2014) ;Burpee *et al.* (2015)). These parameters are determined after a sensitivity analysis with the purpose of identifying the appropriate values to result in a fan-like delta shape but elongated so that it covers as much as possible a larger area. The median grain size D_{50} is decreased to 225 µm because it is known that less coarse material results in more elongated deltas (Caldwell and Edmonds 2014). Sediment concentration is increased in this case. However, the cohesive input is chosen to be much higher than the non-cohesive (0.5 kg/m^3 and 0.2 kg/m^3 respectively) because higher cohesion tends to transform the delta from a fan-like to a bird's foot shape (Edmonds and Slingerland 2010) and thus these become larger. Despite the increases and decreases of several parameters (Table 2), these remain within ranges that do retain a fan delta shape as much as possible. The selection of the setting parameters and the factors for delta morphology are further discussed in chapter 7.1.

Bathymetry output

With these input parameters and forcing, the model ran for 34 days until the bathymetry in Figure 15A was developed. It can be seen that the multichannel system covers an area of approximately 4.8 km x 8 km (Figure 15B) instead of 1.5 km x 3.2 km in the first model version. There is more than 4 km space between the channels end and the two lateral boundaries. The pro-delta area can be distinguished by a change in the depth gradient about 6 km far from the upstream river boundary. Its length is about 3 km and ends in a distance of 10 km from the upstream boundary where the bed slope has been imposed. Beyond that point, the depth increases continuously reaching 30 m at the offshore boundary. This bathymetry is then introduced as a bottom boundary condition in the simulations with salinity.

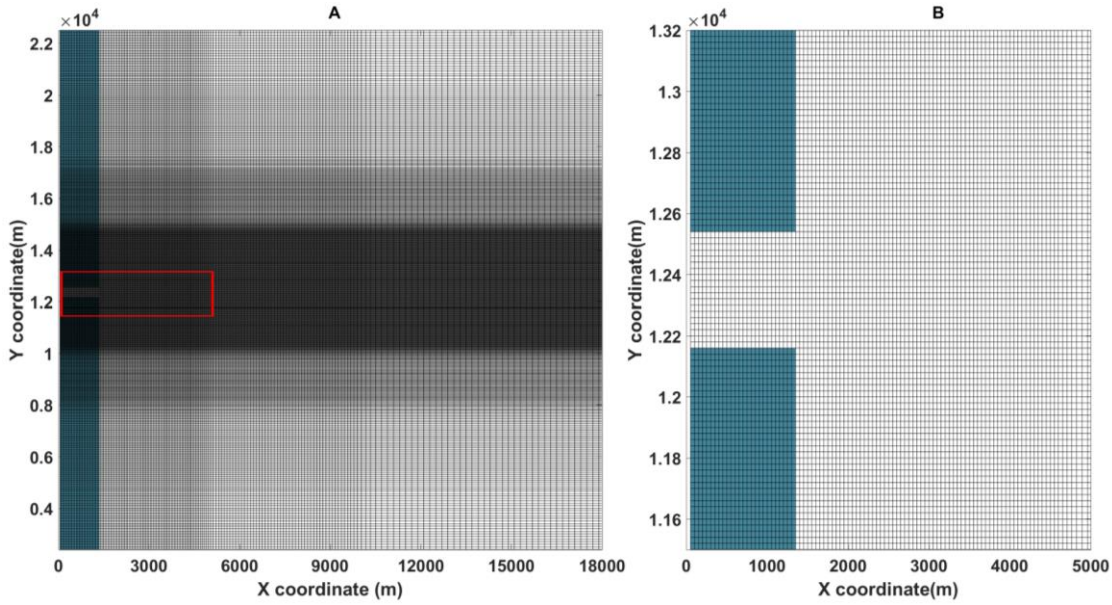

Figure 14 A) The gird of the large model version. B) A zoom in the red box area of panel A so that the resolution around the river inlet is better visualized. Inactive cells are represented by grey colour.

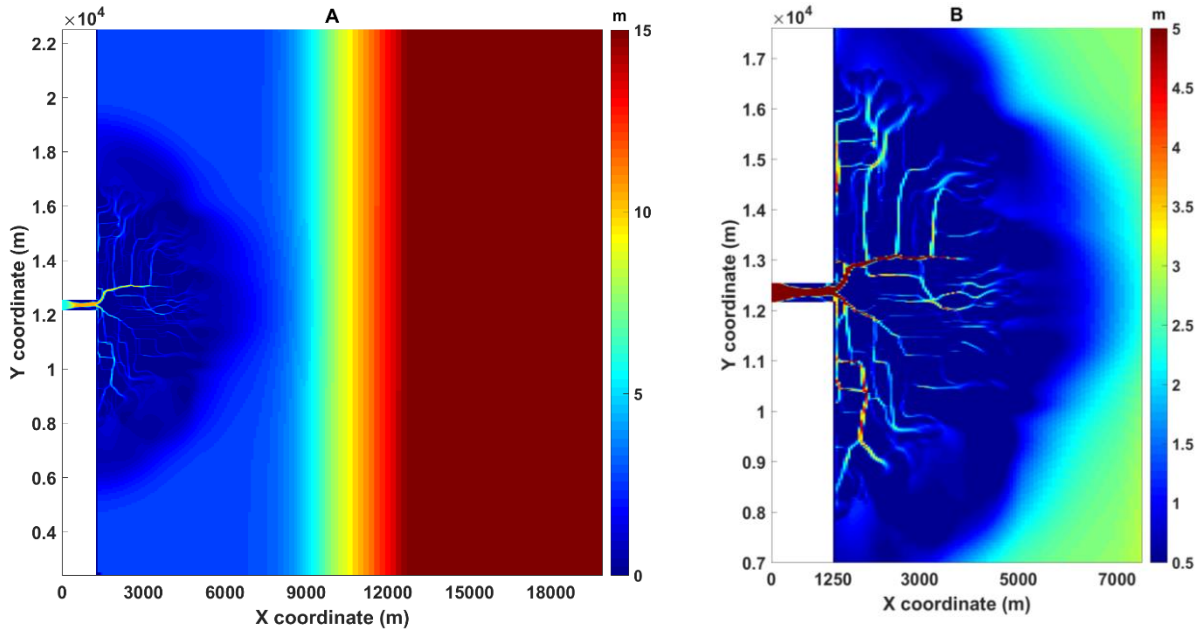

Figure 15 A) The second model version bathymetry. The depth starts to increase at X =10km with a 0.5^0 slope. The depth at the offshore boundary is 30m. B) Zoom in the delta bathymetry.

Table 2 Physical and sediment parameters introduced in the large model version

Parameter	
D_{50} for sand	225μm
Density for hindered settling	1600 kg/m^3
Specific density for sediments	2650 kg/m^3
Initial sediment layer thickness at bed	5 m
Critical bed shear stress for erosion	0.5 N/m^2
Critical bed shear stress for sedimentation	1000 N/m^2
Chezy coefficient	45 m$^{1/2}$/s
Horizontal diffusion	10 m^2/s
Horizontal viscosity	1 m^2/s
Cohesive sediment input	0.5 kg/m^3
Non-cohesive sediment input	0.2 kg/m^3
Morphological factor	175
Time step	12 seconds

3.2. SPIN-UP SALINITY SIMULATIONS SETUP

Simulations including salinity need to be three-dimensional to capture the vertical density variations and its effect on the flow (section 2.1.1). Therefore, the bathymetry output of section 3.1 is introduced in a 3D model each time. The vertical resolution is defined after a sensitivity analysis showing that there is little impact on the results and conclusions of this study from the number of layers. This is probably due to the shallowness of the area of interest delineated by the channels borders and ends. The number of layers is also restricted by computational resources and cost efficiency considering that the simulations time with salinity is one year in each case and that usually requires a substantial amount of time to be completed. In the first model, four sigma layers are implemented. The second model is deeper and so the vertical resolution is increased to eight sigma layers. Bed elevation changes are deactivated and the bathymetry remains constant during the simulation since this consider time scales smaller than those required for morphological changes. No sediment input is introduced. This is a design decision made considering that the focus of this research is on the salinity variations due to changes in the hydrodynamic forcing independent of morphological effects. Coupling with sediments would affect both sediment transport and density stratification but the interplay between them goes beyond the scope of this project (see also section 7.1).

Initial conditions

The spin-up simulations start with a uniform salinity of 30 PSU prescribed everywhere. This is a value close to the typical offshore salinity in the Mississippi Delta (Georgiou et. al 2017). The horizontal diffusion, viscosity and bottom roughness coefficients remain the same with those in the morphological simulations. The vertical diffusion in this 3D model version is resolved by the κ-ε turbulence closure model. In this second order model, the turbulent kinetic energy κ and dissipation rate ε are calculated by transport equations and the mixing length L is computed by this equation:

$$L = C_D \frac{k\sqrt{k}}{\varepsilon} \qquad (7)$$

C_D is a constant relating mixing length. An advantage of the κ-ε model is that stratification is taken into account by the buoyancy terms in the transport equations for κ and ε (Deltares 2013). In the k-ε turbulence closure model both the turbulent energy k and the dissipation ε are produced by production terms representing shear stresses at the bed, surface, and in the flow (Lesser et al., 2004). See the Delft3D-FLOW manual (Deltares, 2013) for a full description of this turbulence model's equations. The κ-ε turbulence closure model is the default option in DELFT3D and it was chosen because it has been successfully implemented for other similar works (de Nijs and Pietrzak, 2012; Martyr-Koller *et al.*, 2017). The results indicated that the physical mechanisms and dynamics of salt transport are accurately reproduced and so it is considered that the vertical resolution and turbulence closure model are suitable for this case.

In the simulations with salinity, the time step is increased to 1 minute in the first and 30 seconds to the second model version. This is done to decrease the computation time of the much longer simulation period (one year) when salinity is included. The use of an implicit scheme (Cyclic method, see section 3.1.1) does not impose any time restrictions and this change does not affect the model's stability.

Boundary conditions

The spin-up simulation in the first model assumes a constant surface water level elevation at the offshore boundary as in the morphological simulation. However, baroclinic pressure terms may lead to strange circulation along the open boundaries (Deltares 2013). This requires changes at the lateral boundaries in order to establish the right flow circulation. Therefore, the Neumann is replaced by a Riemann invariant (see also section 7.1 for more details on this aspect). The salinity at the boundaries is 30 PSU except for the river boundary where the water is fresh (0 PSU). The salt transport is calculated by the 3D advection-diffusion equation for salinity (S):

$$\frac{\partial S}{\partial t} + u\frac{\partial S}{\partial x} + v\frac{\partial S}{\partial y} + w\frac{\partial S}{\partial z} = K_h\frac{\partial^2 S}{\partial x^2} + K_h\frac{\partial^2 S}{\partial y^2} + K_z\frac{\partial^2 S}{\partial z^2} + Ss \qquad (8)$$

K_h , K_z are the horizontal and vertical diffusion coefficients respectively and Ss are source and sink terms.

The model is forced by a constant river discharge (see chapter 4) and for a period of 30 days till a dynamic equilibrium for salinity is achieved. The setup of the spin-up simulations done with the second model is the same. However, a water level equal to the tidal amplitude is prescribed at the offshore boundary for the simulations where tidal forcing is included. Spin-up simulations including tides required longer periods (45 days) to reach quasi-state conditions.

3.3. DATA SCALING

The size of the idealized delta configuration is subject to limitations due to grid resolution, computational efficiency and model stability. As a result, the idealized models include delta configurations that have dimensions much smaller than real ones. For example, the Po Delta that is a relatively small delta covers an area of 685 km^2 (Maicu et al. 2018). This is almost 18 times the delta area of the second model. Inevitably, this sets limitations on the level of forcing parameters like river discharge and tides. The hydrodynamic data in the simulations derives from real deltas but has to be scaled down so that it fits to the model and does not threaten its stability. This is not an unusual technique for idealized models and does not distort the physics of the problem under consideration

because the partial differential equations implemented in the model do not differ from those that would be considered in larger or real scales. In other words, the idealized approach offers the advantage of setting up simplified experiments on a smaller scale in favour of time and cost efficiency (see also section 7.1). On the other hand, it should be noted that even though scaling down is not harmful for the validity of the computations and conclusions, this is not a two way relationship. The idealized model results could not be directly scaled up with respect to a real case. This approach would not lead to safe conclusions. The idealized models are designed to provide answers on the relationship between two parameters but not on their magnitudes (see also section 7.1). Another important element is that magnitudes between the two simulations (morphological and salinity) are not necessarily equal and should not be compared or mixed up. These two simulations are designed for a different purpose each time. For instance, the river discharge implemented in the morphological simulation is on the order of O (10^3). This range is appropriate in this case because a very high discharge is necessary to build the delta. However, this range is not acceptable for the simulations with salinity. Considering the size of the delta, a river discharge of this magnitude would most likely impose freshwater conditions for much longer than expected time and much wider areas. Similarly, the implementation of a close to reality tidal amplitude in the idealized models could impose extreme saline conditions leading to unrealistic and unnatural results. The method of scaling then is very important and should always take into account such considerations.

In our simulations, the flow distribution available from real deltas is scaled down based on the ratio between inertia and gravity forces (Froude number). The Froude number is calculated considering the river cross-section of a real delta and the mean discharge of a certain year. Then a flow velocity for the idealized model is extracted by solving the Froude formula for the idealized delta's river cross-section. Likewise, the scaling of the tidal amplitudes implemented at the offshore boundary when tidal forcing is included is done based on the estuary number. The estuary number (or Canter-Cremers) is a dimensionless number used for the classification of estuaries that expresses the ratio between the amount of the fresh and saline water entering the estuary during the tidal period (Savenije 2005). The estuary number was computed for a number of deltas for which data were available. Then a mean flow is considered for the idealized model based on the scaled flow distribution and this is introduced in the estuary number equation which is solved with respect to the amplitude to get a value for the model. In this way, the ratio between freshwater and saline water volumes is kept equal between the idealized model and a selected real case even though the magnitudes are scaled down.

4. Investigation of spatial and temporal salinity distribution in a river dominated delta through idealized numerical modelling

Constantinos Matsoukis[1], Laurent O. Amoudry[2], Lucy Bricheno[2], Nicoletta Leonardi[1]

(1) University of Liverpool, School of Environmental Sciences, Department of Geography and Planning, Roxby Building, Chatham St., Liverpool L69 7ZT, UK

(2) National Oceanography Centre, Joseph Proudman Building, 6 Brownlow Street, Liverpool, Merseyside, L3 5DA, UK

Corresponding author: c.matsoukis@liverpool.ac.uk

This paper has been published in the Journal of Estuaries and Coasts on January 2021.

First Author Contribution: Conceptualization, Methodology, Software, Pre- and Post-processing, Visualisation, Formal analysis, Writing, Original draft and reviewed versions preparation.

ABSTRACT

The world's river deltas are increasingly vulnerable due to pressures from human activities and environmental change. In deltaic regions, the distribution of salinity controls the resourcing of fresh water for agriculture, aquaculture and human consumption; it also regulates the functioning of critical natural habitats. Despite numerous insightful studies, there are still significant uncertainties on the spatio-temporal patterns of salinity across deltaic systems. In particular, there is a need for a better understanding of the salinity distribution across deltas' channels and for simple predictive relationships linking salinity to deltas' characteristics and environmental conditions. We address this gap through idealized three-dimensional modelling of a typical river-dominated delta configuration and by investigating the relationship between salinity, river discharge and channels' bifurcation order. Model results are then compared with real data from the Mississippi River Delta. Results demonstrate the existence of simple one-dimensional and analytical relationships describing the salinity field in a delta. Salinity and river discharge are exponentially and negatively correlated. The Strahler-Horton method for stream labelling of the delta channels was implemented. It was discovered that salinity increases with decreasing stream order. These useful relationships between salinity and deltas' bulk features and geometry might be applied to real case scenarios to support the investigation of deltas vulnerability to environmental change and the management of deltaic ecosystems.

Keywords: salinity, salt intrusion, river deltas, numerical modelling, idealized river delta models

ACKNOWLEDGEMENTS

The work contained in this paper contains work conducted during a PhD study supported by the Natural Environment Research Council (NERC) EAO Doctoral Training Partnership whose support is gratefully acknowledged. Grant ref NE/L002469/1. Funding support from the School of Environmental Sciences, University of Liverpool are also gratefully acknowledged.

1. INTRODUCTION

Worldwide, half a billion people are currently dependant on deltaic ecosystems. Deltaic deposits are highly fertile regions, desirable sites to perform rural and agricultural activities as well as the centre of other numerous anthropogenic activities. River deltas are extremely vulnerable to both anthropogenic and natural changes such as sea level rise, variations in riverine flow, and changes in

land-use practices (e.g., Paola et al., 2011; Syvitski et al., 2009; Fagherazzi et al., 2015). Continuous efforts are thus required to support the management and sustainability of these delicate ecosystems.

A possible direct consequence of environmental change is an increased salinity in deltaic regions. Increased salinity concentrations can have a severe impact on the anthropogenic activities taking place in river deltas and cause ecological degradation. For instance, increased salinity levels can damage soil cultivation, decrease the quality and availability of water for irrigation and human consumption (Allison,1964; Smedema and Shiati,2002), cause harmful algal blooms (Rosen et al. ,2018), threaten livelihood, and compromise food security (Khanom 2016; Abedin et al., 2013). Increased salinity is currently endangering plant succession, wildlife, and fisheries dynamics in the Louisiana's river deltas (Mississippi, Atchafalaya, and Wax Lake Deltas) (Holm et al. , 2001), Ganges-Brahmaputra delta (Yang et al., 2005; Rahman et al., 2015; Karim et al., 1990; Mondal ,1997) and in the Mekong Delta (CGIAR,2016). Salinity distribution in coastal systems, including river deltas, depends on atmospheric, ocean and riverine forcing (Gong and Shen, 2011). When fresh water from the upstream river mixes with the oceanic water downstream, the density differences in the water column induce a gravitational circulation. The competition between river discharge and ocean forcing determines whether mixing or stratification will prevail at different time scales. In the case of a river dominated system, the river flow has a dominant influence on the salinity (Valle-Levinson and Wilson, 1994; Wong, 1995, Monismith et al. 2002).

Concerns over water resources policy are one of the consequences of impacts of environmental and anthropogenic changes on deltaic systems, such as increased salinity. There is therefore a need for developing simple prognostic methods and tools to support decision and policy making. Even though the salinity field in estuarine systems has been extensively studied, relatively few studies have focused on the spatiotemporal distribution of salinity in river dominated deltas. The relationship between salinity and river flow has been studied indirectly by examining either the time lag of estuarine responses to river forcing (Kranenburg, 1986; MacCready (1999, 2007); Chen et al., 2000; Hetland and Geyer 2004; Lerczak et al. , 2009; Chen 2015) or the salt intrusion response to river flow changes (Monismith et al. 2002; Bowen and Geyer 2003; Gong et al. ,2012). A direct negative correlation between salinity and river discharge has been demonstrated (e.g. Garvine et al., 1992; Denton and Sullivan, 1993; Wong et al., 1995; Petersen et al., 1996), but its applicability and validity have yet to be verified for deltaic systems. A major goal of the present study is to show that simple analytical solutions developed in the past to describe estuarine physics are also applicable to river-dominated deltas. A second objective is to support detection of delta areas at risk from salinization using a channel classification based on stream orders, which has yet to be applied to the specific problem of salt distribution in delta channel networks.

The classification of channels in river networks by stream order was first introduced by Horton (1932, 1945) and revised later by Strahler (1952). It is a powerful technique that sets a hierarchy in branching networks with many tributaries. Despite the existence and development of other schemes such as Scheidegger-Shreve, Milton-Oiller and STORET (Ranalli & Scheidegger 1968; Gleyzer et al. 2004), it is usually preferred in hydrology and geomorphology studies (e.g. Beer and Borgas 1993; Tarboton 1996; Dodds 2000;Cole and Wells 2003; Raff et al. 2003; Reis 2006) because of its simplicity (Smart 1968; Moussa 2009). For example, many authors find it as a useful technique to be incorporated to the geomorphologic instantaneous unit hydrograph (GIUH), (Gupta et al. 1980; Rosso 1984; Gupta and Mesa 1988; Rinaldo et al. 1995; Rodriguez et al. 2005; Kumar et al. 2007; Lee et al. 2008; Moussa 2009). The Strahler-Horton method has also been implemented in many different areas such as statistics (Kovchegov & Zaliapin 2017 and 2020; Yamamoto 2017), neuroscience (Pries &Secomb

2008), computer science (Kemp 1979;Devroye & Kruszewski 1994;Nebel 2000;Chunikhina 2018), biology (Borchert & Slade 1981) and social sciences (Arenas et al. 2004). In this work, an effort is done to adapt it for deltaic systems and test its application to the issue of salinization of delta channel networks. Such an approach can be advantageous for many reasons. River deltas are subjected to tremendous dynamic changes under the influence of natural and human factors and undergo alterations across a wide range of spatial and temporal scales (Zhang et al. 2015; Passalacqua 2017). By implementing a hierarchy scheme to the treelike structure of a delta, scale-dependence can be overcome (Albrecht & Car 2004; Phillips 2016). For example, the Strahler-Horton scheme can summarize spatial and temporal variabilities in river basins despite variations in size (Rodriguez-Iturbe & Rinaldo 2001). A complex natural system (i.e. a system that exhibits structural and functional modularity) is usually hierarchically organized (Wu & David 2002). River deltas display great complexity in channel network structure (Sendrowski & Passalacqua 2017). The set of nodes and links connecting the channels of a network is termed as connectivity (Passalacqua 2017). Connectivity can become important when studying the complexity and evolution of landscapes and/or the interaction between external drivers and system's variables (e.g.in this case, fresh water flow and salinity respectively) (Miller et al. 2012; Bracken et al. 2013; Sendrowski & Passalacqua 2017). This kind of analysis is considered a key element for water management decisions and hydrologic prediction (Western et al. 2001; Bracken et al. 2013; Passalacqua 2017). The stream order method that incorporates all these elements, can be thus extremely useful towards this direction.

In this study, we implement the DELFT3D modelling suite to numerically simulate hydrodynamics and the salinity field for an idealized river-dominated delta. The resulting model data are used to investigate and produce correlations between salinity and delta's features. Field data from the Mississippi river enable a qualitative comparison with the model results.

2. METHODS

DELFT3D (Deltares, 2013) comprises a series of modules to carry out hydrodynamic, morphological, and water quality simulations. DELFT3D-FLOW solves the Navier-Stokes equations for an incompressible flow under the shallow-water and Boussinesq assumptions. Scalar transport (e.g. salinity or temperature) is calculated following an advection-diffusion equation:

$$\frac{\partial S}{\partial t} + u\frac{\partial S}{\partial x} + v\frac{\partial S}{\partial y} + w\frac{\partial S}{\partial z} = K_h\frac{\partial^2 S}{\partial x^2} + K_h\frac{\partial^2 S}{\partial y^2} + K_z\frac{\partial^2 S}{\partial z^2} + Ss \qquad (1)$$

where K_h is the horizontal and K_z the vertical diffusion coefficient and Ss are source and sink terms.

In a 3D case, horizontal diffusion is resolved by the contribution of a 3D turbulence closure model and a user defined coefficient accounting for any unresolved horizontal mixing. In our model, this coefficient is constant and equal to its default value (10 m/s^2) securing the model stability. The selected κ-ε turbulence closure scheme is a two-equation turbulence closure model in which the viscosity (and thus diffusivity) are determined from the turbulent kinetic energy κ and turbulence dissipation rate ε each calculated from a transport equation. The vertical diffusion is exclusively resolved by the turbulence closure model.

The Equation of State calculates the density ρ as a function of temperature and salinity. By default, DELFT3D uses the UNESCO formulation (UNESCO,1981). DELFT3D has been successfully implemented in the past for several applications including the modelling of river deltas, fresh water discharges in bays, stratified density flows and salt intrusion problems (de Nijs and Pietrzak , 2012; Hu & Ding, 2009;

Elhakeem &Elshorbagy, 2013; Martyr-Koller et al., 2017). For more details on the numerical model, a detailed description of DELFT3D can be found in the manual (Deltares,2013).

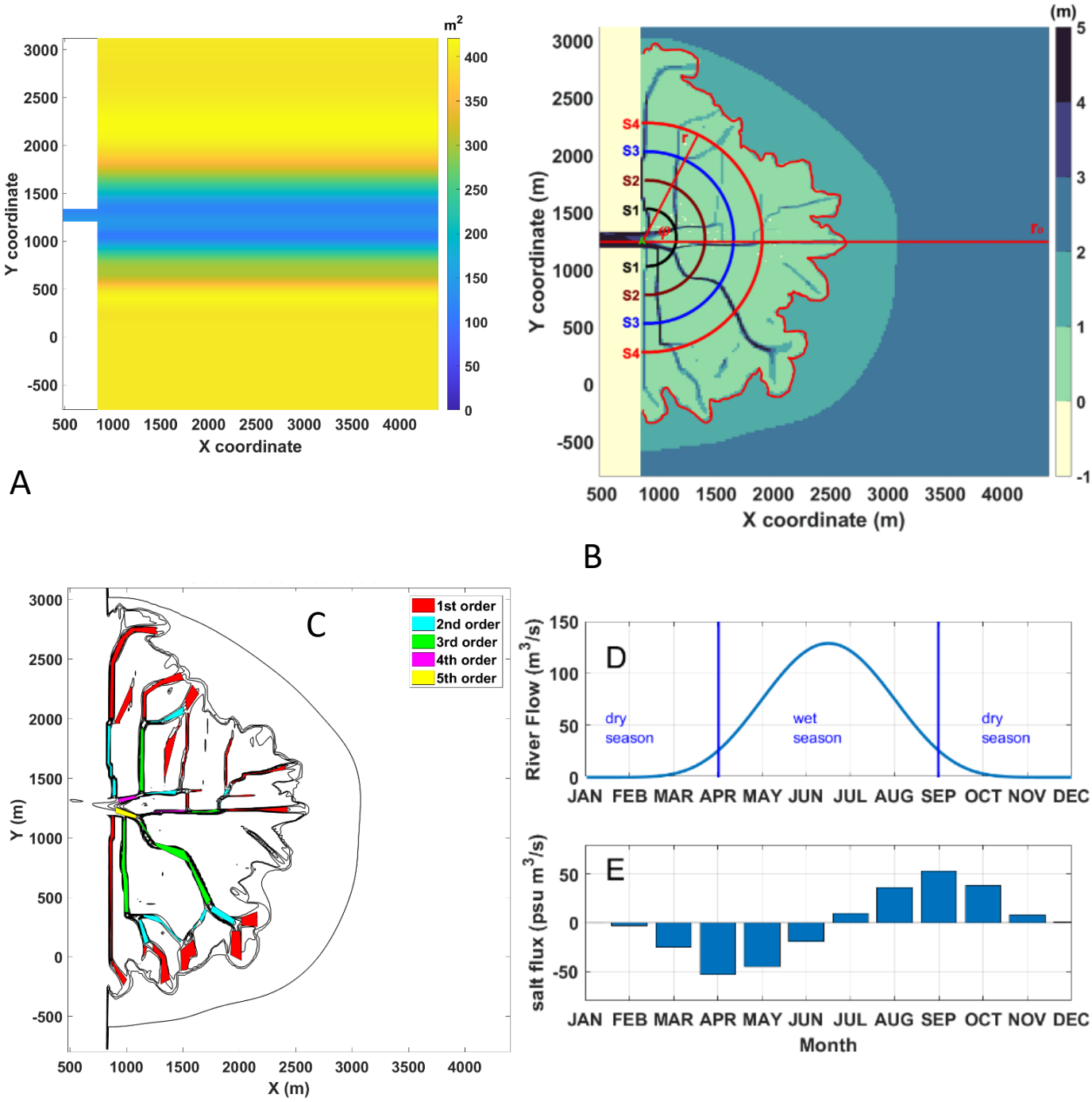

Figure 1A) Model grid. The colours indicate grid cell area. The grid resolution becomes finer in the vicinity of the river inlet. White colour indicates inactive grid cells. X and Y are the coordinates of a Cartesian reference system. B) Bathymetry of the idealized river delta. Negative values in white colour denote land (inactive grid cells).The red line delineates the border between the delta and the ocean. It is defined as the line connecting interdistributary areas between channels with no branches where they meet the sea. Results analysis is done for the area upstream of this borderline. Semicircles S1, S2, S3 and S4 mark the areas where the salinity averaging is done in section 3.3.3.. ϕ is the angle of the semicircles' radius r with the horizontal r_0 along the delta. A' is the common centre of the semicircles colormap (Thyng et al. 2016) C) A sketch with the Strahler-Horton number assigned at each delta channel. Colours represent different stream order number. The stream order number decreases downstream with each channels bifurcation. Channels with no branches are 1st stream order. D) The flow

hydrograph implemented in the model simulation. Vertical lines indicate the borders between the wet season and two dry seasons (one preceding and one succeeding). E) Monthly salt flux as calculated in section 3.1.

2.1 Model setup

2.1.1 Model bathymetric setup

A morphological simulation was initially conducted to create an idealized river delta configuration. The morphology was then "frozen" and maintained constant during the investigation of the salinity field. The model domain has a rectangular grid of 4 km by 4 km. The grid resolution is 20 m in both x and y directions. A finer resolution of 10 m is adapted close to the inlet area to improve accuracy (Figure 1A). The river inlet is 400 m long and 200 m wide. The riverine input used for the creation of the morphology included both cohesive and non-cohesive material in equal percentages. Sediment characteristics and grain sizes were chosen according to findings from morphological studies with idealized modelling (Edmonds and Slingerland ,2010; Caldwell and Edmonds ,2014) so that a semi-circular delta shape was produced accompanied by a high bifurcation order. For this morphological simulation, the model was forced by a constant flow discharge of 900 m^3/s. By setting a morphological factor equal to 70, the bathymetry in Figure B is obtained after a simulation period of 5 days. The created morphology was then introduced as the input bathymetry for the salinity simulations.

2.1.2 Salinity simulations setup and model initialization

Four sigma layers in the vertical direction were used for the simulation of the hydrodynamic and salinity field. A sensitivity test on the number of sigma layers was done by implementing the model with 6 and 8 layers. Indicative numerical results are included in Appendix B and show that the impact of increased vertical resolution is small, probably due to the very shallow nature of the delta, and does not alter the overall conclusions of the study. Further taking into account computational resources required for a full year of simulation, we considered 4 vertical layers sufficient in the present case.

The flow hydrograph for the idealised model is constructed based on real data from the Mississippi River Delta. An annual flow distribution with daily river discharges in the Mississippi is available for 2017 (usgs.gov website, station 07374000). The Mississippi 2017 hydrograph displays an approximate Gaussian distribution with a peak in May. To remove wiggles and irregular fluctuations the beta (B) function is implemented in order to get a new distribution. The B function is given as (Yue et al., 2002):

$$B\,(a,b) = \int_0^1 x^{a-1}\,(1-x)^{b-1}dx \qquad (2)$$

$$0<x<1\ ;\ a,\ b>0$$

where x is variable (the river discharge in this case) and a, b are parameters of the beta probability density function that determine the shape of the variable's distribution. The distribution becomes Gaussian when the parameters are equal. The value of the coefficients determines the sharpness of the hydrograph's peak which becomes sharper for high parameters values. However, this flow rate had to be scaled down to ensure the model's stability. For this reason, the Froude number for a Mississippi's trunk channel section is calculated. By keeping the Froude number equal between the idealized and the real case, a scaled annual flow distribution is worked out for the idealized model's river inlet section. Figure 1D shows the hydrograph implemented in the model. It is symmetric with a peak discharge between June and July and minimum values at the start and the end of the year. To note that the exact timing of the hydrograph within the calendar is arbitrary. The Gaussian function shape is desirable because of its simplicity. It provides a single high peak which allows easy distinction between wet and dry seasons. It might be easier then to detect correlations such as between the river discharge and salinity that would be difficult to discover when using a hydrograph of a more complicated shape. Nevertheless, it can be easily converted to other simple statistical distributions.

Apart from the Mississippi river delta, normal flow distributions can be found in other real cases. The Yangtze River Delta (Chen et al.2001; Lai et al.2014) and the Swan Estuary in Australia (Kurup et al., 1998; Stephens and Imberger, 1996) are examples of water systems demonstrating annual hydrographs often following normal distribution. A spin-up simulation is setup prior to the main one to get initial conditions. The minimum river discharge of Figure 1D hydrograph is implemented in the model with the salinity set equal to 30PSU which is the typical offshore salinity in the Mississippi River Delta. A spin-up run for a period of one month was sufficient to achieve a salinity dynamic equilibrium under the influence of the minimum river discharge that remains constant in the model. The output is introduced as input for salinity initial conditions to the one year simulation.

2.1.3 Boundary conditions

A constant water level is prescribed at the offshore boundary as the main focus of our model was to investigate the discharge-salinity relationship and the relationship between salinity and channel order for a river dominated case. For simplicity, the impact of tides and waves has been thus neglected. The offshore boundary is considered to be a sea boundary with salinity equal to 30 PSU. A Riemann condition is implemented at the lateral boundaries and free transport is allowed to let the model calculate its own hydrodynamic and transport values. The salinity at the river boundary is set to zero. The numerical simulations used to determine the salinity field do not include any mobile sediment input from either the river or the delta bed. The influence of sediments on the baroclinic flow is therefore neglected and the bathymetry is frozen during the simulation. The time step in the salinity simulation is chosen to be 1 minute as the optimum value for both model stability and computational time.

3. RESULTS

3.1 Salinity distribution and salt fluxes

The salinity distribution computed by the model varies seasonally depending on the river discharge. Figure 2 presents maps of monthly averaged salinity field and flow vectors for the driest (December) and wettest (June) months, for both the top and bottom layers. The hydrograph is symmetrical, results for the first and second dry season are identical and here we only show results for the second dry season. Inside the delta, the mean top layer depth is 0.15m and 0.5m at the bottom layer. Maps for every month and all layers can be found in appendix A. The salinity maps highlight a fresh water area, the extent of which varies between dry and wet season on a monthly basis. In this paper, fresh water area refers to all areas where salinity is less than 2 PSU both in the delta channel network and offshore of the delta. Salinity equal to 2PSU is chosen as a threshold of impact to human activities and aquatic life following Kimmerer and Monismith, 1993; Denton R.A 1993; Andrews S.W et al., 2017 (see also section 3.2). There are significant similarities between the fresh water area as defined in this paper and buoyant plume structures as defined in estuarine systems. However, the river input in the present setup flows first into a deltaic zone (see Figure 1B), where fresh water movement and any plume development are strongly constrained by the complex bathymetry. Therefore, we choose to restrict the use of the term plume to the regions offshore of the delta. During the dry season (exemplified in Figure 2 A and C), fresh water (in dark blue colour) is restricted within a narrow area around the river inlet. Salt intrusion in the inlet is indicated by the upstream direction of the flow vectors and by the clustering of isohalines inside the river channel in Figure 2C. In contrast, results for the wet season (Figure 2 B and D) clearly indicate the formation of an offshore buoyant plume: top layer salinities are reduced throughout most of the domain while bottom layer salinities still show a sharp horizontal gradient around the delta limit. In both cases, salinity in the delta is much lower than the high oceanic values observed offshore. The river flow maintains salinity inside the delta within a specific range.

Especially during wet season, the salinity remains below the 2 PSU threshold in a large part of the delta.

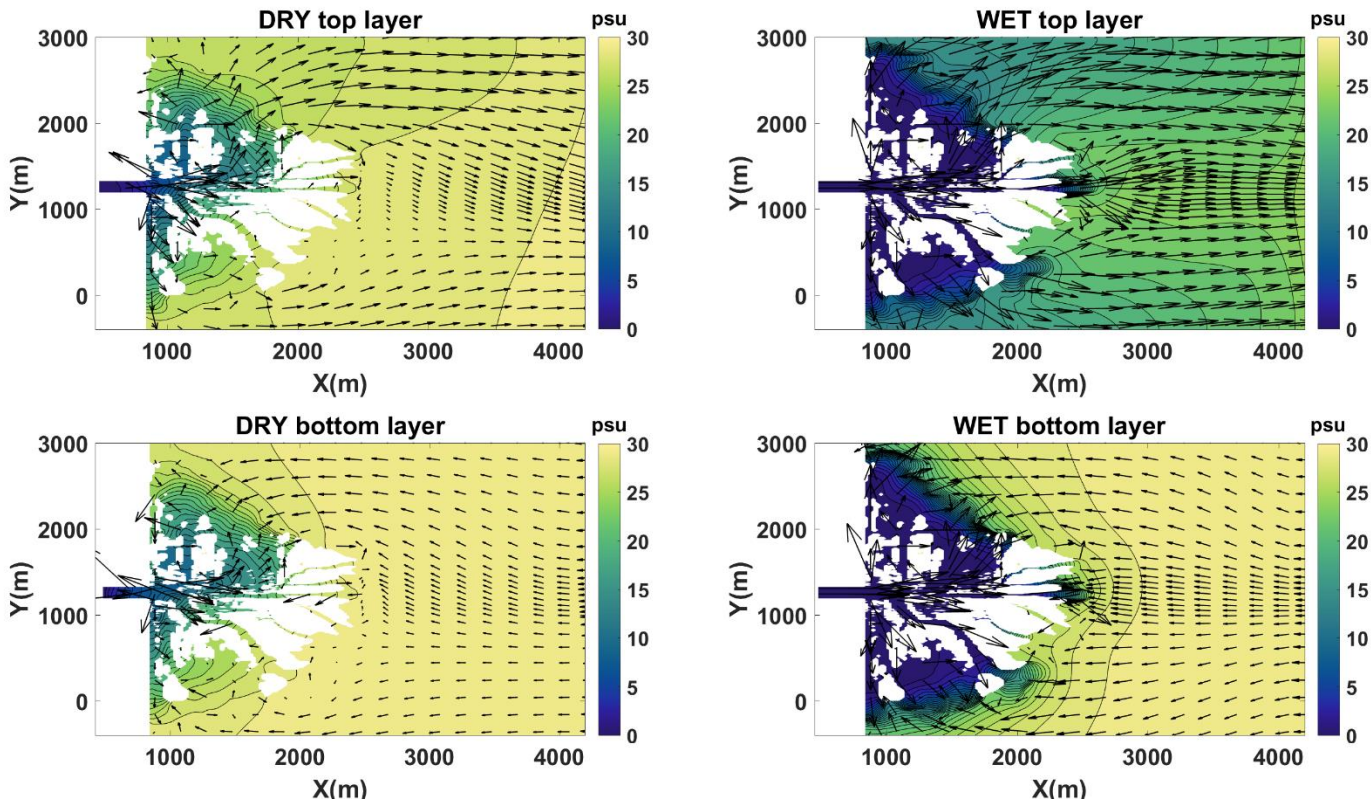

Figure 2 Monthly averaged salinity and flow vectors at (A) driest month at the surface (B) wettest month at the surface (C) driest month at the bottom and D) wettest month at the bottom. White areas indicate dry points and delineate the channels borders*. The isohalines are at 1 psu salinity increment. Grid spacing for flow vectors is 10. colormap (Thyng et al. 2016)*

Figure 2 also presents monthly-averaged flow vectors. The boundary conditions for water elevation, currents, and salinity help generate a baroclinic circulation pattern in the numerical domain: top layer flow vectors indicate an offshore directed flow while the bottom layer flow vectors indicate onshore directed flow. This circulation pattern remains present during both dry and wet periods but its strength appears to be modulated by the river discharge (stronger during wet season). This circulation is an important aspect of the modelling as it provides a critical mechanism for onshore salt flux.

The salt flux $M_s$in the model is calculated following Jia and Li (2012):

$$M_s = \sum_{i=1}^{n} S_i * A_i * V_i \qquad (3)$$

with S, A and V the salinity, area and flow velocity respectively of grid cell i and n the total number of grid cells. Monthly salt flux values are presented in Figure 1E. Negative flux values for the first six months indicate a loss of salt across the model domain. From January (start of the simulation) and until July, the flow rises continuously. As a result, the seaward advection increases causing a decrease of salinity concentrations. On the contrary, from July until the end of the year, the flow declines. As the salinity is constantly 30 PSU at the offshore boundary and because the lateral boundaries do not preclude salt flux, the salinity at this stage increases and its flux becomes positive. It can be seen that the biggest impact of the fresh water flow to the salt mass occurs during the transitional periods between dry and wet season. Salt fluxes are maximum in April (out flux) and September (influx) while

they are minimal during the minimum discharges months (January and December).

3.2 Flushing time

The system's response to the fresh water influence is examined by calculating flushing times. Flushing time (FT) is usually defined as the time required to replace the fresh water volume of a water body (e.g. river delta, bay, and estuary) with the river discharge (Dyer, 1973). The FT was calculated following (Sheldon and Alber, 2002):

$$FT = \frac{\sum_i^n \left(\frac{S_W - S_I}{S_W}\right) V_I}{Q_F} \qquad (4)$$

where $V_I$the grid cell volume, S_w is the seawater salinity at the offshore boundary (30 PSU), S_I is the salinity at each grid point and Q_F the fresh water flow averaged within a certain period. Equation 4 is implemented exclusively to the delta area in the model as defined by the red coloured borderline in Figure B. In the absence of tides the FT variation depends on the fresh water flow fluctuation. In our test case, river discharge is highly variable ranging from periods of very low to periods of very high flows. As a result, the calculation of an instantaneous FT showed high variation during the simulation and could not give a reliable and indicative estimation of the time needed by the system to become fresh in dry and wet seasons. It is preferred then to average the river discharge over longer periods. The determination of the appropriate averaging period is usually an important and difficult issue when calculating FTs.

Various approaches exist for determining the fresh water flow or discharge from using mean monthly or seasonal discharges (e.g., Pilson, 1985; Christian et al., 1991; Lebo et al., 1994), where the mean is taken from long-term records covering many years, to observational discharges, to discharges time-averaged over a user-defined recent past period (e.g. Balls, 1994; Eyre & Twigg, 1997). Here we investigate FTs for the two dry trimesters (January-March and October-December) and the two wet trimesters (April-June and July-September) so the average river discharge of each trimester is taken. A comparison was also done between dry and wet seasons preceding (1st semester) and succeeding (2nd semester) the peak flow. Results can be seen in the bar graph of Figure 3. It was found that more than 2 days are needed for the river flow averaged during dry months to renew the waters while the same process is much faster during the wet months when the FT is less than 6 hours (<0.25 days). Interestingly, the FT between the two dry periods (first and last trimester) is a bit smaller during the last trimester even though the discharge range between the two trimesters is the same. This drop may be due to an influence of antecedent flow since one of these trimesters is preceded by a wet period flushing completely the delta.

Because the use of an average discharge over a long period might be misleading, the date specific method (DSM) is implemented for comparison as introduced by Alber and Sheldon (1999). According to this, the discharge averaging period must be equal to the flushing time itself. An iterative process is then used that starts with a discharge that refers to a starting observation day. The FT calculation is then worked backwards until the averaging period is the closest to the flushing time.

We select two days to be our starting observation point. First, the day of the peak flow and then the day when the minimum flow occurs at the end of the simulation. After the determination of the averaging period, the FT is calculated for the mean and the median discharge for both cases. The mean and median FTs are equal for the maximum flow (0.13 days ~ 3hrs) indicating that the process is very fast at the highest discharges. However, when the time of minimum flow is the starting point, these two numbers differ significantly. The mean flushing time is ten times smaller than the median (17 days and 168 days respectively) because it mitigates the influence of the very low discharges that are present at the end of the simulation. Table 1 shows results for the DSM.

The calculation of FT with the DSM indicates an underestimation of the dry period times and an overestimation of the wet period ones when averaging in trimesters. When the DSM is implemented for the peak discharge, the averaging period is only one day since the water can be renewed very fast in such high discharges. As a result, the median and mean FT with the DSM method are equal because the median and mean discharges for only one day are also equal. This FT was found to be approximately the half of the seasonal one.

The seasonal averaged method overestimates FT because it modulates the effect of the maximum discharges. DSM shows much higher mean and median FT when the minimum flow day is taken as a starting point to find the appropriate averaging period. Mean FT is ~7 times higher in this case because both the averaging period (< 90days) and the discharges are much smaller compared to their mean trimester values. Likewise, the median FT with the DSM is excessively high as a result of the fact that the median value is closer to the very low discharges at the end of the simulation.
The results of the DSM might be more realistic. Considering that low river discharges can sometimes be equal or even smaller than 0.1 m^3/s in the simulation, flushing times between 2-3 days that were found from the seasonal averaging seem to be very small.

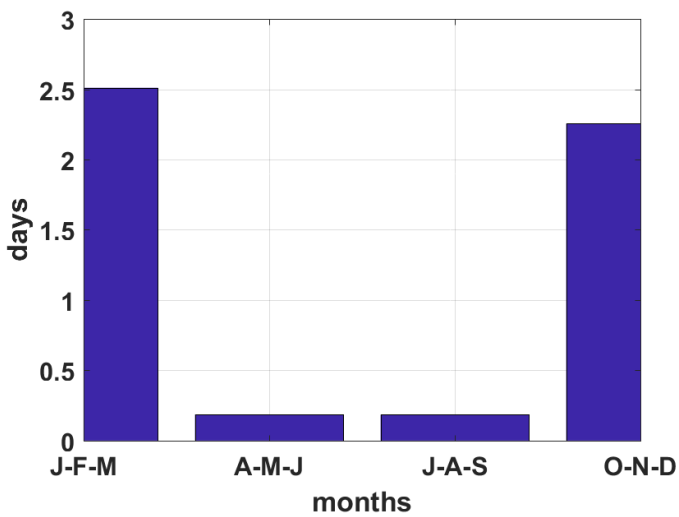

Figure 3 Flushing times calculated with a trimester averaged river discharge

Table 1 Flushing times (FT) of the Date Specific Method

Date of Minimum Flow (31/12)		Date of Maximum Flow (01/07)	
Mean FT (days)	17	Mean FT (days)	0.13
Median FT (days)	168	Median FT (days)	0.13

In addition to the FT calculation, it is important from a management point of view to identify the time period that salinity inside the delta exceeds specific values. Threshold salinity values determine the safety limits for different activities. For instance, drinking water is usually considered potable when salinity < 1psu (Ahmed & Rahman, (2000); Dasgupta (2014); de Vos et al. (2016)) while irrigation water with salinity >4 psu can cause severe reduction of crop yields (Clarke 2015). Marine species present in estuarine habitats have limited tolerance to salinity. The location of the 2-PSU bottom isohaline (commonly denoted in the literature as X2) is considered as an important habitat indicator. X2 has significant statistical relationships with many estuarine resources (e.g. phytoplankton, larvae fish, shrimps, smelt etc.) (Jassby et al.1995, Hutton et al. 2016). It is alternatively often used as a salt intrusion measure (EPA; Schubel et al. 1992; Monismith et al.2002; Andrew et al.2017). In addition, 2 PSU is a threshold for fresh water wetlands conversion to brackish marsh (Conner et al.1997; Wang et al.2020). This is especially true for the Louisiana wetlands and the Mississippi River Delta (Visser et al. 2013) where the majority of vegetation species (e.g. Sagittaria Latifolia, Sagittaria Lancifolia, phragmites australis) survive in conditions less than 2 psu (White et al. 2019).

A critical value of 2 PSU therefore appears to be a sensible threshold that represents requirements for many to most delta ecosystem services. Figure 4 shows an estimation of the time required for salinity to exceed 2 PSU. The time is counted from the moment of highest discharge (hydrograph peak in Figure 1D) to investigate how long the system remains fresh after a wet period. It can be seen that the number of days to surpass the 2 PSU limit decreases seaward. The flushing time is always smaller than the simulation time left after the wet period (180 days left from the peak discharge). Inside the river inlet, the area from the river boundary up to ~100m downstream from the river boundary is always fresh and never exceeds 2 PSU including the deeper portions of the channel. Salt intrusion inside the river inlet starts to develop after approximately 4 months from the wet period when dry conditions recur. Downstream of the river mouth, salinity exceeds 2 PSU within 80-90 days from the wet period and further offshore salinity exceeds 2 PSU much faster and within two months from the wet period.

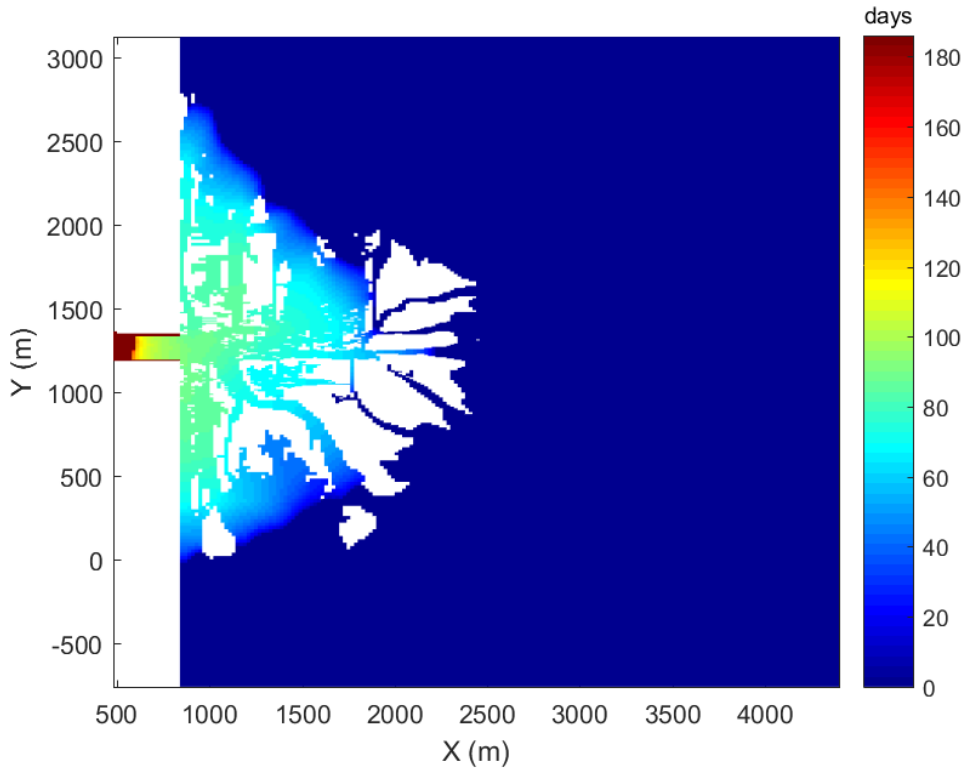

Figure 4 The time (in days) that is needed for salinity to exceed 2psu after the peak discharge (day 181, 1st of July). The maximum number of days (dark red) corresponds to areas where the water remains always fresh and below 2psu. The minimum number of days (dark blue) corresponds to areas where salinity is always above 2psu. White areas indicate dry points.

3.3 Correlations of salinity with river discharge and distance from the river

The salinity response to river flow fluctuations is investigated by looking at the relationship between salinity and river discharge imposed at the river boundary (Figure 1D). Salinity spreads by approximately following semi-circular isohalines (Figure 2). Salinities increase horizontally with the distance r from the river mouth and the angle φ with the x axis (Figure 1B). The variation with φ is influenced by channels characteristics (location, length and width) which also impact isohalines symmetry. To derive simple analytical relationships despite the complex morphology, the depth averaged salinity is averaged within points of equal distance from the river mouth (with the centre at point A', Figure 1B). This simplifies significantly the problem because it filters out by averaging the impact of morphology which is an important aspect in deltas. These points belong to imaginary

semicircles whose radius r represents the distance from the river mouth. We perform this averaging within grid points that are located along the semicircles S1, S2, S3 and S4 of Figure 1B. These semicircles comprise points at a distance of 250m, 500m, 750m and 1000m from the mouth respectively. Figure 5 shows these averaged salinity values as a function of the daily flow (Figure 1D). Dry points (white colour areas in the maps of Figure 2) are not taken into account in the averaging. This means that the salinity is in fact averaged over a sum of arcs with equal distances from the mouth (see section 4.1).

A regression analysis of the results shows a negative and exponential correlation between salinity and river flow for each of the four distances. The highest salinity values are close to the delta border with the sea and lower values are close to the river mouth. At a distance of 250m from the mouth, the water becomes fresh when the river discharge exceeds approximately 40% of its peak value. At a distance of 500m, a higher discharge is needed that should exceed 50% of its peak value to make water fresh. For a distance from the river mouth higher than 500 m, salinity largely declines with increasing discharge but the water remains brackish and salinity never reaches the zero value. Fitting of the results in Figure 5 gives an exponential equation in the following form:

$$S = \alpha * e^{-\beta Q} \qquad (5)$$

S is salinity and Q the river discharge from Figure D. The coefficient α has salinity units and increases seaward while the coefficient β decreases seaward. The parameters values of each semicircle can be seen in Table 2. The fitting lines for each curve are added in black colour in the figure. The fitting lines match extremely well the discrete numerical data at a distance of 750m and 1000m, but minor deviations are present between the fitting lines and the data at 250m and 500m. This may be attributed to the presence of dry points that reduce the number of wet points available for averaging. The fitting was very good for each curve with a coefficient of determination $R^2 \sim 0.99$.

According to Figure 5, the salinity unsurprisingly increases with distance from the river for all discharges so throughout the year. Temporal (annual) averages of the salinity further elucidate the relationship between salinity and the distance r from the river. For this purpose, we considered 15 radial sections every 125 m between 250 m and 2 km from the river mouth. The salinity averaged over the depth and radially (cross-sectional radial average) and over the full year is plotted against the distance r from the river (Figure 6). The complex bathymetry causes the annual salinity to be slightly lower in two specific sections (i.e. 625 m, 1500 m) compared to their upstream neighbour one. Despite this, the spatio-temporally averaged salinity increases with the distance following a curve close to sigmoid (see the fitting approximation in Figure 6) which may also be related to exponential forms. It is reasonable then to assume that the regression analysis solution (equation 5) incorporates both river discharge and distance.

This is an important outcome as it can provide us with information of the expected salinity levels in a delta when the fresh water volume is known. This solution is valid only under certain assumptions because it refers to a non-rotating case and it does not include tides or wind/waves driven mixing. The physical meaning of this equation and the corresponding coefficients together with its limitations are discussed further in section 4.1.

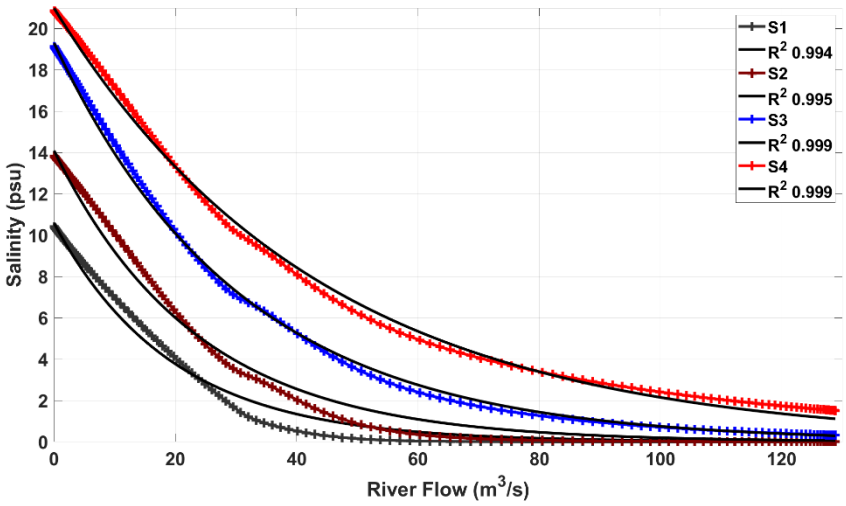

Figure 5 Daily averages along the four semicircles shown in Figure 1B of the depth averaged salinity against the river flow. Each curve displays average values within points of distance 250m, 500m, 750m and 1000m from the river boundary. The fitting lines are added with black colour and the determination coefficient (R^2) is included in the legend

Table 2 Values of α and β coefficients of the exponential equation (eq.5) for each curve in Figure 5

Line	Distance from the river (m)	Base coefficient α	Exponent coefficient β
S1	250	10.5787	0.0516
S2	500	14.0938	0.0427
S3	750	19.2991	0.0325
S4	1000	20.9877	0.0228

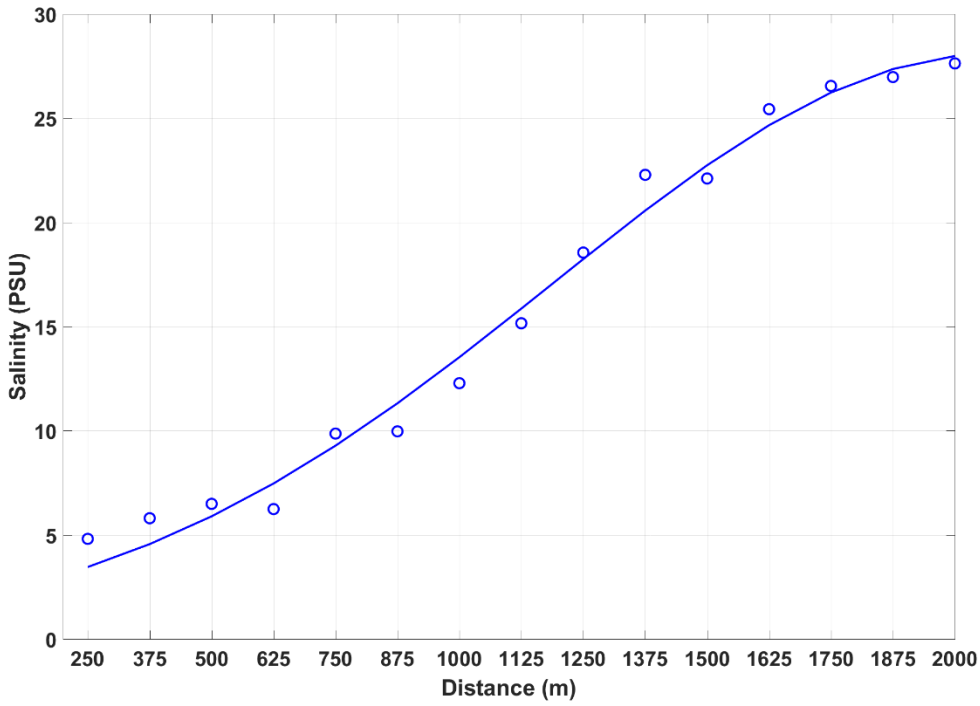

Figure 6 Annual averages of salinity over radial sections against the distance from the river mouth. The averaged values seem to belong in a sigmoid function approximated by the thick blue line.

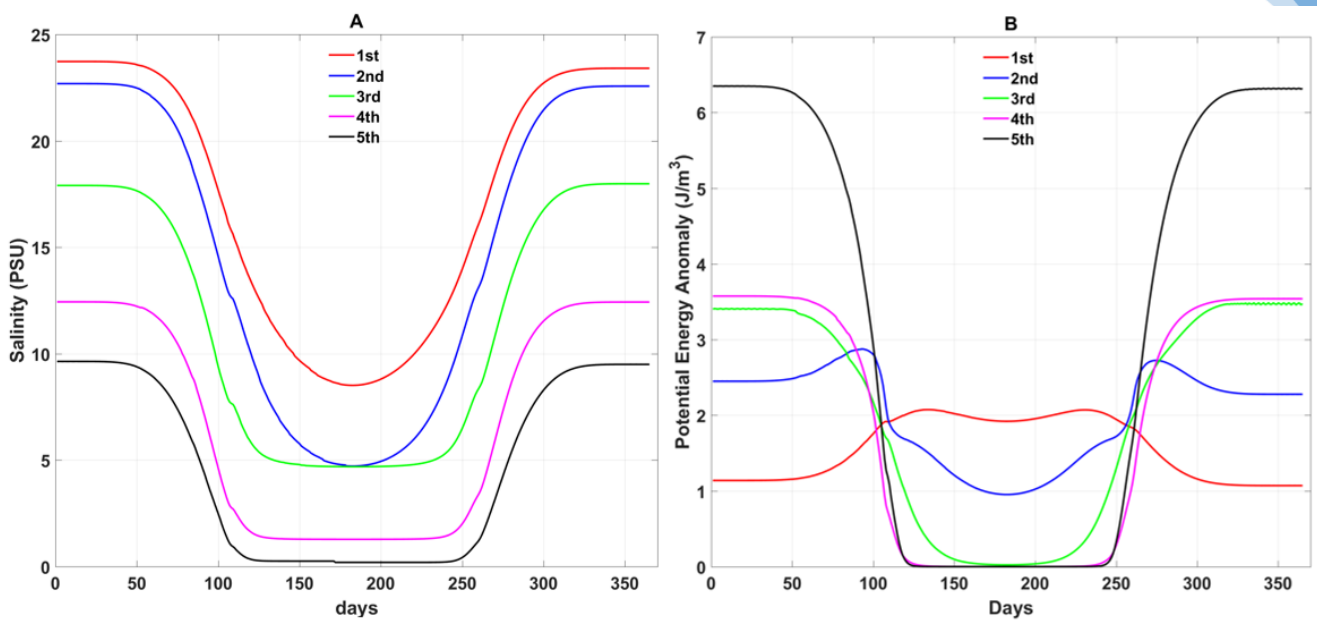

Figure 7 A) The evolution in time of the mean over depth salinity averaged within channels of the same stream order. B) The evolution in time of the potential energy anomaly (PEA) averaged within channels of the same stream order.

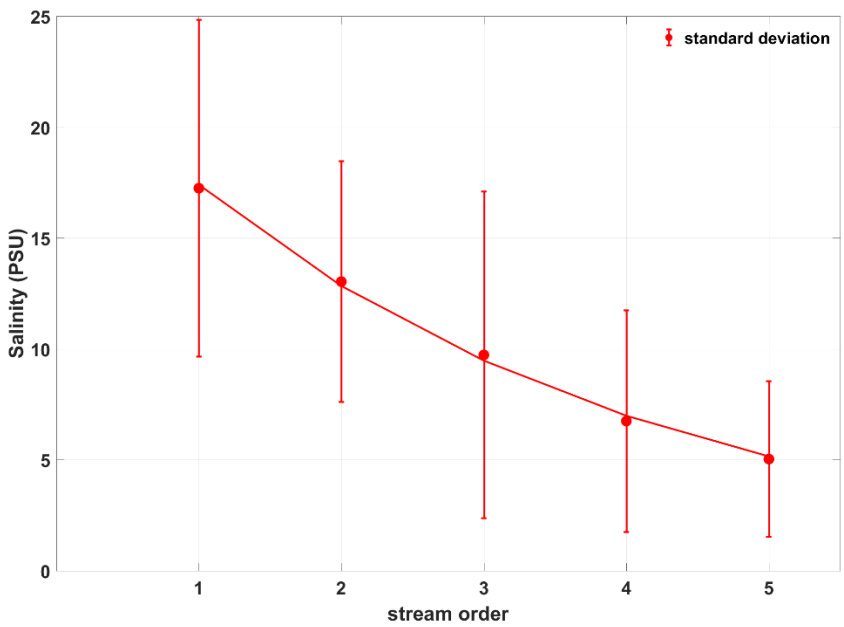

Figure 8 Annual salinity values averaged per stream order. The error bars indicate the standard deviation due to the spatial variability in annual salinities

3.4 Correlations with channel bifurcation order

A stream order number is assigned to each delta channel following the Strahler-Horton method (1952). According to this, first order channels are those with no tributaries at all and second stream order (SO) channels begin at the confluence of two first SO channels. SO increases by one if a channel receives two channels of the same order. When a stream of a given order receives a tributary of lower order, its order does not change. The latter rule though had to be overlooked in several instances, due to the complexity of the delta which includes a variety of formations like closed networks where the method cannot be accurately implemented. In these instances, the stream order number also considers the channel's depth and the number of junctions with neighbours. In our idealized delta,

there are 18 channels of first order, 8 of second order, 4 of third order, 2 of fourth order, and one of 5th order (Figure 1C). Most of the first SO channels are located at the end of the delta and in shallow areas while higher stream order channels are usually closer to the river channel. Nevertheless, stream order number is irrelevant of a channel's position in the network and does not necessarily reflect its relationship with channels in a similar location (Hodgkinson 2009).For example, it can be seen in Figure 1C that the two channels separating at the river mouth are not of the same order. Although someone would expect these two neighbour channels to be of equal order and have similar characteristics because of their proximity, this is not the case. The importance of the stream order labelling lies on the fact that it takes into account the channels connectivity which is higher in the south part (four joints at the 5th SO channel) than in the north (only three joints at the 4th SO channel). Knowing that with each bifurcation both the depth and river discharge decrease (Olariu & Bhattacharya, 2006), it is obvious that the two channels would exhibit differences in their salinity levels despite their locality. The temporal evolution of the depth-averaged salinity averaged within channels of the same SO is shown in Figure 7A. As expected, the time evolution is opposite to the hydrograph for every SO. Salinity increases as the channel stream order decreases and so higher salinity values are present in lower stream order channels. Second and third order channels have an equal minimum because of their geographical proximity. There is also a spatial trend for the duration that the water remains fresh. This amount of time is minimum in first order channels (~1.5 months) and increases upstream with the increase of the stream order number reaching a maximum of 5 months for the 5th stream order. Dry points (land) interfere with channels of 2nd, 3rd and 4th order. Some of them remain submerged after the wet period. This causes a small increase of salinity there during the second semester when a wet period has preceded.

Another important aspect to consider is stratification as it can act as a control on the dynamic evolution of salt intrusion. For example, an increase in river discharge can lead to increased stratification, which in turn may increase residual circulation and near-bed salt intrusion, thus weakening the relationship between salt intrusion and river discharge (e.g., Monismith et al. 2002; Ralston et al. 2008; Lerzcak et al. 2009). Therefore, the stream order analysis is extended to include information on stratification. This is achieved by calculating the potential energy anomaly (PEA), which is the energy required to instantaneously homogenise the water column for a given density stratification (Simpson, 1981; Burchard and Hofmeister, 2008). According to this definition potential energy anomaly ϕ is equal to (Simpson, 1981):

$$\phi = -\frac{1}{D}\int_{-H}^{\eta} gz(\overline{\rho} - \rho)dz \qquad (6)$$

where $\overline{\rho}$ is the depth-averaged density, ρ is the depth-dependent density, H the mean water mean depth, η the surface water elevation, D the total water depth, g gravitational acceleration and z the vertical coordinate.

Figure 7B shows the PEA level when averaged within channels of the same stream order (SO) for the whole simulation period. During the dry season, PEA increases with the decrease of the SO and thus landward, which is related to the increase of channel depth with SO, since deeper channels are more likely to be stratified. The only source of energy to mix the water column in the present numerical setup is the river flow (in absence of ocean and atmospheric forcing), so it is not very surprising that the stratification levels overall decrease with increasing river flow. Increases in river flow also shift the position of the salt intrusion front (see Figure 2 B,D) thus explaining some of the behaviour shown in Figure 7B where stratified regions move seaward (decrease in SO). This leads to maximum PEA for small SO during the wet season.

There appears to be an important shift in the response of salinity and stratification to variable river flow between channels with SO 3 and above versus channel with S0 1 and 2. The increase in river flow is sufficient to completely mix channels with SO3, 4, 5 and result in constant salinity values over (most of) the wet period. In contrast, for channels with SO 1, 2, the increase in river results in an initial increase of stratification, consistent with many estuarine studies (Monismith et al. 2002;MacCready 2004; Ralston et al. 2008; Lerczak et al. 2009; Wei et al. ,2017), before reaching a stage where the river flow is sufficiently high to mix the channels. However, in these two cases, the channels are also too far downstream for the river discharge to completely mix the water column and result in a constant salinity (not dependent of river discharge anymore).

Time averages of salinity curves in Figure 7A produce annual averages per stream order which are presented in Figure 8. The error bars denote the standard deviation due to the overall spatial variability of salinity in channels of equal order. As the SO decreases, the number of channels per SO increases. It would be expected then that higher SO values would exhibit lower standard deviation. However, the spatial variability of SO averaged salinity can be affected by the length and width of channels. This explains the larger variability for SO = 3 than for SO = 2, due to third order channels being longer (and in some cases even wider) than the second order channels (Figure 1C). Even though the relationship portrayed in Figure 8 appears to be consistent with an exponential function, the small number of stream orders (five in this case) makes a quantitative and conclusive regression difficult. Further considering bifurcation orders in natural systems (e.g. only three orders were identified in the Mississippi Delta, see section 3.5), it appears unlikely that a quantitative relationship would be meaningful and representative for a large number of real deltas. Instead, the main result ought to focus on the qualitative relationship that salinity increases with decreasing stream order.

3.5 Comparison with real data

In order to gain confidence in the veracity of the idealised numerical results we have presented, we compare them with real data available from the Mississippi River Delta and examine if similar trends exist in nature. The Mississippi River Delta is chosen for comparison because it is generally classified as a river dominated delta. We used maps with time-series of isohalines every fortnight and with step of 1 psu corresponding to measurements from 2017. These maps are provided by the Lake Pontchartrain Basin Foundation https://saveourlake.org/ within the purposes of the Hydrocoast Program. The Mississippi Delta channels were classified in three stream orders following again the Strahler-Horton method. The maps resolution allows us to identify and name 18 channels as it can be seen in Figure 9. A mean salinity is assigned at every channel calculated as the average value of all the isohalines crossing through a channel for every fortnight (24 values per year). Monthly values are obtained then and salinity is again averaged within channels of the same SO as is done in section 3.4. By averaging, high frequency processes are considered as secondary effects and are included in the filtering. Then, model results of Figure 7A are also monthly averaged to make the comparison with the Mississippi data. The comparison can only be done for SO 1 to 3 as the bifurcation is lower compared to the idealized model. Figure 10A shows the monthly averaged model results for SO 1 to 3. Figure 10B presents the monthly averaged Mississippi data results for SO 1 to 3. The salinity has been normalized in both cases by dividing by its maximum value. The qualitative comparison with results from the idealized modelling is good since salinity increases with decreasing stream order in both cases. Salinity data is then processed in a manner consistent with the averaging undertaken previously to present the relationship between salinity and stream order: i.e. salinity values are time averaged over a year and spatially averaged to result in an annual salinity value for each stream order in the Mississippi (Figure 11). The error bars indicate the standard deviation due to the spatial variability in annual salinities. The qualitative comparison with the results of the idealized model is once again

satisfactory with stream order averaged salinity (and standard deviations) increasing (decreasing) with decreasing (increasing) stream order.

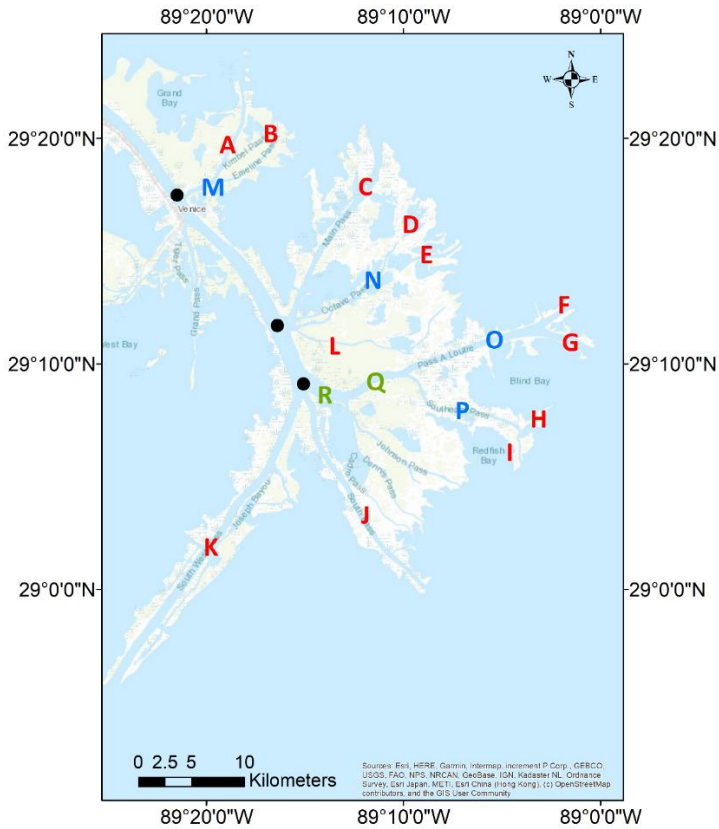

Figure 9 Planar view of the Mississippi River Delta (Courtesy of https://www.google.com/maps/). The capital letters name the channels for which there is available data. Red colour classifies first stream order (SO), blue colour second SO and green colour third SO. The black circles are the reference points to measure distance from the river for every channel at each subdelta.

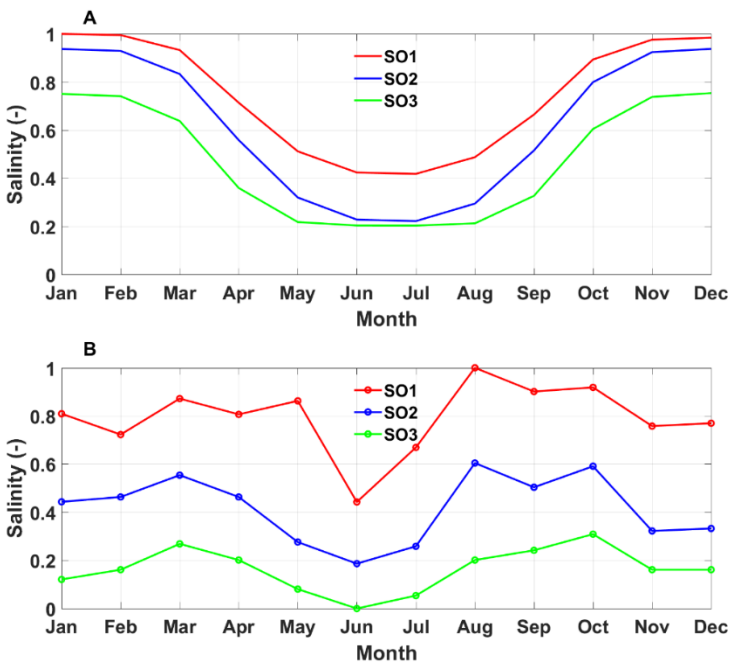

Figure 10 Monthly salinity values averaged within channels of the same stream order (SO) and normalized by their maximum in the A) idealized model and B) Mississippi Delta in 2017.

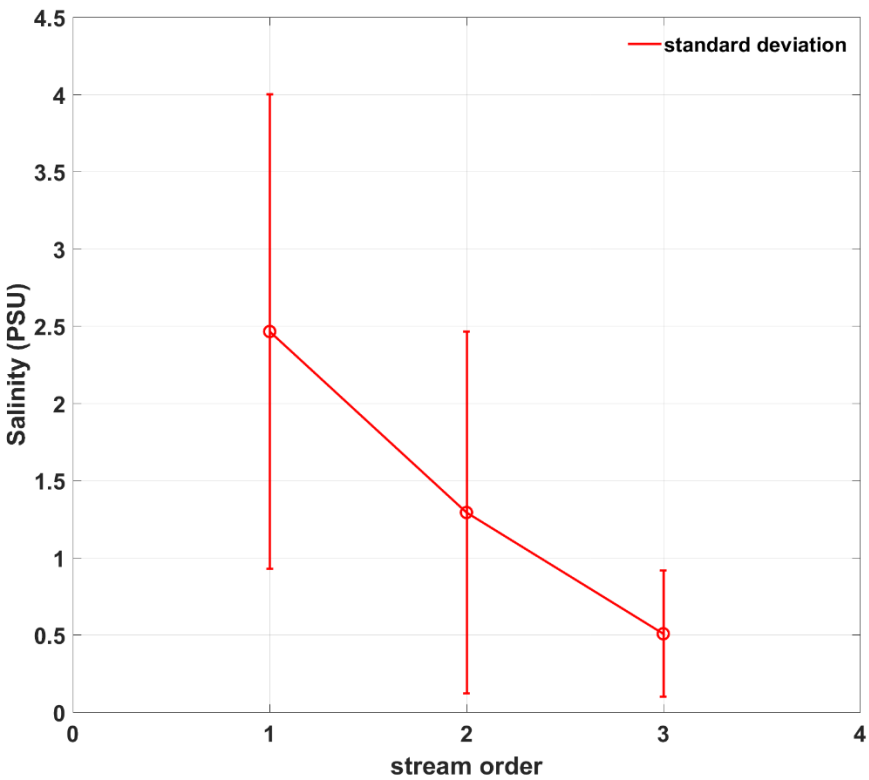

Figure 11 Mean annual salinity averaged within channels of equal order in the Mississippi Delta. Error bars indicate the standard deviation due to the spatial variability.

The methods of section 3.3 are adapted to the Mississippi data and similar plots are reproduced. At first, the salinity is averaged in distances of 5 km, 10 km, 15 km and 20 km from the river. The distance is measured from the three black dots drawn in the main river branch in Figure for each one of the three Mississippi subdeltas. If there is no isohaline crossing exactly at some of these distances, then an interpolation is done between the first upstream and the first downstream isohaline with respect to that distance. Figure 12 presents the salinity-river discharge correlation at each distance from the river (i.e. 5 km, 10 km, 15 km and 20 km) for 2017. The averaged per distance salinity is plotted against the river discharge in Mississippi (available on the usgs.gov website, station 07374000). The river discharge measurements are time averaged to match the number of available salinity observations. These are 25 in total for 2017 (typically two per month but three for July). An exponential regression analysis is done and the R^2 coefficients are shown in Figure 12. The goodness of fit for an exponential correlation is tested by implementing the Kolmogorov – Smirnov test. For a number of 25 samples, as is the number of observations here, the critical value for this test is 0.264 with a 5% uncertainty. If the test-value is below this threshold then the hypothesis that the data follow an exponential relationship can be accepted. An exponential relationship between salinity and river discharge is supported by the test values per curve (reported as ks in Figure 12) for the data at 5 km. An exponential relationship is also supported for the 10 km data, but in this cases at a 10% uncertainty level (critical l value equal to 0.3165).

It can be seen in Figure 12 that the ks values increase with the distance. This expresses the decrease of the river influence with the distance and thus the decrease of the probability for an exponential relationship. In every case, the exponential fitting is weaker in the Mississippi Delta than in the idealized one. This discrepancy is not unexpected considering the numerous differences between the two systems. In the idealized model, we purposefully neglected the impact of tides and other hydrodynamic forcing (waves, storm surge etc.). Even though tidal forcing is weak in the river

dominated Mississippi delta, it may still act as a mixing factor, thus weakening the river discharge influence on the most distant channels (usually of 1st stream order). In addition, the response of salinity to river discharge is likely to be affected by time lag and the system's flow history (e.g. antecedent flow, Denton and Sullivan 1993; Andrews et al., 2017). It should also be noted that the Mississippi maps do not present information of salinity's vertical distribution whereas the analysis with our model results is done for depth averaged salinity. The lack of salinity data in the vertical does not allow a PEA analysis for the Mississippi observations. A more detailed discussion for the inconsistencies between model and real data results for this case can be found in section 4.1.

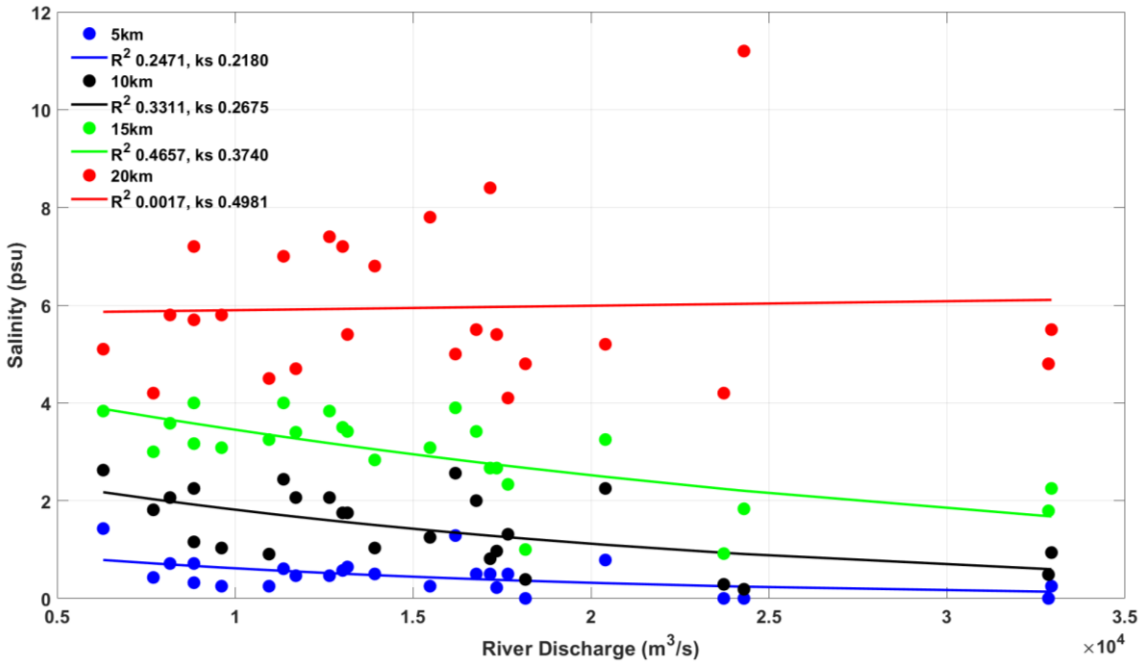

Figure 12 Salinity observations of year 2017 in the Mississippi Delta against river discharge measurements of the same period. The observations are groupped and averaged within distances of 5 km, 10 km,15 km and 20 km from the river, denoted in the graph with different colour. The fitting lines of an exponential regression analysis are added.The determination coefficients (R^2) for each case are included in the legend together with the kolmogorov – Smirnov statistical values (ks) per case. Note that the critical value for a number of 25 samples is 0.264 for a 5% uncertainty and 0.3165 for 10% uncertainty.

4 DISCUSSION

4.1 SALINITY-RIVER DISCHARGE RELATIONSHIP

The idealized model simulates the full three-dimensional baroclinic flow for a typical configuration where there is an upstream river boundary with a varying fresh water inflow and a constant sea boundary condition. In spite of a number of complex processes being accounted for in the idealised numerical model (e.g. complex delta morphology, dynamic flow variability, stratification), the numerical results are well approximated by an exponential relationship between salinity (depth averaged and averaged over arcs) and river discharge (i.e. equation 5).

Denton and Sullivan (1993) developed empirical antecedent flow-salinity relations which are similar to equation 5. The exponential form arises from the solutions of 1D advection-diffusion equations for salt conservation under certain assumptions, initial conditions, and boundary conditions (Crank 1975, Fischer et al.1979, Zimmerman 1988). In particular, solutions similar to equation 5 are found under steady state conditions, for constant cross-sectional area, and for constant dispersion coefficient.

Our delta situation presents similarities and differences with such a simple case. The numerical model does use a constant horizontal diffusion equal to 10 m^2/s, but the other two key assumptions are not a priori satisfied. That the numerical results remain well approximated by equation 5 would seem to indicate that the system remains close to steady state, and therefore that the fresh-water discharge only varies slowly compared to the intrinsic salinity adjustment time scale of the system. The cross-section A used to average results is not constant, and does not vary monotonously with distance from the river because of the complex bathymetry and geometry of the delta. Nevertheless, the numerically derived flow-salinity relationship remains a good fit to an exponential. Such exponential solutions of the advection-diffusion equation have been presented even for non-steady and/or variable coefficients (and thus cross-sections).

For example, Phillip (1994) provided exponential solutions of the advection-diffusion equation in two and three dimensions for a radial flow in the case of variant diffusion coefficient and time-varying flow. Zoppou and Knight (1999) derived exponential solutions to the advection-diffusion equation for spatially variable diffusion and velocity coefficients. In both studies, analytical solutions are expressed only using constant coefficients terms after a series of mathematical transformations of the varying coefficients. It thus seems reasonable to pursue an analogy to the steady state, constant cross-sectional area, and constant dispersion coefficient case for explanatory purposes.

Following from our results, including the different values for the parameters in equation 5 (Table 2), equation (5) can then be rewritten as follows:

$$\overline{S(r,t)} = \overline{S_{max}(r)} * e^{-\beta(r)Q(t)} \qquad (7)$$

Where S the cross-sectional averaged salinity and the overbar denotes depth averaged values. The coefficient α corresponds to the maximum salinity when $Q = 0$. In other words, α is the maximum averaged salinity (S_{max}) in a distance r. In our specific case, the maximum salinity is also the initial one, since Q has values very close to zero at the start of the simulation according to the hydrograph (Figure D). It is logical then that α increases as the radial distance from the mouth increases (Table 2). The coefficient β expresses the effect of distance on the river flow influence which explains why its values decrease as r increases (Table 2).

It is inferred then, that in a river dominated delta, the salinity at a certain distance from the river could be determined based on river discharge charts as Denton and Sullivan (1993) did for the San Francisco Bay, even in non-steady systems and for varying in space cross-sections. It is interesting that despite the non-uniform bathymetry and the unsteady conditions, the problem is successfully approximated with the above method. Since the results in section 3.3 take into account the full range of river discharges over the year, this approach remains valid for the entire simulation period even though the dynamics vary significantly due to significant variations in the fresh water discharge.

The domain undergoes important dynamical changes in time under the influence of the river discharge's high variability in time. The Peclet (Pe) number is a non-dimensional parameter that can be used to monitor the time scales of advective and diffusive processes inside the delta. For a considered length scale λ, Pe can be calculated as:

$$Pe = \frac{U\lambda}{K} \qquad (8)$$

Where U is the fresh water velocity through the river boundary cross-section, λ the length of the inlet (400 m) and K the diffusion coefficient (10 m^2/s here). Figure 13 shows the Pe evolution in time during the simulation. For Pe values less than 1, transport is mainly the result of diffusive processes. This is the case during dry seasons. The horizontal dashed line in Figure marks the threshold of Pe = 1. The curve crosses the threshold for the first time approximately 90 days after the start of the simulation and again 90 days before its end. These two periods of 90 days with Pe < 1 correspond to the two trimesters of dry season (see also Figure 1D). In between these two periods, Pe is larger than 1 which means that advection prevails inside the delta and diffusion becomes less important. This describes the conditions in the delta during the six months period of wet season.

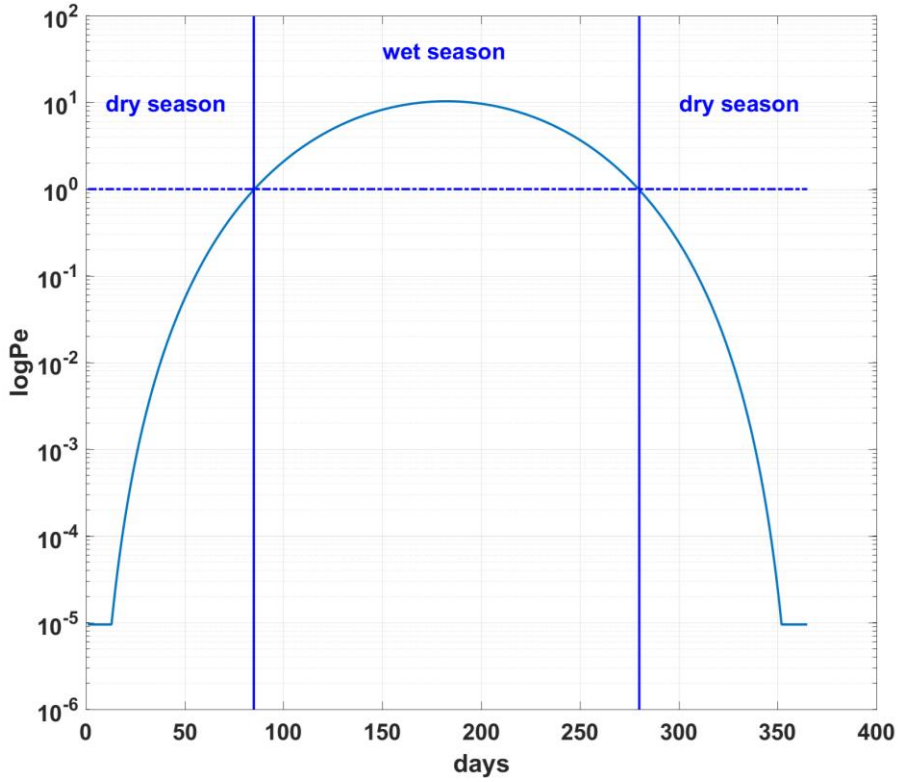

Figure 13 The Peclet (Pe) number evolution in time for a length scale λ equal to the river inlet length. The horizontal dashed line marks the limit between diffusion and advection dominated periods when Pe=1. The vertical lines indicate the times when Pe surpasses or falls below 1 which corresponds to the start of the wet and the dry season respectively.

Several past studies have pointed out the influence that lateral variations of depth, present in our model, have on the longitudinal salinity gradients (Li and O'Donnell 1997; Li et al. 1998; Uncles 2002). This is usually presented as an uneven distribution of vertical mixing causing significant lateral and vertical circulation (Dyer 1977; Valle-Levinson and O'Donnell 1996; Li and O'Donnell 1997). The impact of secondary flows on the along delta salt transport seems to be well incorporated in equation 7 by the depth and radial averaging.

As noted previously, an exponential flow-salinity relationship is much less satisfactory for the Mississippi delta, which should not be entirely surprising given that the assumptions behind equation 7 are far less likely to be valid in natural systems. A critical one is the constant dispersion coefficient (K) which is not a realistic assumption for natural systems. For example, K values in the San Francisco and Willapa bay vary in a range between 10 m^2/s and 1000 m^2/s (Monismith et al. 2002; Banas et al. 2004) while Fischer et al. (1979) summarize its range between 100-300m^2/s based on data from a series of estuaries. Monismith (2010) presents a list of mechanisms for predicting K values in real systems from observations. However, the assumption for a constant diffusion coefficient is a common

practice in modelling studies. In their work for investigation of the dependence of the longitudinal salinity gradient on channel contraction and/or expansion, Gay and O'Donnell (2007) comment on the lack of theoretical reason for implementation of varying K in their model. Moreover, Lewis and Uncles (2002) found better agreement between their model and salinity observations with a constant rather than a varying K.

The uncertainty on the diffusion's magnitude in a real system in addition to the external forcing present in the Mississippi delta could partly justify the weaker exponential fitting (Figure 12). Furthermore, the equation 7 describes a spatio-temporal salinity-flow distribution under important limitations. The exponential correlation is a direct outcome of the dominant role the river flow plays in the modelled case. The presence of other additional forcing mechanisms (i.e. wind, waves, along-shore transport) could alter this correlation because of the changes it would cause to the river flow direction and the fresh water layer shape, thickness and vertical structure. For instance, waves change the flow jet direction from the river mouth and affect its spreading. If the angle between the waves and the shore is high then it causes a deflection of the jet flow downdrift (Nardin & Fagherazzi 2012). Moreover, wave-induced transport causes changes to horizontal salinity gradients and may modify estuarine circulation (Schloen et al.2017). Consequently, the isohalines would not exhibit symmetric and semi-circular shapes as they do in our model results (Figure 2). A flow asymmetry would determine different fresh water areas modifying the results from averaging salinity in Figure 5. We would expect differences to be more pronounced during dry seasons because wet seasons showed river-induced mixing conditions leading to zero salinities inside the delta irrelevant to flow direction (Figure 2 B and D).

Deviations from the simple exponential relationship may also arise from wind forcing intermittently impacting the baroclinic response of the system. For example, down-welling favourable winds constrain fresh waters onshore and increase plume thickness, while upwelling favourable winds tend to promote offshore spreading of fresh water and plume thinning (Barlow 1956; Pullen & Allen 2000; Fong & Geyer 2001; Whitney & Garvin 2005; Choi & Wilkin 2007). Wind forcing also impacts dynamics in estuaries modifying circulation and salt transport (e.g., Scully et al., 2005; Chen and Sanford, 2009; Bolanos et al., 2013). Vertical mixing processes affect fresh water thickness too. For example, wave breaking at the surface leads to enhance mixing and more homogeneous plumes (Gerbi et al., 2013; Gong et al. 2018), while wave-induced circulation usually traps fresh water landward, reducing the surface salinity and increasing the fresh water thickness (Delpey et al. 2014; Rong et al. 2014).

4.2 Bifurcation correlations

Channels classification schemes, such as the Strahler-Horton method implemented here, can be successfully used to relate the salinity with channels hierarchy: salinity increases seaward as the stream order number decreases. Lower salinity should be expected in parts of the delta with higher number of channels junctions which are usually located closer to the fresh water source. Both river discharge and channels depth typically decrease with each bifurcation (Olariu & Battacharya, 2006) and so it is reasonable that salinity becomes higher downstream when the flow influence has weakened and where shallower areas are present. In the idealized model, salinity averaged over time and spatially correlates with stream order number. However, this link can be modulated by the length or the width of the channels, which can vary significantly between different orders. The analysis of the Mississippi data yields similar trends between salinity and stream order, and thus supports the conclusions from the idealized model. Nevertheless, the limited number of stream orders in both the Mississippi and idealized deltas limits a fully quantitative regression and the generalisation of salinity stream order relationships to other natural systems.

Our results also indicate that changes in stratification between different dynamic conditions might also be related to the channels classification. There is a shift in the PEA magnitude inside channels of the same SO number for different flow stages. When dispersion prevails (dry periods), the PEA was found to decrease with the decrease of the SO. In this case, the deeper channels of high SO are more stratified than the others. When advection is dominant (wet period), the most proximal to the river channels are well mixed with PEA becoming zero while channels of low SO order remain partially mixed.

5. CONCLUSIONS

We used an idealized numerical model to investigate the salinity field in a river dominated delta. We modelled salinity variations under the influence of an annual symmetric flow and determined and classified the spatial distribution of salinity during wet and dry seasons, mass balance and flushing time.

Model results indicated that salinity averaged over delta cross-sections decreases exponentially with river discharge. This relationship appears similar to the simple theoretical solution of the 1D advection-diffusion equation under steady conditions and constant diffusion and cross-sectional area.

The implementation of the same methods on salinity-flow data from the Mississippi River Delta showed a weaker exponential correlation between salinity and river discharge. Considering the deviations from the classical assumptions required (i.e. steady-state flow, constant cross-section and diffusion coefficient) and that external forcing not included in our model (e.g. waves, wind etc.) might be present, this is somewhat expected. In spite of this, our analytical expression could work as a best alternative for a first estimation of salinity values when there is lack of data. It provides the opportunity to estimate salinity levels at a certain time and location with respect to the river channel for a known river discharge. This significant outcome could be extremely useful for water management and local authorities. River diversions, dam construction, sea level rise, limited fresh water inflows and prolonged drought periods are a challenge for water supply policies.

Secondly, the Strahler-Horton stream labelling method was introduced and adapted for deltaic systems to achieve a delta channels classification based on their connectivity. A relationship was found to exist between the salinity level and the system's bifurcation. Salinity generally increases as the stream order decreases. Channels of low connectivity (i.e. low number of junctions and nodes) are exposed to high oceanic salinity since they are the farthest from the river. The stream order number method is a scale-independent method that can be easily implemented to other real deltas. The same analysis done with observations from the Mississippi delta agreed with our model results. Therefore, the number of channel branches can be another indicator of high or low salinity in addition to the distance from the river. In the absence of field data, this outcome can be useful for an estimation of delta areas which are more prone to high salinity. Furthermore, the stream order number can be connected to the potential energy anomaly which is used as a measure of stratification. It identifies stratified areas close to the river in dry seasons and far from the river in wet seasons. It should be noted though, that these conclusions are valid only for a river dominated system. The validation of these methods applicability in cases including the impact of tides, waves and different bathymetric conditions will be the topic of a future work.

SUPPLEMENTARY INFORMATION

A. MAP PLOTS WITH SALINITY CONTOURS AND FLOW VECTORS

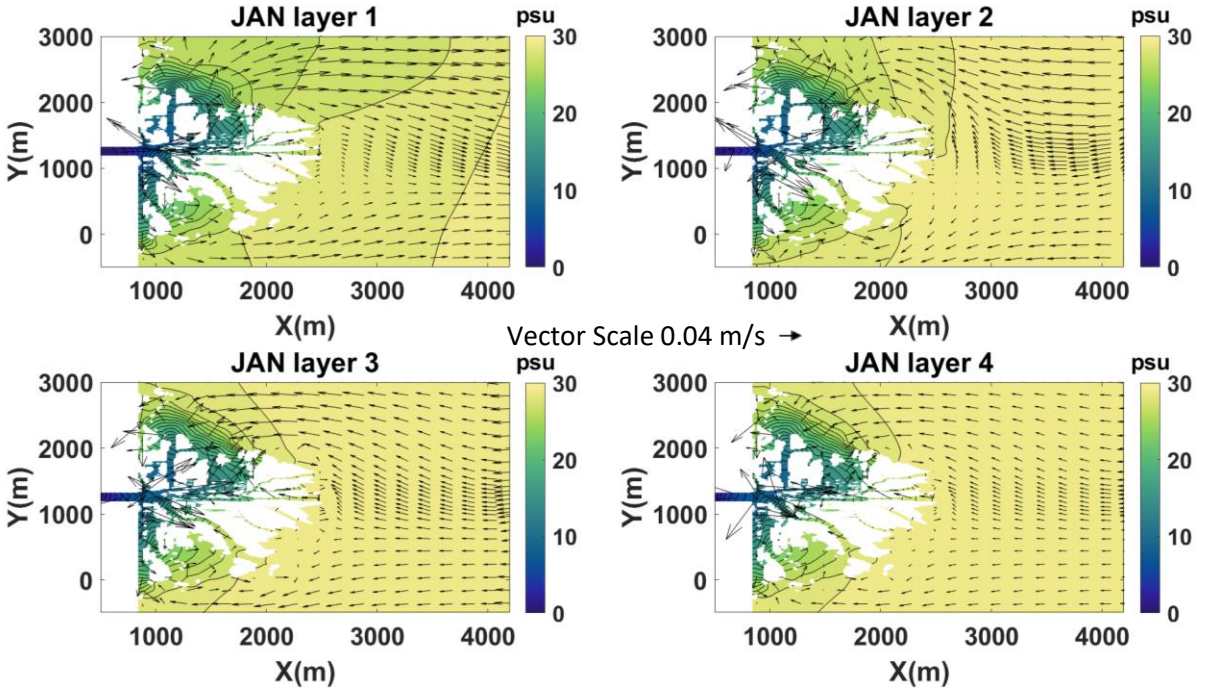

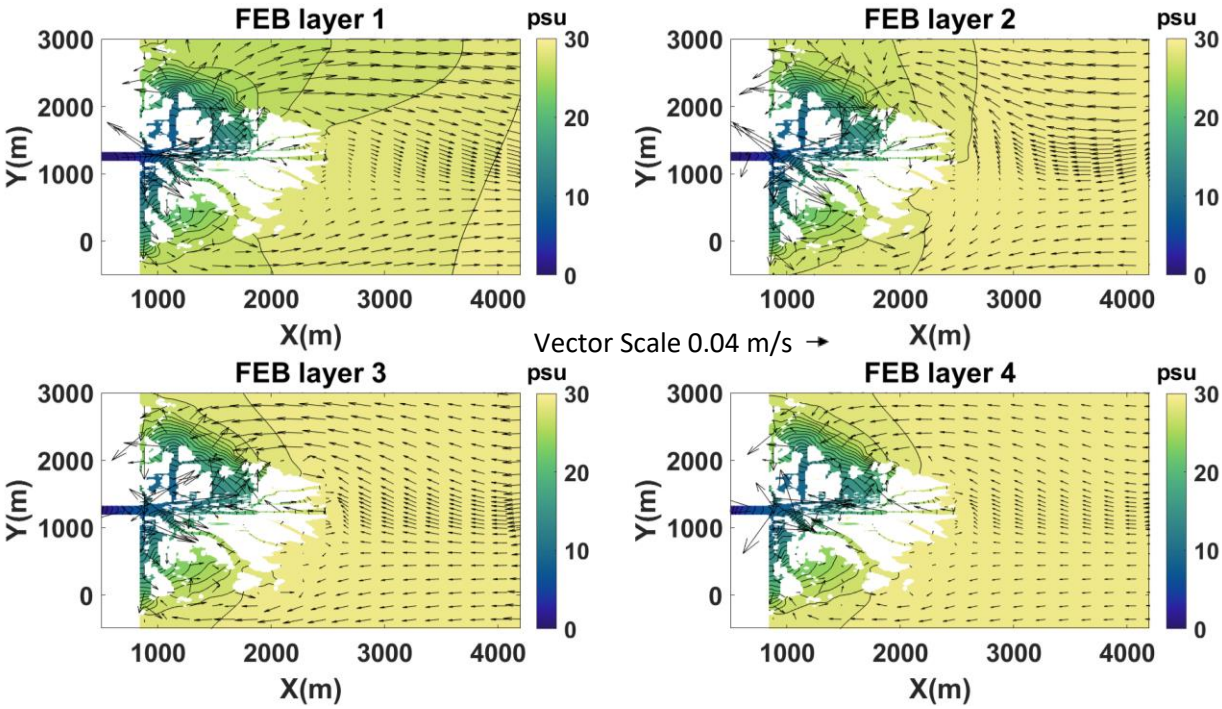

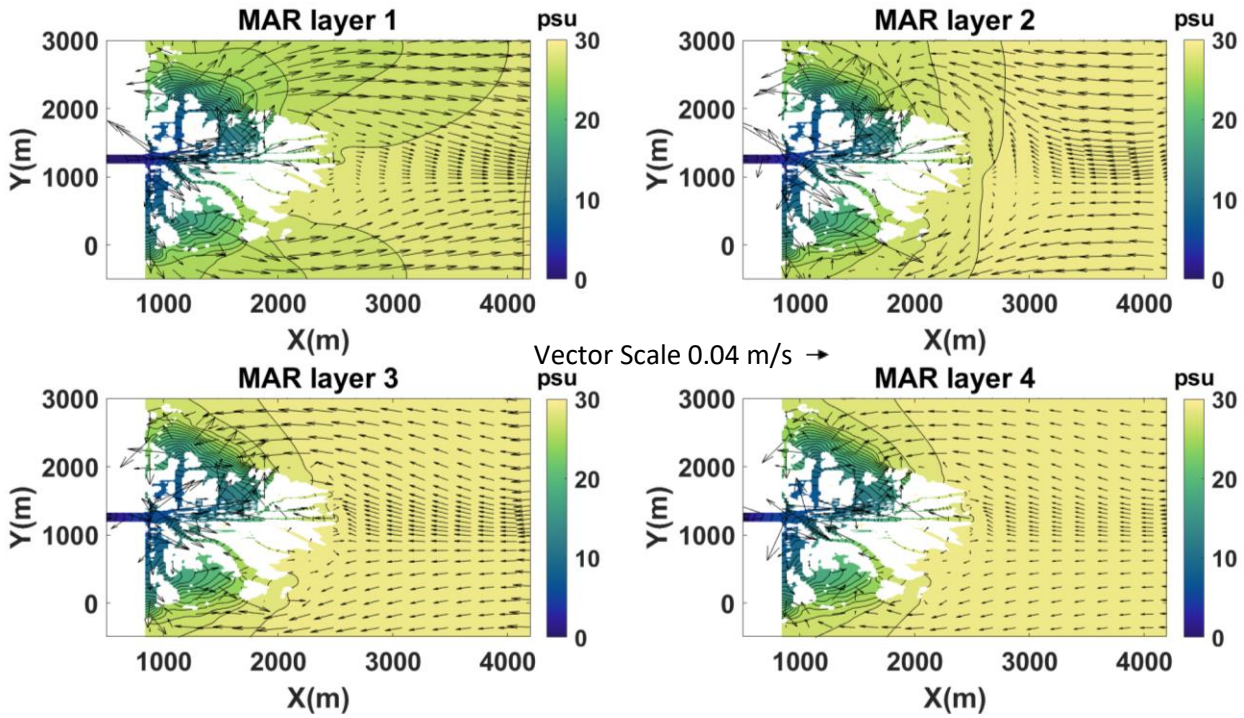
MAR layer 1
MAR layer 2
MAR layer 3
MAR layer 4
psu
Y(m)
X(m)
Vector Scale 0.04 m/s

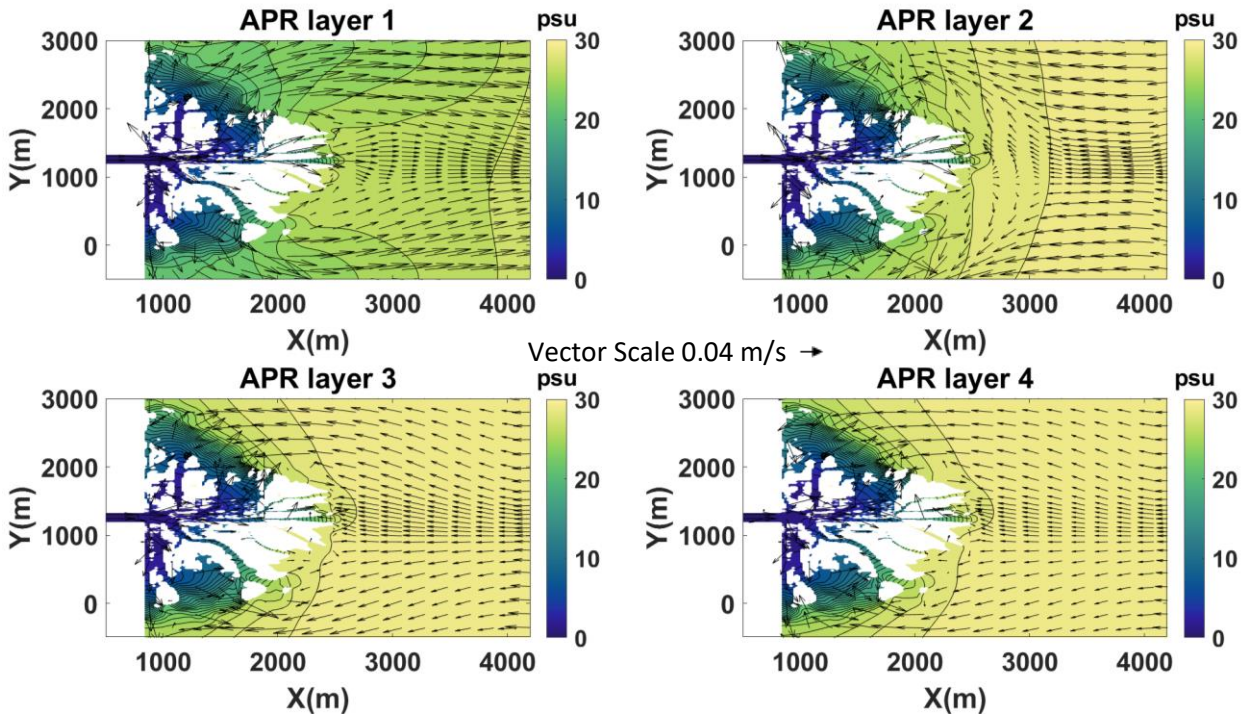
APR layer 1
APR layer 2
APR layer 3
APR layer 4
psu
Y(m)
X(m)
Vector Scale 0.04 m/s

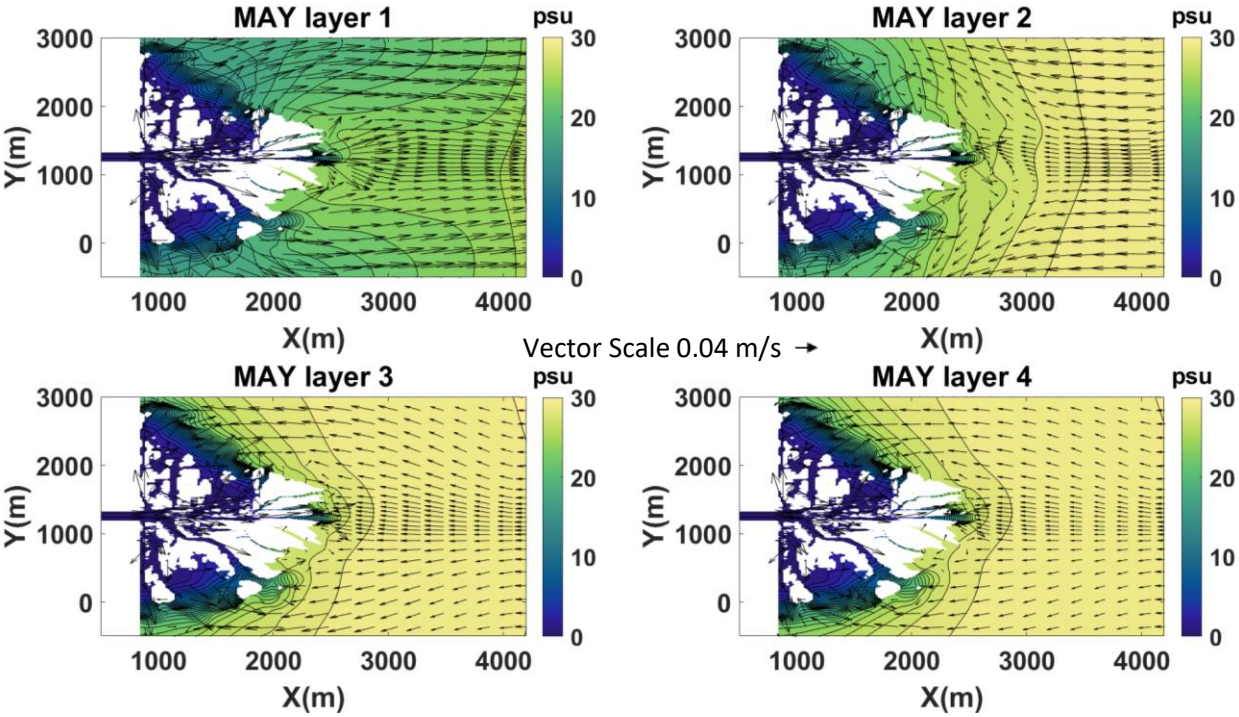
MAY layer 1
MAY layer 2
MAY layer 3
MAY layer 4
psu
30
20
10
0
3000
2000
1000
0
Y(m)
1000
2000
3000
4000
X(m)
Vector Scale 0.04 m/s

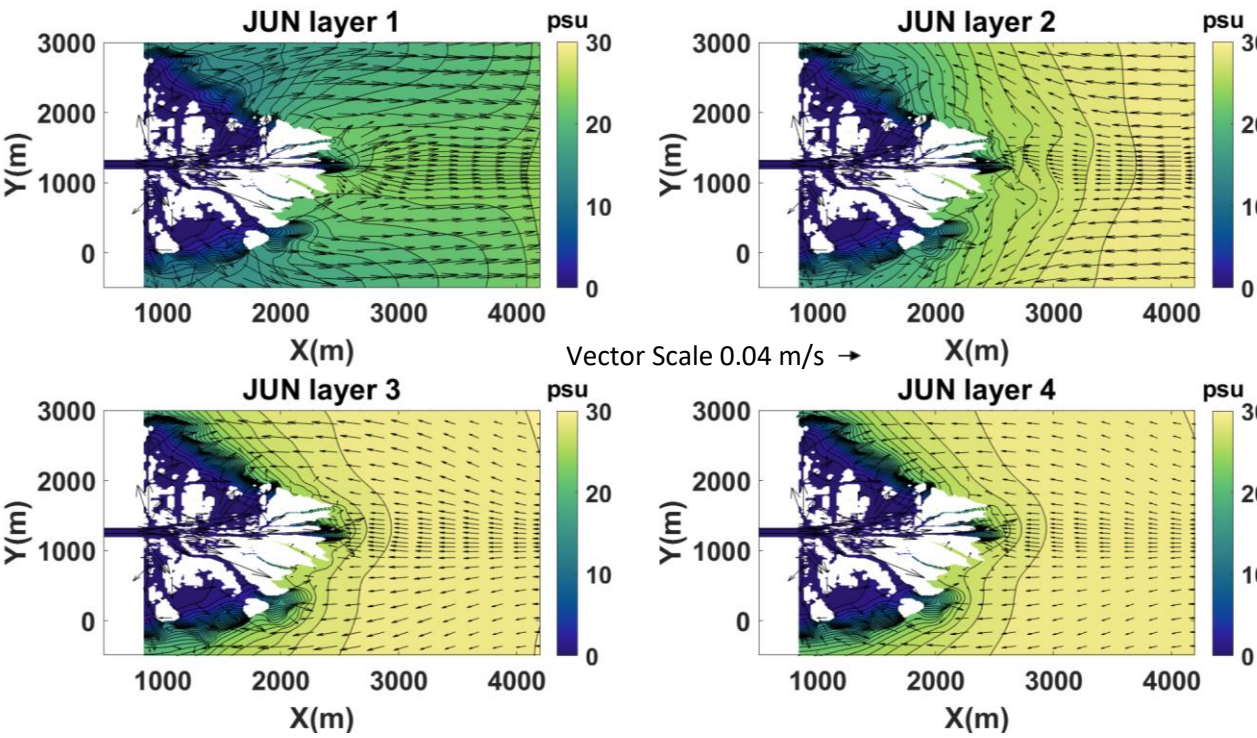
JUN layer 1
JUN layer 2
JUN layer 3
JUN layer 4
psu
30
20
10
0
3000
2000
1000
0
Y(m)
1000
2000
3000
4000
X(m)
Vector Scale 0.04 m/s

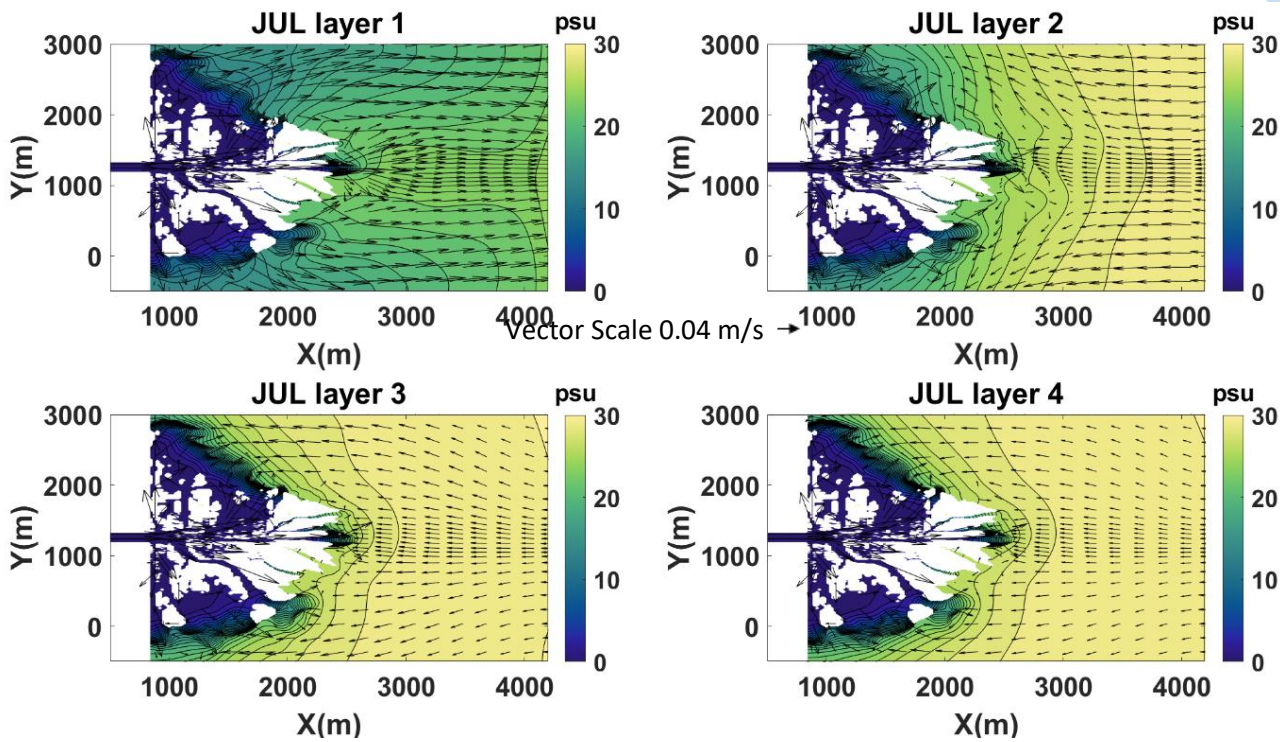
JUL layer 1
JUL layer 2
JUL layer 3
JUL layer 4
psu
Y(m)
X(m)
Vector Scale 0.04 m/s

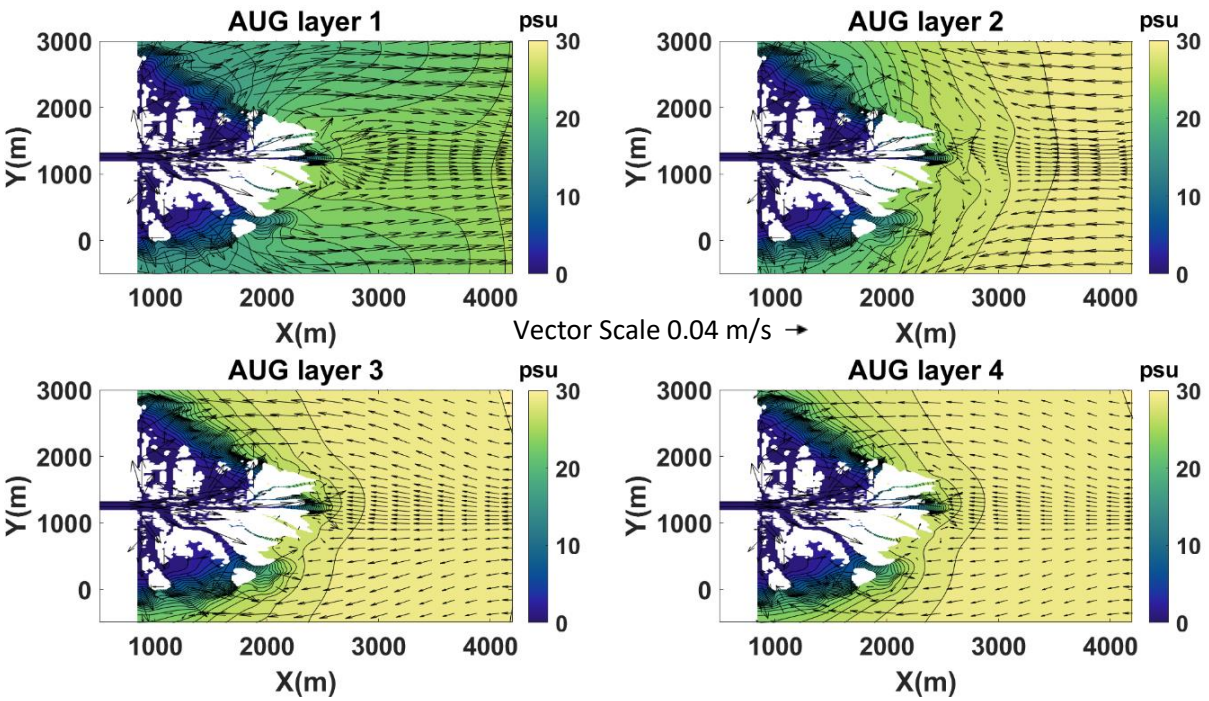
AUG layer 1
AUG layer 2
AUG layer 3
AUG layer 4
psu
Y(m)
X(m)
Vector Scale 0.04 m/s

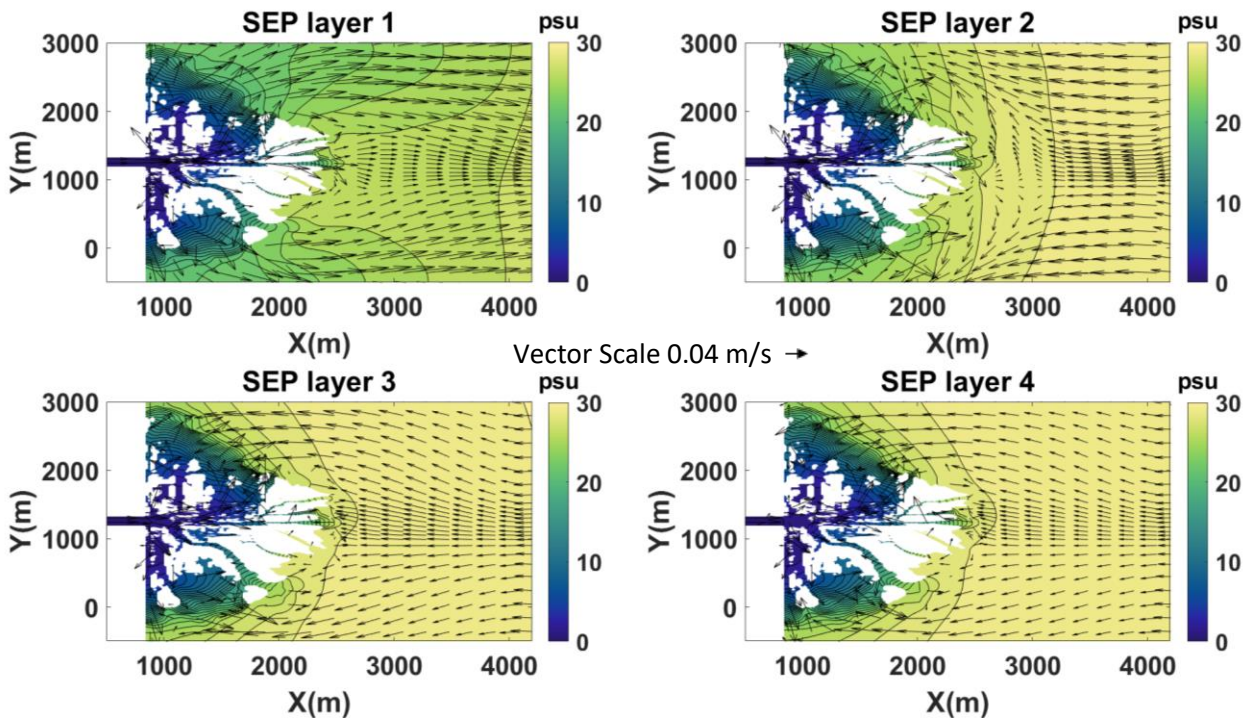
SEP layer 1
SEP layer 2
SEP layer 3
SEP layer 4
psu
30
20
10
0
3000
2000
1000
0
Y(m)
1000
2000
3000
4000
X(m)
Vector Scale 0.04 m/s

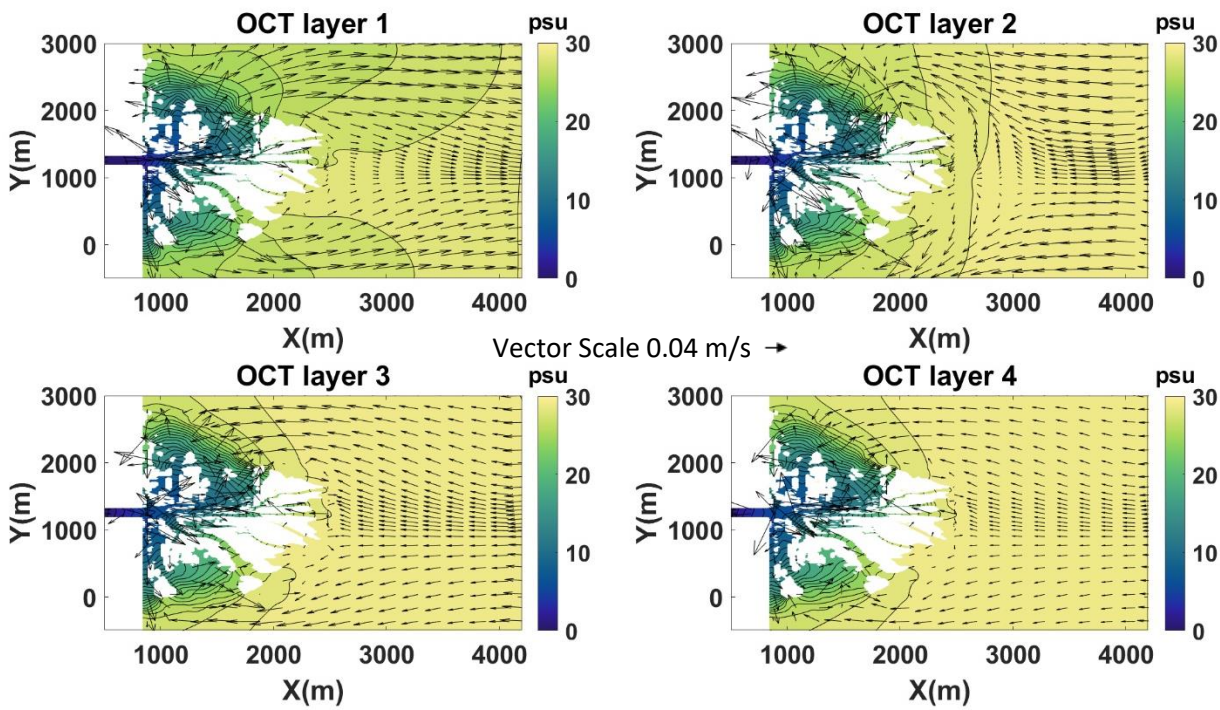
OCT layer 1
OCT layer 2
OCT layer 3
OCT layer 4
psu
30
20
10
0
3000
2000
1000
0
Y(m)
1000
2000
3000
4000
X(m)
Vector Scale 0.04 m/s

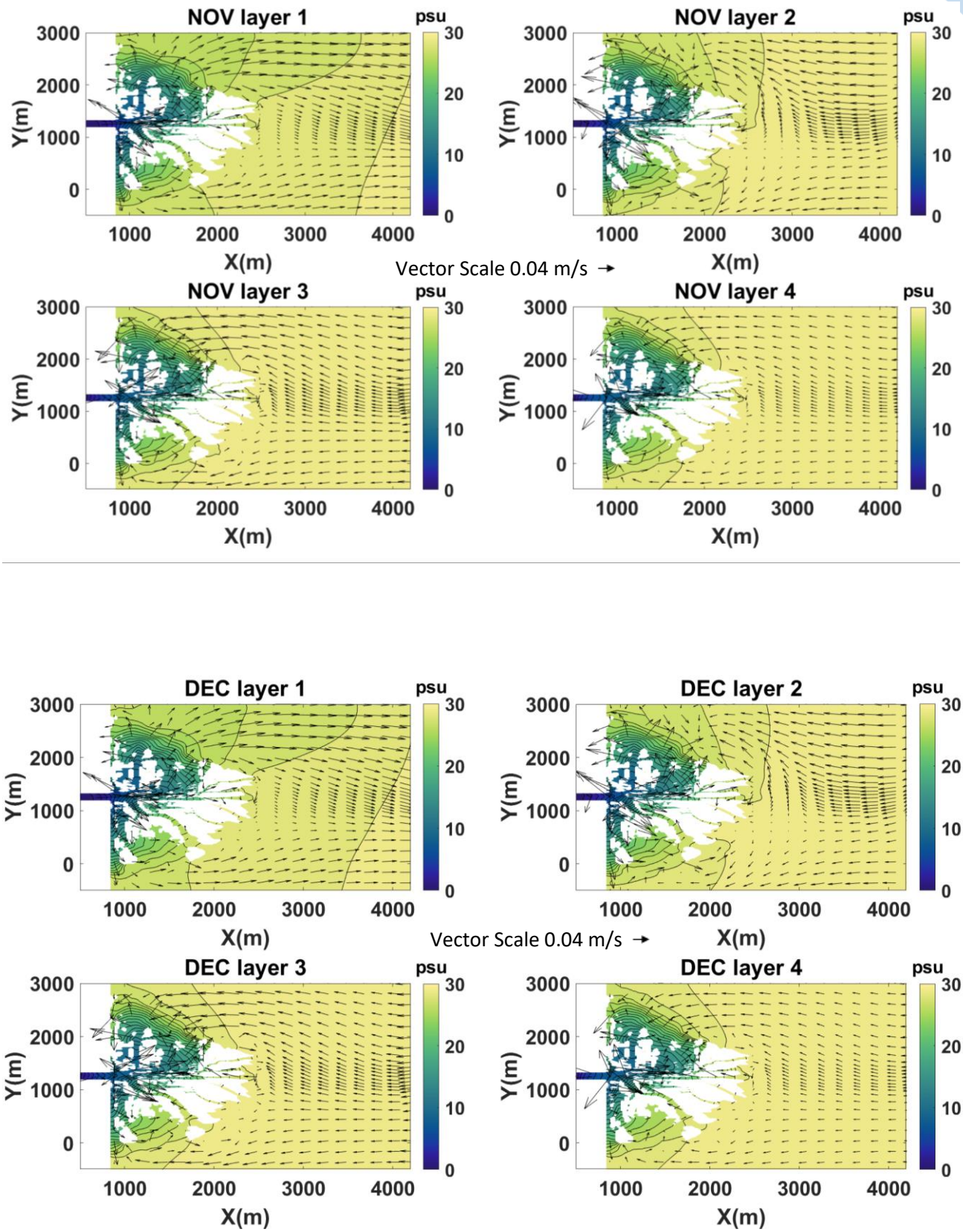

Figure 14 Monthly averaged salinity and flow vectors at every layer and each month. Number 1 corresponds to surface and number 4 to bottom layer. Colormap (Thyng et al.2016).

B. SENSITIVITY TEST ON THE NUMBER OF VERTICAL LAYERS

We present here the results of the sensitivity test on the number of vertical sigma layers. The model was run with 4, 6, and 8 sigma layers and results are summarised into percentage increase of the top-bottom salinity difference (Figure 15) and the impact on the potential energy anomaly averaged within channels of the same stream order (Figure 16). The delta area remains largely unaffected both during the dry season when the largest differences are mainly observed inside the deep river inlet and during the wet season when the largest difference are observed offshore while fresh and well mixed conditions prevail in the delta (see section 3.1). Even though the number of vertical layers does change the magnitude of PEA in Figure 16, it does not affect the qualitative dependence of PEA on stream-order.

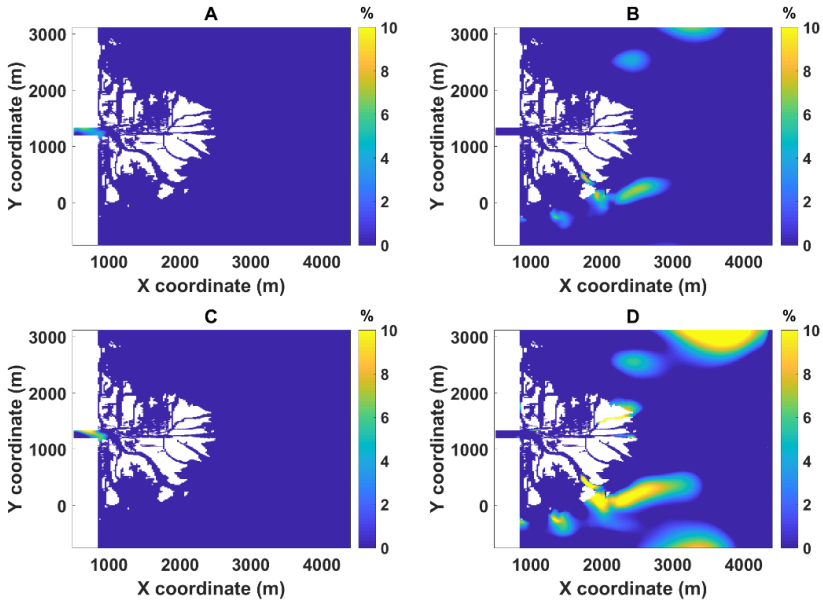

Figure 15 The percentage increase with respect to the simulation of 4 vertical layers in the top to bottom layer salinity differences in the case of A) six layers in the dry season B) eight layers in the dry season C) six layers in the wet season and D) eight layers in the wet season.

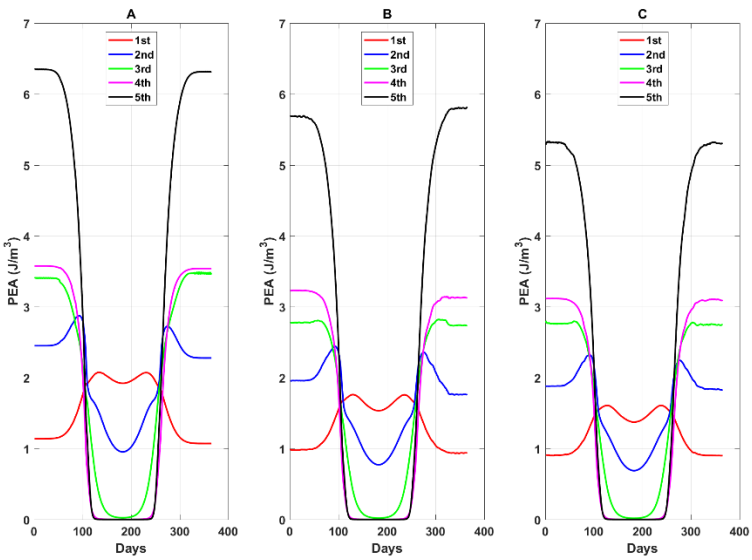

Figure 16 The evolution in time of the potential energy anomaly (PEA) averaged within channels of the same stream order in a simulation with A) four B) six and C) eight vertical layers.

5. Combined impact of river and tide on salinity intrusion in an idealized river delta

Constantinos Matsoukis[1], Laurent O. Amoudry[2], Lucy Bricheno[2], Nicoletta Leonardi[1]

(1) University of Liverpool, School of Environmental Sciences, Department of Geography and Planning, Roxby Building, Chatham St., Liverpool L69 7ZT, UK

(2) National Oceanography Centre, Joseph Proudman Building, 6 Brownlow Street, Liverpool, Merseyside, L3 5DA, UK

Corresponding author: c.matsoukis@liverpool.ac.uk

This paper has been submitted to the Journal of Estuaries and Coasts and is under review

First Author Contribution: Conceptualization, Methodology, Software, Pre- and Post-processing, Visualisation, Formal analysis, Writing, Original draft and reviewed versions preparation.

Link to preceding chapter: This paper extends the work of the previous chapter by investigating the effects of various tidal amplitudes on the salinity of an idealized delta. The methods implemented in the previous paper are repeated to investigate their applicability and validity in the presence of tides.

ABSTRACT

Salinity in deltaic systems is expected to increase in the near future due to sea level rise. This will cause severe environmental consequences because salinity can be detrimental for agriculture, aquaculture and human consumption. Tidal dynamics are affected by changes of the water level. Sea level rise can lead to tidal modulations and so many deltas incur changes in their tidal forcing. However, there is still uncertainty about the consequences of such changes on deltas' salinity. This paper investigates the impact of various tidal amplitudes on the spatiotemporal salinity distribution in deltas through three-dimensional idealized modelling. A series of simulations is carried out where a common hydrograph is implemented and different tidal ranges. Both tide influenced and river dominated cases were considered. Results suggest that small increases to the tidal amplitude in river dominated or low tidal regimes can have positive effects against salinization. Tide induced mixing helps to increase freshwater areas and volumes. The water in the delta remains fresh for longer periods in medium tidal amplitude scenarios representing microtidal regimes. Further increases of the tidal amplitude in meso and macrotidal regimes reverse these effects and reduce freshwater areas and volumes. Our numerical results enable us to test how salinity correlates with channels orders and river discharge in the presence of tides. These correlations are controlled more by bathymetry than tidal forcing. This study provides important insights on how changes in tidal range could impact spatiotemporal salinity distributions in deltas.

Keywords: salinity, river deltas, tidal amplitude, river discharge, idealized modelling

ACKNOWLEDGEMENTS

The work contained in this paper contains work conducted during a PhD study supported by the Natural Environment Research Council (NERC) EAO Doctoral Training Partnership whose support is gratefully acknowledged. Grant ref NE/L002469/1. Funding support from the School of Environmental Sciences, University of Liverpool are also gratefully acknowledged.

1. INTRODUCTION

River deltas are coastal ecosystems with highly fertile soils and productive waters and are attractive places for living and working with dense populations and high economic activity (Ericson et al., 2006; Fagherazzi et al., 2015; Bianchi 2016; Nicholls et al., 2018). Climate change challenges the sustainability and maintenance of deltaic systems worldwide.

Sea level rise (SLR) increases the salinity in deltaic regions and causes an upstream intrusion of the tidal saltwater zone (Gornitz, 1991; Bhuiyan and Dutta, 2012; Hong and Shen, 2012;2020; Bricheno et al. 2021). Saltwater intrusion (SWI) is an important phenomenon in coastal zones that is driven by both anthropogenic (e.g. groundwater extraction) and natural (e.g. tidal inundation) factors (White and Kaplan, 2017; Rahman *et al.*, 2019) and causes serious problems in households, agriculture ,irrigation and industry (Allison, 1964; Smedema and Shiati, 2002; Zhang *et al.*, 2011). Salinization contaminates rivers, aquifers and soils decreasing freshwater storage and water quality (Gornitz, 1991). High salinity reduces soil fertility resulting in low crops yield (Bhuiyan and Dutta, 2012). For example, severe reduction of rice and wheat production is reported in the Bangladesh delta where many freshwater rice paddies have been converted to brackish water shrimp farms (Sarwar, 2005; Bricheno and Wolf, 2018). Conversion of freshwater to brackish or saltwater habitats has also occurred in the Mississippi Delta where serious ecological degradation is taking place because of flooding (Holm and Sasser, 2001; Kaplan *et al.*, 2010). SWI is hazardous for many marine and vegetation species that have limited tolerance to salinity. For instance, some types of phytoplankton, larvae fish and shrimps usually survive only in environments with less than 2 g/kg salinity (Jassby *et al.*, 1995; Hutton *et al.*, 2016). Other vegetation species in the Louisiana wetlands and Mississippi Delta (Sagittaria Latifolia, Sagittaria Lancifolia, phragmites australis) also require less than 2 g/kg salinity (Visser *et al.*, 2012; White *et al.*, 2019). In addition, high salinity may be responsible for plant stress and mortality and hampering of tree production (Kaplan *et al.*, 2010; Bhuiyan and Dutta, 2012). Moreover, human health can be affected by salinization through water consumption. Drinking water should not contain more than 1 g/kg salinity (Vos, 1990; Dasgupta *et al.*, 2015; Sherin *et al.*, 2020). Saline water environment is favourable for the development of microbes related to water borne diseases such as cholera or diarrhoea. Many cholera outbreaks in Bangladesh occurred after flooding because the water supply was contaminated (Sarwar, 2005). Saline water has been also reported as a leading cause for hypertension (Rahman *et al.*, 2019). SWI causes currently similar problems to many deltas worldwide, e.g. Mekong (Eslami *et al.*, 2019), Yangtze (Chen *et al.*, 2001; Dai *et al.*, 2011; Qiu and Zhu, 2015), Pearl River (Liu *et al.*, 2019; Hong *et al.*, 2020), Nile (Frihy, 2003), Mississippi (Day *et al.*, 2005) and Bangladesh (Rahman, 2015; Yang et al. 2015; Bricheno et al.2016;2021; Sherin *et al.*, 2020).

Salt intrusion in estuaries is mainly determined by river discharge, estuary shape, tidal and wave forcing (Nguyen *et al.*, 2008; Dai *et al.*, 2011; Gong and Shen, 2011; Maccready *et al*. 2018). Although the role of river discharge on the salinity is usually dominant, this is low compared to the tidal flow during dry season when salt intrusion matters the most (Nguyen *et al.*, 2008; Zhang *et al.*, 2010). For example, the Yangtze delta presents saltwater intrusion during dry seasons and under strong tidal conditions affecting domestic water usage for millions of people in the city of Shanghai (Qiu and Zhu, 2015).The interaction of freshwater flow and tide establishes an estuarine circulation (or exchange flow) with seaward flow at the top and landward flow at the bottom layer (Pritchard, 1956; Hansen and Rattray, 1965; Deyer 1973;MacCready and Geyer, 2010) although other circulation modes are possible too depending on the level of river and tidal forcing and variations in mixing (Geyer and MacCready, 2014). Landward salt transport is driven either by exchange flow or tidal dispersion (Banas *et al.*, 2004; Lerczak, Geyer and Chant, 2006; MacCready, 2007; MacCready and Geyer, 2010). Tidal processes determine the large-scale salt transport and distribution by influencing stratification and

exchange flow (Liu *et al.*, 2007; MacCready and Geyer, 2010). The exchange flow can be increased by tidal asymmetry especially during flood tides while strain-induced stratification might develop at the ebb tide (Simpson *et al.*, 1990; Jay and Musiak, 1994; MacCready and Geyer, 2010).

Climate change effects on the annual water cycle are expected to cause fluctuations in the river discharge that together with SLR will impact tidal dynamics as well (Bricheno et al.2021). SLR may cause alterations to tidal range and currents on local, regional and global scale (Zhong et al. 2008; Hong and Shen, 2012; Haigh *et al.*, 2020; Hong *et al.*, 2020). These will be more acute over large shallow coastal waters such as deltas while the tides remain unaffected in deeper waters (Nguyen, 2016). Nguyen (2016) identifies the following mechanisms as responsible for these changes in tidal regimes: 1) increase in the tidal wave phase speed 2) direction change 3) tidal friction decrease and 4) frequent flooding of inter-tidal areas. Very flat deltas such as the Mekong will be highly affected. Increases of the tidal range due to SLR have been reported in the Chesapeake Bay (Zhong et al. 2008), Yangtze Delta (Qiu and Zhu, 2015), Bangladesh delta (Bricheno et al. 2021), Mekong delta (Nguyen, 2016), Pearl River Delta (Zhang *et al.*, 2010) and the Eastern Scheldt estuary (Jiang *et al.*, 2020). Hong and Shen (2012) and Chua and Xu (2014) reported an increase of the estuarine circulation in the Chesapeake and San Francisco Bay respectively due to SLR with a consequent increased upstream salt intrusion.

However, tidal amplitude (TA) can both decrease and increase in response to SLR (Green, 2010; Holleman and Stacey, 2014; Carless *et al.*, 2016; Pickering *et al.*, 2017) and changes of TA may be proportional (Idier *et al.*, 2017) or not to mean SLR (Pelling et al. 2013). In an idealized study, Du *et al.* (2018) demonstrated that the tidal range is likely to decrease with SLR in short estuaries with a narrow channel and low-lying shallow areas. This means that deltaic systems may face changes in their tidal forcing with either increases or decreases. Changes in tidal mixing and currents are expected to have implications in saltwater intrusion (Jiang *et al.*, 2020) and thus a delta's salinity distribution. Because the level of these changes can vary a lot globally, there is a need to assess their impact on a system's salinity in a generic and not site-specific manner. This is required in order to take measures and prevent the damage on the human population dependent on deltas and the execution of their activities. There is already enough knowledge on the variation of temporal and spatial salinity distribution in estuaries under the combined forcing of river discharge and tide (Jay, 1991; Turrell et al. 1996; Uncles and Stephens, 1996; Monismith *et al.*, 2002; Bowen and Geyer, 2003; Chen, 2004; Prandle, 2004; Lerczak et al. 2006; Liu *et al.*, 2007; Ralston et al. 2010; Wei et al. 2016) but there is still a gap concerning channelized networks.

This paper presents a modelling study that predicts the changes that different tidal ranges can cause on the spatiotemporal salinity distribution of a static deltaic system where no morphological changes occur. For this purpose, a 3D numerical model is built in Delft3D for an idealized delta configuration. We follow a minimalist idealization concept (Weisberg, 2007), and therefore only retain the core causal factors (influence of river discharge and tides here) controlling a phenomenon (salinity distribution and salt intrusion here). Such an approach relying on idealized or 'exploratory' models (Murray, 2002), in which some processes are intentionally omitted and others are simplified, can offer simpler and better explanations of certain behaviours in systems involving many interacting processes (Murray, 2002).

A series of simulations is carried out for both river dominated and tidally influenced deltas. The model is forced in each case with an upstream freshwater flow varying on a daily basis for a period of one year and a constant offshore tidal boundary condition. For simplicity, low-frequency tidal motions (spring-neap cycle) are omitted and only one semi-diurnal solar tide is considered in each case. This

allows for a direct correspondence between daily discharge values and salinity (when averaged over two tidal cycles) and makes it easier to detect the impact of absolute tidal level on seasonal salinity patterns. Estuarine studies have reported that the tide affects buoyant plumes symmetry (Chao, 1990; Isobe, 2005; Guo and Valle-Levinson, 2007; Lee and Valle-Levinson, 2013). To compare the various amplitudes effects on plumes' symmetry and structure, the Earth's rotation is neglected to avoid an extra source of asymmetry. In the results analysis, an extra emphasis is given on the changes in freshwater areas, volumes and duration of freshwater conditions since this is what matters probably the most in regard to the activities taking place in a delta.

Matsoukis et al.(2021) related salinity with channel order and river discharge. By classifying the delta channels into stream orders based on the Strahler-Horton method (Horton, 1945; Strahler, 1952; Smart, 1968; Gupta and Mesa, 1988; Gleyzer *et al.*, 2004; Reis, 2006; Moussa, 2009; Chunikhina, 2018;Yamamoto, 2020), they found that salinity increases with the decrease of the stream order. They also discovered that radial averages of salinity are negatively and exponentially correlated with river discharge through an equation that resembles solutions of the 1D advection-diffusion equation under certain theoretical assumptions. The applicability and robustness of these methods is tested now for a system that includes tidal forcing.

An additional method is implemented next to the Strahler-Horton one that is commonly referred to as width function. This is a method that describes bifurcation in terms of the number of channel links in some distance from the outflow (Kirkby, 1976). Width function measures a basin's width distribution in space. Many authors implied a connection between a catchment's width and its hydrologic response (Gupta and Mesa, 1988; Rinaldo et al. 1991; Snell and Sivapalan, 1994; Rinaldo *et al.*, 1995; Botter and Rinaldo, 2003). Collischonn *et al.* (2017) investigated any impact of the width function to a catchment's hydrograph shape while much earlier, Kirkby (1976) mentioned the network's width influence to peak discharge timings.

The present work aspires to give an insight on the influence of tidal forcing on the salinity inside deltaic systems that could contribute to the efforts for providing solutions against the issue of salinization in deltas.

2. METHODS

An idealized river delta configuration is built using the Delft3D software (Deltares, 2013). Delft3D comprises a series of modules to simulate flow, waves, water quality, morphology, sediment transport and ecology. It has been successfully implemented in the past for several applications including the modelling of river deltas, fresh water discharges in bays, stratified density flows and salt intrusion problems (Hu *et al.*, 2009; de Nijs and Pietrzak, 2012; Elhakeem and Elshorbagy, 2013; Martyr-Koller *et al.*, 2017). More information on Delft3D can be found in its manual (Deltares 2013). Matsoukis et al. (2021) developed an idealized model to investigate the spatial and temporal salinity distribution in a river dominated delta. The present work extends and improves this model in order to perform simulations with tidal forcing. We refer the reader to Matsoukis et al. (2021) for details on the governing equations solved numerically and focus hereafter on the setup for the present study.

2.1 Model Setup

The model's bathymetry (Figure 1a) derives from a 2D morphological simulation that precedes the simulations with salinity. Its settings can be found in the 'Online resource' and Table S1. It consists of a narrow inlet of 1.3 km length and 380 m width imposed at the west boundary and a complex channels network developed outside the river mouth. The grid cells between the inlet's borders and the two lateral boundaries are inactive. The channels network extends approximately 8 km offshore

of the river inlet mouth (Figure 1b). The depth is set to increase 10 km offshore of the river mouth with a constant 0.5^0 slope reaching 30 m at the offshore boundary. A structured rectangular grid is used that has dimensions 20 km x 22 km and it can be seen in the 'Online Resource' Figure S1. The grid resolution varies from 50 m to 200 m in the X direction and between 20 m and 100 m in the Y direction of a Cartesian co-ordinate system. The resolution is finer within the channelized network (Figure 1b) and becomes coarser offshore and closer to the boundaries.

This scaled idealized delta configuration exhibits many features common in real deltas such as the delta front slope and the pro delta deepening (Hori and Saito 2002; 2007; Goodbred and Saito, 2010) , the erosion in front of the river mouth and the downstream shallowing and widening of the channels (Lamb *et al.*, 2012). Special care was taken to allow enough space in the longitudinal and lateral directions for the offshore buoyant plume to develop. This bathymetry is kept constant for the salinity simulations with various amplitudes even though the strength of the tidal forcing can develop morphological features that are not represented in this case. However, we are looking at relatively short time scales with respect to morphological change and therefore it is reasonable to assume a constant bathymetry. The use of different morphologies would introduce another varying parameter and would severely hinder isolating the effects of tides and rivers. Therefore, the salinity simulations did not include any sediment input.

The salinity simulations require a 3D model setup and thus 8 vertical sigma layers are added. The model was tested with finer vertical resolution as well. However, it was found that there is no significant impact on the numerical results by increasing any further the number of layers, most probably due to the shallowness of the delta. Considering also the computational resources for a full year study, this number is deemed sufficient for this specific case.

In Delft3D, the horizontal diffusion is resolved by the use of a sub-grid turbulence closure model and a user defined coefficient used for calibration. The default Delft3D value is implemented (10 m/s^2) securing the model stability. The vertical diffusion is fully modelled by the κ-ε turbulence closure model.

A spatially constant Chezy coefficient (45 $m^{1/2}$ / s^{-1}) is implemented to account for bed roughness. A cyclic implicit numerical scheme is used and the time step is 30 seconds being the optimum value for both model stability and computational time.

2.2 Hydrodynamic forcing

The model is forced at the river boundary by a flow hydrograph with a Gaussian shape and data covering a one year period. Many deltas (e.g. Yangtze (Lai *et al.*, 2014; Birkinshaw *et al.*, 2017), the Volga (Polonskii and Solodovnikova, 2009), Po Delta (Montanari, 2012), and the Mississippi (usgs.gov)) present annual flow distributions with a single distinct peak usually in the middle of the year. This shape is very convenient because it allows for an easy distinction between wet and dry seasons so that salinity patterns developed during the relevant periods could be easily detected. The hydrograph is built based on real data from the Po Delta for the year 2009 that exhibited a hydrograph with a close to normal distribution. The data are converted first into a cumulative distribution where each daily flow has a probability of occurrence once in 365 days. A beta distribution probability density function (pdf) is then built using the following equation(Yue *et al.*, 2002):

$$B\,(a,b) = \int_0^1 x^{a-1}\,(1-x)^{b-1}\,dx \qquad (1)$$

$$0<x<1\,;\; a,b>0$$

Where x is the variable and a and b are shape parameters. By taking equal shape parameters, a symmetry is obtained with equal flows between the 1st and 2nd semester (day 1 to day 182 and day 183 to day 365 respectively). The flow data need to be scaled down to ensure stability. The flow velocity is kept constant between the real (Po) and the model data but the Po river discharge is divided by the ratio of the Po river's cross-section over the model's one. The implemented scaled hydrograph can be seen in Figure 1e.

A series of five simulations with the same hydrograph but different tidal amplitudes is carried out: two river dominated and three tide-influenced cases. The first river dominated case assumes no tidal water level variation. The four other amplitudes were selected to represent increasing tidal influences. The ratio between fresh water and tidal volume can be expressed by the Canter-Cremers number, also known as the estuary number N , and defined as (Savenije, 2005):

$$N = \frac{Q_f T}{P_t} \qquad (2)$$

Q_f , T and P_t are the fresh water discharge, the tidal period and prism respectively. High and low estuary numbers indicate larger amount of fresh and saline water respectively entering in the system during a tidal period (Savenije, 2005). The tidal amplitudes for our simulations are then selected based on scaling arguments on the estuary number and inspired by real cases. The characteristics of our five simulations are summarised in Table 1. Scenario 2 represents a river dominated case because its estuary number is much higher and its amplitude much lower than the three other scenarios. The estuary number of the three tidally influenced cases decreases as the amplitude increases and so they can be conventionally classified as representative cases of micro-, meso- and macrotidal regimes.

Table 1 Estuary number, tidal amplitudes and classification for each simulation

Scenario	Estuary Number	Scaled Model Tidal Amplitude (m)	Classification
1	**n/a**	**0**	**River Dominated**
2	**0.49**	**0.02**	**River Dominated**
3	**0.073**	**0.15**	**Micro-tide**
4	**0.018**	**0.56**	**Meso-tide**
5	**0.009**	**1.1**	**Macro-tide**

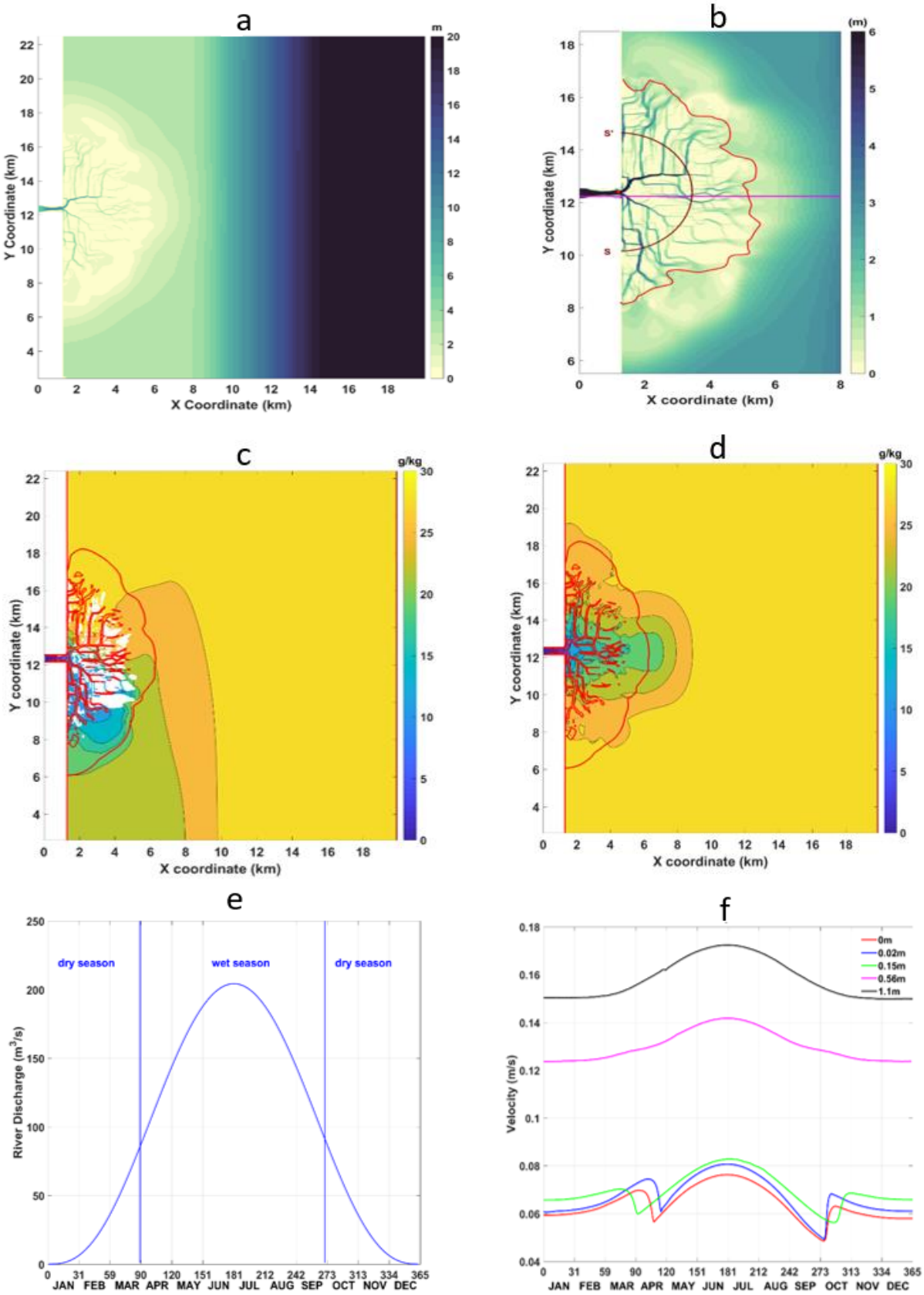

Figure 1 a) Model Bathymetry. The white coloured parallelograms left and right of the river inlet indicate inactive cells. The bathymetry starts to deepen incrementally with a 0.5º slope at X = 10 km. b) Zoom of the bathymetry in the delta area. Notice the much deeper channel on the left of the river inlet (looking seaward). SS' is the semicircle over which salinity is averaged in section 3.5. The red dot is the centre of the semicircle. The magenta horizontal line is the transect where the vertical salinity

distribution is presented in section 3.2 . The red borderline connects the ends of the channels delineating the delta's border. Calculations for Figure 1f and Figure 6 were done for the area upstream of this border. c) ,d) Initial conditions for salinity of Scenario 1 with zero tidal amplitude and Scenario 5 with 1.1 m tidal amplitude respectively. The delta channels and limits are delineated by the red colour line. White areas in panel c indicate dry points above the water level. e) The idealized hydrograph implemented in the model with the corresponding days and months at the horizontal axis. The vertical lines indicate the limit between dry and wet seasons. f) The depth-averaged velocity magnitude for the different tidal amplitudes averaged within the delta limits as delineated by the red borderline in panel b.

2.3 Boundary Conditions

The tide is prescribed at the offshore boundary in the form of a cosine function with its amplitude defined through the Riemann invariant. In Delft3D, the Riemann invariant is introduced as a user-defined parameter with velocity units (Deltares, 2013). An S_2 solar tide is introduced and so the tidal period is 12 hours in every simulation. Such a simplification is reasonably common in idealized modelling (e.g. Guo and Valle-Levinson, 2007) as it significantly simplifies the analysis of the numerical results. Variability due to daily inequalities and at sub-tidal scales (e.g. spring-neap cycles) is neglected with such a tidal forcing but remain beyond the direct scope of the present study. A zero water level gradient (Neumann condition) is implemented at the lateral boundaries. The offshore boundary is considered to be a sea boundary with salinity equal to 30 g/kg. The salinity at the river boundary is set to zero. Free transport is allowed at the lateral boundaries where the model is allowed to calculate its own values. The numerical simulations for salinity do not include any sediment input, the influence of sediments on the baroclinic flow is then neglected and the bathymetry is frozen during the simulation.

2.4 Initial Conditions

A spin-up simulation precedes each one of the five scenarios to generate initial conditions for salinity. In these spin-up simulations, the salinity is set equal to 30 g/kg everywhere except for the river boundary where it is zero. The model in this case is forced by the minimum river flow in Figure 1e, which is equal to the starting value, and the tidal amplitude of each scenario from Table 1. Thus the experiments begin with different initial conditions, dependant on the tidal range. The simulation is stopped when the ratio of salinity and flow velocity over the last two tidal cycles is equal to 1 and quasi-steady state conditions can be assumed. A time period of 45 days is needed for the simulations to reach a quasi-steady state. The initial conditions for the surface layer of Scenario 1 and 5 are presented in Figure 1c and d respectively. The salinity distribution in Figure 1d is symmetric while in Figure 1c is not. The bathymetry is identified as the main cause of this asymmetry in the no tide case because the branch on the left of the delta apex (looking to the sea) is much deeper than the rest of the channels and acts as a flow barrier (Figure 1b). Its depth reaches almost 9 m when the overall mean channels depth is no more than 3 m. This is further discussed in section 3.1.Tidal dynamics are known to affect buoyant plume's symmetry (Chao, 1990; Isobe, 2005; Guo and Valle-Levinson, 2007; Lee and Valle-Levinson, 2013; Leonardi et al.2013). To investigate the tidal effects on the symmetry while bathymetry is already another source of asymmetry, Earth's rotation is not neglected in the simulations as it may also produce spatial asymmetry.

3. RESULTS

3.1 HORIZONTAL SALINITY DISTRIBUTION AND FLOW FIELD EVOLUTION WITH THE TIDAL VARIATION

Map plots in Figure 2 and Figure 3 provide instantaneous isohalines and flow vectors during dry and wet season for each one of the five simulations 3 hours after high water (HW) and low water (LW) respectively at the top layer. Figure 2 displays an instant during ebb and Figure 3 an instant during flood tide. Considering that the period of the solar tide is 12 hours, this means that the tidal level equals the mean water level 3 hours after the HW (MTL_H) and LW (MTL_L). Consequently, the maps

display results for times when the flow velocity at the boundary is closer to its maximum value. The maps show results at two instants 6 months apart: one day (dry season) and 180 days (wet season) after the start of the simulation. The latter corresponds to the day of the maximum and the former to that of the minimum flow.

3.1.1 Salinity variation with seasonality, tidal amplitude and stage

The spatial salinity distribution at the time of minimum flows is asymmetric for the first two scenarios (river dominated cases) because it is affected by the bathymetric asymmetry (see section 2.4). Higher salinity is present on the left and lower on the right of the delta apex (looking seaward) as it can be seen in Figure 2 a,c and Figure 3 a,c. The channels are shallower on the right side and that allows for a faster decrease of salinity under the freshwater influence while this process is impeded by the much deeper channel on the left side of the inlet. The system moves towards a more symmetrical state when higher flows occur during wet season (Figure 2 b,d and Figure 3b,d). The tide can also enhance the flow and override the bathymetric control so that a more symmetric salinity spatial distribution is observed at the maps of the tidally influenced cases for both dry and wet season (panels e-j in Figure 2 and Figure 3). The salinity in the delta is very high during dry seasons. The relevant panels in Figure 2 and Figure 3 (a,c,e,g,i) show that it barely drops below 10 g/kg in the vicinity of the inlet. This signifies salt intrusion in the river inlet. During the wet season (panels b,d,f,h,j in Figure 2 and Figure 3), a deep blue coloured area of low salinity (<5 g/kg) develops. The more symmetric the distribution becomes the more constrained are the areas of low water. Table 2 displays the evolution with the TA of the area with salinity less than 5 g/kg. The area increases progressively with the TA until it reaches the microtide's scenario amplitude (0.15 m). Beyond this threshold, the area decreases as the TA increases so that the macrotide scenario demonstrates the lowest value. Even though the low TA in Scenario 2 enlarges the area compared to Scenario 1 (no tide), the difference between the two cases is not significant.

In the absence of tides (Figure 2a, c and Figure 3 a, c), the salinity beyond the abscissa of 10 km reaches sea water values (more than 27 g/kg) at dry seasons. On the contrary, during the wet season, the isohalines are clustered in the vicinity of the bed slope developing sharp horizontal gradients parallel to the bed (Figure 2 b,d and Figure 3 b,d). In the presence of tides, the enhanced fresh water flow causes sharper horizontal gradients outside of the delta where an offshore buoyant plume starts to develop.

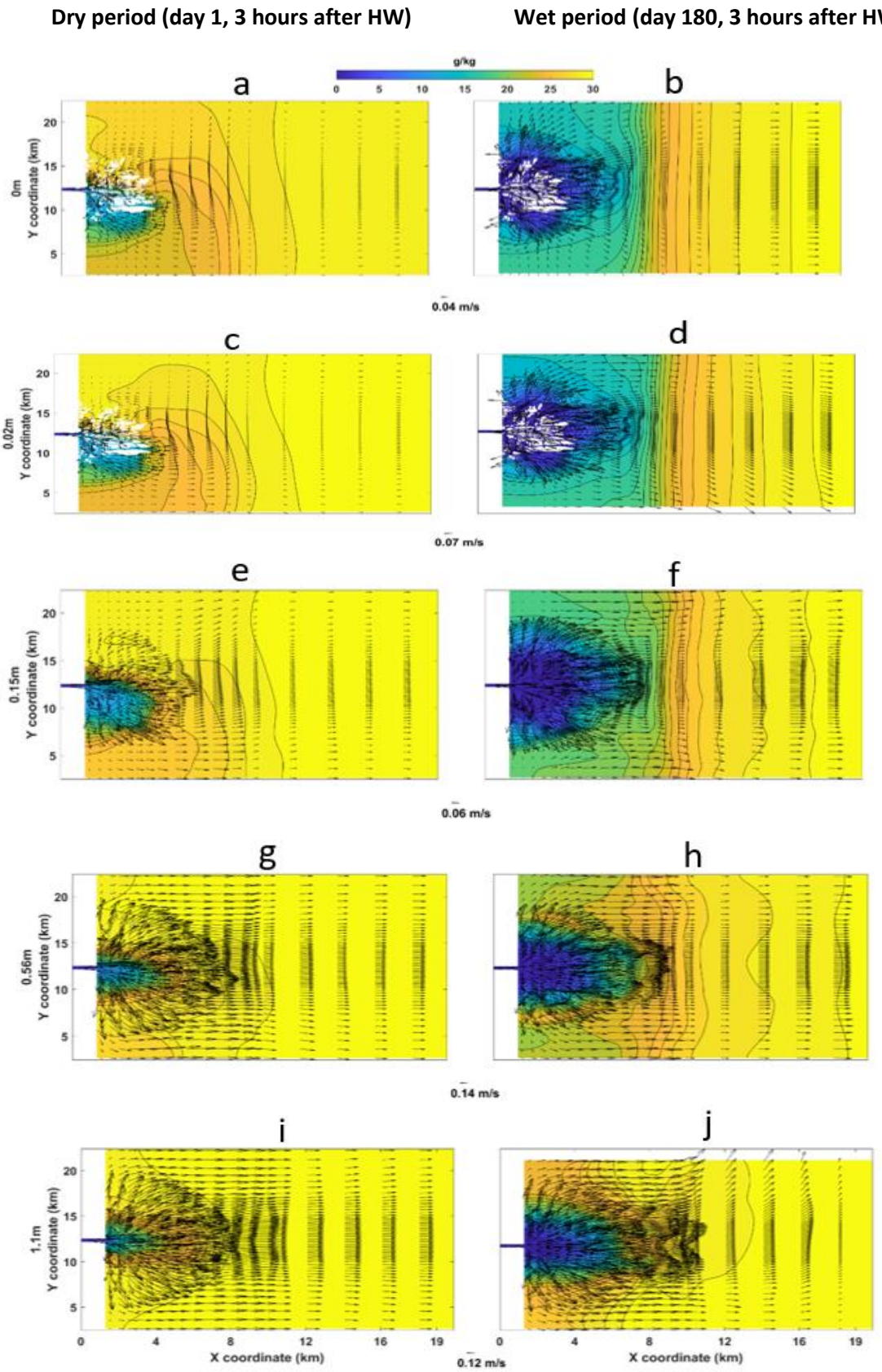

Figure 2 Salinity and flow vectors at the top layer 1 day (dry season) and 180 days (wet season) after the start of the simulation for all amplitudes. The map plots show the salinity and flow conditions 3 hours after High Water (ebb tide). Salinity increments are at 1 g/kg. Flow vector spacing is 10.

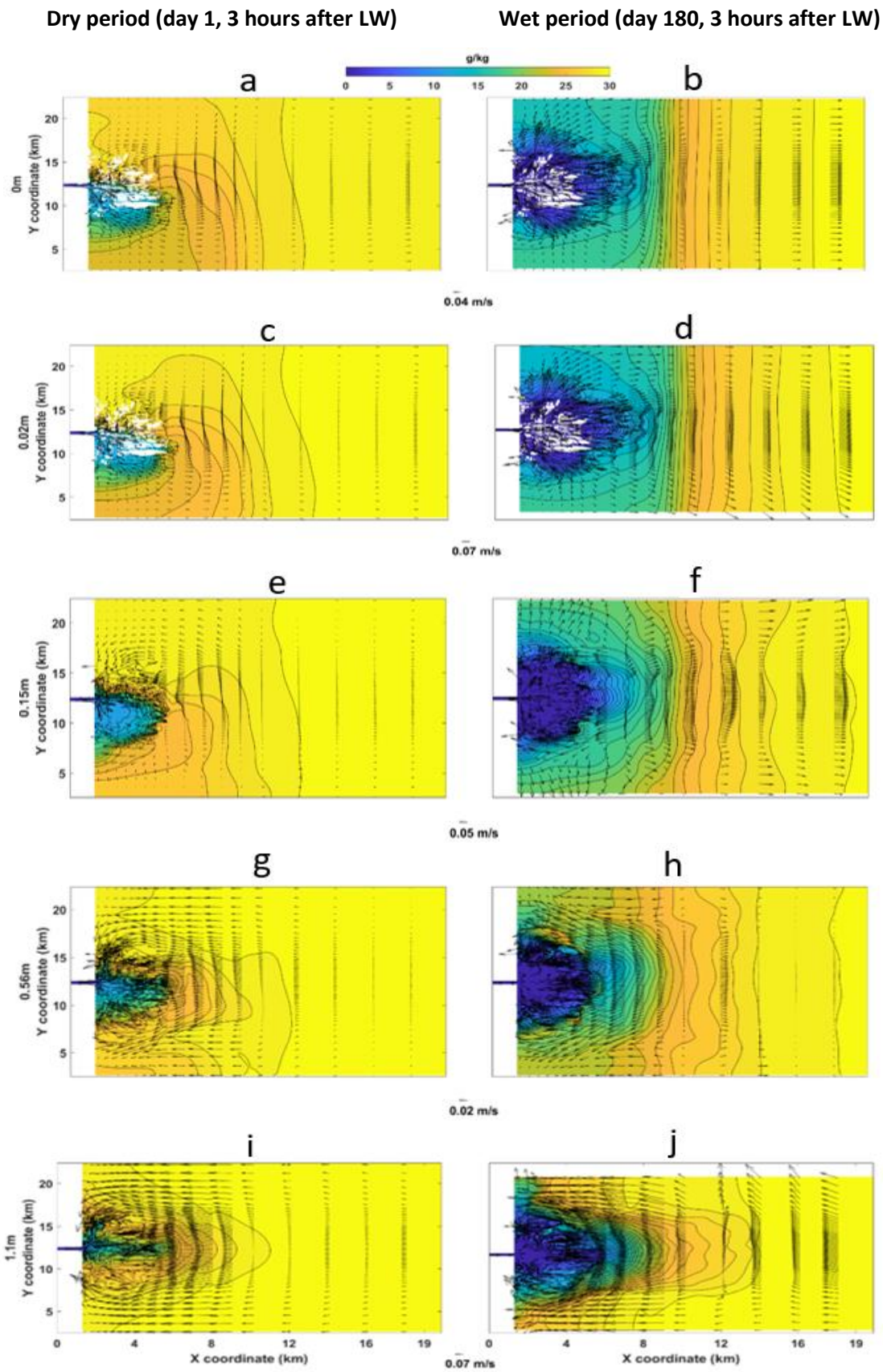

Figure 3 The same content as in Figure 2 but 3hours after Low Water (flood tide). The 0 m amplitude maps are identical but they are included to facilitate the comparison with the other amplitudes.

Table 2 The area within the 5 g/kg isohaline 3hours after LW (flood) and HW (ebb), 180 days after the start of the simulation

AREA ON DAY 180 (km^2) WET SEASON					
Amplitude	0m	0.02m	0.15m	0.56m	1.1m
MTL_L	25.51	25.79	31.51	22.75	18.02
MTL_H	25.51	25.57	29.08	16.20	9.60

Table 3 Fresh water area at times of high water (HW), low water (LW), 3hours before LW (MTL_H) and 3 hours before HW (MTL_L) 180 days after the start of the simulation

AREA ON THE 30th of June (km^2) WET SEASON					
Amplitude	0m	0.02m	0.15m	0.56m	1.1m
LW	16.72	18.30	21.79	14.30	8.27
MTL_L	16.72	18.62	20.95	14.26	10.15
HW	16.72	17.64	15.98	7.28	5.16
MTL_H	16.72	17.94	16.40	8.24	5.54

3.1.2 Flow variation

The two river dominated cases exhibit a common feature which is the presence of dry points inside the delta (white coloured areas in Figure 2 a,b,c,d and Figure 3 a,b,c,d) that lie above the mean water level. In the tidal case (Figure 2 e-j and Figure 3 e-j), fresh water is trapped in these areas but remains stagnant as no flow currents develop between these points.

In the river dominated cases, the high lateral salinity gradients across the inlet observed at dry season have a strong influence on the flow direction. Onshore and offshore flow develops at the high and low salinity areas respectively (Figure 2 a,c and Fgure 3 a, c). The offshore flow magnitude is stronger since the horizontal salinity gradients are higher in this case. The flow becomes parallel to the offshore boundary at the bed slope following the horizontal salinity gradients orientation (see section 3.1.1). During wet season, the flow becomes unidirectional (Figure 2 b,d and Figure 3 b,d).

During flood tide (Figure 3), Scenarios 3, 4 and 5 develop different flow patterns at the deep area downstream of the bed slope. In Scenario 3, the river discharge prevails over the tidal flow imposing a unidirectional seaward flow (Figure 3 e,f). However, landward flow at the flood tide can still be seen in the shallower area upstream of the slope where the delta lies. The flow direction turns landward at the flood tide with its magnitude increasing as the TA becomes higher (compare flow vectors between Figure 3 g, h and Figure 3 i, j).

A better illustration of the flow magnitude increase by the tide can be seen in Figure 1f. The horizontal velocity in the delta is averaged over depth and space (upstream of the red borderline in Figure 1b) and over two tidal cycles to get its daily evolution. The velocity magnitude of Scenarios 4 and 5 is more than double that of the three others and resembles the shape of the hydrograph (Figure 1e) with lower values at dry and higher values at the wet season. On the contrary, the first three scenarios exhibit a short period of velocity decrease (increase) in the 1st (2nd) semester. This is a feature that reflects the impact of the bathymetric asymmetry on the flow jet. When the river discharge is low, the crossflow is downward and the jet turns to the right of the inlet (looking seaward). The jet tends to become

symmetric as the river discharge increases in time. During this transition stage between the asymmetric and symmetric flow jets, the crossflow tends to zero and that causes a decrease of the resultant velocity. With the crossflow almost zero, the total velocity continues to rise following again the hydrograph's shape. The opposite process occurs at the 2nd semester. Figure f clearly shows that the simulations are separated in two groups: Scenarios 1,2 and 3 with salinity distribution constrained by the bathymetry while Scenarios 4 and 5 remain unaffected. In the rest of the paper, the first three scenarios will be referred as bathymetry controlled and the two others as non-bathymetry controlled scenarios.

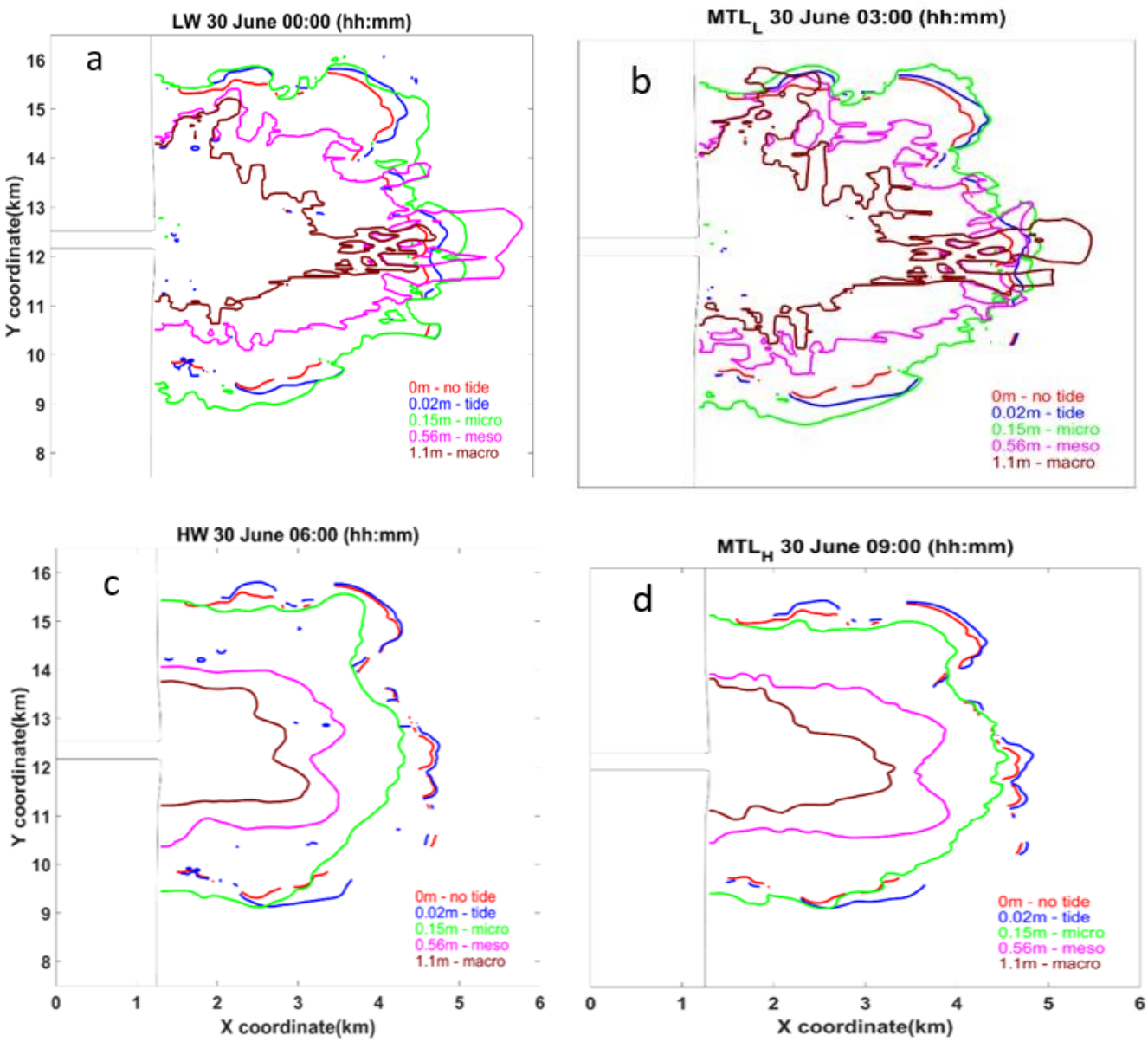

Figure 4 The position of the 2 g/kg isohaline for every amplitude 180 days after the start of the simulation at the surface layer and at times of a) LW, b) 3 hours after LW, c) HW and d) 3 hours after HW. Colours denote the different tidal amplitudes.

3.1.3 Intratidal effect of tidal amplitude variation on the freshwater area

In this study the 2 g/kg isohaline is taken as the limit of the freshwater area (FWA) because this value is generally considered as a threshold of impact to human activities and aquatic life (Schubel, 1992; Monismith *et al.*, 2002; Andrews et al.2017). Figure 2 and Figure 3 indicated that during periods of low flows (left column panels) the salinity is much higher than this threshold. As the river discharge increases in time reaching its peak, the salinity decreases and drops below the 2 g/kg threshold at some instant between the minimum (day 1) and maximum flow (day 180). Figure 4 displays the limits of the 2 g/kg isohaline for the five simulations with different TA at the day of the maximum flow (180 days from the start) and at four instances of the tidal cycle: 1) LW, 2) three hours after LW (MTL_L), 3) HW and 4) three hours after HW (MTL_H). The area within these limits is defined as the freshwater area (FWA).

The no tide isohaline does not vary within the tidal cycle but is included for comparison. The contour lines of the river dominated cases (blue and red colour) are interrupted because of the presence of the dry exposed areas (see the white coloured areas in Figure 2 a, b, c, d and Figure 3 a, b, c, d). In addition, single spots with salinity equal to 2 g/kg appear inside the delta (the blue colour covers the red). These are most likely caused by 'ponding' where fresh water is trapped around the dry areas. Overall, the FWA shows different patterns between flood (panels a,b) and ebb (panels c,d) tide. The 2 g/kg isohaline is smoother at the ebb tide when both river and tidal flow act seaward. The landward tidal flow during flood tide causes lateral changes to the contours shape while an offshore buoyant plume tends to form in the meso and macrotide scenarios (Figure 4 a and b). This leads to a wider FWA during flood (top panels) than ebb tide (bottom panels) in every scenario. In addition, it causes a gradual increase to this area when the amplitude rises from 0 m to 0.15 m while at the ebb tide this occurs only between the two rived dominated cases (Scenario 2 shows higher FWA than Scenario 1). Any increase of the amplitude above these thresholds results in a decrease of the FWA. The FWA variation with the amplitude and the tide can be seen quantitatively in Table 3. These results indicate different salinity response to TA changes depending on the tide (flood or ebb).

3.2 VERTICAL SALINITY DISTRIBUTION IN THE TIDE DOMINATED SCENARIOS

The results in section 3.1 present the spatial salinity distribution in the horizontal direction and revealed the development of an offshore buoyant plume in the tidally influenced scenarios (Figure 2 f,h,j and Figure 3 f,h,j). The plume is the result of buoyant inflow from riverine water entering the delta and has become fully developed at the maximum flow day (~day 180, 01/07). Figure 5 illustrates the vertical salinity distribution along a transect with start and end points at the upstream (X = 0 km) and the bed slope location (X = 10 km) respectively following the magenta coloured line in Figure 1b. Figure 5 displays the vertical salinity distribution on the day of the maximum river discharge (180 days from the start, 1st of July) at the times of the maximum velocity during ebb (panels a,b,c) and flood (panels d,e,f) tide.

The starting point of the offshore buoyant plume may be set conventionally at the delta end (X ~ 5km). The 18 g/kg isohaline (light green colour) seems to delineate best the front between the buoyant water and the ambient seawater with salinity more than 20 g/kg (orange and yellow colour). This front is inclined in the microtide scenario at both tidal stages (Figure 5 a,d). The buoyant inflow causes the lower density water to move faster offshore compared to the denser bottom water. This indicates the development of a surface advected plume. At the ebb tide (Figure 5a), the isohalines have been tilted and stratification is expected to occur at the end of the ebb stage. On the other hand, the flood tide (Figure 5d) pushes the isohalines landward in order to destabilize stratification and develops a bottom

boundary layer at the front location which is capped by the pycnocline. This resembles what is reported by observations of turbulence in shallow estuaries that are characterized by a well-mixed bottom boundary layer being capped by a stable density gradient in shallow estuaries (Stacey and Ralston, 2005). The front location moves further downstream as the velocity increases (i.e. the amplitude increases). As the tidal level increases, tide-induced vertical mixing leads to plume structures that occupy the entire water column. This is very clear in panel c referring to the macrotide scenario. The mesotide scenario (Figure 5 b,e) seems to develop an intermediate plume type between those of the microtide (surface advected) and macrotide (bottom advected). While the plume is in contact with the bottom for some distance, it is detached further downstream where it keeps moving offshore with its front closer to the surface. This is more pronounced at the flood tide (Figure 5e) because the counteraction between landward tidal and seaward river flow tends to lengthen the plume at the surface (see also Figure 2h and Figure 3h). Something similar occurs at the macrotide case (Figure 5f) with the surface layer being deeper in this case since the macrotide bottom advected plume reaches higher depths. Conclusively, a tidal amplitude increase may convert progressively a surface advected to bottom advected plume. In addition, it results in a further offshore front displacement.

Alongside to the buoyant plume structure, Figure 5 gives also an image of the FWA length along this section which is denoted by the dark blue colour. This length is seen to decrease with the amplitude increase before the LW time (ebb tide, panels a,b,c) reflecting the influence of higher tidal prisms on the delta's salinity. On the contrary, it increases with the amplitude in an instant during flood tide probably because the higher tidal flows cause a lengthening when acting against the river flow similarly to what happens with the plume's length at the same times.

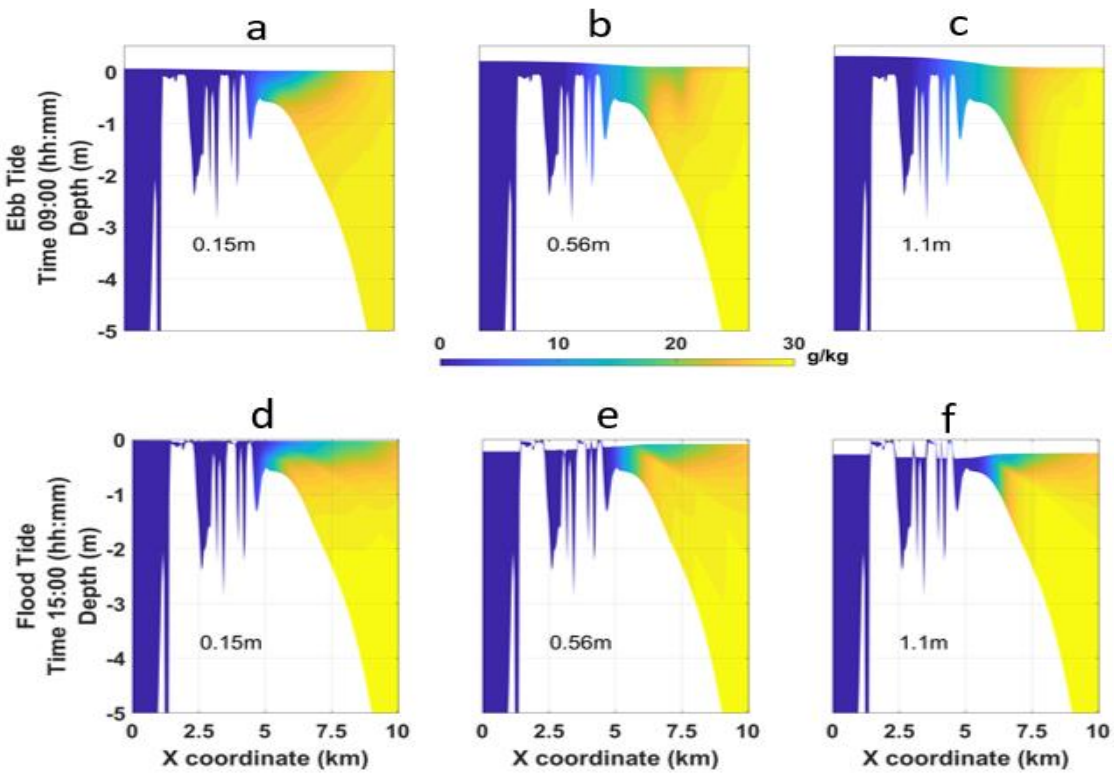

Figure 5 The vertical salinity distribution through the delta along the transect denoted by the magenta colour line in Figure 1b for the three tide-influenced scenarios. Left panels correspond to microtide (0.15m), middle panels to mesotide (0.56m) and right panels to the macrotide scenario (1.1m). Results are presented on the day of maximum flow, 180 days from the start of the simulation and at the time of the maximum velocity during the ebb (a,b,c) and flood (d,e,f) tide.

3.3 FRESH WATER VOLUME EVOLUTION IN TIME WITH THE TIDE AMPLITUDE

To get an overview of the tidal variation impact on the fresh water conditions, the fresh water volume (FWV) of the delta (area upstream of the red borderline in Figure 1b) is calculated. FWV is defined as the product of a segment's fresh water fraction times its volume. Considering the grid cells of the idealized model as segments, FWV is calculated by the following equation (Alber and Sheldon, 1999):

$$\sum_{i=1}^{n}\left[\left(\frac{S_0 - S_i}{S_o}\right) * Vol_i\right] \qquad (3)$$

where n is the number of grid cells, S_o is the oceanic salinity equal to 30 g/kg, S_i is the depth averaged salinity of a grid cell i and Vol_i its volume. Figure 6 depicts the evolution in time of the FWV for the various amplitudes and at the times of maximum (HW, panel a) and minimum (LW, panel b) water volume in the delta. The calculation in equation 3 is done by introducing the salinity values at the times of HW and LW of the first tidal cycle of the day. The FWV evolution follows the hydrograph's shape (Figure 1e) with maximum values at periods of high and minimum at periods of low flows. The FWV curves are affected by the shape of the spatial salinity distribution (section 3.1.1 and 3.1.2). The rate of FWV increase (1st semester) or decrease (2nd semester) changes when the spatial distribution transforms from an asymmetric to symmetric shape and vice versa. This is more obvious in the three bathymetry controlled scenarios (1,2 and 3). The time instants of these changes agree with the corresponding changes of velocity magnitude in Figure 1f. Therefore, the FWV curves are not symmetric with respect to their peak because the spatial distribution remains symmetric more time in the 2nd semester due to the salinity's slower response to decreasing river discharges (Savenije 2005).

At HW times (Figure 6a), FWV of the three bathymetry controlled scenarios is higher than the two others at all times. The FWV of the two river dominated scenarios is almost equal during the entire simulation period. At the wet season, when the high river discharge increases mixing, the difference between the river and tidally influenced cases becomes larger.

At the ebb tide, an amount of sea water leaves the delta while river discharge still flows in it. For this reason, the FWV is higher for every scenario (except for the no tide case) at times of LW (Figure 6b). The tidal cases exhibit higher FWV than the river dominated ones. The reason is that in the absence of tides (and thus tide-induced mixing), the river discharge does not manage to reach downstream areas very far from the inlet where the water remains either partially mixed or stratified. The difference becomes larger at high flow periods (wet season) when combined tidal and freshwater flow usually increase mixing. This does not concern Scenario 5 (maximum TA = 1.1 m) where the FWV increase during wet season is limited so that it is equalled by FWV of Scenario 2. Interestingly, microtide and mesotide scenarios have comparable FWV at most times and an equal maximum occurring in the middle of the year (day 180,1st of July).

According to these results, a TA increase will most likely have different effect on the delta's salinity between HW and LW. Significant decrease can be expected at HW. On the other hand, tidal level increase could be beneficial to some extent at LW.

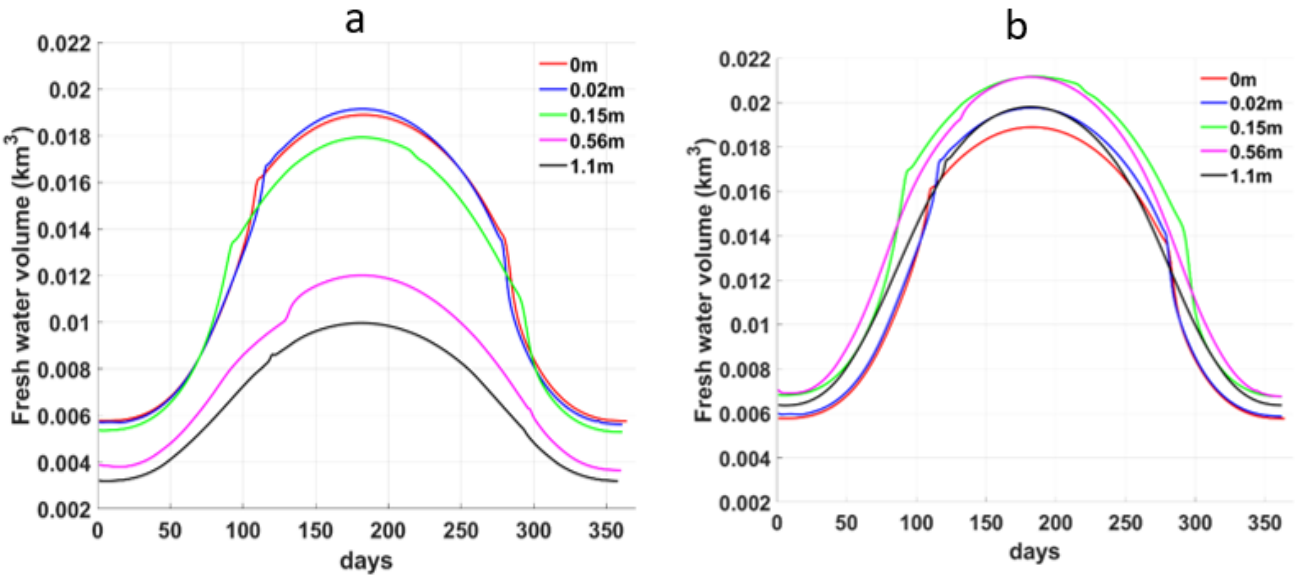

Figure 6 Daily evolution of the fresh water volume in the delta for each scenario at times of a) HW and b) LW for the first tidal cycle of the day.

3.4 CORRELATIONS BETWEEN SALINITY AND DELTA'S BIFURCATION

Stream order

The delta channels are classified and assigned a stream order number (SO) according to the Strahler-Horton method (Strahler 1952) as presented in Figure 7a. To exclude low lying regions of the delta plain, channels shallower than half a meter were not considered. Independent channels disconnected from the main network were also neglected. By this, 57 channels were identified and classified. This idealized delta has a 4th order bifurcation (four stream orders). Branchless channels are of first order. The order increases upstream when two channels of equal order make a junction. If a channel meets with another channel of lower order, its order does not change. Then, the mean over depth salinity is averaged within channels of equal order. The result is further averaged over two tidal cycles to get daily values of the mean per SO salinity. Figure 8 a, b and c show the evolution in time of these averages per SO for Scenario 1, 3 and 5 (TA = 0 m / 0.15 m / 1.1 m respectively). The same plots for Scenario 2 and 4 can be found in the 'Online Resource' (Figure S2 A and B). Figure 8 c exhibits a clear trend with salinity increasing as the SO decreases at all times. On the contrary, this trend is present only at periods of high flows (wet season) in Figure 8a and b where the various orders overlap each other at the start and the end of the year and do not follow a constant succession. The stream orders in Figure 7a expand in space in a somehow semi-circular or symmetric manner so that SO1 channels are located at the end of the delta and SO4 close to the river inlet. It seems then that the trend of increasing salinity with decreasing SO does not apply for the bathymetry controlled scenarios when the spatial salinity distribution is not symmetric.

The bathymetry effect is overcome with the flow enhancement by the TA increase (Figure 1f). In Figure 8a (no tide) the first three orders overlap with each other while in Figure 8b (TA = 0.15 m) only the two first orders do overlap. With the TA increase, the system moves progressively from a state of no symmetry to a symmetric one where the salinity-SO correlation applies again. It looks like the stream order number rule (hereafter SON) works better for symmetric salinity distributions.

Width Function

Since the SON rule was not successful for periods with no symmetric salinity distribution, an alternative solution is needed to relate salinity with delta's bifurcation. Other stream labelling methods (e.g. Horton, Miller-Oiller, Scheidegger) do not serve this purpose because they follow a procedure of channels ordering very similar to the Strahler-Horton. Nevertheless, the width function (WF) offers the opportunity to summarize the delta's bifurcation in terms of channel links rather than the channels themselves (see section 1). It is adapted then for the present idealized delta model. The delta network is divided into three areas by three vertical lines of equal distance (1.1 km) between them (Figure 7b). These lines are drawn starting from the river mouth and until the end of the delta where there are no other junctions. For the width function method to be applicable, its distribution in space must exhibit a certain skewness (positive or negative). With the current space step, a positive skewness appears with the number of junctions reducing downstream as the delta's cross section does. In the following text, the three vertical lines (A, B and C Figure 7b) are referred as generations following Kirkby (1976). The width of each generation is the number of junctions between two successive generations. For example, the width of generation B is the number of junctions between the borderlines of generation B and A. The width A is the number of junctions between generation A and the vertical line crossing through the river mouth (X = 1250 m). Figure 8 d, e and f show the evolution in time of the mean over depth salinity averaged within channels belonging to the same generation for scenarios 1,3 and 5 (TA = 0 m / 0.15 m / 1.1 m respectively). Results for Scenario 2 and 4 can be found in the 'Online Resource' (Figure S2 C and D). The salinity is averaged again within two tidal cycles to get daily values. It is observed that the range of the lateral averages in the WF figures is much smaller than that of the radial averages in the SO ones because channels far from the river mouth and closer to the lateral boundaries are included in every generation increasing these averages. The results show that SO and WF methods may be complementary. In Figure 8d (no tide) and e (microtide), salinity decreases with the width increase only for low flow periods while in Figure 8f (macrotide) this happens at all times. There is an indication that when the SON rule is not applicable the WF can be and vice versa.

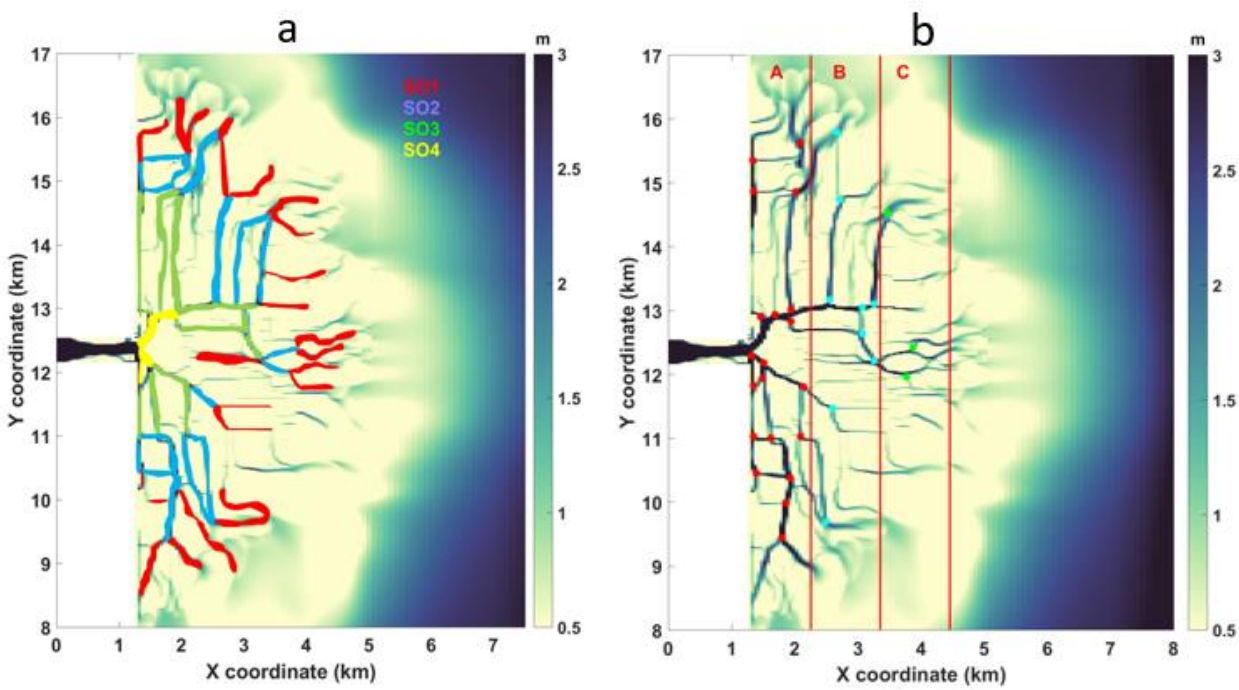

Figure 7 a) A sketch of the delta with the channels coloured by their stream order (SO) number. First order corresponds to branchless channels. The SO increases upstream at every junction between channels of equal order. b) Schematic

representation of the width function method. The junctions between delta channels are denoted by coloured circles. Each colour corresponds to a different generation group that is limited between the vertical lines A,B and C. The lines are drawn with a step of 1.1km between them. The generation A line is drawn 1.1km from the shore. The width of a generation equals the number of the coloured circles per generation group. According to this, the width of A,B and C is 20,9 and 3 respectively.

Fresh water conditions duration in space

Taking a salinity equal to 2 g/kg as a fresh water threshold value (see section 3.1.3), the SO and WF methods could be used in order to determine an indicative time that the water in the delta remains fresh (i.e. the average salinity is < 2 g/kg) in each scenario. Figure 9 illustrates the number of days that the mean over depth salinity remains below 2 g/kg when averaged within channels of the same SO (panel a) and within the same generation (panel b). Both figures project a spatial image of the time that fresh water conditions prevail based on a radial (Figure 9 a) and lateral (Figure 9 b) averaging. In Figure 9a the freshwater conditions duration (FWD) increases in every scenario upstream as the SO does too. FWD rises too as the TA increases from 0 m to 0.15 m. However, this positive effect does not concern channels of SO3 and 4 of Scenario 2 (TA = 0.02 m) that lie close to the inlet and are subject to limited influence from the low tidal level of these scenarios. Within the three tidal cases, the FWD reduces with the TA increase.

Figure 9b shows a common order between generations for every scenario (i.e. B>C>A). However, the lateral salinity averages in Scenarios 4 and 5 do not fall below 2 g/kg at all. This indicates that in the case of very high amplitudes, the fresh water does not reach distant areas laterally and any influence from the river flow is mainly transmitted longitudinally. A paradox is that FWD is minimum in generation A (GA) which is the closest to the delta apex (Figure 7b) and is also smaller than that of generation C (GC) which is the most distant section. The reason is the delta width which is the maximum in GA (equal to 20) and the minimum in GC (equal to 3). This means that GA is the longest section including areas with higher salinity in large lateral distances from the river. On the other hand, GC covers the smallest delta section and thus salinity averages are lower. Consequently, the delta remains fresh for longer periods within the borders of generation B where the delta has its medium width equal to 9.

The microtide scenario emerges in both methods as the one with the longest fresh water period at every order and generation. It is also the only case where even the very distant channels of SO1 become fresh at least for some time (Figure 9a). The calculation of the FWD based on radial and lateral salinity averages may provide some useful conclusions by combining their results. For example, the SO3 channels that become fresh during wet season for 140 days in e.g. Scenario 4 (Figure 9a) are most probably only those located in straight distance from the inlet and not sideways (Figure 7a) since Scenario 4 does not exhibit any results for lateral averages in Figure 9b. In addition, it seems that the delta's cross-sections size may indicate areas of high or low salinity.

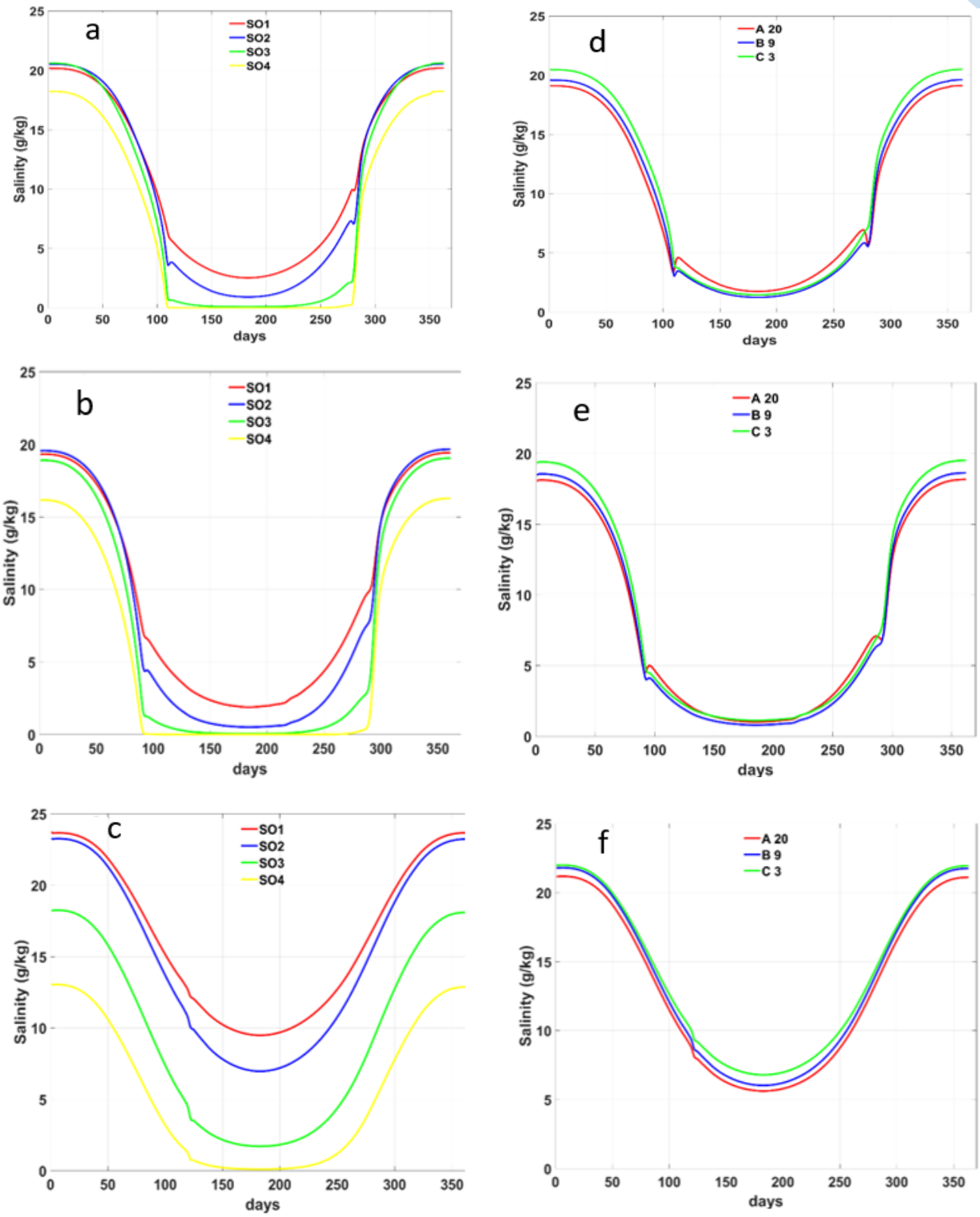

Figure 8 The evolution in time of the mean over depth salinity averaged within channels of the same stream order in a) notide, b) microtide and c) macrotide scenarios. The evolution in time of the mean over depth salinity averaged within channel branches of a generation group in d) notide,e) microtide and f) macrotide scenarios.

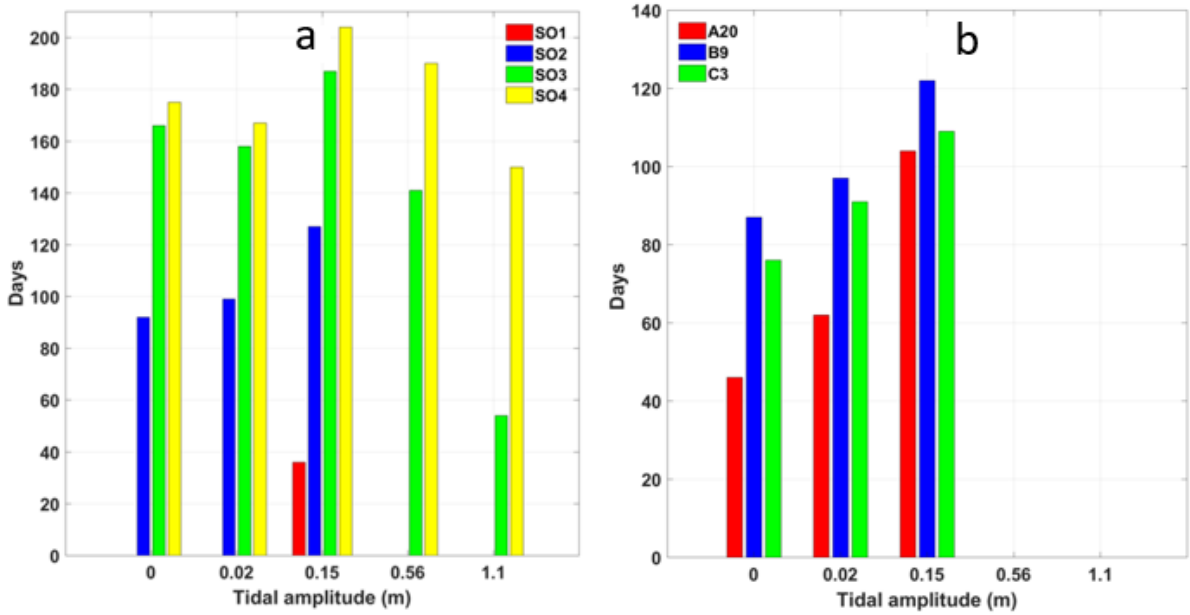

Figure 9 The time in days that the depth averaged salinity remains below 2 g/kg when averaged within channels of the same a) stream order and b) generation group. In order to obtain daily values, the salinity is averaged over two tidal cycles.

3.5 CORRELATION BETWEEN SALINITY AND RIVER-DISCHARGE

Building on Matsoukis et al. (2021), the existence of an exponential salinity (S) - river discharge (Q) correlation in the presence of tides is further investigated. The mean over depth salinity is radially averaged over a semi-circle with its centre at the river mouth (Figure 1b). Figure 10 a and b shows the daily variation between the radially averaged salinity and river discharge for each scenario. Since the hydrograph is symmetric, data for the first semester are used only. A regression analysis between S and Q verifies an exponential correlation for high amplitudes (Figure 10b) which can be justified by both the very high R^2 coefficients and the fitting curves denoted by black colour.

In contrast, the S-Q curves in Figure 10a indicate the existence of a flow threshold which determines two different regimes for the S-Q distribution. It was found that below a threshold, salinity and river discharge are better correlated by a double exponential equation in the following form:

$$S = \alpha_1 * exp^{\beta_1 Q} + \alpha_2 * exp^{\beta_2 Q} \qquad (4)$$

with $\alpha_1 < 0$, $\alpha_2 > 0$, $\beta_1 > 0$, $\beta_2 < 0$. The theory behind equation 4 is further discussed in section 4.2.2. The parts of the S-Q curves that are better fitted by eq. (4) are extracted from Figure 10a and presented separately in Figure 10 c. The included fitting curves (in black colour) and the high values (close to 1) of the R^2 coefficients support the assumption of a double exponential fitting. The value of the flow threshold determining the nature of the fitting equation varies with the TA in Figure 10 c. This depends at the moment the spatial distribution changes from an asymmetric to symmetric distribution. Since this happens earlier in Scenario 3 and later in Scenario 2 (Figure 1f), the flow threshold is higher in the latter and lower in the former. Above the threshold, the S-Q distribution returns to a single exponential form.

The reason for the difference in the S-Q distribution between the high (Scenario 4 and 5) and low amplitude cases (Scenario 1, 2 and 3) is the bathymetric asymmetry but this is discussed in more details in section 4.2.2.

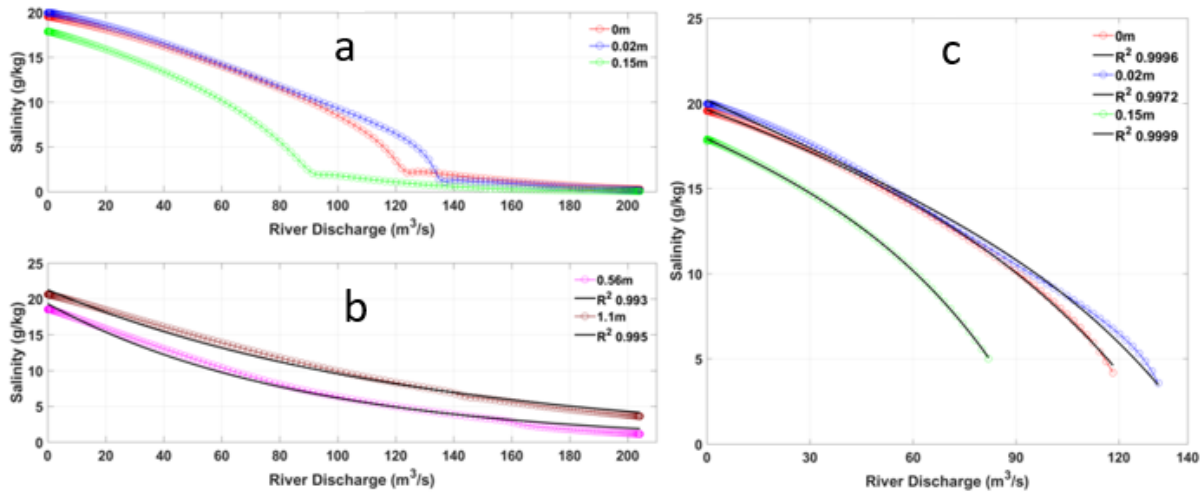

Figure 10 Daily averages of the depth averaged salinity averaged over the SS' semicircle shown in Figure 1b against the daily river discharge (Figure 1f) for a) Scenario 1,2 and 3 and b) Scenario 4 and 5. The tidal amplitude of each simulation is added on the legend. The black lines in panel b are the fitting curves after a regression analysis for a single term exponential equation. The R^2 coefficients for an exponential fitting are included in the legend. c) The salinity (S)-river discharge (Q) curves of panel a cut for a shorter period during which the two magnitudes seem to have a very good fit for a double exponential equation. The R^2 coefficients for the double exponential fitting are displayed in the legend.

4. DISCUSSION

4.1 Impact of the tidal amplitude variation on the salinity distribution

The presence of tides in the system may have several positive effects. For example, when the river discharge is low (dry season), the riverine flow may not be able to transfer fresh water in long distances leaving the downstream parts of the delta with high salinity. Tide-induced mixing though can decrease the salinity in these outer areas. This is the reason why the FWV is higher in the tidal cases at the times of the minimum water level (LW) compared to the river dominated cases (Figure 6b). However, these positive effects may reverse if the TA increases too much and starts decreasing the FWV (Figure 6a). Results indicated that low tide systems may benefit by a TA increase while highly tide dominated systems will not. In the latter case, a decrease of the TA due to SLR could be beneficial for such systems. Within the context of this manuscript, the microtide case (Scenario 3, TA=0.15 m and flow/tide ratio equal to 0.073) represents the boundary between river dominated and tidal influenced cases. The TA increase from 0 m to 0.15 m results in wider low salinity areas (Table 2 and Table 3) and lead to more symmetric spatial salinity distribution (Figure 2 and Figure 3). Therefore, the microtide case provides wider areas of low salinity (<5 g/kg) and fresh water (<2 g/kg) and keeps the delta fresh for the longest period (Figure 9). In contrast, further increase of the TA resulted in a significant reduction of the low salinity areas, fresh water periods and volumes in the delta.

The above should be interpreted as an indication that potential increases of tidal amplitude due to SLR to river dominated systems would have a positive effect against salinization. On the contrary, TA increase by SLR in a meso or macrotidal regime could increase salinity intrusion. This conclusion is of paramount importance for the investigation of future impact on deltas due to SLR and tidal level variations and the efforts against salinization.

Tidal motion imposes several mechanisms on buoyant inflow. Garvine (1999) identifies enhanced vertical (tidal) mixing, tidal straining and subtidal flow nonlinearities as some of them. These may be the cause behind the differences in the spatial salinity distribution due to TA variations. At low flow times (panels a,c,e,g,i in Figure 2 and Figure 3), freshwater flow is directed to the right of the delta apex decreasing the salinity but leaving almost unaffected the areas left of it. The TA increase leads to

more symmetric shapes (compare between panels a,c,e and g,i in Figure 2 and Figure 3). Such tidal effect has been observed on buoyant plumes deflected to the right under the influence of the Coriolis force (in the northern hemisphere) or in the presence of ambient crossflows (Chao and Boicourt, 1986; Chao, 1988; O'Donnell, 1990; Lie-yaw Oye, 1992; Kourafalou *et al.*, 1996; Narayanan and Garvine, 2002; Lee and Valle-Levinson, 2013; Cole and Hetland, 2016). Since none of these parameters is included in these simulations the asymmetry in the present case can only be ascribed to the bathymetry (see section 2.4). Many plume studies argued on the effect of high tidal forcing that diminishes such deflections. Chao (1990) has stated that the tidal residual circulation enhances the plume growth and limits the coastal jet. Garvine (1999) noticed that tidal forcing restricts the plume advection in the across-shelf direction decreasing significantly the upshelf and downshelf penetration. This tidal effect towards more symmetric plumes is a common conclusion in a number of other papers concerning buoyant plume structures under tidal influence (Chao, 1990; Isobe, 2005; Guo and Valle-Levinson, 2007; Lee and Valle-Levinson, 2013).

At high flow times (panels b,d,f,h,j in Figure 2 and Figure 3), the TA increase constrains the size of the low salinity area (blue coloured with salinity less than 5 g/kg) but causes also the development of an offshore buoyant plume. The plume lengthens at flood tide (Figure 3) when tide acts landward and river flow seaward. The freshwater plume develops a density front with important dynamics such as flow nonlinearities and influences the shelf circulation at the bottom boundary layer (Csanady, 1984; Wright, 1989; Chapman and Lentz, 1994). Increases of the inflow velocity move the front farther downstream (Yankovsky and Chapman (1997)) and this can be seen in the results of Figure 5. The frontal location moved downstream as the amplitude increased because the flow becomes stronger in this case. Many of the features in Figure 5 may imply tidal straining effects. Simpson *et al.*, (1990) talk about a distortion of the initially vertical isohalines at the start of the ebb that are later distorted by differential displacement. The isohalines tilting in Figure 5a probably reflects this kind of distortion under the effect of advection from buoyant inflow. This process is expected to reverse at the flood tide that acts in favour of mixing and destabilizes stratification (Figure 5d). This kind of effects are less visible in the meso and macrotidal cases because a different type of plume is developed that comes in contact with the bottom for a certain length. Yankovsky and Chapman, (1997) studied the buoyant plumes vertical structure and classified them as surface or bottom-advected. In the latter, the plume occupies the entire water column and the density front extends from the surface to the bottom. In the former, the plume is confined in a thin layer close to the surface and spreads offshore having no contact with the bottom. They identified also a third plume type in an intermediate stage between surface and bottom advected. In this case, the plumes spread offshore in contact with the bottom but beyond some distance the upper part of it detaches from the bottom. It is generally considered that higher tidal amplitudes act in favour of bottom advected plumes while stronger river discharge tends to stratify the water column developing surface advected plumes (e.g. Yankovsky and Chapman, 1997; Guo and Valle-Levinson, 2007). The results in section 3.2 indicate a progressive plume conversion from surface to bottom advected as the TA increases. From the three tidally influenced scenarios, the lower amplitude simulation (Scenario 3) develops a surface advected offshore plume irrespective of the tidal stage (Figure 5a,d). Plumes of this kind may cause stratification and anoxic conditions at the bottom layers and low oxygen can have environmental consequences to the aquatic life (Chant, 2012). For example, riverine waters are responsible for recurrent summertime hypoxia at the bottom waters of the river dominated Mississippi Delta (Schiller *et al.*, 2011). In this context, the microtide amplitude is not so beneficial because contaminants (e.g. organic matter, pesticides, toxic chemicals) from activities such as municipal wastes, industry and agriculture are trapped decreasing the water quality.

Figure 5 b and e indicate that the mesotide scenario develops an intermediate plume that lifts off in a certain distance from the delta end. Atkinson (1993) mentions similarities between the depth of detachment and the depth of maximum flow jet penetration. The plume liftoff occurs in a distance of approximately 6 km from the river boundary where the bed starts to deepen. At this site, it is not hydraulically possible anymore for the freshwater flow to be any deeper (Atkinson, 1993). The detachment depth is shorter at the flood tide because of increased entrainment (mixing) (Atkinson, 1993; Chen and MacDonald, 2006). However, this also reduces the salinity in the detached part of the plume (Figure 5e). The thickness of this detached plume layer is higher in the macrotide scenario (Figure 5f) probably due to the higher tidal flow even though its length at the surface is shorter.

4.2 Impact of tides and bathymetry on the salinity distribution

4.2.1 Stream labelling and bifurcation methods

Previous work (Matsoukis et al.2021) indicated that the salinity is expected to increase as the SO decreases in a river dominated delta. This was tested again in this new idealized delta used for simulations including tides. The tide does not seem to modify this relationship as the same distribution between salinity and SO is observed in Figure 8c (macrotide case). The bathymetry was identified as a factor that influences and prevents this correlation. Due to its nature (symmetric distribution of SO), the SON scheme could not be implemented when the salinity distribution is not symmetric. At these times, the width function scheme proved to be a successful alternative. Averaging the salinity laterally and not radially leads to a similar relationship with salinity decreasing as the width increases. This is very convenient since the two methods appear to be complementary to each other. If the salinity does not decrease with a SO increase, it does decrease with the width increase and vice versa. In addition, the WF rule is successful when the river discharge is low while the SON is mostly associated with high flows.

The duration that each method is applicable and the time of interchange between them might be important to know. The time of shift from SON to WF rule could indicate the duration of low and high flow periods, the threshold values between them and the shape of the spatial salinity distribution. Figure 11 gives a timeline of the period and duration each method applies in the five scenarios. The timeline shows that SO rule applies for the whole simulation period in the mesotide case (TA=0.56 m) while both methods apply at all times in the macrotide case (TA = 1.1 m). A conclusion can be drawn here because it seems that high amplitude scenarios develop salinity distributions that satisfy both methods independent of seasonal flow variations. Therefore, the timeline is discussed only for the three bathymetry controlled scenarios that demand the use of both methods for a correlation between salinity and delta's geometry.

In the 1st semester, the WF implemented at low flow periods is valid only for 90 days in the microtide case. It remains valid though for longer times in Scenario 1 (109 days) and Scenario 2 (116 days). The one week difference between the two river-dominated scenarios means that the spatial salinity distribution becomes symmetric one week later in Scenario 2 than in Scenario 1.This agrees with Figure 1f that shows one week difference at the time moments the velocity starts to increase before the peak flow (see section 3.1.2). That the velocity starts to increase after a short break is indicative that the flow has become symmetric. Notice also that in the 2nd semester the velocity starts to fall (after a short break) at the same time for these two scenarios (281 days after the start). Figure 11 shows that the SON rule stops to be applicable at the same time for both river dominated cases (also 281 days after the start). This correspondence between the times that the delta's velocity magnitude changes and the times of SON and WF interchange exists in the microtide case as well. SON is applicable for the maximum time in the microtide case compared to the river dominated cases which

is not a surprise knowing that the fresh water period associated with relatively higher flows is longer in Scenario 3 (Figure 9).

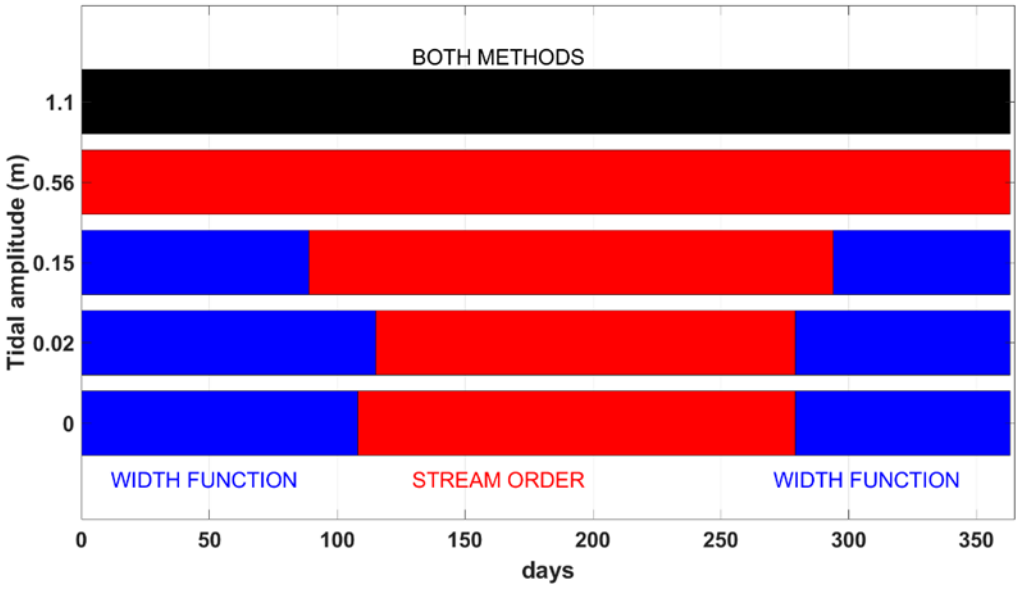

Figure 11 A timeline that shows the number of days that salinity decreases with the increase of the stream order or the delta's width (width function) against the tidal amplitude implemented in each scenario. Salinity decreases with the stream order increase during the entire simulation when the tidal amplitude is 0.56m. The salinity decreases with both the stream order and width increase during the entire simulation when the tidal amplitude is 1.1m (black bar).

4.2.2 Salinity – river discharge relationship

The analysis in section 3.5 tested the existence of an S-Q exponential correlation in every scenario following the work by Matsoukis et al. (2021). The authors argued also that the exponential solution in this case approximates solutions of the 1D advection-diffusion equation under certain theoretical assumptions which are also exponential. The tide does not seem to modify this correlation as it can be seen in Figure 10b for the mesotide and macrotide cases. However, Figure 10a shows a different kind of distribution between S and Q for the bathymetry controlled scenarios. Instead of the tide, the bathymetry does influence the S-Q correlation as it does in the salinity-SO relationship. A regression analysis indicates that the depth and radially averaged salinity in the delta can be better approximated by an exponential equation with two terms (eq.4). This equation could also be a solution of the 1D advection-diffusion equation but for different boundary conditions.

The much deeper channel on the left of the delta apex (Figure 1b) causes a significant decrease of the flow velocity compared to the rest of the delta and impinges the spreading of freshwater beyond of it. In fact, it acts as a flow boundary. Fischer et al. (1979) presented a series of analytical solutions of the diffusion equation under several initial and boundary conditions. They considered the case of a mass concentration spreading in a 1D system where there is a wall at some distance preventing the flow beyond of it. In this case, the solution is a double exponential equation which is the outcome of the superposition of the real solution (single term exponential) plus an imaginary one that would be the solution if the wall was not present. It seems that the fitting equation (eq.4) is similar to this theoretical case. Equation 4 can be divided in two parts as follows:

$$\begin{cases} S = A + B \\ A = \alpha_1 * exp^{\beta_1 Q} \ , A < 0, \beta_1 > 0 \\ B = \alpha_2 * exp^{\beta_2 Q} \ , B > 0, \beta_2 < 0 \end{cases} \quad (5)$$

In the original theoretical case of a wall, the two terms A and B are positive and their exponent coefficients negative so that the concentration of the pollutant increases in front of the wall. The present case is slightly different because the deeper river branch is not impermeable and fixed as a wall would be. Fresh water flows through the channel and downstream of it but not in a constant rate. The salinity is under the influence of two parameters: the freshwater flow that decreases the salinity and the deeper channel that delays this process. The latter influence weakens in time while the former is enhanced. The signs of the exponent coefficients in equation 5 indicate that A is a growth and B a decay term. It can be inferred then that the negative term A represents the river discharge influence and the positive term B that of the deep channel that delays the rate of salinity decrease for some time. When the river discharge exceeds a threshold overcoming the deep channel's influence, the S-Q relationship returns into a single exponential form.

An interesting finding is that these flow thresholds are equal in each case with the flow at the times of interchange between WF and SO as presented in Figure 11. The flow thresholds and the day of interchange between WF and SO are given in Table 4. Notice that the variation of the flow and the day index in the hydrograph is the same.

Table 4 The value and index in the hydrograph of the maximum flow in each S-Q curve of the three bathymetry controlled simulations in Figure 10 and the flow magnitude at the time of interchange from WF to SO in Figure 11. The time instant of interchange from WF to SO method coincides with the time instant of interchange from double to single exponential equation between salinity and river discharge.

Tidal amplitude	**0m**	**0.02m**	**0.15m**
Flow threshold (m^3/s)	**120**	**133**	**87**
Day index in the hydrograph	**109**	**116**	**92**
Day of interchange between WF and SO	**109**	**116**	**92**

5. CONCLUSIONS

A 3D idealized delta model was built in Delft3D to investigate the combined impact of tides and varying river flow on the salinity in deltaic systems. The model was forced by an annual fresh water flow from the river head and a tidal level prescribed at the offshore boundary. A symmetric hydrograph of Gaussian shape was implemented with very low and high flows allowing to detect different patterns developed at both dry and wet seasons. A series of five simulations with different amplitudes was carried out where both river dominated and tidally influenced cases were considered.

Changes in the tidal amplitude in deltaic systems may have either positive or negative effects depending on their initial state. Increases of amplitude in river dominated or low tidal systems were found to offer several advantages. The tide enhances the mixing in the delta and widens areas of brackish or fresh water. This flow enhancement is beneficial during the low flows periods because it helps to override bathymetric effects that produce asymmetric spatial salinity distribution leaving large areas with very high salinity. Tidal amplitude and river discharge increases lead progressively to more symmetric distributions. In addition, imposing medium tidal amplitudes extends the time the delta remains fresh during the wet season. Tide-induced mixing increases the fresh water volume in the delta compared to the river dominated cases where the river discharge influence on the salinity weakens in the most distant from the delta apex areas that remain either partially mixed or stratified

during the wet season. However, the freshwater is constrained in narrow areas around the inlet and its volume decreases significantly when the amplitude corresponds to meso and macrotide regimes. This results in the delta containing freshwater for shorter time periods compared to the river dominated and microtide cases. Tidal amplitude increases in such systems will deteriorate the conditions in terms of salinization. In such cases, an amplitude decrease would be favourable instead.

An offshore buoyant plume develops at flood tides with its vertical structure being determined by the tidal amplitude. Low amplitudes favour surface advected and high amplitudes bottom advected plumes. Surface advected plumes may have several consequences on the water quality offshore of the delta counterbalancing the positive effects of tides inside the delta in low and medium amplitude regimes.

Finally, the role of bathymetry was found to be important because it affects the spatial salinity distribution. This has an impact on several salinity correlations that were found to exist in a previous idealized study done for a case without tides. The salinity increases as the channels order decreases as long as its distribution remains symmetric and unaffected by bathymetry. In this case, the width function is suggested as an alternative where the salinity decreases as the width increases. The stream order method was successful at times of high and the width function at times of low flows. Asymmetric distributions do affect also the exponential correlation between radial salinity averages and river discharge. As long as the spatial salinity distribution is not symmetric, the two magnitudes are correlated by a double exponential equation that shows similarities with the solution of the 1D advection-diffusion equation in the presence of a wall boundary preventing the flow behind of it. Therefore, it is inferred that the methods are not affected by tidal forcing but can be sensitive to bathymetric differences.

6. SUPPLEMENTARY INFORMATION

Table S3 Main setting parameters of the 2D morphological simulation

Parameter	Value
Simulation period	**34 days**
River discharge	**3000 m^3/s**
Offshore tidal level	**0 m**
Cohesive sediment fraction concentration	**0.5 kg/m^3**
Non cohesive sediment fraction concentration	**0.2 kg/m^3**
Morphological factor	**175**
Time step	**12 seconds**
Spatially constant Chezy roughness coefficient	**45 $m^{1/2}/s^{-1}$**

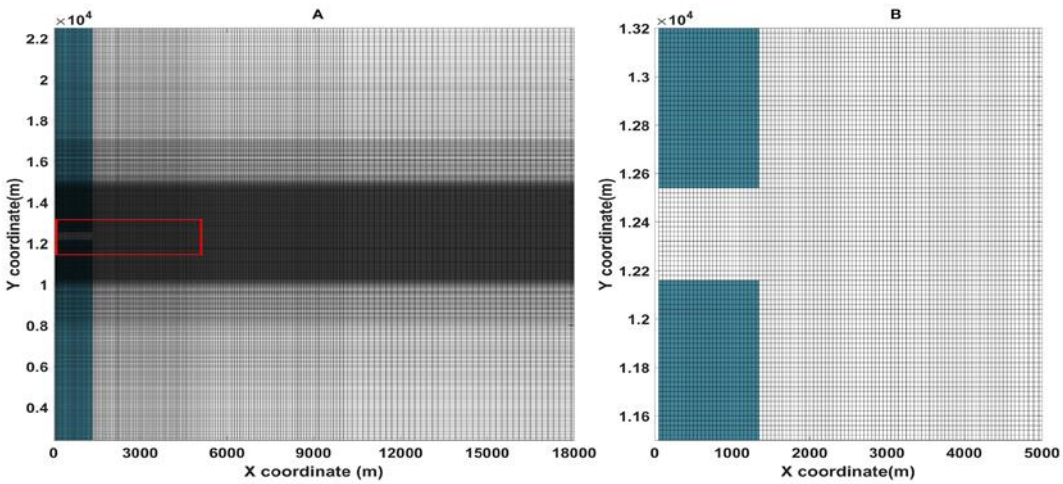

Figure S16 A) The model grid. Blue coloured areas are dry cells and white coloured wet ones. B) Zoom in the red box area in A) to show finer resolution in the inlet vicinity.

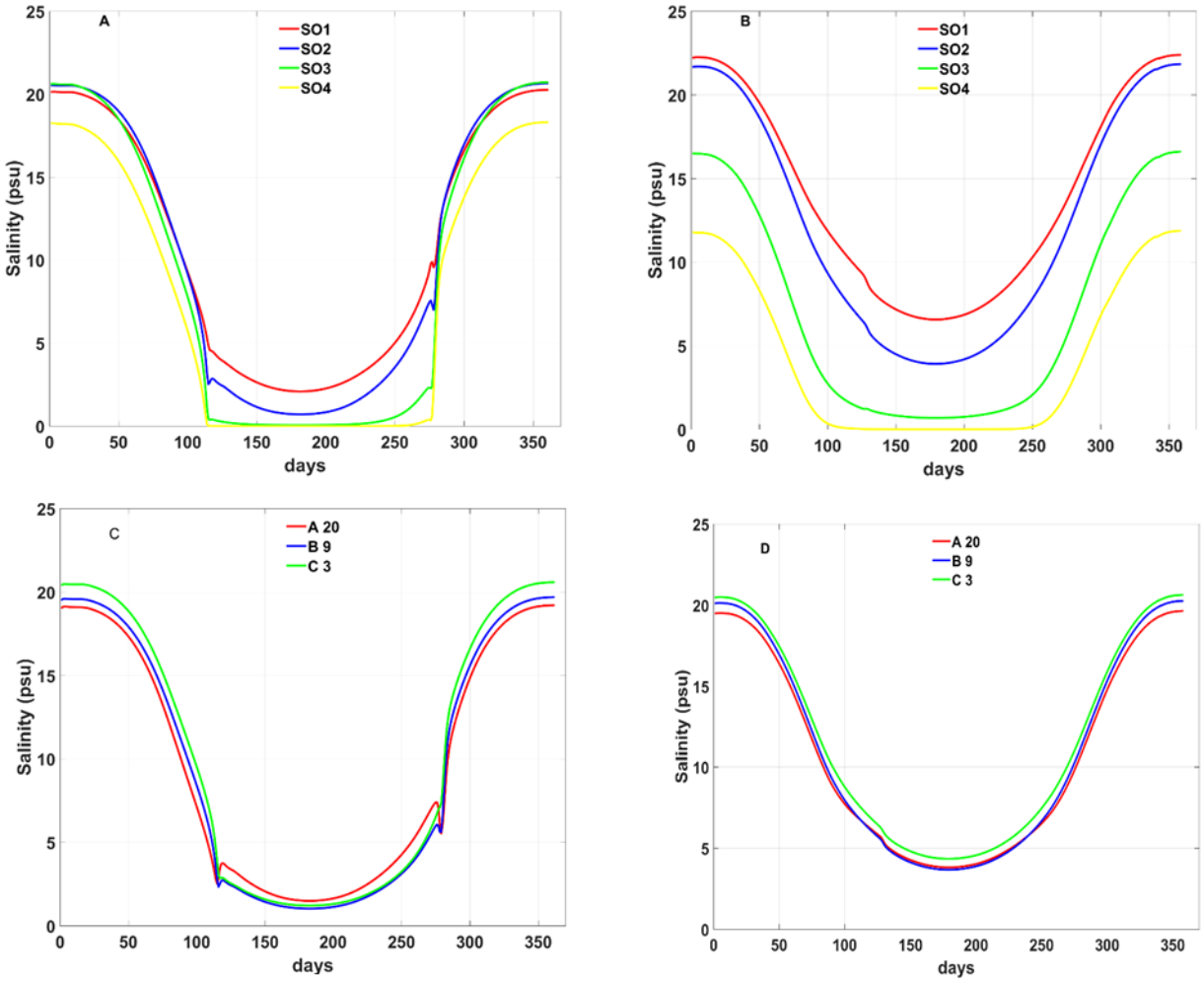

Figure S17 The evolution in time of the mean over depth salinity when averaged within channels of equal SO in Scenario 2 and Scenario 4 respectively. C,D)The evolution in time of the mean over depth salinity when averaged within channels belonging in the same generation group for Scenario 2 and Scenario 4 respectively.

6. The effect of hydrographs shape on river deltas salinization

Constantinos Matsoukis[1], Laurent O. Amoudry[2], Lucy Bricheno[2], Nicoletta Leonardi[1]

(1) University of Liverpool, School of Environmental Sciences, Department of Geography and Planning, Roxby Building, Chatham St., Liverpool L69 7ZT, UK

(2) National Oceanography Centre, Joseph Proudman Building, 6 Brownlow Street, Liverpool, Merseyside, L3 5DA, UK

Corresponding author: c.matsoukis@liverpool.ac.uk

This paper has been submitted to the Water Resources Journal and is now under review

First Author Contribution: Conceptualization, Methodology, Software, Pre- and Post-processing, Visualisation, Formal analysis, Writing, Original draft and reviewed versions preparation.

Link to preceding chapters: This paper uses the idealized model implemented in the previous paper. It extends the work of chapter 4 by implementing a number of different hydrographs in a system with no tides. The goal is to assess the effect of various annual hydrographs shape on the salinity.

Key Points:

- The shape of annual hydrographs influences the level of salinity in river deltas and can contribute to a more sustainable water management.
- The peak flow magnitude and hydrographs tails determine freshwater areas, residence and renewal times and stratification.
- Salinity responds slower to flow decreases than increases and decreases faster with higher hydrographs slopes.

ABSTRACT

Excessive salinity can harm ecosystems and compromise the various anthropogenic activities that take place in river deltas. The issue of salinization is expected to exacerbate due to natural and/or anthropogenic climate change. Water regulations are required to secure a sufficient water supply in conditions of limited water volume availability. Research is ongoing in seek of the optimum flow distribution establishing longer-lasting and fresher conditions in deltas. In this study a three–dimensional (3D) numerical model was used to unravel the influence of hydrographs shape on the deltas salinity. Our results show that it is possible to improve the freshwater conditions in deltas without seeking for additional water resources but by modifying the water distribution. The peak flow magnitude and timing and the tails of a hydrograph were found to be important parameters affecting stratification, freshwater residence and renewal times. Hydrographs having lighter tails and smaller range were the most successful in keeping the delta and its river inlet fresher for longer periods. Salinity distributions showed a slower response to decreasing rather than increasing river discharges. An increase in the flow rate can achieve a desired salinity standard in much shorter time. Hydrographs with heavier tails can push the salt intrusion limit further away and are more efficient in mixing the water column. However, they present low freshwater residence and high water renewal times. These

results have implications for coastal scientists and stakeholders dealing with the management of freshwater resources in river deltas across the world.

PLAIN LANGUAGE SUMMARY

High salt concentration is detrimental for the anthropogenic activities taking place in river deltas. Natural or anthropogenic climate change can increase the salt water threatening the deltas sustainability. Limited freshwater availability demands the design of new water management policy to secure a sufficient water supply. It is speculated that the problem can be solved with friendlier environmental instead of technical solutions. This study investigates the effect of different annual freshwater flow distributions on the deltas salinity. By implementing numerical modelling for an idealized river delta, it was discovered that it is possible to establish longer-lasting freshwater conditions. Attributes of a hydrograph such as the peak flow magnitude, timing and its tails were found to be important parameters. Hydrographs with light tails can keep the delta fresh for longer times while higher peak flows can result in freshwater covering larger areas and decrease stratification. For equal flow ranges, the salinity was found to decrease faster than increasing. Higher flow rates can decrease salinity to a desired standard in shorter time. These results have implications for coastal scientists and stakeholders dealing with the management of freshwater resources in river deltas across the world.

1. INTRODUCTION

Rising sea level and decreasing streamflow threaten water resourcing and freshwater availability by exacerbating salt intrusion in low lying areas such as deltas (Zhou *et al.*, 2017). Salt intrusion (SI) is a serious problem that affects households, agriculture, irrigation and industry (Allison, 1964; Smedema and Shiati, 2002; Zhang *et al.*, 2011) because rivers and aquifers contaminated by high salinity decrease freshwater storage and water quality (Gornitz, 1991). In addition, SI reduces soil fertility resulting in low crops yield (Bhuiyan and Dutta, 2012), threatens vegetation and marine species with limited salinity tolerance (Visser *et al.*, 2012; White *et al.*, 2019), increases plants mortality (Kaplan *et al.*, 2010; Bhuiyan and Dutta, 2012) and affects human health (Sarwar, 2005; Rahman *et al.*, 2019).

Many deltas face already the consequences of salt intrusion including the Mekong in Vietnam (Nguyen and Savenije, 2006; Trieu and Phong, 2015; Eslami *et al.*, 2019) the Ganges-Brahmaputra in Bangladesh (Nobi and Das Gupta, 1997; Bhuiyan and Dutta, 2012; Rahman, 2015; Yang *et al.*, 2015; Bricheno, Wolf and Islam, 2016; Sherin *et al.*, 2020; Bricheno, Wolf and Sun, 2021), the Mississippi in the Gulf of Mexico (Holm and Sasser, 2001; Day *et al.*, 2005; Das *et al.*, 2012) , the Yangtze in China (Chen *et al.*, 2001; Hu and Ding, 2009; Dai *et al.*, 2011; Qiu and Zhu, 2015), the Pearl River (Liu *et al.*, 2019; Hong *et al.*, 2020) and the Nile Delta (Frihy, 2003). Unfortunately, limitations in water supply come along with an increase in water demand because of population growth, economic development and land use change (Phan *et al.*, 2018).

Sustainable water management and enhanced water conservation practices are necessary for the available water supply to meet with the future demand (Dawadi and Ahmad, 2013). These practices often rely on the scientific consensus that salt intrusion reduces as river discharge increases (Garvine et al. 1992; Gong and Shen, 2011). In the absence of tides or other driving mechanisms (i.e. atmospheric or oceanic forcing) the river discharge dominates the salinity distribution (Valle-Levinson and Wilson, 1994; Wong, 1995; Monismith *et al.*, 2002). During the 20th century, water management relied on technical and engineering solutions (Ha *et al.*, 2018). The so called 'hard-path' approach

consisted of dams, aqueducts, pipelines and complex treatment plants (Gleick, 2003). However, this type of solutions often comes with a cost. For example, tens of millions of people have been displaced by their homes due to water related projects (Adams 2000) while the flows reaching many deltas are not adequate anymore and this has several consequences for the local environment and population (Gleick, 2003). Recently, the need for more adaptive management to sustain freshwater resources has been identified (Ha *et al.*, 2018; Zevenbergen *et al.*, 2018). A 'soft-path' approach for water is now promoted that would include regulatory policies for better use of existing water resources than seeking for additional ones (Gleick, 2002). In this context, an efficient water usage is preferred with equitable distribution and sustainable system operation over time while local communities should be also included in water management decisions (Gleick 2002; Wolff and Gleick 2002; Gleick 2003). Within this concept, the problem of salt intrusion in deltas could probably be mitigated by an efficient water management of a catchment's freshwater availability instead of resorting to technical solutions. This could be achieved for example by storing a certain amount of water that is available during a wet season and supply it during the next dry season when the demand for freshwater is higher. Coastal reservoirs -water storage structures constructed at a river estuary or other coastal area to store fresh water and control water resources- have already been constructed in China, South Korea, Hong Kong and Singapore (Tabarestani and Fuladfar 2021; Yuan and Wu, 2020). Independent of a hard or soft path, the main management strategy is to affect river discharge, which is likely to cause changes to the annual hydrograph. Even though salinity response to changes in river discharges has been studied extensively in estuaries (Garvine et al.1992; Wong, 1995; Uncles and Stephens, 1996; MacCready, 1999; Chen et al. 2000; Monismith *et al.*, 2002; Bowen & Geyer 2003; Banas *et al.*, 2004; Chen, 2004; Hetland and Geyer, 2004; Brockway *et al.*, 2006; Liu *et al.*, 2007; Lerczak et al.2009; Gong and Shen, 2011; Wei et al. 2016) it is still unclear if and how this changes in the presence of a channelized network.

The present study investigates the effect of various annual flow distributions of equal water volume on the salt intrusion. The paper tries to answer questions such as: 1) how does salinity respond to flow changes, 2) what is the impact on salinity from hydrographs shape changes depending on the cause of change, 3) which is the most appropriate flow distribution to minimize stratification and 4) which hydrograph ensures high water quality (i.e. low salinity) and for how long.

The answer to the last question derives from measuring flushing and residence times that are useful tools to assess the efficacy and adequacy of a certain flow distribution for averting the salt intrusion (Choi and Lee, 2004; Sámano *et al.*, 2012). Flushing time (FT) is defined as the time required for the cumulative freshwater inflow to equal the amount of freshwater originally present in the region (Dyer 1973; Sheldon and Alber, 2002). The simplest and most common method for the FT calculation is the freshwater fraction in which the freshwater volume is divided by the freshwater input (Lauff 1967; Dyer 1973; Fischer et al. 1979; Williams, 1986). A difficulty on the determination of the freshwater volume and input arises in the case of unsteady flow and tidal conditions. Many researchers implemented the method by taking averages over a certain period (Pilson 1985;Christian et al.1991;Asselin & Spaulding 1993;Balls, 1994; Lebo et al. 1994; Swanson & Mendelson 1996;Eyre and Twigg, 1997;Chan Hilton et al. 1998; Alber and Sheldon, 1999; Hagy, Boynton and Sanford, 2000; Huang and Spaulding, 2002; Sheldon and Alber, 2002; Huang, 2007). Alber and Sheldon (1999) proposed a specific technique to determine the appropriate averaging period of the river discharge by assuming that this should be equal or very close to the flushing time itself. They tested their method in Georgia Estuaries. Whereas the FT is a unique value representative of an entire water body, the residence time (RT) is a measure of spatial variation (Choi and Lee, 2004; Sámano *et al.*, 2012). It is defined as the remaining time that a particle will spend in a defined region after first arriving at some

starting location (Zimmerman, 1976; Sheldon and Alber, 2002). Therefore, the RT is applied within a restricted geographical area such as an estuary, a water basin or a box model (Hagy et al. 2000; Sheldon and Alber, 2002; Sámano *et al.*, 2012).The knowledge of a particle's RT is important because pollutants exert most of their effects only if their biochemical scales are smaller than that (Wang et al. 2004; Yuan et al. 2007). In the case of freshwater, RT would mean the time between entering and leaving a domain and therefore might also be called as the transit time (Sheldon and Alber, 2002).

A freshwater RT would normally correspond to a certain salinity threshold. The acceptable salinity levels can vary depending on the various aforementioned activities. For irrigation and agriculture, some studies accept salinity of up to 4 PSU (Clarke *et al.*, 2015) but others suggest values below 2.5 PSU (Đạt et al.2011). Some marine (e.g. phytoplankton, larvae fish, shrimps, smelt etc.) and vegetation (e.g. Sagittaria Latifolia, Sagittaria Lancifolia, phragmites australis) species do not survive in environments with more than 2 PSU salinity (Jassby *et al.*, 1995; Visser *et al.*, 2012; Hutton *et al.*, 2016; White *et al.*, 2019; Wang *et al.*, 2020). Salinity in drinking water must be less than 1 PSU to avoid the development of germs related to water borne diseases like cholera (Ahmed & Rahmad;Sarwar, 2005; Dasgupta *et al.*, 2015). Overall, a critical threshold of 2 PSU appears to satisfy most of these requirements and thus the bottom 2 PSU isohaline (commonly denoted in the literature as X2) is often used as an indicator for salt intrusion (Schubel, 1992; Monismith *et al.*,1996,2002; Herbold and Vendlinkski, 2012; Andrews et al. 2017). Therefore, the freshwater RT in this study is defined as the time that the salinity remains below 2 PSU.

For the purposes of this study, a 3D numerical model for an idealized delta configuration is built in Delft3D and five simulations with different flow distributions are carried out. The implemented hydrographs follow typical distributions that can be often found in real deltas. The paper aspires to provide answers through the idealized modelling for a more sustainable use of freshwater resources in deltaic systems.

2 METHODS

2.1 Model setup

The present work uses a 3D model with an idealized delta configuration that can be seen in Figure 1F. The model that was built in Delft3D (Deltares, 2014) encompasses a larger area with dimensions 20 km x 22 km but the area of interest for this research contains only the delta configuration with its channels and interdistributary areas (Figure 1f). Results outside of the delta and throughout the deeper offshore area are not presented as they are out of this paper's scope. The model's bathymetry remains constant during the simulations and there is no sediment input. Bed level changes are not considered so that the impact of flow distributions on the salinity is isolated from any morphological effects. The vertical resolution consists of eight sigma layers. The default Delft3D values for horizontal diffusion and viscosity are introduced in the model equal to 10 m^2/s and 1 m^2/s respectively. A spatially constant Chezy coefficient (45 $m^{1/2} / s^{-1}$) is implemented to account for bed roughness. A cyclic implicit numerical scheme is used and the time step is 30 seconds being the optimum value for both model stability and computational time. The model's grid resolution and bathymetry can be found in the Appendix (Figure 8, Figure 9 and Table 3).

2.2 Hydrodynamic forcing

The model is forced with an annual river flow distribution. Five simulations are setup with hydrographs of equal water volume but different shape each time. A real flow distribution with data from the Po Delta for 2009 (Montanari, 2012) is used to construct the hydrographs. The data are converted first

into a cumulative distribution where each daily flow has a probability of occurrence once in 365 days. A beta distribution is then built using the following equation (Yue *et al.*, 2002):

$$B\ (\alpha, \beta) = \int_0^1 x^{\alpha-1}\ (1-x)^{\beta-1} dx \qquad (1)$$

$$0<x<1\ ;\ \alpha, \beta > 0$$

Where x is the variable and the shape of the hydrograph is determined by the shape parameters α and β. The normalized probability distribution is then converted to a flow distribution by multiplying by the annual water volume of the real hydrograph (Po Delta in 2009). However, the data need to be scaled down to fit the model's dimensions and ensure its stability. The scaling is done based on the river cross-sections' ratio between the real (Po Delta) and the idealized delta. The produced hydrographs can be seen in panels a-e of Figure 1. Table 1 presents the basic statistic parameters for each beta distribution. Equal shape parameters result into symmetric hydrographs (Figure 1 a,b,c) and the higher their value the higher the peak is. When α is smaller than β a positively skewed hydrograph occurs (Figure 1d). The hydrograph exhibits negative skewness when b is smaller than a (Figure 1e).

The five hydrographs in Figure 1 can be qualitatively classified based on their shape and the tails of each distribution as: 1) Platykurtic (light tails and low peak), 2) Mesokurtic (relatively light tails and medium peak), 3) Leptokurtic (heavy tails and high peak), 4) Positively skewed (long tail on the right) and 5) Negatively skewed (long tail on the left). All of them correspond to seasonal regimes with a pronounced wet season (Hansford et al. 2020). The distinction between heavy and light tails in this paper is defined as follows: heavy tails indicate distributions with larger probability of getting an outlier (e.g. leptokurtic) and light tails indicate distributions that go to zero faster than the exponential distribution (e.g. platykurtic) (Bryson 1974;Glen 2016).

Annual flow distributions with shapes close to the hydrographs of Figure 1 are recorded often in many real deltas. For example, right skewed hydrographs (Figure 1d) were reported in deltas located at the Gulf of Mexico including the Wax Lake Delta in the years between 2006 and 2010 (Shaw et al. 2013) and the Mississippi Delta between 1993 and 2012 (Kolker et al. 2018). Based on large data records from internet data bases and national agencies, Latrubesse et al. (2005) showed that the Mekong and the Ganges-Brahmaputra river catchments develop usually left skewed annual hydrographs (Figure 1e). The Yangtze delta sees its peak flow often in the middle of the year at some time during the wet season that occurs between May and September (Birkinshaw *et al.*, 2017). Such flow distributions are similar to that of Figure 1c and have been reported in the years between 1996 and 2005 (Lai *et al.*, 2014; Birkinshaw *et al.*, 2017) in the Yangtze Delta. In addition, when Hansford et al. (2020) averaged daily flow data for the period 1978-2009 in the Parana Delta (Argentina), they detected an annual flow hydrograph very similar to a platykurtic distribution (Figure 1a). Finally, mesokurtic hydrographs as the one in Figure 1b have been observed in the Colorado and Nile deltas. Averaged annual hydrographs for the 1950-1993 period in the Colorado (Pitlick and Cress ;2000) and flow distributions at several stations in the Nile (Eldardiry and Hossain, 2019) confirm this. The averaged over the years 1984-1996 annual hydrograph in the Niger Delta also exhibited a mesokurtic hydrograph shape (Lienou *et al.*, 2010).

2.3 Boundary Conditions

The effects of tides and the Coriolis force are neglected in order to isolate the influence on salinity from the various flow distributions. A zero water level is implemented at the offshore boundary while the Riemann condition (in the form of a zero velocity variant) applies in the lateral boundaries. Fresh water is assumed at the upstream river boundary and seawater salinity (30PSU) at the offshore and lateral boundaries.

2.4 Initial Conditions

A spin-up simulation precedes each time to get a dynamic equilibrium for salinity to be introduced as initial conditions. A uniform salinity equal to 30 PSU is implemented in the model except for the river upstream boundary where zero salinity is imposed. It is decided to spin-up the model with the initial flow of each hydrograph in Figure 1. These are very small but non-zero values and this reduces the time required to reach a dynamic equilibrium. In this way, the simulations will start from dry season (low flows) conditions. The river flow in the spin-up model is constant and the simulation is stopped after 30 days when steady state conditions are reached in all cases.

Table 1 Statistical Parameters for each hydrograph type

Scenario	Shape parameters	Kurtosis	Qmax (m^3/s)	Qmean (m^3/s)
Platykurtic	a =b = 2	2.14	140	93
Mesokurtic	a =b = 4	2.45	204	93
Leptokurtic	a = b =8	2.68	293	93
PosSkewed	a = 2 b= 4	2.62	197	93
NegSkewed	a = 4 b= 2	2.62	197	93

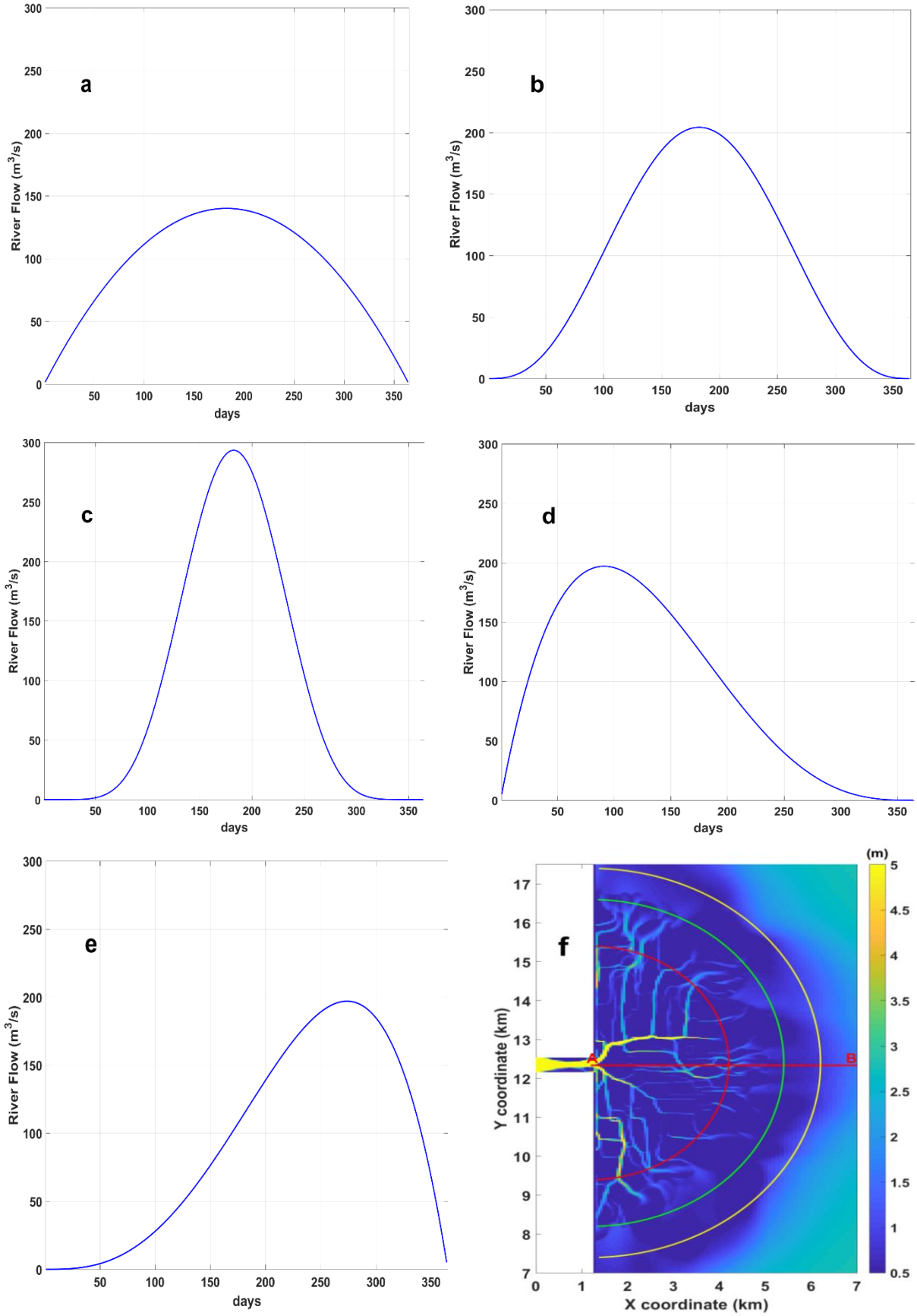
a
b
c
d
e
f
River Flow (m3/s)
days
Y coordinate (km)
X coordinate (km)
(m)
A
B

Figure 1 The hydrographs implemented in the model: a) Platykurtic b)Mesokurtic c) Leptokurtic d) Left Skewed and e) Right Skewed flow distribution for one year. f) The delta bathymetry. The red line AB measures the 6km distance from the river mouth (point A) corresponding to the length of the salt intrusion curve displayed in Figure 5b. The coloured semicircles with their centre at point A and radius 3km (red), 4.2km (green) and 5km (yellow) visualize the cross sections over which salinity is averaged for the result analysis in sections 3.1, 3.2 and 3.4.

3 RESULTS

3.1 Salinity response to river discharge changes

Previous studies detected a hysteresis on the salinity's temporal response to flow changes in estuaries (Hetland and Geyer 2004; Savenije 2005; Chen 2015). The salinity responds slower to flow decreases than increases. An investigation follows on the existence or not of this hysteresis in the idealized delta for the symmetric and skewed hydrographs in separate. To do this, the salinity is first averaged over depth and over a radial cross-section of 3 km distance from the mouth. Then, this is plotted either in time and/or against the river discharge. The decision to show results for this particular radial section (3 km) for both symmetric and skewed distributions is taken with the consideration that it is probably safer to assess the salinity response in a location with medium influence of the river discharge where the water does not become completely fresh. This is a somewhat arbitrary decision but it does not affect much the conclusions. The same analysis but for a section closer to the river (1 km) (available in the Appendix, Figure 10 and Figure 11) shows similar results.

3.1.1 Symmetric Hydrographs

Figure 2a displays the mean over depth daily salinity averaged over a radial cross-section of 3 km distance (red semicircle in Figure 1f) from the mouth at every date for the three symmetric distributions. The bottom axis shows the dates of the 1st semester and the corresponding salinity for each day denoted by dotted lines. During the 1st semester the salinity decreases monotonously. The top axis shows the dates of the 2nd semester in reverse order starting from right to the left and the corresponding salinity for each day is denoted by circled lines. During the 2nd semester the salinity increases monotonously. The unique daily values of the river discharge from each one of the three symmetric hydrographs are also added in the plot displayed as continuous lines and with its scale being on the right axis. Due to the symmetry, the dates on the top are projections of the dates on the bottom axis of equal river discharges. Therefore, the points of intersection of a vertical line drawn in Figure 2a with the dotted and circled lines give us the salinity level at days of equal flow.

Figure 2a shows that initially, the order between the three symmetric distributions is as follows: $S_{leptokurtic} > S_{mesokurtic} > S_{platykurtic}$ because the relationship between the river discharge (Q) magnitude of the three symmetric distributions follows the opposite order $Q_{platykurtic} > Q_{mesokurtic} > Q_{leptokurtic}$. The order between the river discharges changes as the flow increases in the 1st semester and so does that of the salinity. $S_{leptokurtic}$ falls below $S_{platykurtic}$ at first and $S_{mesokurtic}$ a few days later. The dates of the intersection between the salinity curves correspond to the dates of intersection between the flow curves in each case which means that the salinity becomes lower in one simulation when its flow becomes higher than the flow of another simulation.

The opposite procedure takes place at the 2nd semester and as long as the flow decreases. The salinity of the leptokurtic hydrograph becomes higher than the mesokurtic and then than the platykurtic salinity.

Figure 2a indicates that there is a hysteresis on the salinity's response between increasing and decreasing flows. For example, the leptokurtic salinity falls below the platykurtic one in the 1st semester on the 5th of May. This means that the change occurs only 55 days before the peak flow day

on the 1st of July. On the contrary, the leptokurtic salinity becomes higher than the platykurtic one in the 2nd semester on the 10th of September. This is 72 days far from the 1st of July (peak flow day) which shows a delay in comparison to the interchange in the 1st semester between the two simulations. Similar conclusions can be drawn when comparing between any couple of simulations.

In addition, it can be seen that there is a time frame in each simulation when the salinity in the 2nd semester is always lower compared to its corresponding date of equal flow in the 1st semester. This indicates that the salinity might not be equal at dates of equal flow depending on whether the flow is increasing or decreasing and whether the peak flow has occurred already or not. However, this effect is not present for very low flows (at the start of the simulation) or very high ones while getting closer to the peak flow day. In this case, the salinity is equal for equal flows independent of increasing or decreasing river discharge.

To get a clearer image of this salinity asymmetry between 1st and 2nd semester, the salinity differences of more than 0.5 PSU between the two semesters are plotted in Figure 2b for each day and each simulation separately. The maximum salinity difference increases with the peak flow magnitude but the duration of salinity differences decreases with it. For example, differences in salinity between the two semesters can reach 10 PSU in the leptokurtic case but they are present only for approximately 1.5 months. On the contrary, the maximum salinity difference in the platykurtic case is 8PSU but differences are present for 2.5 months instead.

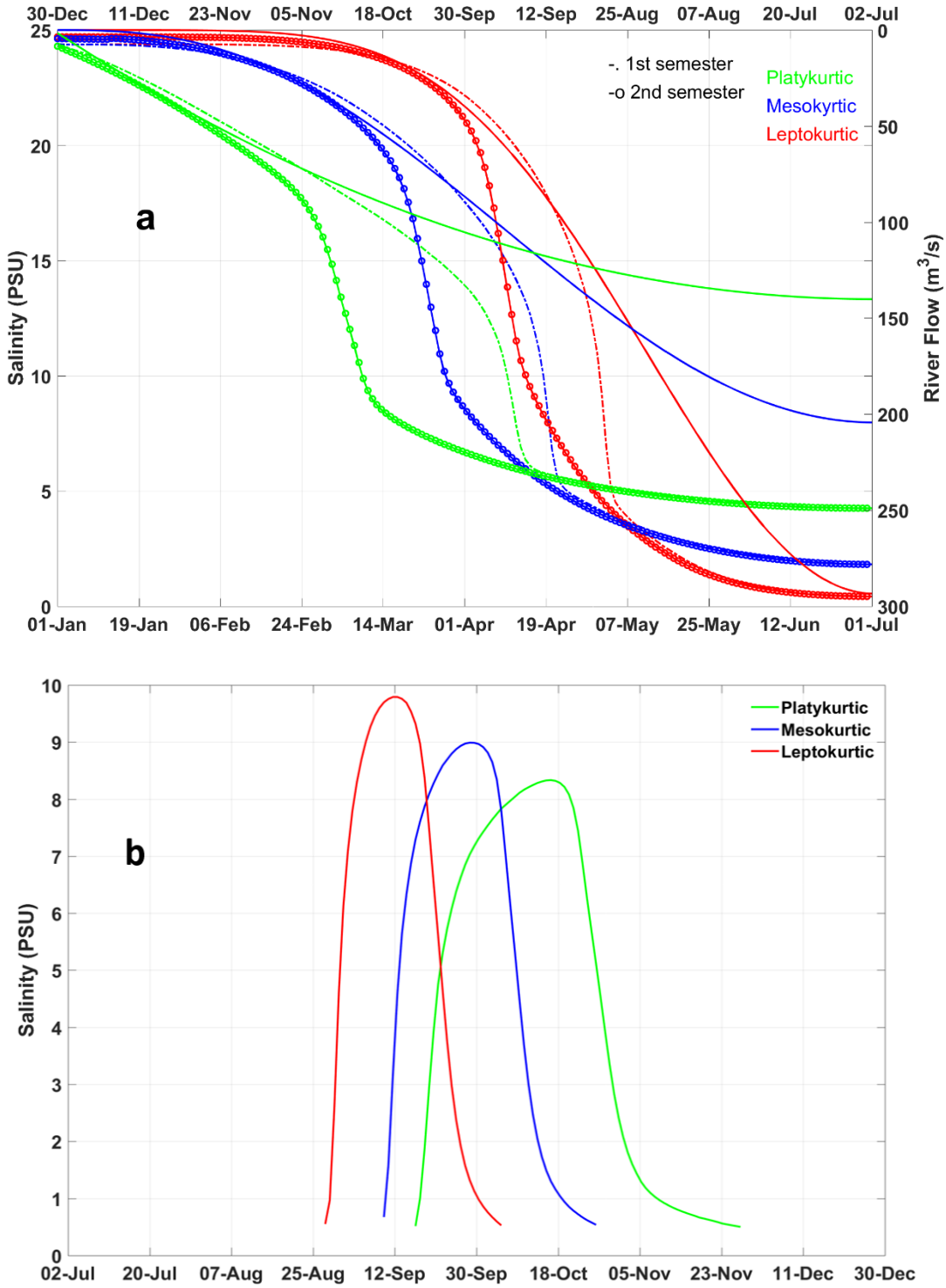

Figure 2 a) A comparison of the mean over depth salinity averaged over a distance of 3km from the river mouth between the three symmetric distributions. Bottom axis shows the dates of the 1st semester. The dotted lines denote salinity in the 1st semester. Top axis shows the dates of the 2nd semester moving from right to the left. Circled lines denote salinity in the 2nd semester increasing from right to the left. The river discharge of each symmetric distribution is added with continuous lines and with its scale on the right axis. The flow increases from 1st of January until 1st of July following the bottom axis and decreases from 2nd of July until 31 of December following the top axis. b) A timeline of the salinity differences above 0.5 PSU between the 1st and 2nd semester for each symmetric distribution.

3.1.2 Skewed hydrographs

The analysis for the two skewed hydrographs is presented in a different manner since the flow range remains the same in both cases. Figure 3 displays the salinity averaged over depth and over the radial cross section 3 km far from the mouth against the river discharge. The positive skewed case shows almost equal salinity between the start and the end of the simulation. The long tail covers a period of 9 months with decreasing flows that allows the salinity to recover and return to its initial state. In contrast, the salinity for the negative skewed hydrograph is about 1 PSU lower at the end of the simulation compared to its initial value. In this case, the simulation ends with the short tail that covers a period of only 3 months with a very sharp flow decrease that does not allow the salinity to recover.

There are indications of a hysteresis in salinity's response to flow changes in Figure 3 as well. Both simulations exhibit a time frame with lower salinity during the decreasing flow periods compared to equal discharges at increasing flow periods. The salinity is lower in the short tail for the negative skewed and in the long tail for the positive skewed case.

Similarly to what is observed in Figure 2a for the symmetric hydrographs, there is a flow range with equal salinity. This occurs during high flow periods. When the flow is between 120 m^3/s and 200 m^3/s the salinity is equal between the two skewed hydrograph simulations. This means that for very high flows, the salinity's response is independent of skewness and of increasing or decreasing flows.

The flow range in the short and long tails is equal in both simulations and varies between very low discharges and the peak flow that is close to 200 m^3/s. The short and long tail seem to cause the same level of salinity variation as this fluctuates between 0 PSU and 24 PSU. This indicates that by increasing the flow rate a salinity standard could be achieved in much shorter time.

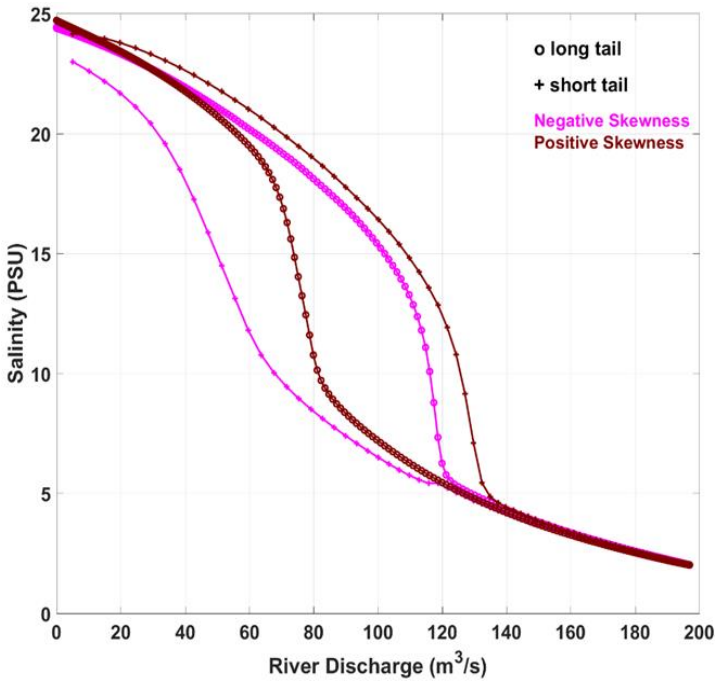

Figure 3 The mean over depth salinity averaged over a distance of 3 km far from the river mouth against the river discharge for the two skewed hydrographs. The circles correspond to the dates of the long tail and the crosses to those of the short tail.

3.2 Stratification

Changes in the river discharge affect the stratification. Increases in the river discharge usually result in stronger stratification (Monismith *et al.*, 2002; MacCready, 2004; Ralston, Geyer and Lerczak, 2008; Lerczak, Geyer and Ralston, 2009; Wei et al. 2016) with high top to bottom density differences. Therefore, the influence of the flow distribution on the stratification is measured in this section by taking the difference of the top to bottom layer salinity. To visualize the results, the top to bottom salinity differences are averaged over radial cross-sections like it was done in section 3.1. The averaging is done over points in a distance of 3 km and 5 km from the river mouth (red and yellow semicircles in Figure 1f) to compare results between shallow locations in the delta front (i.e. area including delta channels) and deeper ones at the pro-delta (i.e. delta area beyond the channels ends) (Hori & Saito 2007). The evolution in time of the stratification is presented for both symmetric and skewed flow distributions and for both radial sections in Figure 4.

The shape of the hydrograph does not seem to affect the range of stratification which remains similar between the five cases in each section (3km and 5km). This range is relatively small at the 3 km section (Figure 4a and b) which is the shallower one where mixing occurs under the influence of stronger bottom friction. The three symmetric hydrographs (Figure 4a) show a stratification level that increases initially following the hydrographs shape. For example, the leptokurtic curve demonstrates heavier tails and almost constant stratification for the period that the hydrograph has also heavier tails. At the same time, the platykurtic curve demonstrates light tails with a sharp increase of stratification in accordance with the sharp flow increase in Figure 1a. As the river discharge increases continuously, it crosses a threshold above which it manages to mix the water column despite the absence of other contributors (e.g. tide-induced mixing). This is most probably accompanied by a seaward shift of the salt intrusion length. The level of mixing depends on the level of the peak flow. The higher the peak the lower the stratification is. In that sense, the leptokurtic is the more efficient hydrograph against stratification while the decrease of stratification in the platykurtic is not substantial. The skewed hydrographs (Figure 4b) present similar results. Initially, the stratification increases following the flow increase but it drops when the river discharge is high enough to mix the waters. This occurs earlier in the positively skewed case, 40 days after the start of the simulation and during the short tail. It occurs later in the negatively skewed simulation, 170 days after the start and during the long tail. In both cases, the stratification starts to increase again when the river discharge drops below a threshold value when it cannot mix the water anymore. After this point and till the end of the simulation, the top to bottom salinity differences follow the flow distribution.

In the deeper waters (5 km radial section, Figure 4c and d), the stratification follows the flow distribution and increases/decreases when the river discharge does increase/decrease too irrespective of the hydrograph shape. Its value reaches its maximum at the time of the peak flow. Accordingly, the higher the peak flow the higher the stratification can become and this is why the leptokurtic shows the maximum top to bottom salinity difference (17 PSU) and the platykurtic the minimum one (13 PSU). In the same concept, the two skewed simulations (Figure 4d) show an equal maximum stratification occurring though at different time moments following the difference in the position of their peak on the hydrograph.

Changes in the spatial salinity distribution are reflected in Figure 4c and d as spikes, one before and another one after the peak flow. As the flow increases, the freshwater spreads radially in wider areas resulting in more symmetric spatial distributions. An example of a change in the spatial salinity distribution for the platykurtic hydrograph is given in the Appendix (Figure 12). At the moment this change occurs, the rate of stratification increase/decrease in the 1st/ 2nd semester also changes. The

time period between the spike and the peak flow is longer in the 2nd semester when the flow decreases as a result of the slower salinity's response to decreasing than increasing flows.

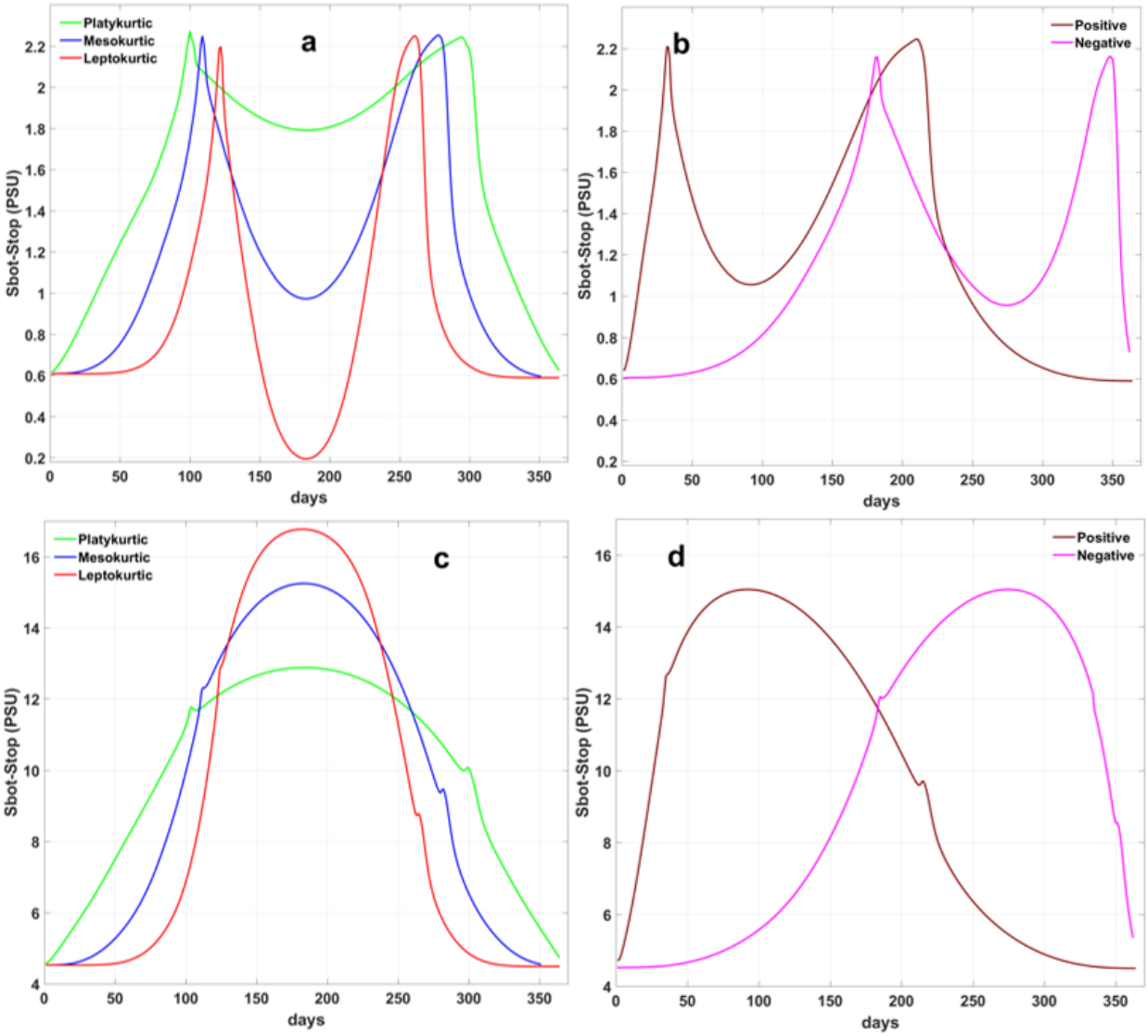

Figure 4 a), b) The evolution in time of the top to bottom layer difference of the radially averaged salinity in a distance 3 km from the mouth in the symmetric and skewed flow distributions respectively. c), d) The evolution in time of the top to bottom layer difference of the radially averaged salinity in a distance 5 km from the mouth in the symmetric and skewed flow distributions respectively.

3.3 Salt intrusion in the inlet

Sustained drought periods may result in salt intrusion inside the river mouth. This is often defined by the location of the 2 PSU bottom isohaline (Schubel, 1992; Monismith *et al.*,1996,2002; Herbold and Vendlinkski, 2012; Andrews et al. 2017). The time that the salinity at the bottom of the river mouth remains below 2 PSU is measured for each simulation with the intention to detect the flow distribution that keeps the river mouth fresh for the most time. Figure 5a shows the level of the bottom salinity at the river mouth (point A in Figure 1f) for the whole simulation period in each case. The five simulations start from a dry season state with very high salinity at the bottom of the mouth meaning that there is salt intrusion in the inlet. The intrusion is averted when the river flows become higher during the wet season. It is identified from Figure 5 that the river discharge at the time the salinity falls below 2 PSU is approximately 100 m^3/s in each case. The rate at which the flow rises in each

hydrograph until it reaches this threshold determines the moment that the inlet's salt intrusion disappears first. The earliest this can happen is for the positive skewed and the latest for the negative skewed hydrograph. The time period that the inlet remains fresh is determined by the hydrographs' tails and the peak flow position. Table 2 displays the total number of days and the days after the peak flow that the bottom salinity at the mouth is less than 2 PSU. The symmetric distributions indicate that the lighter the tails (platykurtic) the longer the inlet is fresh (210 days). The positive skewed case, which also shows light tails but for shorter time, exhibits the second longer period (189 days). Being antisymmetric to the positive, the negative skewed hydrograph keeps the inlet fresh for a long period as well (179 days). However, the fact that its peak occurs much later in time seems to have an effect by cutting out 10 days making it equal to the mesokurtic hydrograph. The minimum duration of all (147 days) corresponds to the leptokurtic as it has the heavier tails. The results are a bit different when the time is measured after the peak flow. In this case, the positive skewed hydrograph exhibits the longer duration (126 days) with the platykurtic being second now (119 days). This indicates that it might be better to force a peak flow to occur early in the year in order to establish a fresh water system for longer periods. This is further supported by the fact that the negative skewed hydrograph manages to keep the bottom salinity at the mouth below 2PSU only for 80 days, even 2 days less than in the leptokurtic hydrograph.

Table 2 The total duration and the time after the peak flow that the bottom salinity is less than 2 PSU at the river mouth

Case	Total Duration (days)	Duration after the Peak (days)
Platykurtic	210	119
Mesokurtic	179	100
Leptokurtic	147	82
PosSkewed	189	126
NegSkewed	179	80

3.4 Salinity longitudinal distribution

Possible effects of the hydrographs shape on the salinity longitudinal distribution are investigated in this section. In Figure 5b, the mean over depth and annual averages of salinity in the delta are averaged over radial cross sections every 300 m along a distance of 6 km from the river mouth (see cross-section AB in Figure 1f). This technique follows the concept of the salt intrusion curves, often used in other studies to measure cross-sectional salinity averages from the estuary mouth's to its head (Savenije, 1993; Nguyen and Savenije, 2006; Nguyen et al., 2008; Zhang et al., 2011). The annual salinity average at the river mouth is above the 2 PSU threshold in every case. This is probably caused by the long periods of heavy tails (meaning very low flows) at all hydrographs except for the platykurtic one. Having the lightest tails of all, the platykutic case presents the lowest salinity value and closest to the 2 PSU threshold at the river mouth. The spatial salinity distribution in the delta increases gradually downstream. The rate of salinity increase between two successive sections is not constant because in contrast to their length, the depth of the radial cross-sections does not increase monotonously downstream. The shape of the five curves in Figure 5b is very similar and does not seem to be affected by the shape of the hydrograph. A border exists 4.2 km far from the river mouth where

downstream of it the salinity is equal between the platykurtic, mesokurtic and the two skewed hydrographs. The green semi-circle in Figure 1f denotes the radial section of 4.2 km. This is located at the border between the delta front and the pro-delta. Upstream of this border, hydrographs with lighter tails (platykurtic) provide a salt intrusion curve of the lowest salinity. Hydrographs with similar peaks and flow ranges, such as the positive skewed and the mesokurtic provide exactly the same spatial salinity distribution in the delta. The salinity in the negative skewed is slightly higher than them. This indicates a negative effect of moving the peak closer to the end instead of the start of the hydrograph as it causes an increase of salinity. Downstream of the green semicircle, in the absence of complex bathymetry and in deeper waters (pro-delta), the salt intrusion curve is the same for all cases with the exception of the leptokurtic hydrograph that still shows the highest salinity. It appears then that the salinity in deep areas is less affected by changes in a hydrograph shape.

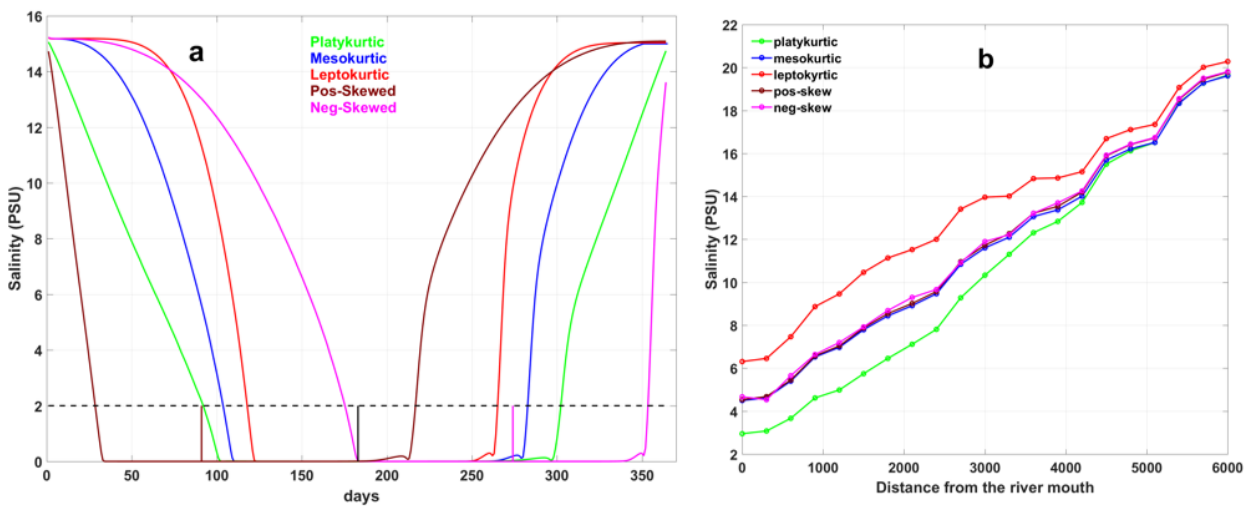

Figure 5 a) Time series of the bottom salinity at the river mouth (point A in Figure 1f). Each colour represents results for a simulation with a different hydrograph. The dashed black line draws the 2PSU threshold. The short brown, magenta and black vertical lines indicate the time moment of the peak flow on the horizontal axis for the positive skewed, negative skewed and symmetric distributions equal to 91,274 and 183 days respectively. b) Annual averages of the mean over depth salinity when averaged radially every 300 m along a distance of 6km from the river mouth.

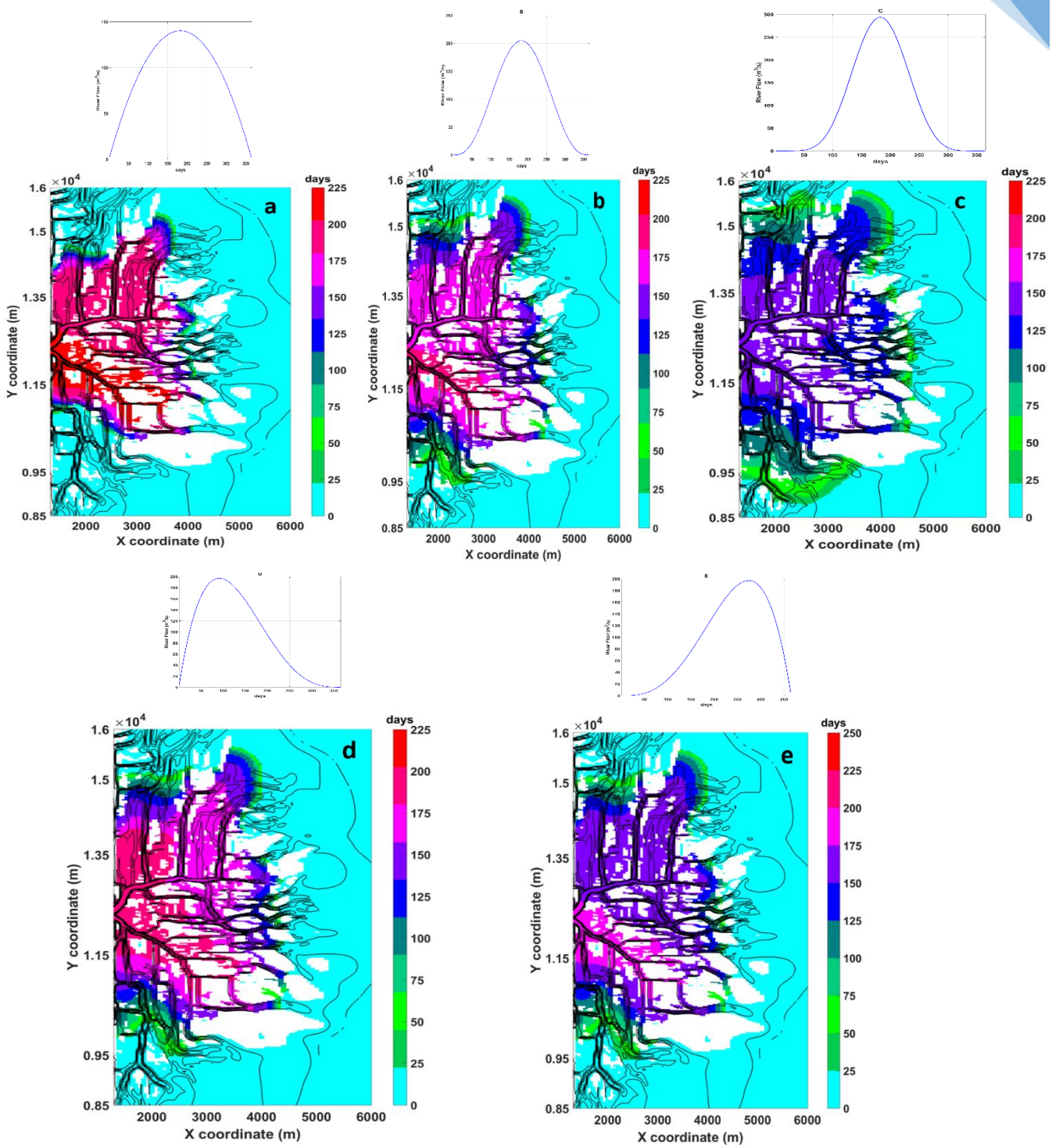

Figure 6 The time in days that salinity is less than 2 PSU in the delta for the a)Platykurtic b)Mesokurtic c)Leptokurtic d)Positive and e) Negative skewed hydrograph cases. The hydrograph corresponding to each plot is added on top of it as a miniature. The black lines in the background delineate the delta channels. White coloured spaces denote dry areas. The river inlet has been taken out from the maps and the abscissa is set to start at the river mouth. Cyan coloured areas never become fresh.

3.5 Freshwater residence time

Considering the water to be fresh as long as its salinity remains below 2 PSU, its residence (or transit) time is calculated to determine how long the delta remains fresh in each simulation and to what extent. Figure 6 includes maps of the delta for each simulation displaying the total time in days that the depth averaged salinity remains below 2 PSU. The delta channels borders are delineated in the background (in black colour) to visualise the size of the area that becomes fresh in each case. The cyan colour in these maps represents areas that never become fresh (freshwater RT is zero). In every case, the tendency is that the time salinity remains below 2 PSU decreases downstream in long distances from the river mouth. The peak flow seems to be the determinant factor for the extent that becomes fresh. This is almost the same for the mesokurtic (Figure 6b) and the two skewed cases (Figure 6d,e) because their maximum flows are very close (204 m^3/s in the mesokurtic and 197 m^3/s in the skewed hydrographs).

In the symmetric distributions, the delta area that becomes fresh increases with increasing peak flow. Hence, every delta channel becomes fresh when the leptokurtic hydrograph is implemented - with the exception of the two most distant ones at the top left and bottom left corner of the map. On the contrary, a more limited delta area becomes fresh with the platykurtic hydrograph (Figure 6a) compared to the other hydrograph cases. Interestingly though, this case provides the longest fresh water conditions period. The delta is fresh in relatively small or medium distances from the mouth for almost 7 months. The duration of a freshwater period for a symmetric distribution decreases as the tails of the hydrograph become heavier. This is why the maximum time that salinity can be below 2 PSU with the leptokurtic hydrograph is only 5 months (Figure 6c). In the case of the skewed hydrographs the positive one (Figure 6d) keeps the delta fresh for more time than the negative (Figure 6e) highlighting the importance of its hydrograph slope that shows a rapid flow rise in the 1st semester and an early in time peak discharge. The hydrograph's slope is identified as another crucial factor because the two cases exhibiting the faster rate of flow rise in the 1st semester (platykurtic and right skewed) provided the longer fresh water conditions in the delta.

In the map plots, differences in the duration within certain areas of the delta indicate bathymetry effects. There seems to be a difference of 25 days in the duration between the right and left sides of the inlet (looking seaward) (Figure 6a,b,d). The latter is deeper and thus the higher bottom salinity reduces the duration in comparison to the shallower areas right of the inlet. This difference is more pronounced in the negative skewed case (Figure 6e) when the dry season is prolonged and the low fresh water flows do not manage to decrease the salinity in the deeper areas. On the other hand, this separation between deep and shallow areas is not present in the leptokurtic case (Figure 6c) because the peak flow is very high and distributes symmetrically the fresh water throughout the delta.

3.6 Flushing times

The flushing time (FT) in each of the five simulations is calculated by the following equation (Dyer 1973; Alber and Sheldon, 1999):

$$FT = \frac{\sum_i^n \left(\frac{S_{SW} - S_i}{S_{SW}}\right) V_i}{Q_F} \qquad (2)$$

For a total number n of grid cells i , V_i and S_i are its volume and salinity respectively. S_{SW} is the sea water salinity (in this case equal to 30PSU) and Q_F an averaged over a time frame river discharge. The

determination of the appropriate period of averaging for the calculation of Q_F can be a complex issue. In this paper, the Date Specific Method (DSM) is used as introduced by Alber and Sheldon (1999). The method assumes that the averaging period must be equal to the FT. By selecting an observation day as a starting point, the FT is calculated through an iterative process working backwards and stops when its value equals the period over which the river discharge is averaged.

The FT was measured twice after determining the averaging period first by setting the start at the day of the maximum flow and second at the last day of the simulation. Figure 7a displays the FT for both starting days. The five simulations show comparable results when the maximum flow day is considered the starting point. In this case, the averaging period is only one day because the river flow is so high that replaces immediately the salt with fresh water and so Q_F in equation 2 is also Q_{max}. Consequently, the FTs are about 1 day and the differences between the five simulations are in the order of a few hours. The order of the FT between the five hydrographs follows the order of their peaks and the higher the flow the lower the FT is.

If the last day of the simulation is taken as the observation day to determine the averaging period, the differences in the FT between each hydrograph are more significant. The negative skewed hydrograph exhibits the lowest FT (4 days) because it contains the highest flows at its end. The symmetric distributions show a progressive decrease of the FT as the hydrographs tails become lighter. As a result, the leptokurtic hydrograph requires the most time for water renewal (17 days) with the positive skewed one demonstrating similar values since its heavy long tail occurs at the end of the simulation.

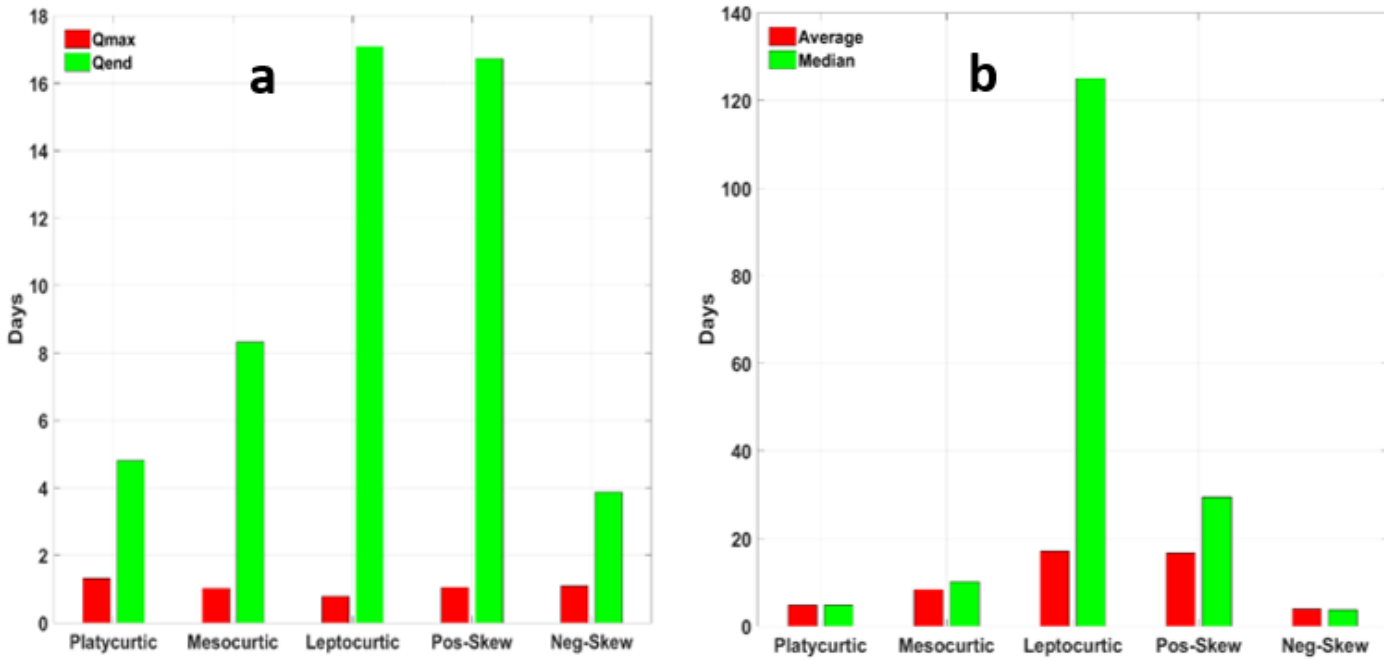

Figure 7 The flushing time for each simulation calculated using the Date Specific Method (DSM) to determine the river discharge averaging period. a) Comparison of the flushing time measured with the average river discharge over a period with the starting date at the day of the maximum flow (Qmax, red bars) and the last day of the simulation (Qend, green bars).b) Comparison of the flushing time measured with the average (red bars) and the median (green bars) river discharge over a period with a starting date at the last day of the simulation

However, since most of the hydrographs contain very low river discharges at the end of their simulation, it is possible that the average discharge Q_{end} introduced in equation 2 might lead to an

underestimation of the FT when the starting date is the last one. For this reason, the calculation of the FT is repeated for this specific case by introducing the median discharge over the averaging period instead of its mean value. Figure 7b provides a comparison between the FTs measured with the median and the average discharge. The outcome is very interesting because even though the relationship of the FTs between the various hydrographs remains the same, the values in some cases are quite different. In the leptokurtic case, the median FT is more than 120 days (4 months) while the average one was just 17 days. Clearly, the average discharge leads to an underestimation for a hydrograph with very heavy tails. Similarly, the positive skewed hydrograph that also exhibits heavy tails at the end of the simulation gave a higher median FT (30 days) than its average one (17 days). In addition, the median FT uncovers a significant difference of the time required for water renewal between the leptokurtic and the positive skewed hydrograph which was not detected when the average discharge was used. The positive skewed hydrograph exchanges water 3 months faster than the leptokurtic according to the median FT calculation.

4 DISCUSSION

4.1 Salinity response to river discharges

Results in section 3.1 indicate the existence of an asymmetry in the salinity response to flow changes. The salinity responds slower to decreasing than increasing flow independent of the hydrographs shape. This asymmetry has been identified in several estuarine studies as well (Blanton et al. 2001; Hetland & Geyer, 2004; Savenije 2005;MacCready, 2007; Uddin and Haque, 2010; Chen, 2015). Savenije (2005) simply states that the replacement of fresh with salt water takes more time. Hetland & Geyer (2004) attributed the asymmetry in the estuarine response to the increase of the bottom drag when the flow decreases. The idealized delta presents a complex and asymmetric bathymetry so that it would be reasonable to assume an effect of the bottom drag to the salinity response. For example, Figure 6 shows higher freshwater RT in the shallower parts of the delta for some simulations. However, Figure 2a shows that this asymmetry does not concern periods with very high or very low flows. At these times, the salinity is equal for equal flows between the two semesters irrespective of whether the flow increases or decreases. The peak flow magnitude seems to have a strong influence. The higher the peak the shorter the asymmetry period is and the higher the salinity decrease is too (Figure 2b). This could be similar to the shorter adjustment times to large peaks in estuaries that Chen (2015) reported. In contrast to Hetland and Geyer (2004), Chen (2015) claims that the asymmetry is caused by two other factors: non-linearity of the salt flux and large variations in the river forcing. The results in section 3.1 present a direct dependence of the salinity response timescale to the flow. Monismith (2017) states that this is true only in systems close to steady state although the relationship is not linear. This is most probably true for the present case since the hydrographs of Figure 1 assume slow flow changes and this justifies the direct dependence of salinity response to river discharge observed in the results. In addition, Monismith (2017) examined if it is possible to take advantage of this asymmetry and achieve a specific salinity standard with flow variations of lower freshwater volumes compared to a constant flow for the same time frame. The outcome was that the flow needed to obtain a certain salinity value (e.g. 2 PSU) increases as the period of flow variation increases. Similarly, Figure 6c indicates that to sustain the 2 PSU salinity threshold in its most distance position, higher flow would be required to vary for a longer period. However, this would result in an increase of the freshwater volume compared to the other hydrographs.

The response asymmetry of salinity to flow changes can be well detected in the skewed hydrographs too (Figure 3). The effect of high flow periods when the salinity does not vary between increasing or

decreasing flows is also present. Most importantly though, the conclusion is that for a given flow range a standard salinity decrease could be achieved in much shorter time if the flow rate is increased or in other words if the hydrographs tails become sharper.

The latter outcome could be extremely useful in terms of water management as it seems that for a given flow range, the increase of its rate can decrease faster the salinity and remarkably improve the conditions in the delta. The faster rate of flow change (lighter tails) is also what probably makes the platykurtic hydrograph a preferable option compared to the leptokurtic one since it sustains freshwater conditions in the delta for longer periods. This would prolong the period that the various anthropogenic activities could take place safely in the delta even though the leptokurtic hydrograph could achieve larger salinity decrease but for a limited time.

4.2 Drivers of hydrographs shape change and its impact on salinity

Deltas can be found at all latitudes and climatic zones (Roberts, Weimer and Slatt, 2012). Although not absolute, a hydrograph's shape could be indicative of certain climate zones. Climate change will affect hydrological regimes in the future which can reflect as changes in hydrographs shape. Riverine flow changes result from either natural climate variability (NCV) (Deser *et al.*, 2012) or anthropogenic climate change (ACC) (Zhang and Delworth, 2018). NCV influences riverine floods magnitude and timing (Merz *et al.*, 2014; François *et al.*, 2019). Atmospheric processes such as intensified precipitation (Viglione et al. 2016) can increase riverine flood peak discharges (Hall *et al.*, 2014; Zhang *et al.*, 2015). Such increases may result in hydrographs like the leptokurtic in Figure 1c that presents a sharp peak. This type of hydrograph with large differences between maximum and minimum flows is often found in monsoonal climates (Hansford et al. 2020). The results analysis in section 3 indicates that peak flow increases could result in an offshore displacement of the salt intrusion length, freshening of a larger area in the delta, mixing of the water column with freshwater and fast renewal times during this period. However, this positive effect would be only temporary if it is not accompanied by an increase of the streamflow throughout the year and the delta's salinity will shortly recover to its pre-peak flow state. A platykurtic hydrograph that has lower peak but smaller differences between maximum and minimum flows is more successful in retaining the delta fresh for longer periods. Increases of peak flows magnitude with thus similar effects may arise by ACC as well as for example urbanization and land use changes that decrease soil infiltration and weaken the natural buffering effect (Vogel et al.2011; Prosdocimi et al. 2015; François *et al.*, 2019).

Warmer temperatures have led to earlier spring discharges in rivers affected by snowmelt (IPCC 2007;Matti *et al.*, 2017;Bloschl et al. 2017). The positively skewed hydrograph's peak is of similar magnitude to the mesokurtic and the negative skewed one but occurs earlier in time. An earlier occurrence of the same magnitude peak flow shows to have an advantage in terms of keeping the delta and its river mouth fresh for longer periods compared to the two other cases. Despite this, the annual and spatial averaged salinity remains the same between these three cases. Moreover, the earlier spring peak discharge shifts the river runoff away from the summer and the autumn which are the months with the highest water demand and so special consideration should be taken in these conditions (IPCC 2007). On the other hand, polar warming has caused a delay of winter floods in the North Sea and some sectors in the Meditteranean Coast (Bloschl et al. 2017). In the hydrographs of Figure 1, when the peak flow is positioned late in time (negative skewed) the freshwater residence

time is much lower compared to other cases of equal peak flow. However, the winter's water renewal time may become faster in this case because of the higher flows during this period.

Rises of temperature, increases of evaporation and warming of the oceans in recent years has intensified droughts that have also become more frequent (IPCC 2007). In addition, reduction of runoff in many regions is assumed to be the result of a poleward expansion of the subtropical dry zone due to anthropogenic climate warming (Lu et al.2007; Milly *et al.*, 2008). Conversion of delta regions to arid zones due to sustained drought periods could modify their annual hydrographs into a mesokurtic shape which is the hydrograph type usually met in these zones (Hansford et al. 2020) as is the case for the Colorado and Nile deltas (Day *et al.*, 2021). The effect on salinity would depend mainly on the peak flow change. If the peak flow increases then an offshore displacement of the salt intrusion zone should be expected, a decrease of stratification and freshwater residence times together with a delay in water renewal times. The reverse effects should be expected if the peak flow decreases.

4.3 Effects of flow distributions on stratification

The evolution of stratification in time with flow changes depends a lot on bathymetry. In deep waters, it follows the hydrographs shape consistent with what is reported in many estuarine studies (Monismith et al., 2002; MacCready, 2004, 2007; Ralston et al.2008; Lerczak et al.2009; Wei et al. 2016). The level of stratification increases with the flow increase so that the leptokurtic hydrograph exhibits the maximum and the leptokurtic the minimum top to bottom salinity differences. In shallow waters, the link between the stratification and the hydrograph shape breaks when the river discharge is sufficient to mix completely the water column. This is expected to happen in areas closer to the river mouth where the depth is shallower and the river discharge's influence stronger. This difference of stratification between deep and shallow areas is not surprising and has been reported earlier. For example, Sridevi et al. (2015) observed something similar in the Godavari estuary where the top to bottom salinity differences varied along the estuary due to bathymetric differences. Stratification was higher in deeper stations and lower in the shallow ones. Several conclusions can be drawn considering this result.

If the interest regarding stratification is focused inside the delta and in areas closer to the river mouth, a flow distribution that follows the leptokurtic hydrograph shows several advantages. It presents longer periods with either mixed waters or very low vertical salinity differences compared to the other hydrographs. It should be noted though that during low flow periods, the salinity can be high despite low vertical differences Special consideration should be taken then concerning the salinity thresholds of different activities taking place in the delta. The two skewed and the mesokurtic hydrographs demonstrate a very similar stratification range in accordance with their flow range. This is an indication that the level of stratification is more sensitive to the peak flow magnitude than its position in the hydrograph.

The range of stratification is much higher in the deeper areas (Figure 4c and d) and that can be explained by the weakening of the bottom friction that leads to stronger stratification (Monismith et al., 1996; Shaha et al., 2012). This can have several environmental consequences even though deeper areas are located downstream and closer to the sea where the activities taking place in the delta may not be so much affected. Stratification may cause anoxic conditions at the bottom layers and low oxygen can have environmental consequences to the aquatic life (Chant, 2012). For example, riverine

waters are responsible for recurrent summertime hypoxia at the bottom waters of the river dominated Mississippi Delta (Schiller et al., 2011).

4.4 Hydrograph shape effects on water renewal and freshwater residence times

The results of sections 3.5 and 3.6 indicate that each hydrograph type has certain advantages and disadvantages. Therefore, the decision on the selection of an optimum hydrograph in regard to water quality should be per case and according to water management demands. The peak flow magnitude and the tails of each hydrograph are important parameters affecting freshwater RT and water renewal time. An incremental increase of the peak flow results in a seaward salt intrusion limit displacement due to the negative correlation between river discharge and salinity (Garvine et al. 1992; Wong, 1995; Liu et al., 2001, 2007; Monismith et al., 2002; Becker et al. 2010). This is reflected in the panels of Figure 6 as an increase of the freshwater area with the peak flow increase. The freshwater area and RT follow an opposite trend. A peak flow increase results in a freshwater area increase but RT decrease. This is a consequence of the heavier tails that the higher peak flows hydrographs exhibit. For example, the leptokurtic hydrograph shows the lowest RT because of its sharp peak and the uneven flow distribution throughout the year. For the same reason, the leptokurtic dry season FT is also the maximum one since the freshwater cannot be fast enough replenished in such low flow conditions. The effect of heavy tails causes also the leptokurtic hydrograph to present the maximum annual and space averaged salinity while the platykurtic shows the minimum.

Hydrographs of similar flow range and peak flows (e.g. skewed and mesokurtic) make fresh almost equal areas (Figure 6). However, the RT may vary between them because of bathymetry or the time of the peak flow in the hydrograph. For example, the positive skewed hydrograph shows higher RT which indicates positive effect of an early peak river discharge. In contrast, when the peak flow is positioned at the end of the year (negative skewed) the RT decreases significantly. In the last case, bathymetric effects are more pronounced because the difference in the RT between shallow and deeper areas is much higher than the two other cases.

FT is known to vary a lot with seasonality (Ensign et al. 2004) and this results in different order of FTs between the five hydrographs during wet and dry season. FT gets shorter values during wet and higher during dry seasons. The critical parameters for the FT are the peak flow in the wet and the hydrographs tails in the dry season. However, the effect of the tails in the second case is much stronger than that of the peak discharges in the first case. The hydrographs shape does not influence significantly the FT during wet seasons. Although the FT decreases with the peak flow increase the difference is only within the range of hours. On the contrary, the FT increases by days as the tails become heavier. The selection of the statistical river discharge value to be introduced in the freshwater fraction method equation is very important in the case of heavy tails such as those of the leptokurtic and positively skewed hydrographs. The use of an average over a period of very low discharges such as those included in hydrographs with heavy tails can decrease the FT and provide an unrealistic estimation of the renewal time (Alber & Sheldon, 1999). The use of the median discharge is proposed instead.

5. CONCLUSIONS

This study investigated the influence of different shape but equal volume flow distributions on the salinity in deltaic systems. A 3D numerical model built in Delft3D for an idealized delta configuration was used. A series of five simulations was carried out with three hydrographs of symmetric distributions but of different peak flow magnitude and two skewed ones (positive and negative). The

results showed a hysteresis between increasing and decreasing river discharge for every distribution. The salinity response is slower to river discharge decreases than increases similar to what is observed in estuaries. This asymmetry is mitigated in periods of very high or very low flows. In addition, an increase of the flow rate could result in a salinity standard in much shorter time.

Natural climate variability and anthropogenic climate change modify the hydrological regimes of many deltas causing changes to their annual hydrograph shapes. Modifications in the shape of the annual hydrographs can have positive or negative effects on the stratification, freshwater conditions, and water renewal and residence times.

The relationship between stratification and hydrographs is much affected by bathymetry. There are two different responses of stratification to flow changes observed. The top to bottom salinity differences in deeper water areas follow exactly the hydrographs shape. This means that leptokurtic hydrographs cause higher stratification. This outcome is though reversed when the focus is in shallower areas. In this case, the river discharge manages to mix the vertical column with freshwater so that stratification decreases with the increase of the river discharge making the leptokurtic hydrograph the most efficient case for mixing. The stratification is more sensitive to peak flow magnitude than position in the hydrograph because flow distributions of similar flow range present a similar range of stratification levels.

Freshwater areas, renewal and residence times depend on a hydrograph's peak flow magnitude and tails. The time with freshwater in the delta increases when the hydrograph's tails are light and the maximum to minimum flow differences become smaller to allow a more even distribution of the water volume throughout the year. The bathymetry can affect the residence time because shallow areas remain fresh for longer time. Freshwater areas and residence times follow an opposite trend. The latter increases with the decrease of the peak and the former decreases.

The flushing time does not vary significantly during wet seasons between the different types of hydrographs. It does vary though in the range of days or months during dry season. In low flow periods, the flushing time increases as the hydrograph's tails become heavier. For the water renewal time calculation in heavy tails hydrographs (e.g. leptokurtic and positively skewed), the use of the median instead of the average discharge is suggested to avoid an underestimation of the flushing time by mitigating the effect of very low flows.

The work in this paper aspires to contribute in the efforts for a more sustainable water management in river deltas under the challenges of climate change and water demand increase. The results indicate that it is possible to mitigate salt intrusion issues by water supply regulations. Each type of the annual flow distribution investigated in the present work demonstrates its own advantages and disadvantages. The selection of the most appropriate one probably can depend on many parameters. For example, the choice might be different if the goal is just to reduce the salinity in the delta than cause further mixing or push fresh water further away from the river. Nevertheless, the present study focused on river flow forcing only and so further research might be needed to determine the influence of other parameters such as for example tide-induced mixing.

Acknowledgments

The work contained in this paper contains work conducted during a PhD study supported by the Natural Environment Research Council (NERC) EAO Doctoral Training Partnership whose support is

gratefully acknowledged. Grant ref NE/L002469/1. Funding support from the School of Environmental Sciences, University of Liverpool are also gratefully acknowledged.

6. SUPPLEMENTARY INFORMATION

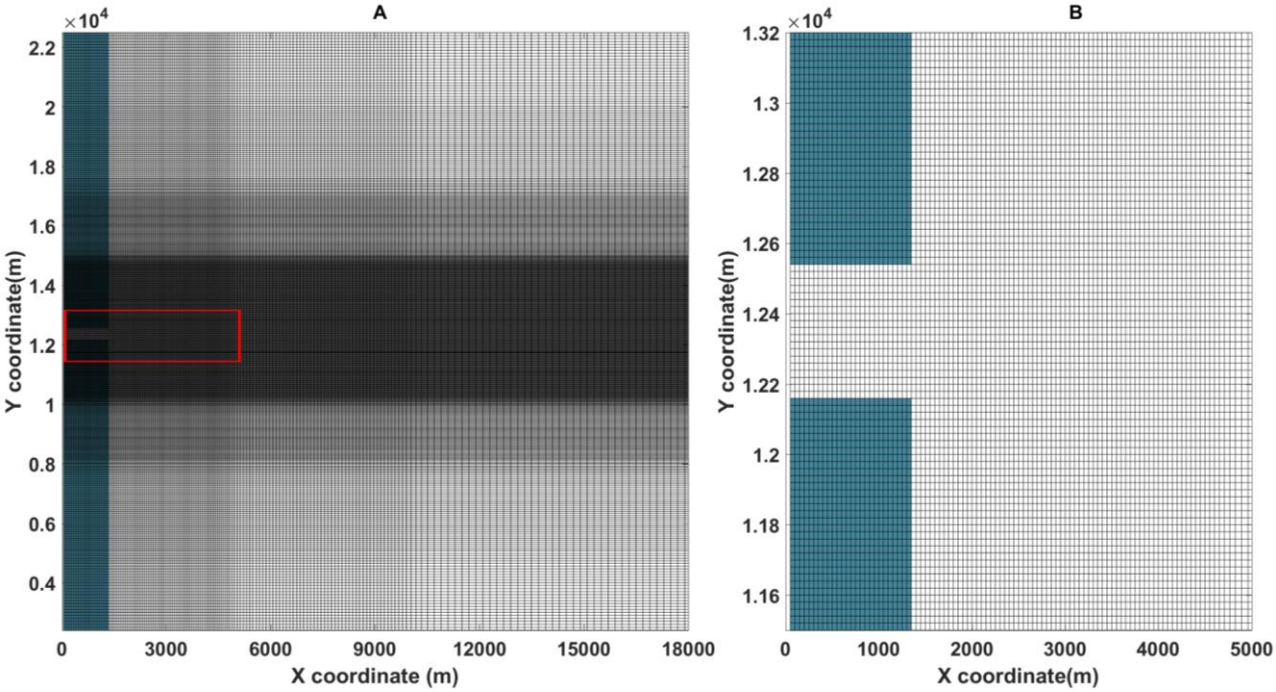

Figure 8 A) The model grid B) Zoom within the limits of the red box in A.

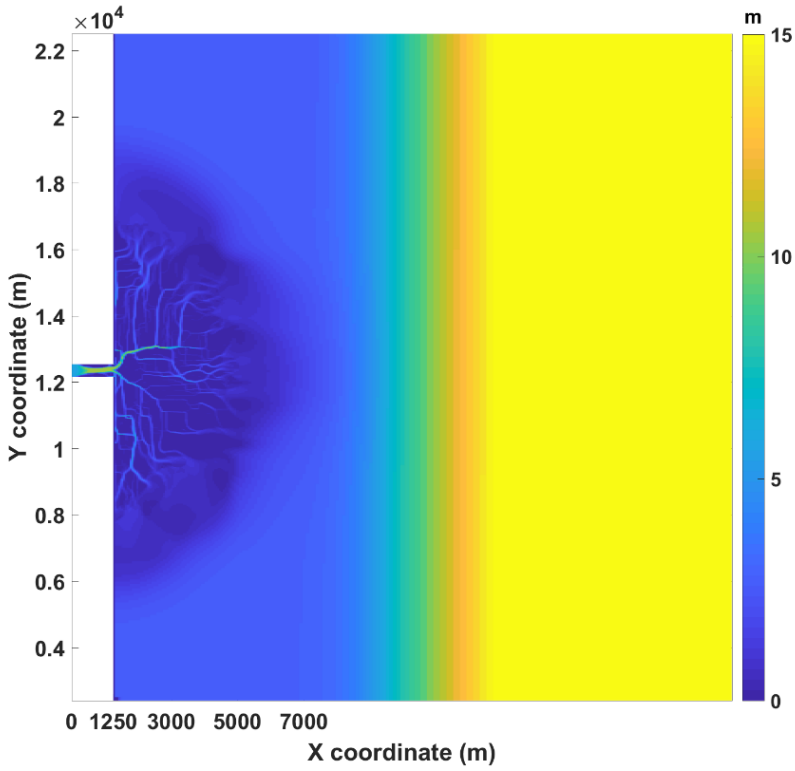

Figure 9 The model bathymetry

Parameter	
D_{50} for sand	225µm
Settling velocity for mud	0.25 mm/s
Density for hindered settling	1600 kg/m^3
Specific density for sediments	2650 kg/m^3
Critical bed shear stress for erosion	1 N/m^2
Critical bed shear stress for sedimentation	1000 N/m^2
Chezy coefficient	45 m$^{1/2}$/s
Horizontal diffusion	10 m^2/s
Horizontal viscosity	1 m^2/s
Cohesive sediment input	0.2 kg/m^3
Non-cohesive sediment input	0.5 kg/m^3
Morphological factor	175
Time step	12 seconds

Table 3 Physical and sediment parameters for the morphological simulation

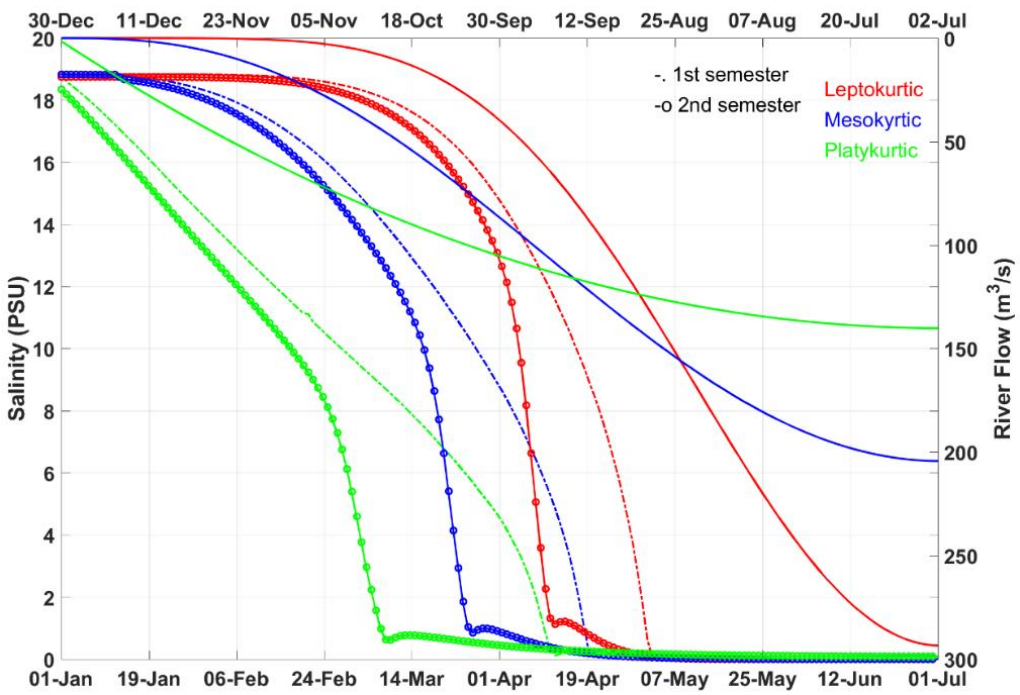

Figure 10 Same content as in Figure 2a (manuscript) but for a radial section 1 km far from the river mouth

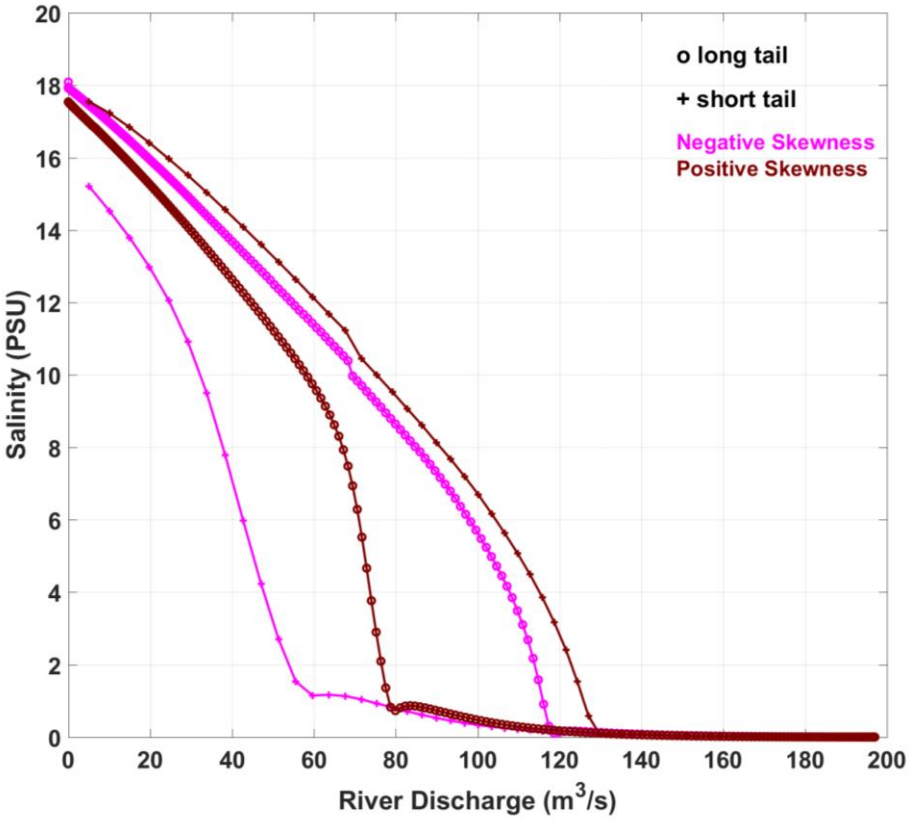

Figure 11 Same content as in Figure 3 (manuscript) but for a radial section 1 km far from the river mouth

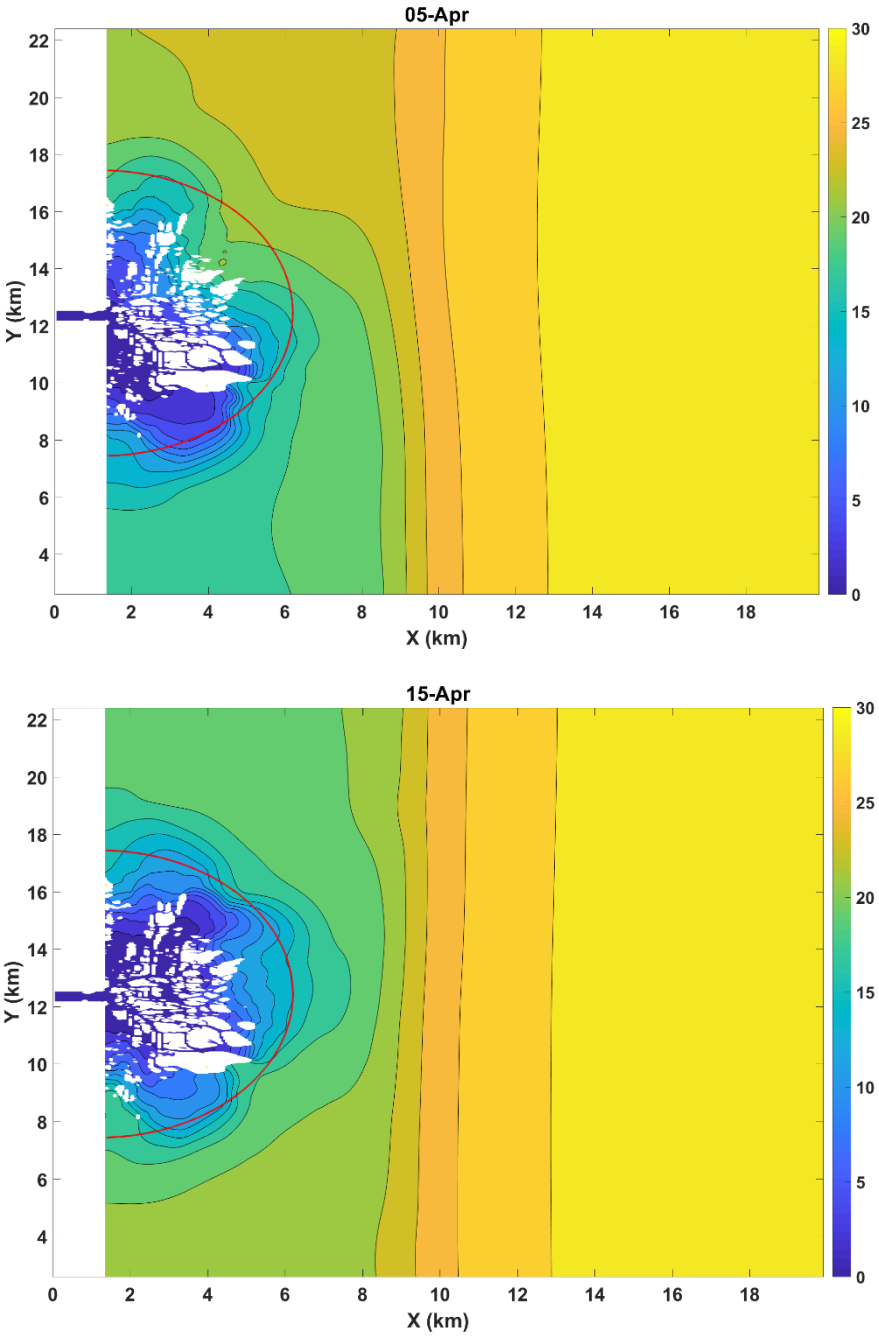

Figure 12 The spatial salinity distribution at the surface layer in the platykurtic simulation at two different instants in the 1st semester. White coloured areas lie above the mean water level. The red semicircle indicates the 5 km radial section over which the salinity is averaged in section 3.2. Notice the difference in the spatial distribution between the 5th and the 15th of April. The distribution has become more symmetric on the 15th of April. The shape of the distribution changes at some time between the 5th and the 10th of April and that is reflected as a spike in Figure 4c. Similar changes of the spatial salinity distribution were detected for the two other symmetric and the two skewed hydrographs.

7 DISCUSSION

This chapter is an effort to combine common elements included in the three papers presented in chapters 4,5 and 6. The first paper (chapter 4) constitutes the foundation basis of this work. The second paper (chapter 5) is an extension that includes the same methods but implemented in the presence of tides. The third one (chapter 6) is an attempt to investigate methods of better water management by implementing the model used in chapter 5. The results of these papers could be unified to some extent in order to provide overall conclusions from the work included in these three publications. The chapter is divided in seven sections. Each one discusses separately key elements from specific topics presented in this dissertation. The various sections summarize -where necessary- results from the papers that refer to the same or similar topics. They also elaborate further where required on the significance and importance of this work's findings.

7.1 The role of idealized modelling and its challenges

The simulation through idealized modelling of the various physical and dynamic processes that take place in a delta has been successful because a number of correlations were exported and several interesting inferences were extracted that hopefully will contribute and assist in further research in this field. This project proposes and supports the use and development of idealized models as an alternative method for research in deltas. Idealized models can be of great help because the access to extensive and accurate real data is not always possible in every delta worldwide. In addition, deltas differ in many ways between each other depending on morphology and hydrodynamic forcing and so conclusions from site-specific research may lack universality.

The idealization approach adopted here refers to what is also called a 'minimalized' concept (Weisberg, 2007), meaning the construction of a model that includes only the core causal factors that give rise to a phenomenon. Using a minimalized concept, the present work was divided in three main categories. First, the influence of seasonally varying fresh water flow on the salinity in the absence of tides was investigated. Later, various tidal levels were added to see their impact on salinity and finally the effect of different hydrograph shapes was assessed but without considering tides. The advantage from the use of such 'exploratory' (Murray, 2002) models is that by omitting certain system parameters, the effect of a single causal factor can be better illustrated. This is very useful in the case of systems involving many interconnected processes (Murray, 2002). Exploratory models are not intended to reproduce specific cases, but to investigate general behaviours (Murray 2003). Results from such models lead to conclusions that can have generality and provide explanations on the effect of causal factors. Idealized models explain by accurately representing a set of difference-making causal factors isolated from other less important causes (Rice 2019).

Limitations of idealization

Of course, there can always be a level of uncertainty when trying to transfer directly conclusions from idealized studies into real cases. Nonlinearities that govern the relationship between various parameters in a real system may not lead to the exact same conditions predicted by an idealized model. Therefore, there might be limitations in the interpretation of idealized modelling results for real cases. In every case, idealized models are not intended to replace real case ones because they may not be able to capture non-linear effects between the various parameters and their results can be only qualitatively reliable and not quantitatively. In fact, idealized and real models should be rather viewed as complementary and not in juxtaposition between them because they are designed for different purposes. Real models are orientated to a "specific problem solving" and to a lesser degree to a fundamental physical analysis while the ideal ones are orientated towards to " a knowledge obtaining" without specific reference to a particular practical problem in hand.

Within the context of this work, the two most important physical factors driving the phenomenon of salinity intrusion and spreading in deltas have been examined, that is, the fresh water (river) discharge and the incoming tide. Evidently, there are also other factors that could be potentially involved such as winds blowing at periods very strong or precipitation and heat exchange at the sea surface. Needless to say that these could introduce other nonlinearities of their own and, therefore, this leaves able room for further research in the future within this adopted idealized scheme that could eventually reveal more on the contribution of each of these drivers to the entire process.

Scaling

As it has been stated in section 3.3 and explained in the methods sections of chapters 4, 5 and 6, this study's idealized models are scaled. Scaling is usually done when something cannot be directly studied due to size (too large or too small) or speed (too slow or too fast). In the present project, scaling down was necessary to simulate the physical processes at scales as small as is practical given limitations of computing power. Building of a model that would correspond to natural sizes is impractical in this case. A model with very large dimensions would result in very long and time-consuming simulations. In addition, stability issues would require changes to the resolution of the model which could lead to a non-realistic and deficient bathymetry as it will be explained later.

It is imperative for a scaled numerical model to represent fairly the physical processes of the under study phenomenon. Therefore, scaling requires a qualitative similarity, i.e. the same physical processes are present in an experiment (i.e. idealized model) and a prototype (i.e. a real delta) and a quantitative similarity meaning that the proportions between the scaled variables correspond to those in the prototype (Ransom et al. 1998). These two concepts are manifest in the form of the three basic similarity principles, i.e. geometric, kinematic and dynamic similarity (Ransom et al. 1998). The last two principles are ensured by the fact that the physical laws implemented in the model are the same that describe the physical processes in nature. Therefore, scaling is not harmful for the model's validity because the governing laws (e.g. momentum and advection-diffusion equations) describing the system's fundamental physical processes still hold in this case and are universal. Geometric similarity has been achieved by developing an idealized delta configuration that exhibits most of the features expected to be present in a real delta bathymetry.

Bathymetry

Each delta has its own characteristics in terms of morphology, geology, size, and hydrodynamic conditions, land uses etc. This complexity of deltas configuration render the building of a 3D model for an idealized delta a difficult, time-consuming, challenging and laborious task. The successful development of a delta morphology with the typical river channels curvature and meandering demands a meticulous determination of the setup parameters. The delta morphology depends on hydrodynamic forcing and sediment properties. The hydrodynamic conditions define the delta type (river, tide or wave dominated (Galloway, 1975) and the sediments its size and shape (Edmonds and Slingerland, 2007, 2010; Edmonds et al. 2011; Caldwell and Edmonds, 2014). The building up procedure was largely based on the methods and findings of the works by Edmonds and Slingerland (2010), Geleynse et al. (2011) and Caldwell and Edmonds (2014). Both delta bathymetries exhibit many typical delta features such as the delta front slope and the pro delta deepening (Hori and Saito 2002; 2007; Goodbred and Saito, 2010) , the erosion in front of the river mouth and the downstream shallowing and widening of the channels (Lamb et al., 2012).

The building up of the two models did not consider tidal forcing even though this is included in chapter 5. Yet, deltas develop very different geometries depending on the strength of river and tide (Galloway, 1975). However, the use of a single bathymetry in chapter 5 is necessary to isolate the direct effects

of tides from any bathymetric influences. The bathymetry must be kept the same so that the results from simulations with different amplitudes are comparable. Otherwise, the effect of tides will be intertwined with other parameters. For the same reason, morphological changes have been omitted in this study since it is known that density stratification can have an impact on sediment transport and vice versa.

Grid resolution

There were a few challenges and difficulties detected while building the delta bathymetry. The grid resolution appears to be a crucial factor for the development of a realistic delta morphology. Coarse resolution produces channels of constant width usually equal to one or two times the grid space step. Adjacent cells transform abruptly from dry to wet. The result is a network with straight channels and no curvature or meandering. The resolution has to be as finer as possible so that the flow erodes the bed and the suspended sediments are deposited unevenly between adjacent cells forming channels of various widths. Earlier idealized delta studies using Delft3D on which this work was based on (e.g. Liu et al.2020, Burpee et. al.2015, Caldwell and Edmonds 2014, Edmonds and Slingerland 2009) all used a 625 m^2 (25 m x 25 m) grid cell area that is fit for the purpose. However, a very fine resolution requires a relatively small model area regarding computational efficiency. The first model in this study has small dimensions and the grid resolution close to the inlet reduced to 20 m x 10 m so this is not a problem in this case. As mentioned in section 3.1.2, the study of tidal effects would require a larger model as is the second one presented here with dimensions 22 km x 20 km. The reasons for a larger model are also stated in section 3.1.2. In this case, the resolution could not be so fine because the model becomes cumbersome for one year simulations and/or unstable for the river flow magnitude of the morphological simulation that is quite high in $O(10^3)$ (section 3.1.2.2). Despite that, the second model's grid cell size is not far from that of the other studies (1 km^2 instead of 625 m^2). As it was discussed earlier, the output bathymetry provides a realistic morphology with many common delta features (Figure 14).

Model testing

Another challenge in idealization is model testing. Since these models are simplified and have left out intentionally certain processes (e.g. waves), the predictions should not involve the magnitudes of the model-dependent variables but the trends in how these variables (e.g. salinity) respond in various conditions (e.g. river or tidal forcing). Consequently, the value of idealized model results can only be qualitatively and not quantitatively assessed. A good example in this study is the implementation of the Strahler-Horton method that provided a non-scalable trend between salinity and stream order (see also section 7.3). However, idealized models are often criticized for their simplifications. A source of criticism is the uncertainty on the level of agreement between idealized model results and nature. It should not be taken for granted that the interactions the idealized model presents always exist in nature. Therefore, the idealized model's results are usually tested for consistency with existing knowledge. For example, this project's idealized models exhibited patterns that agree with what is observed in nature. The development of a baroclinic circulation with offshore flow at the top and onshore at the bottom layers, the increase/decrease of stratification with the increase/decrease of the river discharge and the effect of tides on the buoyant plumes' symmetry and vertical structures are only some of them. This is very supportive and reassuring on the results validity. On the other hand, such results alone do not guarantee the same behaviour in nature but they show that the extracted conclusions are at least plausible. To support this argument, the model behaviour must be tested with field observations as well. In chapter 4, the methods implemented for model's results analysis were repeated for a real case and showed satisfactory agreement. Finally, it should be noted

that idealized (or process-based) models are designed for explanation purposes and cannot be readily applied for other purposes (Murray, 2002).

Boundary conditions

The selection and implementation of boundary conditions is usually a tricky but significant matter because they are so important to obtain valid, reliable numerical results of physical meaning and overall value. The validity of the boundary conditions was assessed based on the resulted flow circulation and the salinity distribution. The latter should not be disturbed or constrained by the boundaries and the former should ensure that the current vectors are always parallel to the lateral and perpendicular to the offshore boundary irrespective of their sign.

The morphological simulations are executed with a Neumann condition at the lateral boundaries. By this, a zero water level gradient is assumed along the boundary. The Neumann condition can be prescribed only at cross-shore boundaries in combination with a water level boundary at the seaward boundary (Deltares, 2013). This setup is satisfied in the morphological simulations. However, the inclusion of baroclinic terms in the momentum equations and the densimetric differences that these cause affect the water field and currents velocity direction. Therefore, changes to the boundary conditions are required in the simulations with salinity compared to the morphological ones to ensure that the correct flow circulation is established. It was discovered that a Riemann condition at the cross-shore boundaries is more appropriate in this case. This is because the Riemann boundary condition represents a weakly reflective boundary that prevents reflections at the open boundary. This is imperative to avoid boundary effects and constraints on the salinity distribution. A zero flow along the boundary is imposed and the water level is computed by the model based on the known-depth field and assuming a zero water level in the reference plane (Deltares, 2013).

For transport (i.e. salinity), the boundary conditions should match its initial value. Otherwise, the baroclinic pressure gradient can cause severe water level gradients (Deltares, 2013). For this reason, the salinity in the spin-up simulations is prescribed equal to 30 PSU at all open boundaries except the river where it is assumed that the water is fresh. This is not a problem for the sea boundary which is assumed to be the origin of salt water in the system and is at certain distance from the delta. It could be an issue though for the lateral boundaries in case the prescribed value has an impact on the salinity inside the delta. To preclude this, the diffusion along the lateral boundary gridlines was reduced. In this way, the model was allowed to calculate its own values at the boundaries independent of the prescribed value. This could be verified by the salinity isohalines in the map plots of chapters 4 and 5 that show the isohalines making angles with the lateral boundaries. The figures show clearly that the isohalines are not constrained by the boundaries and the plume is allowed to develop uninhibited by the imposed salinity at the boundaries.

When there is tide at the sea boundary, harmonic boundary conditions are prescribed. The tide is implemented in the model in the form of a cosine function with its amplitude defined through the Riemann invariant. This was done because this type of boundary conditions ensured a flow perpendicular to the offshore boundary at all times. However, it was discovered that the implementation of the Riemann invariant at the cross-shore boundaries were inappropriate in the presence of tides and caused unrealistic flow circulation. As a consequence, they were replaced by the Neumann condition. To avoid reflections at the open boundaries and any impact on the salinity, the baroclinic terms were deactivated. This is an option available in Delft3D that is recommended for such cases (Deltares, 2013). Boundary conditions for all cases are summarized in Table 3.

Table 3 The boundary conditions implemented at the cross-shore and offshore model boundaries for each type of simulation

Simulation	Cross-Shore	Offshore
Morphology	Neumann	Water Level
Salinity without tides	Riemann	Water Level
Salinity with tide	Neumann	Riemann

7.2 Salinity Seasonal Variation

The salinity distribution in a coastal system depends on freshwater flow, tidal and atmospheric forcing (Bowen and Geyer 2003; Banas *et al.*, 2004; Gong and Shen, 2011; Maccready, Geyer and Burchard, 2018). In this study the effects of the latter have been neglected and the focus is on the river discharge and tidal level variations. The results indicated significant seasonal variation of the spatial salinity distribution caused by high dynamic flow variability. The patterns developed in the delta are quite different between dry and wet seasons in both river dominated and tidally influenced systems. In low flow periods, the freshwater area (taken as the limits of the 2 PSU isohaline) in the system without tides (chapter 4) is confined in the vicinity of the inlet. Diffusive processes prevail and the freshwater transport is slow. The potential energy is high close to the mouth due to the high vertical salinity gradients that develop. The result is that a salt wedge forms at the bottom of the river mouth indicating salt intrusion in the inlet. The flow acts seaward at the surface but landward at the bottom layer.

A density front with high horizontal salinity gradients develops further downstream but inside the delta plain area. In this case, the outer areas of the delta that are in close proximity with the sea are fully mixed but the salinity indicates seawater values. Lateral variations of the density front during dry seasons can become important in the case of transverse depth variations (Wong, 1994). In estuaries, it has been observed that inflow is stronger in the deep and outflow in the shallower sections (Wong, 1994; Valle-Levinson et al. 2000; Geyer and MacCready, 2014). The delta configuration that was used for the simulations including tides (chapter 5) presented a lateral bathymetric asymmetry with deeper channels on the left and shallower ones on the right of the inlet looking seaward. This causes high lateral salinity gradients at low flow periods because the salinity is high in the deep and low in the shallow channels. As a result, onshore flow develops at the deep and offshore at the shallow ones.

Such bathymetric effects can be overridden in the presence of tides because of an increase in the flow circulation and currents in the delta. The flow jet and consequently the salinity distribution tend to become more symmetric. This corresponds to both dry and wet seasons. The result is a decrease of the gradients in the lateral but an increase in the longitudinal direction because the density front moves offshore to the well mixed (with seawater) distant areas. The effect of the tides on the velocity currents inside the delta and the development of more symmetric plumes has been reported in many estuarine studies (Chao, 1990; Garvine, 1999; Isobe, 2005; Guo and Valle-Levinson, 2007; Leonardi et al. 2013;Lee and Valle-Levinson, 2013).

In high flow periods, the freshwater is spread radially in longer distances. Potential energy (and thus buoyancy) decreases because the higher river discharges manage to mix the water column in a quite large area. This area becomes even wider in the presence of tides due to tide-induced mixing. Delta channels that would remain saline in a river dominated system could be fresh if tidal level increases. However, there is a limit to these tide-related positive effects. If the tidal range reaches meso- or macro-tidal levels, the low salinity areas reduce in size leaving many of the channels outside of the freshwater zone.

Like the tides, higher river discharge can also override bathymetric effects and so the spatial salinity distribution becomes symmetric and close to semi-circular. Freshwater and low salinity areas expand further both laterally and longitudinally. The density front that lies inside the delta during dry seasons is displaced offshore. However, bathymetric effects can still be present but outside of the delta. Most deltas exhibit a gradual depth increase beyond the channels end that can become very sharp further offshore (Hori and Saito 2007; Goodbred and Saito 2010). It was found that the radial isohalines can be affected by bottom changes. They tend to become parallel to the offshore sea boundary as they approach steeper bed slopes and constant salinity gradients may develop in the lateral direction. In the presence of tides though and when the buoyant offshore plume becomes prominent, the horizontal salinity gradients decrease close to the lateral boundaries and the isohalines tend to become radial again.

7.3 Salinity correlations with the distributary network

The use of stream labelling methods to relate stream networks to landscape processes is common in hydrology and geomorphology. They are useful tools providing information on the geometry and topology of river networks. The use of such methods in deltas was tested in this project. It is proposed that stream labelling schemes can be adapted in order to relate salinity with the delta's geometry. The classification of delta channels into stream orders following the Strahler-Horton (1952) method uncovered the existence of a relationship between salinity and channels order. The salinity increases as the order decreases. This happens because the low order channels are located far from the freshwater source while high order channels lie close to it. Moreover, the river discharge decreases with every bifurcation and is distributed through the new branches (Yalin 1992). The amount of freshwater that reaches the channels end is insufficient to decrease adequately the salinity in those distant areas.

Through the Strahler-Horton method, a deltaic system is characterized by a non-dimensional integer value. The number of orders identified in a delta provides information on the level of bifurcation, connectivity (Passalacqua 2017), channels number and size. A high order number likely implies a large delta that includes longer channels with many bifurcations. Knowing that salinity reduces upstream as the order increases, channels likely to be more saline than others could be identified. This could be very useful if there is lack of data. Availability of detailed data through a delta's channels is usually limited. Most often, observation campaigns provide sparse data in distinct points and modelling studies are required to obtain a detailed image of the salinity distribution within the channelized network.

Validity

A disadvantage of stream labelling methods is their dependence on map scale resolution (Ranalli and Scheidegger, 1968). Sometimes it may not be possible to detect every single channel in a map and so the ordering may not be accurate. The difficulty refers mostly to the identification of first order channels. These are terminal distributaries channels (see section 1.4), free of branches and relatively small located at the ends of the delta and may not always be detectable in a map. In addition, some of them may be only seasonally active (Olariu and Bhattacharya, 2006) and so it is uncertain which of them should be included in the ordering. The development of state of the art mapping tools (e.g. GIS) though seems to diminish significantly this issue.

In any case, this does not put in doubt the validity of this method which in reality is independent of the map resolution. The Strahler-Horton scheme reveals a non-scalable trend between channels order and salinity which is independent of the number of orders or the level of salinity. Even if the estimated bifurcation order of a real system is lower than its actual one, the salinity will still decrease with the

increase of the stream order. For example, when the method was implemented in the Mississippi Delta, the channels were classified into three orders only. This was done based on the maps resolution including salinity data from field observations although many aerial photos of the area suggest that this delta's bifurcation order is probably much higher (see Figure 16). The data analysis disclosed the same trend existing in the idealized model showing that salinity did decrease with the increase of the order. The implementation of the stream ordering in a real delta follows the argument of section 7.1 about model testing. The idealized model was used to develop a trend between variables and not a relationship between their magnitudes. This proved to be successful because the trend is present in both cases (idealized and real one). In addition, the stream order method has been implemented successfully in two different idealized deltas of different bifurcation (chapter 4 and 5). The fact that this trend exists in two deltas of different type (idealized fan delta versus real bird's foot delta) is also very supportive of its validity. It is also important to note that the trend was not affected by changes in the forcing since it is present in both river and tide dominated systems.

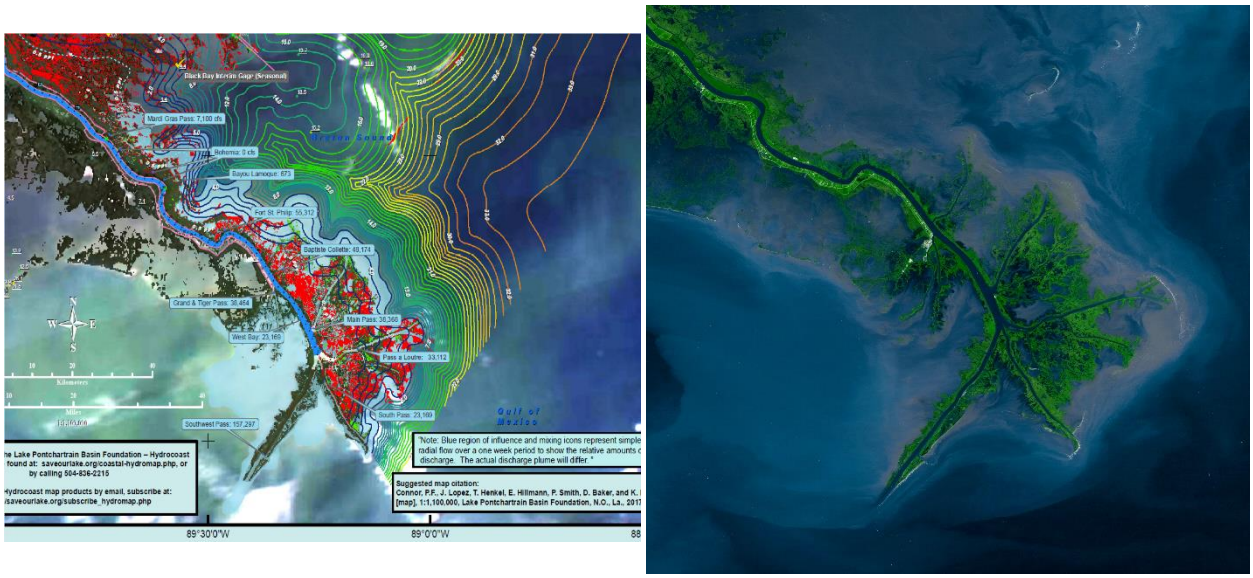

Figure 16 The map on the left is one of the maps including salinity observations in the Mississippi Delta that was used for data analysis in chapter 4 (available at https://scienceforourcoast.org/pc-programs/coastal/hydrocoast-access-form/). The map on the right is a photo of the Mississippi Delta taken by NASA (https://visibleearth.nasa.gov/images/8103/mississippi-river-delta). It is obvious that the observations map is too dense with too much information and is possible that some channels that can be detected in the NASA photo may have been left out. However, this does not affect the validity of the salinity-stream order trend.

Limitations

Nonetheless, there are instances where this relationship does not apply. The stream order number increases upstream throughout the delta in an almost symmetric and semi-circular manner. Although channels of a certain order will not necessarily be close to each other and might be located at various areas within the delta (close or far from the river), averaging the salinity per stream order is close to radial averaging. If for any reason the spatial salinity distribution is not symmetric then these radial averages might not decrease monotonously with the order increase. Apparently, factors affecting the spatial distribution (e.g. winds or waves) could modify the salinity-stream order relationship. The second delta configuration of the larger model version presented a bathymetric asymmetry with much deeper channels on the left of the river inlet. High bathymetric differences and asymmetries in a delta can result in asymmetric salinity distributions. As long as these are present the salinity cannot be directly correlated with the stream order. Deeper channels usually contain more salinity than shallower ones that require less water volume to become fresh. Higher freshwater flows override

these bathymetric effects. Then the jet flow is distributed symmetrically and so does the salinity. In the case of significant flow seasonality, the salinity-stream order relationship in deltas with bathymetric irregularities applies better during high flows season. Such bathymetric irregularities do not seem to be a problem in tide dominated deltas because the tide increases the flow velocity and results in more symmetric distributions. Nevertheless, the tide needs to be above a threshold for this to occur. Thus the salinity-stream order trend is expected to be present mostly in meso and macrotidal regimes. The method is applicable for longer times as the tidal level increases and retains salinity distributions symmetric for longer periods.

Alternative methods

Despite that, correlations between salinity and delta's geometry are possible even when its distribution is not symmetric. The present study suggests the width function as an alternative to the Strahler-Horton method. By this, the number of channels junctions replaces their order. The term width refers to the number of junctions (or links) within a certain space step along the delta. The number of channels links between equal space distances could be measured in a way that the width evolution in space follows a skewed distribution. Usually deltas present a positively skewed width function distribution because the channels junctions reduce downstream. The width is also another way to describe the changes in space of the delta's cross-section. Hence, the salinity correlation with the width represents the salinity distribution with the delta's cross-section. The implementation of the width function proved to be very convenient because it develops the same correlation with salinity that the stream order does. The salinity decreases as the width increases because the number of channels bifurcations is higher closer to the river inlet. The width function method applicability seems to depend on the type of horizontal salinity distribution as well. Averaging the salinity within channels between successive distance steps defined by vertical lines through the delta's cross-section results in lateral averaging. It is normal then for these lateral salinity averages to increase downstream while moving closer to the sea. This method proved to be successful when there were high salinity differences in the lateral direction. Consequently, the width function and stream order could be complementary to each other because the former applied better when the salinity distribution was symmetric and the latter when it was not. Alternatively, the stream order method is more successful during high flows and the width function during low flows periods. However, both methods are applicable in tide dominated deltas independent of seasonality. Significant tidal forcing develops horizontal salinity distributions that satisfy both methods.

To overcome the issue with symmetric and asymmetric salinity distributions, other stream labelling methods were tested too. For example, Horton's, Milton-Ollier's, Scheidegger's and STORET location coding system were considered. However, they do not seem to offer any advantage mostly because they follow a very similar approach to the Strahler-Horton method. Therefore, the use of stream order and width functions is proposed to be used either separately or combined with each other.

7.4 Vertical Salinity Distribution

The salinity vertical distribution was assessed in all three papers. In chapter 4, the potential energy anomaly (PEA) was considered in order to measure the evolution in time of stratification under seasonal flows. PEA is a magnitude that expresses the amount of kinetic energy necessary to fully mix the water column (Rippeth et al. 2001; Burchard and Hofmeister, 2008; de Boer et al. 2008; Formats, 2014). Averaging PEA within channels of equal order resulted in a trend very similar to that between salinity and stream order. However, the trend in this case is not independent of seasonality. During low flow periods, PEA increases with the order increase. This happens because channels of high order are deeper and located closer to the river mouth. Downstream channels are usually shallower and

therefore less likely to be stratified. Instead, they can be mixed at these times but with salt water due to their proximity with the sea. During high flow periods, the trend reverses. PEA increases with the decrease of the order. High order channels become fresh because they are in close proximity with the river channel. Low order channels move from mixed to partially mixed conditions under the influence of higher discharges. Consequently, the PEA variation in time of the low order channels is much smaller than that of the high order ones.

In chapter 6, the stratification was measured by taking the top to bottom salinity differences. These were considered over two radial sections (in and out of the delta) including both channels and interdistributary areas. The results indicate different evolution in time of stratification depending on the distance from the mouth. The complex morphology of a delta seems to alter the typical relationship of increasing/decreasing stratification with the increase/decrease of river discharge (Monismith *et al.*, 2002; MacCready, 2004; Ralston et al. 2008; Lerczak et al. 2009; Wei et al. 2016). Considering a Gaussian hydrograph, the top to bottom salinity differences inside the delta increase/decrease with the increase/decrease of the river flow until a threshold. When the flow becomes larger/smaller than the threshold the vertical salinity differences start to decrease/increase. Outside of the channels network, in the deeper delta front and pro-delta areas, the evolution in time of stratification follows the changes in the flow distribution independent of seasonality. The evolution of stratification in time follows the hydrograph.

Parameters affecting stratification

The above indicate that both bathymetry (shallow or deep channels) and distance from the mouth are critical factors for stratification. The salinity's response to seasonal flow variations in the vertical direction is not uniform over space. This could be better visualized in Figure 16 that illustrates a map of PEA in an instant at low (panel A) and another at high (panel B) flow periods. Figure 16A shows a gradual decrease of PEA in space along a transect that starts from the river boundary and ends at the end of the channels. This reflects the decrease of the river influence as the distance from the mouth increases and causes the downstream channels to become mixed (with sea water). The channels on the left and on the right of the mouth are also mixed but with high and low salinity water respectively. The wet season map (Figure 16B) shows that PEA increases progressively in space. The delta has become fully mixed due to the higher discharges. However, the low order channels (of 1st order usually) exhibit higher PEA values than before because the higher discharge reaches these areas and increases the vertical salinity gradients.

In addition to bathymetry and distance from the mouth, the hydrodynamic forcing and in particular the presence or not of tides is another important parameter for stratification. Figure 17 C and D illustrate maps of PEA for the same instants as in Figure 16 A and B but for a case including tide (mesotide). Figure 17 C demonstrates that the delta is divided in two zones with their borderline at X ~= 4 km. Channels located upstream of this border are stratified but channels beyond of it are mixed. A comparison between panels A (no tide) and panel C (with tide) shows that more channels are stratified closer to the mouth in the latter than in the former case. This happens because the tide increases the flow currents in the delta (section 7.2) which results in an increase of stratification. At the same time, tide-induced mixing makes more delta channels mixed in the areas downstream of the border (X ~= 4 km). However, it is likely that most of these channels are mixed with salt water. Figure 17 D presents lower PEA at every position compared to Figure 17 B (no tide) indicating the contribution of tide-induced mixing that in combination with high discharges almost eliminates stratification.

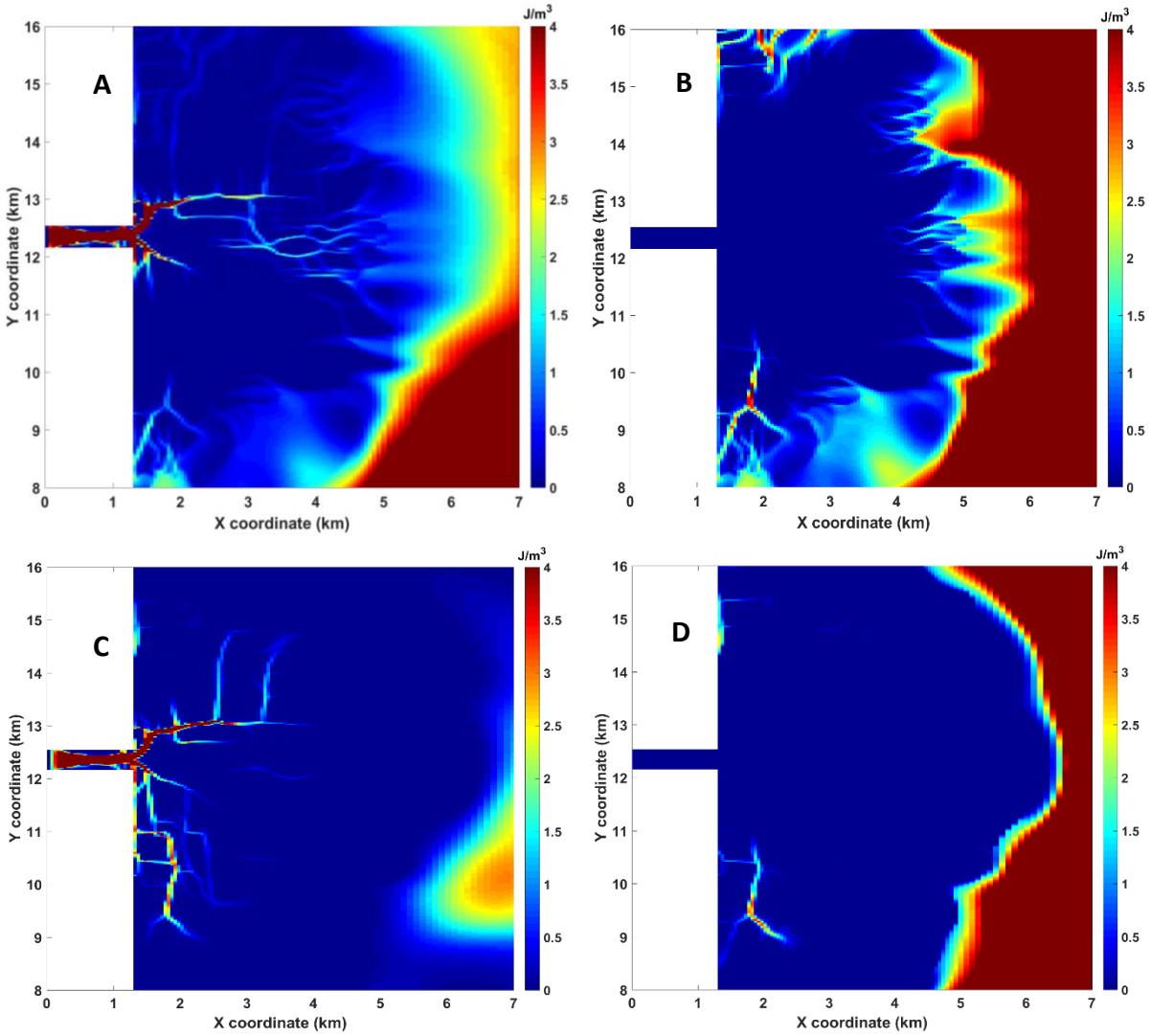

Figure 17 (A, B) Potential energy anomaly in the delta configuration used for chapters 5 and 6 in an instant during the dry and the wet season respectively without tidal forcing. (C,D) Potential energy anomaly in the delta configuration used for chapters 5 and 6 in an instant during the dry and the wet season respectively including tidal forcing.

Buoyant plumes vertical structure

Moreover, the work in chapter 5 focused on the vertical structure of the offshore buoyant plume that is a common feature in both river and tide dominated systems. This is more prominent during wet season and flood tide when the tidal and river flow counteract to each other. The plume's vertical structure depends on the level of tidal forcing and transforms progressively from a surface to bottom advected type as the amplitude increases. River dominated and microtide systems are expected to present surface advected plumes that move offshore through a low density layer close to the surface. This stratifies the water column with serious consequences for aquatic life and water quality (Chant, 2012). One of them can be hypoxia (low levels of oxygen at the bottom layers) that can increase mortality of fish and prey species and reduce growth and production (Diaz et al. 2019). For example, hypoxia has been reported to occur in the micro-tide estuaries of Pearl River and Chesapeake Bay (Sun et al. 2020). In contrast, the plume in macrotidal regimes occupies the full vertical column and remains in contact with the bottom due to tide-induced turbulence providing mixing. Therefore, an increase of the tidal range leading to bottom advected plumes may have a positive effect on issues such as

hypoxia. For instance, active oxygen replenishment from the atmosphere is observed in the macrotidal Scheldt and Chikugo estuaries (Sun et al. 2020). Finally, mesotide regimes can develop a plume of intermediate type which is initially connected with the bottom but detaches from it further downstream at higher depths when the flow is not hydraulically possible to move any deeper (Atkinson, 1993).

7.5 Salinity - river discharge relationship

The river discharge has a dominant role on the salinity distribution that becomes even more important in the absence of tides and other driving mechanisms such as winds and waves (Garvine et al., 1992; Denton and Sullivan, 1993; Valle-Levinson and Wilson, 1994; Wong, 1995;Wong et al., 1995; Petersen et al., 1996;Monismith *et al.*, 2002). This strong dependency of salinity on flow is fundamental in estuarine physics. In the past, empirical curves have been developed that relate the salt intrusion length with river discharge through power laws (Hansen and Rattray 1965; MacCready 1999; Monismith et al. 2002; Heltand and Geyer 2004). The exponent in the power law has been measured to be -1/3 although other values have been reported as well (Monismith et al. 2002; MacWilliams et al. 2015). Water quality managers are particularly interested in the salt intrusion response to flow changes. The salinity response to river discharge changes has been the topic of many studies (Kranenburg 1986; MacCready (1999, 2007); Chen et al., 2000; Monismith 2002; Hetland and Geyer 2004; Lerczak et al. , 2009; Chen 2015). Scientists have identified asymmetries in the salinity response to flow changes. Salinity responds slower to flow decreases than increases (Chen 2000; Chen 2015; Hetland and Geyer 2004; Monismith 2017). The asymmetry is attributed to non-linear processes (Chen 2015; Monismith 2017). This hysteresis was also detected in the findings of chapter 6 for every type of flow distribution in a channelized network.

However, the determination of the salt intrusion length in a channelized network is not as straightforward as in estuaries. The deltas have a complex and irregular morphology which makes the definition of salt intrusion length difficult. With this consideration, an attempt was done in this project to correlate directly salinity with river discharge. The motivation was to summarize if possible the complex dynamics and processes modelled in this idealized delta configuration and reduce the dimensionality of the problem. Estuarine studies have identified a strong negative correlation between river discharge and salinity (Garvine et al., 1992; Denton and Sullivan, 1993; Wong et al., 1995; Petersen et al., 1996). It is also known from theory that if we consider a 1D estuary of constant cross-section in a steady-state system and with constant diffusion, this correlation can be expressed through an exponential equation (Crank 1975, Fischer et al.1979, Zimmerman 1988). The boundary conditions for the equation to be valid are a seawater salinity at the offshore boundary and freshwater in a very long distance from it with the longitudinal x direction increasing upstream. The equation is the solution of the 1D advection-diffusion equation under these assumptions.

In the present work, it was discovered that the 3D modelling results could be successfully summarized by a similar equation. This is achieved through a process of averaging the salinity over depth and over radial cross-sections. The model setup satisfies some of the theoretical assumptions such as the constant diffusion coefficient and the boundary conditions. The salinity at the offshore boundary was set equal to 30 PSU and freshwater is assumed at the upstream river boundary. On the other hand, the flow is not constant and the radial cross-sections vary irregularly in space due to the delta's complex morphology. In spite of all these, the equation holds for the entire simulation period. It could be inferred then that the flow in the model changes slowly compared to the salinity adjustment time scale and therefore the system must remain close to steady state. In addition, exponential equations are common solutions of the diffusion equation and have been reported in the literature even for non-steady conditions and variable cross-sections (Philipp 1994; Zoppou and Knight 1999). Relevant

studies showed that the variable parameters of the equation can be reduced through mathematical formulations and expressed exclusively by constant coefficients. Therefore, it seems reasonable to assume a resemblance between the model results derived equation and the theoretical solution of the 1D advection-diffusion equation.

Advantages

The fact that the system's complex dynamics and dimensionality can be successfully summarized into a simple 1D equation with reference to estuarine theory is a great asset. The equation incorporates successfully many processes and parameters that are interconnected to each other such as the complex morphology, dynamic flow variability, and horizontal and vertical density gradients. This simple relationship between salinity and river discharge offers many advantages. River discharge measurements are usually more frequent and easier to find than salinity. Most of the times, salinity data in channels are sparse and limited. The exponential equation offers the opportunity to estimate the salinity in a certain distance from the river mouth and at a certain time moment based on river discharge observations. Considering that access to water flow data is usually much easier and available for a larger number of locations, a relationship that links directly salinity with river discharge can be of great value for the industry and water management authorities.

Limitations

However, the implementation of this relationship in real systems may be subject to several limitations. For example, constant diffusion in a natural system is usually not realistic. The horizontal diffusion in many real estuaries is known to vary in O(10 m^2/s – 1000 m^2/s). Despite that, the use of a constant diffusion coefficient is common in modelling studies and has been justified (Lewis and Uncles, 2003; Gay and O'Donnell, 2007) after good agreement between model and salinity observations in a number of estuaries.

The method was later tested in a real delta using data from the Mississippi Delta that is categorized as a river dominated system and the tide is low (mean tidal range is 0.35m according to Levin (1993)). The results analysis shows a satisfactory fitting for an exponential correlation between salinity and river discharge but mostly in short to medium distances from the river. There are a number of parameters to which this discrepancy can be ascribed. For example, the diffusion varies spatially in the Mississippi delta in contrast to the model. The river influence becomes weaker in longer distances where other forcing parameters may become more influential (e.g. winds, waves and tides). In any case, a complete agreement between idealized and real data could not be expected for the reasons that were discussed in section 7.1.

Parameters affecting the equation

The method has been repeated in the second larger model in chapter 5 in an effort to assess its applicability in systems including tides and any influence that these may have on the exponential salinity-river discharge relationship. The tide does not seem to affect this relationship. Simulations where higher tidal amplitudes were considered (meso-tide and macro-tide scenarios) developed exponential correlations between salinity and river discharge similar to those detected without tide (chapter 4). It seems though that this relationship is sensitive to other parameters. When the river discharge is low, bathymetric differences within the delta lead to asymmetric spatial salinity distribution (section 7.2). During these times, the salinity and river discharge correlate better through a double instead of single term exponential equation. When the hydrodynamic forcing increases (due to either higher discharges or tidal amplitudes), the salinity distribution becomes symmetric again and the correlation returns to a single term exponential equation.

The double exponential equation has also theoretical reference. Fischer et al. (1979) reported that this kind of equation is a solution to the 1D advection-diffusion equation in the special case of a wall presence blocking the flow behind of it. The correspondence between this special theoretical case and the model results equation might not be direct but allows for a better understanding of the physical mechanisms behind it. The theoretical solution assumes an impermeable wall and the idealized delta bathymetry can exhibit areas that could act as flow obstacles similar to a wall (e.g. deeper channels). However, there is a crucial difference between the theory and the model. An obstacle in the model, such as a very deep channel, is not impermeable but only delays the flow over and beyond of it instead of fully preventing it. Therefore, the level of its 'permeability' depends on the level of hydrodynamic forcing (low or high). This difference between model and theoretical equation is reflected on the opposite signs of the two exponential terms. In the theoretical case, both terms are positive so that the salinity upstream of the wall increases continuously in time. On the contrary, the model's solution includes a positive term that expresses the delay in the decrease of salinity from an obstacle and a negative one referring to the river discharge effect on salinity. The latter is a growth term that increases in time as the flow increases and the former a decay term that decreases in time while the effect from the deep channel reduces.

The tides do not constitute a factor that would alter the nature of the equation (exponential distribution) between salinity and river discharge because they act in favour of symmetric salinity distributions and not against it. Other types of forcing that cause flow asymmetries may result in deviations from the original equation. These may include for example Coriolis force effects, waves and wind forcing (see more details in section 4.1 of chapter 4). Overall, the analytical equation remains a valuable and useful tool for salinity prediction despite its limitations.

7.6 Implications in salinity from changes in the hydrographs shape

The previous section emphasized on the strong dependency of salinity on the river discharge. The negative correlation indicates that an increase of river discharge decreases salt intrusion (Garvine et al. 1992; Gong and Shen, 2011) that is an issue from which many deltas suffer already. The annual flow distribution can be indicative of seasons when the risk of salt intrusion is higher in a delta. Deltas can present high flow seasonality that results in various salinity patterns as discussed in section 7.2. Therefore, it is important to study the impact of changes in the hydrographs shape on the deltas salinity distribution. Changes to the shape of annual flow distributions can occur due to either natural climate variability or anthropogenic climate change (Desser et al. 2012; Zhang and Delworth 2018). For example, an increase of the peak flow could be the result of either intensified precipitation or urbanization and changes in land use (Vogel et al.2011; Viglione et al. 2016; Prosdocimi et al. 2015; François et al., 2019). On the other hand, intensified drought periods caused by natural or anthropogenic climate warming could decrease the peak flows. In addition, changes to the timing of the peak flows can be caused by polar warming and earlier snowmelt (IPCC 2007; Matti et al., 2017; Bloschl et al. 2017). Modifications of the annual flow distributions can have a direct impact on the freshwater availability. Shortages of freshwater supply would exacerbate salt intrusion problems. In the past, water management practices were restricted in technical solutions (Ha et al., 2018). The need for cost effective and friendly environmental solutions forces us to alternative paths seeking more adaptive methods (Ha et al., 2018; Zevenbergen et al., 2018).

The work in chapter 6 investigated if it is possible to improve the conditions in a delta through better management of existing water resources than seeking for additional ones. The results demonstrated that different types of hydrographs exhibit several advantages and disadvantages against salinization. Critical parameters are the peak flow magnitude and timing and the hydrographs slopes affecting freshwater areas, residence and renewal times and stratification. Therefore, water management

policy could be regulated based on this knowledge depending on the case. For example, hydrographs with very sharp peaks presented much lower levels of stratification and larger freshwater areas in the delta. On the other hand, these hydrographs can contain very large differences between maximum and minimum flows with the latter prevailing for longer periods. In this case, any benefit would be temporary. In addition, freshwater renewal could be very slow during dry seasons. Flow distributions with lower peaks but higher flow rates during dry seasons can provide freshwater conditions in the delta for longer time. A similar effect is possible by moving the peak flow closer to the start of the hydrograph. The disadvantage though in these two cases is that the salt intrusion limit is transferred landward. If the peak flow is displaced closer to the end of the hydrograph, the freshwater renewal will become faster at that time but this would be counterbalanced by a decrease of the total time with freshwater in the delta. Table 4 presents a summary of the effects for the various types of hydrographs. Conclusively, the shape of annual hydrographs influences the level of salinity in river deltas and can indeed contribute to a more sustainable water management. Special consideration should be taken though to ensure that any imposed changes on the flow distribution would be the appropriate regarding the priorities and needs of a certain system

Table 4 A summary of the effects in stratification, flushing and residence times and freshwater areas of hydrographs with certain characteristics

Characteristics	Stratification	Flushing time	Residence Time	Freshwater Areas
Sharp tails and low max to min discharge differences	Low effectiveness in the delta, stratification can be high even in wet seasons	Fast water renewal in both dry and wet seasons	High residence times , the water can be fresh for months in medium to high order channels	Restricted areas leaving out low order channels
Sharp peak, long periods with low flows and high max to min discharge differences	Can provide full mixing during wet season inside the delta	Very slow water renewal, could take months during dry seasons	Very low residence times, fresh water leaves the delta faster than in other cases	Vey wide areas that can cover temporarily the entire delta
Peak flow closer to the start, falling limb on the right	Medium effectiveness, small decrease of stratification in wet seasons	Slow water renewal in both seasons, could be a couple of weeks	High residence times , the water can be fresh for months in medium to high order channels	Wide areas could include some of the low order channels
Peak flow closer to the end, rising limb on the left	Medium effectiveness, small decrease of stratification in wet seasons	Fast water renewal, requires a couple of days in both seasons	Low residence times, could be even shorter in deeper channels	Wide areas could include some of the low order channels

7.7 Flushing and residence times

In this project, the effect of flow seasonality on flushing times was assessed. Flushing time (FT) calculation is quite sensitive to the river discharge implemented in its equation. It is important for the river discharge to be as much representative as possible for the period of investigation to avoid overestimations and/or underestimations. In this study, instantaneous and seasonal flushing times were tested at first (chapter 4). Instantaneous flushing time in the case of high flow variability between dry and wet seasons proved to be unreliable because it cannot provide a representative water renewal time. Averaging seasonally (every three months in a full year simulation) the river discharge demonstrated the significant reduction in flushing times during wet periods when it can be only a few hours compared to a few days in the dry seasons. It revealed also a few hours decrease of dry period flushing time when it follows a long wet season. Nonetheless, the fact that the river discharge is averaged over such a long period is still concerning. Therefore, the Date Specific Method (DSM) as introduced by Alber and Sheldon (1999) was used additionally for comparison. The advantage is that it proposes a method to determine the appropriate time frame to average the river discharge. The implementation of the DSM disclosed much higher differences between dry and wet season flushing times compared to the seasonal averaging method. Therefore, it is inferred that seasonal averaging is also unreliable because it leads to FT overestimation for wet and underestimation for dry seasons. The reason is that by averaging the river discharge over very long periods the effect of very low or very high discharges is mitigated. The DSM provides much more realistic and reliable results and therefore it is qualified as the best technique.

Freshwater renewal times are long in deltas facing salinization. In chapter 6, the effect of various flow distributions on the FT is investigated to detect what kind of hydrographs could provide shorter FT. The DSM was used following the conclusions of chapter 4 and this provided a better evaluation on the FT calculation. In addition to the river discharge averaging period, important parameters affecting the flushing time calculations were found to be :1) the statistical value of river discharge (e.g. mean or median), 2) the starting date of the calculation and the 3) preceding flow conditions. Dry season flushing times are more sensitive to these parameters. They can be much longer if long periods with decreasing flow have preceded. In such cases, the use of a mean discharge over the averaging period is not recommended because it mitigates the effect of low discharges and results in much lower flushing times. The use of the median discharge is proposed instead so that the effect of long low flow periods is not neglected. Wet season flushing times are less sensitive to these parameters because the higher the flow the faster the water renewal takes place irrespective of the preceding conditions. The wet season flushing time seems to depend exclusively on the river discharge magnitude. Finally, it was discovered that the hydrographs shape has a bigger impact on the dry season FT and much less on the wet season one that can be very low even in the range of hours. Hydrographs with lighter tails (meaning faster rate of flow changes) present faster freshwater renewal.

The residence time (RT) calculation of a particle or pollutant into a system is more straightforward as it derives directly from the model results. The concept of residence time was adapted in this project to determine the time that salinity remains below critical levels for a number of activities (e.g. water consumption, survival of vegetation and marine species, crops yield, irrigation and agriculture etc.). Many studies consider the 2 PSU salinity as a representative threshold limit that satisfies these requirements in most deltas (Schubel, 1992; Monismith et al.,1996,2002; Herbold and Vendlinkski, 2012; Andrews et al. 2017). Therefore, the freshwater residence time as defined in this study is a critical parameter that determines the time period when various anthropogenic activities can safely take place in the delta.

Freshwater RT is shorter in downstream regions because these are located far from the freshwater source. These include channels of low stream order. In contrast, areas and higher order channels that are closer to the river channel can remain fresh for much longer times even in the range of months. However, there is always a threat for salt intrusion in the inlet in the case of sustained drought periods. It is possible to increase the freshwater RT with the appropriate freshwater management. Hydrographs with lighter tails (e.g. platykurtic and positively skewed) exhibit longer freshwater residence times because of the faster flow rates. The evolution in space of the freshwater RT does not change in the presence of tides. However, changes in the tidal range can have an impact. An increase of the tidal amplitude until a certain level can increase the freshwater RT everywhere due to tide-induced mixing. For example, it was found that a simulation for a micro-tidal regime provided the highest times with freshwater for every channel order and it was the only case that the most distant channels (first order) became fresh for some time. Positive effects from the tide reverse though when the amplitude increases above a threshold. In this case, the freshwater residence time decreases with the increase of the amplitude.

8 CONCLUSIONS

This research work ended up to important conclusions that hopefully could contribute further in the effort to understand better the cause of changes in salinity distribution in a delta and to develop methods and techniques to alleviate the impact of increased salinity levels. The conclusions of this work could be separated in three categories, these that refer to : i) the influence of different forcing parameters (river discharge and tides) and bathymetry, ii) the assessment and outcome from the implementation of innovative methods and techniques and iii) the suggestions for better water management to mitigate or avert salinization issues. Conclusions of the first category are listed below:

1) Salinity can undergo considerable seasonal variations in the case of high dynamic flow variability. Deltaic systems can face serious threats during low flows periods. The freshwater can be confined in very narrow areas in close proximity to the river mouth and so its volume might not be sufficient for the execution of certain activities (e.g. irrigation, farming etc.). The conditions could become even more critical if the dry season is prolonged and salt intrusion occurs at the river mouth.
   In high flows periods, the freshwater can spread radially in wider areas and longer distances from the river mouth. Fully mixed conditions can be developed depending on the flow magnitude and the entire delta may become fresh when the flow reaches its maximum.
2) Changes of the tidal range could have either positive or negative effects against salinization. The tide increases the flow currents in the delta and acts in favour of symmetric spatial salinity distributions. Consequently, freshwater areas close to the mouth could increase. In the more downstream areas, tide-induced mixing decreases salinity increasing freshwater volumes. Therefore, increases of the tidal amplitude could be beneficial in river dominated deltas that face salt intrusion issues. On the contrary, an increase of the tidal range in mesotidal and macrotidal regimes could increase salinization. In this case, freshwater areas become constrained and freshwater volumes decrease as the amplitude increases.
3) The bathymetry is an important parameter that can affect the salinity distribution. Its impact is higher at low flow periods when the bottom friction is stronger. If the river discharge is not sufficient, the freshwater might not be able to spread radially and so an asymmetric salinity distribution develops with high horizontal gradients in the lateral direction. This can have an impact on detected salinity correlations with channels order and river discharge. The complex and relatively shallow bathymetry inside the delta allows the river discharge to fully mix the water column in some distance from the river mouth depending on its magnitude. This results in a decrease of stratification with the increase of river discharge which is counterintuitive to what is reported in estuarine studies.

The implementation of innovative methods and techniques lead to some interesting and useful conclusions that follow:

1) Topological methods (e.g. stream labelling) could be successfully implemented in deltas to correlate salinity with a non-dimensional parameter that takes only integer values. If the delta channels are classified based on their order according to the Strahler-Horton method, a trend appears with salinity increasing as the stream order decreases. This is convenient because it allows to identify channels expected to be more saline than others. However, this trend is sensitive to the spatial salinity distribution and might not be present as long as this is not symmetric. Sources of asymmetry could be the Coriolis force, intermittent wind and waves forcing as well as bathymetric effects. In this project, only the latter case was studied. If and when bathymetric effects cause asymmetric salinity distribution, the Strahler-Horton method

could be replaced by the width function. The width is the number of channels links between equal space steps along the delta and represents changes in the delta's cross-section. The width correlates with salinity in a similar way to the channels order. Salinity increases as the width decreases.

The two methods could be combined because stream order applies better during high flows and width function during low flows periods. Nevertheless, salinity distributions that satisfy both methods can be developed in systems with significant tidal forcing (e.g. mesotide and macrotide).

2) It is possible to develop analytical relationships with reference to the theory that summarize the complex dynamics of deltaic systems and reduce dimensionality. Depth and radial averaged salinity is negatively and exponentially correlated with the river discharge. This is valid for both river and tide dominated deltas. The exponential equation is very similar to the solution of the 1D advection-diffusion equation in steady state conditions and for constant cross-sections and diffusion. Therefore, its applicability in real systems is subject to limitations. Deviations from a direct exponential equation may be due to variable diffusion and cross-sections and/or other type of external forcing (e.g. wind, waves, Coriolis force).

   If the bathymetry exhibits features that could act as flow sinks (e.g. very deep channels compared to their neighbour ones), the salinity and river discharge correlate better through a double exponential equation. This is expected to be valid as long as the bathymetry causes the salinity distribution to not be symmetric and usually occurs during low flows periods. The double exponential equation is also linked to a theoretical case which is the solution of the 1D advection-diffusion equation in the special case that there is a wall acting as a closed boundary.

3) The determination of the freshwater renewal time depends a lot on the averaging period of the river discharge. Estimation of instantaneous flushing times is not useful in systems with high flow dynamic variability and calculations with seasonal averaging of river discharges can lead to overestimations or underestimations. For the purposes of this study, the Date Specific Method (DSM) by Alber and Sheldon (1999) has provided the most reliable results. Flushing times in the order of hours during wet seasons but in the order of days (or even months) in dry seasons were estimated. Special consideration must be taken in the case of hydrographs with heavy tails (e.g. leptokurtic distribution) where the use of the median instead of the mean river discharge over a certain period is recommended so that the effect of long low flow periods is not neglected. Hydrographs with steeper slopes (e.g. platykurtic, positively skewed) can renew the freshwater faster.

Investigation of the effect of various flow distributions on salinity lead to the following main conclusions:

1) The shape of annual hydrographs influences the level of salinity in river deltas and can contribute to a more sustainable water management.
2) The peak flow position in the hydrograph, its magnitude and the hydrographs tails determine freshwater areas, residence and renewal times and stratification. Hydrographs of equal peak flow present equal freshwater areas irrespective of their shape. Hydrographs with their peak positioned closer to the start present longer freshwater residence times and are more effective against salt intrusion. An increase of the peak flow can displace the salt intrusion limit seaward and decrease stratification especially in shallow areas.
3) Salinity responds slower to flow decreases than increases.
4) A certain salinity standard could be achieved in much shorter time if the rate of flow change increases and the hydrographs tails become lighter.

9 FUTURE WORK

This PhD project sets the ground for further research on this topic. There is a lot of space to extend the work done in this project and investigate topics that have not been discussed and addressed in this case. For example, wave dominated deltas have not been considered. It would be very interesting to implement many of the methods of the present study into this type of deltas. Wave dominated deltas can have a complex morphology that includes very often shore-parallel mouth bars. The angle with which the waves approach the shore affects the flow jet direction and spreading (Nardin and Fagherazzi 2012) while wave-induced transport has an impact on horizontal salinity gradients and estuarine circulation (Schloen et al. 2017). It is speculated that many relationships and correlations presented in this thesis could be largely affected in such environments. Similar impact can be expected from wind forcing. Upwelling and downwelling favourable winds move freshwater offshore and onshore respectively (Barlow 1956; Pullen & Allen 2000; Fong & Geyer 2001; Whitney & Garvin 2005; Choi & Wilkin 2007). This onshore/offshore transport of freshwater could alter significantly the conclusions of seasonal salinity variation depending on when the intermittent wind forcing occurs and for how long it lasts. It would be worthy to study this in the case of a wave dominated system due to the presence of wind-generated waves. In addition, the work done here for tidally influenced systems has purposefully neglected the impact of spring-neap tides on salinity. However, this could be important for salt intrusion since stratification is usually more pronounced during neap-tides. The inclusion of spring-neap tides can be a quite complicated issue. The spring-neap effect on salt intrusion is not straight forward because there are different responses to various estuaries. For example, in well-mixed or salt wedge estuaries, saltwater intrudes more landward during spring than neap tides while the opposite occurs in partially mixed estuaries (Gong and Shen 2011). It would be interesting to investigate this effect in tidal dominated deltas and detect similarities/differences with different types of estuaries.

The effect of density stratification on the sediment transport has also been neglected in this study. This was done deliberately to preclude morphological changes. The salinity distribution is subject to changes only by varying hydrodynamic forcing. However, many mega deltas around the world (e.g. Ganges-Brahmaputra) have large sediment flux loads that can cause morphological changes due to sediment deposits (Rahman et al. 2018). Thus, the interplay between sediments and stratification in deltas is an important parameter that would require further investigation. Shear stresses and rates of sediment transport may be inhibited by density stratification (Moodie et al.2017). Vertical salinity gradients can depress turbulence and sediments resuspension (Li et al. 2018). Changes to stratification due to tidal straining would limit sediments suspension in the lower water column during ebb but allow it in higher water layers during flood tide (Scully and Friedrichs 2003). In its turn, vertical distribution of suspended sediments may enhance stratification (Li et al. 2018)). A comparison of sediment transport in deltas between different regimes would be valuable. For example, wind and wave-driven transport can move sediments offshore while these may be constrained onshore in very stratified conditions (Flores et al. 2017). Finally, another interesting plan would be to combine the work of chapter 5 and 6 in order to assess the influence of different hydrograph shapes on salinity in systems where the tidal level is significant and cannot be neglected.

10 BIBLIOGRAPHY

Abedin Md.A, Habiba U., Shaw R., (2013). 'Salinity Scenario in Mekong, Ganges, and Indus River Deltas, Water Insecurity: A Social Dilemma Community', *Environment and Disaster Risk Management*, Vol. 13,pp. 115-138

Adams W. (2000).'World Commission on Dams, Dams and Development: A New Framework for Decision-Making'.ch.1, pp.1-28. EarthScan London.

Ahmed, M.F., and M. Rahman. (2000.) 'Water supply and sanitation: Rural and low income urban communities. Dhaka: ITN-Bangladesh', Center for Water Supply and Waste Management, BUET.

Akter, A. ,Tanim, A. H. (2021) 'Salinity Distribution in River Network of a Partially Mixed Estuary', *Journal of Waterway, Port, Coastal, and Ocean Engineering*, 147(2), p. 04020055. doi: 10.1061/(asce)ww.1943-5460.0000621.

Alber, M. , Sheldon, J. E. (1999) 'Use of a date-specific method to examine variability in the flushing times of Georgia estuaries', *Estuarine, Coastal and Shelf Science*, 49(4), pp. 469–482. doi: 10.1006/ecss.1999.0515.

Albrecht J., Car A., (2004). GIS Analysis for Scale-sensitive Environmental Modelling Based on Hierarchy Theory, GIS for Earth Surface Systems.

Allison, L. E. (1964) 'Salinity In Relation To Irrigation', *Advances in Agronomy*, 16(C), pp. 139–180. doi: 10.1016/S0065-2113(08)60023-1.

Allison, M. A. (1998) 'Historical changes in the Ganges-Brahmaputra delta front', *Journal of Coastal Research*, 14(4), pp. 1269–1275.

Allison, M. A., Dallon Weathers, H. and Meselhe, E. A. (2017) 'Bottom morphology in the Song Hau distributary channel, Mekong River Delta, Vietnam', *Continental Shelf Research*. Elsevier Ltd, 147(October 2016), pp. 51–61. doi: 10.1016/j.csr.2017.05.010.

Andrews, S. W., Gross, E. S. and Hutton, P. H. (2017) 'Modeling salt intrusion in the San Francisco Estuary prior to anthropogenic influence', *Continental Shelf Research*. Elsevier Ltd, 146(May), pp. 58–81. doi: 10.1016/j.csr.2017.07.010.

Anh, D. T., Hoang L.P., Bui M.D, Rutschmann, P. (2018) 'Simulating future flows and salinity intrusion using combined one- and two-dimensional hydrodynamic modelling-the case of Hau River, Vietnamese Mekong Delta', *Water (Switzerland)*, 10(7). doi: 10.3390/w10070897.

Anh, D. T., Bui, M. D., Rutschmann, P. (2015) 'Impact of climate change on salinity intrusion in the Mekong Delta', in *14th International Conference on Environmental Science and Technology*.

Arenas, A.; Danon, L.; Díaz-Guilera, A.; Gleiser, P. M.; Guimerá, R. 2004. Community analysis in social networks, *European Physical Journal B*, vol.38 (2): p.373–380. doi:10.1140/epjb/e2004-00130-1.

Atkinson, J. F. (1993) 'Detachment of Buoyant Surface Jets Discharged on Slope', *Journal of Hydraulic Engineering*, 119(8), pp. 878–894. doi: 10.1061/(asce)0733-9429(1993)119:8(878).

Balls, P. W. (1994) 'Nutrient Inputs to Estuaries from Nine Scottish East Coast Rivers; Influence of Estuarine Processes on Inputs to the North Sea', *Estuarine, Coastal and Shelf Science*, pp. 329–352. doi: 10.1006/ecss.1994.1068.

Banas, N. S., Hickey, B.M., MacCready, P., Newton J.A. (2004) 'Dynamics of Willapa Bay, Washington: A highly unsteady, partially mixed estuary', *Journal of Physical Oceanography*, 34(11), pp. 2413–2427. doi: 10.1175/JPO2637.1.

Banas, N. S., Hickey, B.M. (2005) 'Mapping exchange and residence time in a model of Willapa Bay, Washington, a branching, macrotidal estuary'. *Journal of Geophysical Research,* vol.110, C11011.

Banavar, J. R., Maritan, A. and Rinaldo, A. (1999) 'Size and form in efficient transportation networks', *Nature*, 399(6732), pp. 130–132. doi: 10.1038/20144.

Barlow J.P., (1956). 'Effect of Wind on Salinity Distribution in an Estuary', *Journal of Marine Research*, Vol.15, p. 193-203.

Bates, C. C. (1953) 'Rational theory of delta formation',*Bulletin of American Association of petroleum geolgists',* vol. 37(9), pp. 2119–2162.

Becherer, J., Stacey, M. T., Umlauf, L., Burchard, H. (2015). 'Lateral circulation generates flood tide stratification and estuarine exchange flow in a curved tidal inlet'. *Journal of Physical Oceanography*, vol. 45(3), pp. 638–656.

Becker , M.L., Luettich Jr., R.A., Mallin, M.A.(2010) 'Hydrodynamic behaviour of the Cape Fear River and estuarine system: A synthesis and observational investigation of discharge-salinity intrusion relationships' , *Estuarine Coastal and Shelf Science,* vol.88,pp.407-418. doi:10.1016/j.ecss.2010.04.022

Beer, T., and M. Borgas (1993). 'Horton's laws and the fractal nature of streams', *Water Resources Research*, vol.29(5), pp. 1475– 1487.

Bellafiore, D., Ferrarin C., Maicu F., Manfe G.,Lorenzetti G., Umgiesser G., Zaggia L., Valle-Levinson,A. (2021) 'Saltwater Intrusion in a Mediterranean Delta Under a Changing Climate', *Journal of Geophysical Research: Oceans*, 126(2), pp. 1–23. doi: 10.1029/2020JC016437.

Bhuiyan, M. J. A. N., Dutta, D. (2012) 'Assessing impacts of sea level rise on river salinity in the Gorai river network, Bangladesh', *Estuarine, Coastal and Shelf Science*. Elsevier Ltd, 96(1), pp. 219–227. doi: 10.1016/j.ecss.2011.11.005.

Birkinshaw, S. J., Guerreiro SB, Nicholson A, Liang Q, Quinn P, Zhang L, He B, Yin J, Fowler HJ.(2017) 'Climate change impacts on Yangtze River discharge at the Three Gorges Dam', *Hydrology and Earth System Sciences*, 21(4), pp. 1911–1927. doi: 10.5194/hess-21-1911-2017.

Biswal, B. , Marani, M. (2010) 'Geomorphological origin of recession curves', *Geophysical Research Letters*, 37(24), pp. 1–5. doi: 10.1029/2010GL045415.

Blanton, J., Alber, M. and Sheldon, J. (2001) 'Salinity response of the Satilla River estuary to seasonal changes in freshwater discharge', *Proceedings of the 2001 Georgia Water Resources Conference*, pp. 1–4. Available at: http://gce-lter.marsci.uga.edu/public/files/pubs/Blanton_gwrc.pdf.

Bloschl G. et al. (2017). 'Changing climate shifts timing of European flods',*Science*,vol.357,issue 6351,pp.588-590. DOI: 10.1126/science.aan2506

Blum, M.D., Tornqvist, T.E. (2000) 'Fluvial response to climate and sea-level change: a review and look forward'. *Sedimentology* ,vol.47 (Suppl.), 1–48.

de Boer, G. J., Pietrzak, J. D. and Winterwerp, J. C. (2008) 'Using the potential energy anomaly equation to investigate tidal straining and advection of stratification in a region of freshwater influence', *Ocean Modelling*, 22(1–2), pp. 1–11. doi: 10.1016/j.ocemod.2007.12.003.

Bolaños, R. , Brown, J.M. , Amoudry, L.O. , Souza, A.J. , (2013). 'Tidal, riverine, and wind influences on the circulation of a macrotidal estuary'. *Journal of Physical Oceanography*, vol. 43 (1), p.29–50.

Bolin, B. and H. Rodhe (1973) A note on the concepts of age distribution and transit time in natural reservoirs. Tellus , vol.25, pp.58–62.

Bondar C.(1968). 'Hydraulic and hydrological conditions of the Black Sea waters penetration into the Danube mouths', *Studii de Hydrologie.*

Borchert, Rolf; Slade, Norman A. (1981). 'Bifurcation ratios and the adaptive geometry of tree', *Botanical Gazette*, vol.142 (3): pp.394–401, doi:10.1086/33723

Botter, G., Rinaldo, A. (2003) 'Scale effect on geomorphologic and kinematic dispersion', *Water Resources Research*, 39(10), pp. 1–10. doi: 10.1029/2003WR002154.

Bowen, M. M.,Geyer, W.R. (2003) 'Salt transport and the time-dependent salt balance of a partially stratified estuary', *Journal of Geophysical Research*, 108(C5), pp. 1–15. doi: 10.1029/2001jc001231.

Bracken, L.J., Wainwright, J., Ali, G.A., Tetzlaff, D., Smith, M.W., Reaney, S.M., Roy, A.G., (2013). 'Concepts of hydrological connectivity: Research approaches, pathways and future agendas', *Earth Science Reviews*, vol.119,pp.17-34. https://doi.org/10.1016/j.earscirev.2013.02.001.

Bricheno, L. M., Wolf, J. , Sun, Y. (2021) 'Saline intrusion in the Ganges-Brahmaputra-Meghna megadelta', *Estuarine, Coastal and Shelf Science*. Elsevier Ltd, 252, p. 107246. doi: 10.1016/j.ecss.2021.107246.

Bricheno, L.M,Wolf, J. (2018).'Modelling Tidal River Salinity in Coastal Bangladesh', chapter 17 in Ecosystems Services for Well-Being Deltas,Integrated Assessment for Policy Analysis. https://doi.org/10.1007/978-3-319-71093-8

Bricheno, L. M., Wolf, J. and Islam, S. (2016) 'Tidal intrusion within a mega delta: An unstructured grid modelling approach', *Estuarine, Coastal and Shelf Science*. The Authors, 182, pp. 12–26. doi: 10.1016/j.ecss.2016.09.014.

Brockway, R. ,Bowers D., Hoguane A., Dove V., Vassele V. (2006) 'A note on salt intrusion in funnel-shaped estuaries: Application to the Incomati estuary, Mozambique', *Estuarine, Coastal and Shelf Science*, 66(1–2), pp. 1–5. doi: 10.1016/j.ecss.2005.07.014.

Brunier, G., Anthony, E.J., Goichot M., Provansal M., Dussouillez , P. (2014) 'Recent morphological changes in the Mekong and Bassac river channels, Mekong delta: The marked impact of river-bed mining and implications for delta destabilisation', *Geomorphology*. Elsevier B.V., 224, pp. 177–191. doi: 10.1016/j.geomorph.2014.07.009.

Bryson , M.(1974). 'Heavy tailed distributions: Properties and Tests'.*Technometrics* vol.16(1),pp.61-68.

Burchard, H., Hetland, R.D., Schulz, E., Schuttelaars, H.M. (2011). 'Drivers of residual estuarine circulation in tidally energetic estuaries: straight and irrotational channels with parabolic cross section', *Journal of Physical Oceanography* ,vol.41,pp.548–570

Burchard, H., Hetland, R. D. (2010) 'Quantifying the contributions of tidal straining and gravitational circulation to residual circulation in periodically stratified tidal estuaries', *Journal of Physical Oceanography*, 40(6), pp. 1243–1262. doi: 10.1175/2010JPO4270.1.

Burchard, H. , Hofmeister, R. (2008) 'A dynamic equation for the potential energy anomaly for analysing mixing and stratification in estuaries and coastal seas', *Estuarine, Coastal and Shelf Science*, 77(4), pp. 679–687. doi: 10.1016/j.ecss.2007.10.025.

Burpee, A. P., Slingerland, R.L., Edmonds,D.A., Parsons,D. , Best,J., Cederberg,J., McGuffin,A., Caldwell,R., Nijhuis, A., Royce, J. (2015) 'Grain-size controls on the morphology and internal geometry of river-dominated deltas', *Journal of Sedimentary Research*, 85(6), pp. 699–714. doi: 10.2110/jsr.2015.39.

Caldwell ,R., Edmonds, D.A. (2014) 'The effects of sediment properties on deltaic processes and morphologies: A numerical modeling study', *Journal of Geophysical Research*, pp. 961–982. doi: 10.1002/2013JF002871.Received.

Carless, S. J., Greena J.A.M, Pelling H.E., Wilmes S.B. (2016) 'Effects of future sea-level rise on tidal processes on the Patagonian Shelf', *Journal of Marine Systems*. The Authors, 163, pp. 113–124. doi: 10.1016/j.jmarsys.2016.07.007.

CGIAR, (2016) 'Assessment Report: Drought and Salinity Intrusion in the MekongRiver Delta of Vietnam'. CGIAR Research Centres in Southeast Asia, 25–28 April 2016

Chant, R. J. (2012) *Interactions between Estuaries and Coasts: River Plumes - Their Formation, Transport, and Dispersal*, *Treatise on Estuarine and Coastal Science*. Elsevier Inc. doi: 10.1016/B978-0-12-374711-2.00209-6.

Chant , R.J.(2010).' Estuarine secondary circulation'. Contemporary issues in estuarine physics,chapter 5, pp. 100-124, edited by A.Valle-Levinson. Cambridge University press.

Chant, R. J., Stoner, A.W. (2001). 'Particle trapping in a stratified flood-dominated estuary'. *Journal of Marine Research*, vol.59, pp.29–51.

Chao, S. Y. (1988) 'Wind driven motion of estuarine plumes', *Journal of Physical Oceanography*, 18(1), pp. 1144–1166. doi: 10.16309/j.cnki.issn.1007-1776.2003.03.004.

Chao, S. Y. (1990) 'Tidal modulation of estuarine plumes', *Journal of Physical Oceanography*, pp. 1115–1123. doi: 10.1175/1520-0485(1990)020<1115:TMOEP>2.0.CO;2.

Chao, S. Y. , Boicourt, W. C. (1986) 'Onset of estuarine plumes.', *J. Phys. Oceanogr.*, pp. 2137–2149. doi: 10.1016/0198-0254(87)90056-2.

Chapman, D. C. , Lentz, S. J. (1994) 'Trapping of a coastal density front by the bottom boundary layer', *Journal of Physical Oceanography*, pp. 1464–1479. doi: 10.1175/1520-0485(1994)024<1464:TOACDF>2.0.CO;2.

Chatwin, P. C. (1976) 'Some remarks on the maintenance of the salinity distribution in estuaries', *Estuarine and Coastal Marine Science*, 4(5), pp. 555–566. doi: 10.1016/0302-3524(76)90030-X.

Chen, W., Chen,K., Kuang, C., Zhu,D.Z., He,L., Mao,X., Liang,H., Song,H. (2016) 'Influence of sea level rise on saline water intrusion in the Yangtze River Estuary, China', *Applied Ocean Research*. Elsevier B.V., 54, pp. 12–25. doi: 10.1016/j.apor.2015.11.002.

Chen, Y., Zuo, J., Zou, H., Zhang, M., Zhang, K.(2016) 'Responses of estuarine salinity and transport processes to sea level rise in the Zhujiang (Pearl River) Estuary', *Acta Oceanologica Sinica*, 35(5), pp. 38–48. doi: 10.1007/s13131-016-0857-2.

Chen, S. N. (2015) 'Asymmetric estuarine responses to changes in river forcing: A consequence of nonlinear salt flux', *Journal of Physical Oceanography*, 45(11), pp. 2836–2847. doi: 10.1175/JPO-D-15-0085.1.

Chen, S. N., Geyer, W. R., Ralston, D. K., &Lerczak, J. A. (2012). 'Estuarine exchange flow quantified with isohaline coordinates: Contrasting long and short estuaries'. *Journal of Physical Oceanography*, vol. 42(5), pp. 748–763.

Chen S., and L. P. Sanford, (2009). 'Axial wind effects on stratification and longitudinal salt transport in an idealized, partially mixed estuary'. *Journal of Physical Oceanography*, vol.39, pp.1905–1920.

Chen, X. J. (2004) 'Modeling hydrodynamics and salt transport in the Alafia River estuary, Florida during May 1999-December 2001', *Estuarine, Coastal and Shelf Science*, 61(3), pp. 477–490. doi: 10.1016/j.ecss.2004.06.012.

Chen, X., Zong Y. , Zhang E., Xu J., Li S. (2001) 'Human impacts on the Changjiang (Yangtze) River basin, China, with special reference to the impacts on the dry season water discharges into the sea', *Geomorphology*, vol. 41(2), pp. 111–123. doi: 10.1016/S0169-555X(01)00109-X.

Chen Z., Li J., Shen H., Zhanghua W., (2001). 'Yangtze River of China: historical analysis of discharge variability and sediment flux', *Geomorphology*, vol. 41, pp.77-91.

Chen, X., Flannery, M.S., Moore, D.L.(2000) 'Response times of salinity in relation to changes in freshwater inflows in the Lower Hillsborough River, Florida', *Estuaries,* vol.23, no5,p.735-742.

Chen, X. , Zong, Y. (1999) 'Major impacts of sea-level rise on agriculture in the Yangtze delta area around Shanghai', *Applied Geography*, 19(1), pp. 69–84. doi: 10.1016/S0143-6228(98)00035-6.

Chen, F. and MacDonald, D. G. (2006) 'Role of mixing in the structure and evolution of a buoyant discharge plume', *Journal of Geophysical Research: Oceans*, 111(11), pp. 1–13. doi: 10.1029/2006JC003563.

Chen, X., Zong Y. , Zhang E., Xu J., Li S. (2001) 'Human impacts on the Changjiang (Yangtze) River basin, China, with special reference to the impacts on the dry season water discharges into the sea', *Geomorphology*, 41(2), pp. 111–123. doi: 10.1016/S0169-555X(01)00109-X.

Choi B., Wilkin J.L., (2007). 'The effect of Wind on the Dispersal of the Hudson River Plume' *Journal of Physical Oceanography*. Vol.37, p. 1878-1897. doi:10.1175/JPO3081.1

Chorley, R.J., Schum, S.A., Sugden, D.E., 1984. 'Geomorphology'. Methuen, New York, 811.

Christian, R. R., Boyer, J. N. & Stanley, D. W. (1991). 'Multi-year distribution patterns of nutrients within the Neuse River Estuary, North Carolina'. *Marine Ecology Progress Series*, Vol. 71, pp.259–274.

Chua, V. P. and Xu, M. (2014) 'Impacts of sea-level rise on estuarine circulation: An idealized estuary and San Francisco Bay', *Journal of Marine Systems*. Elsevier B.V., 139, pp. 58–67. doi: 10.1016/j.jmarsys.2014.05.012.

Chunikhina, E.V. (2018). 'Information Theoretical Analysis of Self-Similar Trees' PhD Thesis, School of Electrical Engineering and Computer Science, Oregon State University.

Chunikhina, E. V. (2018) 'Entropy rates for Horton self-similar trees', School of EECS, Oregon State University, Corvallis, OR 977330 pp. 1–20.

Clarke D., Williams S., Jahiruddin M., Parks K., Salehin M. (2015). 'Projections of on-farm salinity in coastal Bangladesh'. *Environmental Science Processes and Impacts*, vol.17, pp.1127-1136.

Coffey, T. (2017) 'Comparison of Flow Dynamics and Bifurcation Angles in Tributary and Distributary Channel Networks'. Available at : http://scholarworks.uark.edu/etdhttp://scholarworks.uark.edu/etd/1890.

Cole, K. L. , Hetland, R. D. (2016) 'The effects of rotation and river discharge on net mixing in small-mouth Kelvin number plumes', *Journal of Physical Oceanography*, 46(5), pp. 1421–1436. doi: 10.1175/JPO-D-13-0271.1.

Cole T.M, Wells S.A, (2003). 'CE-QUAL-W2: A two-dimensional, laterally averaged, hydrodynamic and water quality model, version 3.1'. Available at http://www.cee.pdx.edu/w2.

Coleman, J.M.,Wright, L.D. (1975). 'Modern river deltas: Variability of processes and sand bodies'. In: Broussard, M.L. (Ed.), Deltas: Models for Exploration. *Houston Geologic Society*, pp. 99–149.

Collischonn, W., Fleischmann, A., Paiva, R. C. D., & Mejia, A. (2017). 'Hydraulic causes for basin hydrograph skewness'. *Water Resources Research*, vol.53, pp.10603– 10618. https://doi.org/10.1002/ 2017WR021543

Conner, W. H., McLeod, K. W., & McCarron, J. K. (1997). 'Flooding and salinity effects on growth and survival of four common forested wetland species'. *Wetland Ecology and Management,* vol.5, p.99–109.

Crank,J. (1975). 'Methods of solution when the diffusion coefficient is constant. The Mathematics of Diffusion'. Brunel Universitry Uxbridge,Clarendon Press,Oxford, pp.11-15.

Csanady, G. T. (1984) 'Circulation induced by river inflow in well mixed water over a sloping continental shelf.', *J. PHYS. OCEANOGR.*, 14(11, Nov. 1984), pp. 1703–1711. doi: 10.1175/1520-0485(1984)0142.0.CO;2.

Dalrymple, R. W. , Choi, K. (2007) 'Morphologic and facies trends through the fluvial-marine transition in tide-dominated depositional systems: A schematic framework for environmental and sequence-stratigraphic interpretation', *Earth-Science Reviews*, 81(3–4), pp. 135–174. doi: 10.1016/j.earscirev.2006.10.002.

Dai, Z., Chu A. , Stive M., , Zhang X., Yan H. (2011) 'Unusual salinity conditions in the Yangtze Estuary in 2006: Impacts of an extreme drought or of the three gorges dam?', *Ambio*, 40(5), pp. 496–505. doi: 10.1007/s13280-011-0148-2.

Das, A., Justic D. , Inoue M., Hoda A., Huang H., Park D. (2012) 'Impacts of Mississippi River diversions on salinity gradients in a deltaic Louisiana estuary: Ecological and management implications', *Estuarine, Coastal and Shelf Science*. Elsevier Ltd, 111, pp. 17–26. doi: 10.1016/j.ecss.2012.06.005.

Dasgupta, S., Kamal F.A., Khan Z.H., Choudhury S., Nishat A. (2015) 'River salinity and climate change: Evidence from coastal Bangladesh', *World Scientific Reference on Asia and the World Economy*, (March), pp. 205–242. doi: 10.1142/9789814578622_0031.

Đạt, T. Q., Trung, N. H. & Likitdecharote, K. (2011) 'Modeling the influence of river discharge and sea level rise on salinity intrusion in the Mekong Delta. in The 1st Environment Asia International Conference on 'Environmental Supporting in Food and Energy Security: Crisis and Opportunity 21', Thai Society of Higher Education Institutes on Environment, 21(b). doi: 10.13140/RG.2.1.3110.3522.

Dat, T. Q. K. L. (2010) 'Effects of sea water level rise and low flow on salinity intrusion in Mekong Delta', in *International Conference for a Sustainable Greater Mekong Subregion*.

Davis, R. A. , Dalrymple, R. W. (2010a) 'Principles of tidal sedimentology', in *Principles of Tidal Sedimentology*, pp. 1–621. doi: 10.1007/978-94-007-0123-6.

Davis, R. A. , Dalrymple, R. W. (2010b) 'Principles of tidal sedimentology', *Principles of Tidal Sedimentology*, pp. 1–621. doi: 10.1007/978-94-007-0123-6.

Dawadi, S. ,Ahmad, S. (2013) 'Evaluating the impact of demand-side management on water resources under changing climatic conditions and increasing population', *Journal of Environmental Management*. Elsevier Ltd, vol.114, pp. 261–275. doi: 10.1016/j.jenvman.2012.10.015.

Day, J. W., Barras J., Clairain E., Johnston J., Justic D., Kemp G.P, Ko J.Y, Lane R., Mitsch W.J., Steyer G., Templet P., Yanez-Arancibia A. (2005) 'Implications of global climatic change and energy cost and

availability for the restoration of the Mississippi delta', *Ecological Engineering*, 24(4 SPEC. ISS.), pp. 253–265. doi: 10.1016/j.ecoleng.2004.11.015.

Day, J., Goodman R., Chen Z., Hunter R., Giosan L., Wang Y. (2021) 'Deltas in arid environments', *Water (Switzerland)*, 13(12). doi: 10.3390/w13121677.

Dazzi, R. , Tomasino, M. (1975) 'Mathematical model of salinity intrusion in the delta of the Po River', in *Coastal Engineering*, pp. 2302–2321.

Delpey M.T., Ardhuin F., Otheguy P., Jouon A. (2014). 'Effects of waves on coastal water dispersion in a small estuary bay'. *Journal of Geophysical Research: Oceans*, Vol.119, p 70-86. doi:10.1002/2013JC009466.

Deltares, (2013). 'Delft3D-Flow: Simulation of Multi-Dimensional Hydrodynamic Flows and Transport Phenomena, Including Sediments-User Manual', Hydro-Morphodynamics, version 3.15.34158. Deltares, Delft, Netherlands.

Deng , Y. (2016).'River-Delta Systems: A significant deposition location of global coal-measure source rocks'. *Journal of Earth Science,* no 4,vol.27, p.631-641. DOI: 10.1007/s12583-016-0710-8

Denton R.A, (1993)a. 'Accounting for antecedent Conditions in Seawater Intrusion Modelling - Applications for the San Francisco Bay Delta'. *Hydraulic Engineering*, vol.1 ASCE National Conference, San Francisco. July 1993. pp. 448-453.

Denton A.R., Sullivan D.G, (1993). 'Antecedent Flow-Salinity Relations: Application to Delta Planning Models', rep. for Contra Costa Water District.

Desser C.,Knutti R.,Solomon S., Phillips A.S. (2012). 'Communication of the role of natural variability in future North America climate', *Natural Climate Change,* vol.2, pp.775-779. DOI: 10.1038/NCLIMATE1562

Devroye, L. , Kruszewski, P. (1995) 'A note on the Horton-Strahler number for random trees', *Information Processing Letters*, 56(2), pp. 95–99. doi: 10.1016/0020-0190(95)00114-R.

Diaz, R.J., Rosenberg, R., Sturdivant, K. (2019.' Hypoxia in estuaries and semi-enclosed seas', chapter 2.5 in Ocean deoxygenation: Everyones's problem, causes , impacts, consequences and solutions. IUCN.Global Marine and Polar Programme,pp. 85-102

Dodds, P. S. , Rothman, D. H. (2000) 'S Caling , U Niversality , and', *Networks*, 28, pp. 571–610.

Dodds, P. S. , Rothman, D. H. (2001) 'Geometry of river networks. I. Scaling, fluctuations, and deviations', *Physical Review E - Statistical Physics, Plasmas, Fluids, and Related Interdisciplinary Topics*, 63(1), pp. 1–13. doi: 10.1103/PhysRevE.63.016115.

Dronkers, J., Zimmerman, J.T.F. (1982) 'Some principles of mixing in tidal lagoons'. In Proceedings of the International Symposium on Coastal Lagoons, Bordeaux, France. *Oceanologica Acta*.

Du, J., Shen J. , Zhang Y.J. , Ye F., Liu Z., Wang Z., Wang Y.P. , Yu X., Sisson M., Wang H.V. (2018) 'Tidal Response to Sea-Level Rise in Different Types of Estuaries: The Importance of Length, Bathymetry, and Geometry', *Geophysical Research Letters*, 45(1), pp. 227–235. doi: 10.1002/2017GL075963.

Dun, O. (2011) 'Migration and Displacement Triggered by Floods in the Mekong Delta', *International Migration*, 49(SUPPL.1). doi: 10.1111/j.1468-2435.2010.00646.x.

Dyer K.R.(1973). 'Estuaries: A Physical Introduction'. John Wiley and sons,London UK.

Dyer, K.R., (1977). 'Lateral circulation effects in estuaries'. Symposium on Geophysics of Estuaries,

National Academy of Sciences, Washington, D.C., 1977.

Edmonds, D., Slingerland, R., Best,J., Parsons, D., Smith , N. (2010) 'Response of river-dominated delta channel networks to permanent changes in river discharge', *Geophysical Research Letters*, 37(12), pp. 1–5. doi: 10.1029/2010GL043269.

Edmonds, D. A., Shaw, J. B., Mohrig, D. (2011) 'Topset-dominated deltas: A new model for river delta stratigraphy', *Geology*, 39(12), pp. 1175–1178. doi: 10.1130/G32358.1.

Edmonds, D. A. , Slingerland, R. L. (2007) 'Mechanics of river mouth bar formation: Implications for the morphodynamics of delta distributary networks', *Journal of Geophysical Research: Earth Surface*, 112(2), pp. 1–14. doi: 10.1029/2006JF000574.

Edmonds, D. A. , Slingerland, R. L. (2010) 'Significant effect of sediment cohesion on deltamorphology', *Nature Geoscience*. Nature Publishing Group, 3(2), pp. 105–109. doi: 10.1038/ngeo730.

Eldardiry, H. ,Hossain, F. (2019) 'Understanding reservoir operating rules in the transboundary nile river basin using macroscale hydrologic modeling with satellite measurements', *Journal of Hydrometeorology*, vol. 20(11), pp. 2253–2269. doi: 10.1175/JHM-D-19-0058.1.

Elhakeem A., Elshorbagy W. ,(2013). 'Evaluation of the long-term variability of seawater salinity and temperature in response to natural and anthropogenic stressors in the Arabian Gulf'. *Marine Pollution Bulletin*, vol.76,pp.355-359.

Elliott, T. (1986) 'Deltas', *Sedimentary Environments and Facies* (H.G. Reading, Ed.), Blackwell Scientific, Oxford, pp.113–154.

Ensign, S. H., Halls, J. N., Mallin, M. A. (2004) 'Application of digital bathymetry data in an analysis of flushing times of two large estuaries', *Computers and Geosciences*, 30(5), pp. 501–511. doi: 10.1016/j.cageo.2004.03.015.

Ericson, J. P., Vorosmarty, C.J., Dingman, S.L., Ward, L.G., Meybeck,M. (2006) 'Effective sea-level rise and deltas: Causes of change and human dimension implications', *Global and Planetary Change*, 50(1–2), pp. 63–82. doi: 10.1016/j.gloplacha.2005.07.004.

Eslami, S., Hoekstra P., Trung N.N, Kantoush S.A., Van Binh D., Dung D.D., Quang T.T. , van der Vegt M. (2019) 'Tidal amplification and salt intrusion in the Mekong Delta driven by anthropogenic sediment starvation', *Scientific Reports*, 9(1), pp. 1–10. doi: 10.1038/s41598-019-55018-9.

Eyre, B. , Twigg, C. (1997) 'Nutrient behaviour during post-flood recovery of the richmond river estuary northern NSW, Australia', *Estuarine, Coastal and Shelf Science*, 44(3), pp. 311–326. doi: 10.1006/ecss.1996.0124.

Fagherazzi, S. (2008) 'Self-organization of tidal deltas', *Proceedings of the National Academy of Sciences of the United States of America*, 105(48), pp. 18692–18695. doi: 10.1073/pnas.0806668105.

Fagherazzi, S., Edmonds, D.A., Nardin, W., Leonardi, N., Canestrelli, A., Falcini, F., Jerolmack, D.J., Mariotti, G., Rowland, J.C. and Slingerland, R.L., (2015). 'Dynamics of river mouth deposits'. *Reviews of Geophysics*, vol. 53(3), pp.642-672.

Feely, R. A., Alin,S.R., Newton , J., Sabine, C.L, Warner, M., Devol, A., Krembs C., Maloy, C. (2010) 'The combined effects of ocean acidification, mixing, and respiration on pH and carbonate saturation in an urbanized estuary', *Estuarine, Coastal and Shelf Science*. Elsevier Ltd, 88(4), pp. 442–449. doi: 10.1016/j.ecss.2010.05.004.

Fisher, W.L., Brown, L.F., Scott, A.T., McGowen, J.H., (1969). 'Delta systems in the exploration for oil

and gas'. *Bur. Econ. Geol.* University of Texas, Austin, 78.

Fischer, H. B., E. J. List, J. Imberger, R. C.Y. Koh and N. H. Brooks (1979)' Mixing in Inland and Coastal Waters'. Academic Press, New York.

Flores, R.P.,Rijnsburger, S., Horner-Divine, A.R., Souza, A.J.,Pietrzak, J.D. (2017). 'The impact of storms and stratification on sediment transport in the Rhine region of freshwater influence', *Journal of Geophysical Research: Oceans',* vol.122, pp.4456-4477, doi:10.1002/2016JC012362.

Fong D.A., Geyer W.R. (2001). 'Response of a river plume during an upwelling favourable wind event' *Journal of Geophysical Research*, vol.106, NO.C1, p1067-1084.

Fong, D. A. , Geyer, W. R. (2002) 'The alongshore transport of freshwater in a surface-trapped river plume', *Journal of Physical Oceanography*, 32(3), pp. 957–972. doi: 10.1175/1520-0485(2002)032<0957:TATOFI>2.0.CO;2.

Formats, F. (2014) 'Journal of Geophysical Research Oceans', *Journal of Geophysical Research: Oceans*, (119), pp. 3868–3882. doi: 10.1002/2014JC010325.Received.

Francois, B., Schlef, K.E., Wi,S., Brown, C.M. (2019). 'Design considerations for riverine floods in a changing climate – A review', *Journal of Hydrology*, vol.547,pp. 557-573. https://doi.org/10.1016/j.jhydrol.2019.04.068

Frihy, O. E. (2003) 'The nile delta-Alexandria coast: Vulnerability to sea-level rise, consequences and adaptation', *Mitigation and Adaptation Strategies for Global Change*, 8(2), pp. 115–138. doi: 10.1023/A:1026015824714.

Fryirs, K. (2013) '(Dis)Connectivity in catchment sediment cascades: A fresh look at the sediment delivery problem', *Earth Surface Processes and Landforms*, 38(1), pp. 30–46. doi: 10.1002/esp.3242.

Galloway, W. E. (2007) 'Process Framework for Describing the Morphologic and Stratigraphic Evolution of Deltaic Depositional Systems', (September).

Garvine, R.W, McCarthy R.K., Wong K., (1992). 'The Axial Salinity Distribution in the Delaware Estuary and its Weak Response to River Discharge', *Estuarine Coastal and Shelf Science* vol. 35, pp. 157-165.

Garvine, R. W. (1995) 'A dynamical system for classifying buoyant coastal discharges', *Continental Shelf Research*, 15(13), pp. 1585–1596. doi: 10.1016/0278-4343(94)00065-U.

Garvine, R. W. (1999) 'Penetration of buoyant coastal discharge onto the continental shelf: A numerical model experiment', *Journal of Physical Oceanography*, 29(8 PART 2), pp. 1892–1909. doi: 10.1175/1520-0485(1999)029<1892:pobcdo>2.0.co;2.

Gay, P. S. , O'Donnell, J. (2007) 'A simple advection-dispersion model for the salt distribution in linearly tapered estuaries', *Journal of Geophysical Research: Oceans*, 112(7), pp. 1–12. doi: 10.1029/2006JC003840.

Geleynse, N., Storms, J.E.A, Stive, M.J.F., Jagers, H.R.A., Walstra, D.J.R. (2010) 'Modeling of a mixed-load fluvio-deltaic system', *Geophysical Research Letters*, 37(5), pp. 1–7. doi: 10.1029/2009GL042000.

Geleynse, N. , Storms, J.E.A, Walstra, D.J.R., Jagers, H.R.A.,Wang, Z.B., Stive, M.J.F. (2011) 'Controls on river delta formation; insights from numerical modelling', *Earth and Planetary Science Letters*. Elsevier B.V., 302(1–2), pp. 217–226. doi: 10.1016/j.epsl.2010.12.013.

Georgiou, I.Y,Gaweesh,A., Hanegan, K.,Yocum, T. (2017). 'Flow distribution and salt-wedge

propagation in the lower Mississippi River and Delta Multi-Dimensional Modeling using FVCOM Mississippi River Hydrodynamic and Delta Management Study'.

Gerbi G.P. ,Chant R.J. , Wilkin J.L.(2013). 'Breaking Surface Wave Effects on River Plume Dynamics during Upwelling – Favorable Winds'. *Journal of Physical Oceanography*, Vol.43, p. 1959-1980. doi:10.1175/JPO-D-12-0185.1.

Geyer, W. R., Ralston, D. K., Chen,J.-L (2020). 'Mechanisms of exchange flow in an estuary with a narrow, deep channel and wide, shallow shoals'. *Journal of Geophysical Research: Oceans*, 125, e2020JC016092. https:// doi.org/10.1029/2020JC016092

Geyer, W. R., MacCready, P. (2014) 'The estuarine circulation', *Annual Review of Fluid Mechanics*, 46, pp. 175–197. doi: 10.1146/annurev-fluid-010313-141302.

Geyer , W.R.(2010).'Estuarine salinity structure and circulation'.Contemporary issues in estuarine physics,chapter 2,pp. 12-26, edited by A.Valle-Levinson. Cambridge University press.

Geyer, W. R., Chant R.J., Houghton,R. (2008). 'Tidal and spring–neap variations in horizontal dispersion in a partially mixed estuary'. *Journal of Geophysical Research* vol. 113, C07023, doi:10.1029/2007JC004644.

Gleick, P. H. (2002) ' Soft paths water', *Nature*, 418(July).

Gleick, P. H. (2003) 'Global Freshwater Resources: Soft-Path Solutions for the 21st Century', *Science*, 302(5650), pp. 1524–1528. doi: 10.1126/science.1089967.

Glen, S.(2016). 'Heavy-Tailed distribution and light-tailed distribution: Definition & Examples', from 'Elementary Statistics for the rest of us!' https://www.statisticshowto.com/heavy-tailed-distribution/

Gleyzer ,A., Denisyuk, M., Rimmer, A., Salingar, Y. (2004). 'A fast recursive GIS algorithm for computing Strahler stream order in braided and non-braided networks'. *Journal of the American Water Resources Association*, pp.937-946.

Gong, W. , Shen, J. (2011) 'The response of salt intrusion to changes in river discharge and tidal mixing during the dry season in the Modaomen Estuary, China', *Continental Shelf Research*. Elsevier, 31(7–8), pp. 769–788. doi: 10.1016/j.csr.2011.01.011.

Gong, W., Shen, J. , Jia, L. (2013) 'Salt intrusion during the dry season in the Huangmaohai Estuary, Pearl River Delta, China', *Journal of Marine Systems*. Elsevier B.V., 111–112, pp. 235–252. doi: 10.1016/j.jmarsys.2012.11.006.

Gong, W., Maa, J.P.Y, Hong,B., Shen, J. (2014) 'Salt transport during a dry season in the Modaomen Estuary, Pearl River Delta, China', *Ocean and Coastal Management*. Elsevier Ltd, 100, pp. 139–150. doi: 10.1016/j.ocecoaman.2014.03.024.

Gong W., Lin Z., Chen Y., Chen Z., Zhang H. (2018). Effect of winds and waves on salt intrusion in the Pearl River Estuary. *Ocean Sciences,* Vol. 14, pp.139-159. https://doi.org/10.5194/os-14-139-2018.

Gornitz, V. (1991) 'Global coastal hazards from future sea level rise', *Palaeogeography, Palaeoclimatology, Palaeoecology*, 89(4), pp. 379–398. doi: 10.1016/0031-0182(91)90173-O.

Green, J. A. M. (2010) 'Ocean tides and resonance', *Ocean Dynamics*, 60(5), pp. 1243–1253. doi: 10.1007/s10236-010-0331-1.

Gugliotta, M., Saito, Y., Nguyen, V.L., Oahn Ta, T.K., Nakashima , R., Tamura ,T., Uehara, K.,Katsuki, K., Yamamoto, S. (2017) 'Process regime, salinity, morphological, and sedimentary trends along the fluvial to marine transition zone of the mixed-energy Mekong River delta, Vietnam', *Continental*

Shelf Research. Elsevier Ltd, 147(March), pp. 7–26. doi: 10.1016/j.csr.2017.03.001.

Guo, X. , Valle-Levinson, A. (2007) 'Tidal effects on estuarine circulation and outflow plume in the Chesapeake Bay', *Continental Shelf Research*, 27(1), pp. 20–42. doi: 10.1016/j.csr.2006.08.009.

Gupta, V. K. , Mesa, O. J. (1988) 'Runoff generation and hydrologic response via channel network geomorphology - Recent progress and open problems', *Journal of Hydrology*, 102(1–4), pp. 3–28. doi: 10.1016/0022-1694(88)90089-3.

Gupta, V. K., Waymire, E. , Wang, C. T. (1980) 'A representation of an instantaneous unit hydrograph from geomorphology', *Water Resources Research*, 16(5), pp. 855–862. doi: 10.1029/WR016i005p00855.

Ha, T. P., Dieperink C., Dang Tri V.P., Otter H.S., Hoekstra P. (2018) 'Governance conditions for adaptive freshwater management in the Vietnamese Mekong Delta', *Journal of Hydrology*, 557, pp. 116–127. doi: 10.1016/j.jhydrol.2017.12.024.

Haigh, I. D., Pickering M.D, Mattias Green J.A., Arbic B.K., Arns A., Dangendorf S., Hill D.F., Horsburgh K., Howard T., Idier D., Jay D.A., Janicke L., Lee S.B., Muller M., Schindelegger M., Talke S.A., Wilmes S.B., Woodworth P.L. (2020) 'The Tides They Are A-Changin': A Comprehensive Review of Past and Future Nonastronomical Changes in Tides, Their Driving Mechanisms, and Future Implications', *Reviews of Geophysics*, 58(1), pp. 1–39. doi: 10.1029/2018RG000636.

Hagy, J. D., Boynton, W. R. , Sanford, L. P. (2000) 'Estimation of net physical transport and hydraulic residence times for a coastal plain estuary using box models', *Estuaries*, 23(3), pp. 328–340. doi: 10.2307/1353325.

Haines, A. T., Finlayson, B. L., McMahon, T. A. (1988) 'A global classification of river regimes', *Applied Geography*, vol. 8(4), pp. 255–272. doi: 10.1016/0143-6228(88)90035-5.

Hall, J. et al. (2014). 'Understanding flood regime changes in Europe: a state-of-the-art assessment', *Hydrology and Earth System Sciences,* vol.18, pp.2735-2772. doi:10.5194/hess-18-2735-2014

Hansen,D.V., Rattray,M.Jr. (1965) 'Gravitational Circulation in Straits & Estuaries', *Journal of Marine Research*, 23(2), pp. 104–122.

Hansford, M. R., Plink-Björklund, P. ,Jones, E. R. (2020) 'Global quantitative analyses of river discharge variability and hydrograph shape with respect to climate types', *Earth-Science Reviews*. Elsevier, vol. 200, pp. 102977. doi: 10.1016/j.earscirev.2019.102977.

Hasslet, S.K. (2000) 'Coastal Systems, routledge introductions to environmental series', Routledge.Taylor and Francis Group.

Heap , A.D, Bryce,S., Ryan, D.A.(2004).'Facies evolution in Holocene estuaries and deltas: a large sample-statistical study from Australia', *Sedimentary Geology,* vol.168, pp.1-17. doi:10.1016/j.sedgeo.2004.01.016

Heckmann, T., Schwanghart, W., Phillips, J. D. (2015) 'Graph theory-Recent developments of its application in geomorphology', *Geomorphology*. Elsevier B.V., 243, pp. 130–146. doi: 10.1016/j.geomorph.2014.12.024.

Herbold and Vendlinkski (2012) 'Modeling Estuarine Habitat in the Bay Delta, Unifying One and Three Dimensional Approaches to Modeling X2 and the Low Salinity Zone',www.epa.gov.

Herrera-León, S., Lucay F., Kraslawski A., Cisternas LA., Galvez E.D. (2018) 'Optimization Approach to Designing Water Supply Systems in Non-Coastal Areas Suffering from Water Scarcity', *Water Resources Management*, vol. 32(7), pp. 2457–2473. doi: 10.1007/s11269-018-1939-z.

Hetland, R. D. (2005) 'Relating river plume structure to vertical mixing', *Journal of Physical Oceanography*, 35(9), pp. 1667–1688. doi: 10.1175/JPO2774.1.

Hetland, R. D. , Geyer, W. R. (2004) 'An idealized study of the structure of long, partially mixed estuaries', *Journal of Physical Oceanography*, 34(12), pp. 2677–2691. doi: 10.1175/JPO2646.1.

Hodgkinson J.H.,(2009). 'Geological control of physiography in southeast Queensland: a multi-scale analysis using GIS'. PhD Thesis, Queensland University of Technology.

Hoitink, A. J. F., Wang, Z.B., Vermeulen, B., Huismans, Y., Kastner, K.. (2017) 'Tidal controls on river delta morphology', *Nature Geoscience*, 10(9), pp. 637–645. doi: 10.1038/ngeo3000.

Hoitink, A. J. F. , Jay, D. A. (2016) 'Tidal river dynamics: Implications for deltas', *Reviews of Geophysics*, 54(1), pp. 240–272. doi: 10.1002/2015RG000507.

Holleman, R. C. , Stacey, M. T. (2014) 'Coupling of sea level rise, tidal amplification, and inundation', *Journal of Physical Oceanography*, 44(5), pp. 1439–1455. doi: 10.1175/JPO-D-13-0214.1.

Holm, J. , Sasser, C. E. (2001) 'Differential salinity response between two Mississippi River subdeltas: Implications for changes in plant composition', *Estuaries*, 24(1), pp. 78–89. doi: 10.2307/1352815.

Hong, B., Liua Z., Shen J., Wu H., Gong W., Xu H., Wang D. (2020) 'Potential physical impacts of sea-level rise on the Pearl River Estuary, China', *Journal of Marine Systems*. Elsevier, 201(August 2019), p. 103245. doi: 10.1016/j.jmarsys.2019.103245.

Hong, B., Liua Z., Shen J., Wu H., Gong W., Xu H., Wang D. (2020) 'Potential physical impacts of sea-level rise on the Pearl River Estuary, China', *Journal of Marine Systems*. Elsevier, 201(August 2019), p. 103245. doi: 10.1016/j.jmarsys.2019.103245.

Hong, B. , Shen, J. (2012) 'Responses of estuarine salinity and transport processes to potential future sea-level rise in the Chesapeake Bay', *Estuarine, Coastal and Shelf Science*. Elsevier Ltd, 104–105, pp. 33–45. doi: 10.1016/j.ecss.2012.03.014.

Hood, W. G. (2010) 'Delta distributary dynamics in the Skagit River Delta (Washington, USA): Extending, testing, and applying avulsion theory in a tidal system', *Geomorphology*. Elsevier B.V., vol. 123(1–2), pp. 154–164. doi: 10.1016/j.geomorph.2010.07.007.

Hori K., Saito, Y. (2007) 'Classification , Architecture and Evolution of Large-river Deltas', chapter 6 in Large Deltas: Geomorphology and Management. edited by A.Gupta , John Wiley and Sons, Ltd.

Hori, K., Saito, Y., Zhao Q., Wang, P. (2002) 'Architecture and evolution of the tide-dominated Changjiang (Yangtze) River delta, China', *Sedimentary Geology*, vol. 146, pp. 249–264.

Horner-Devine, A. R., Hetland, R. D., MacDonald, D. G. (2015) 'Mixing and transport in coastal river plumes', *Annual Review of Fluid Mechanics*, 47, pp. 569–594. doi: 10.1146/annurev-fluid-010313-141408.

Horton , R.E (1932). 'Drainage-basin characteristics', EoS Trans.AGU, vol.13, pp.350-361.

Horton, R. E. (1945) 'Erosional development of streams and their drainage basins; hydrophysical approach to quantitative morphology ',*Bulletin of the geological society of America,* , vol. 56(March), pp. 275–370.

Hu, K., Ding P., Wang Z., Yang S. (2009) 'A 2D/3D hydrodynamic and sediment transport model for the Yangtze Estuary, China', *Journal of Marine Systems*. Elsevier B.V., 77(1–2), pp. 114–136. doi: 10.1016/j.jmarsys.2008.11.014.

Hu, K., Ding, P. (2009) 'The effect of deep waterway constructions on hydrodynamics and salinities in Yangtze Estuary, China', *Journal of Coastal Research*, (SPEC. ISSUE 56), pp. 961–965.

Huang, W. (2007) 'Hydrodynamic modeling of flushing time in a small estuary of North Bay, Florida, USA', *Estuarine, Coastal and Shelf Science*, 74(4), pp. 722–731. doi: 10.1016/j.ecss.2007.05.016.

Huang, W., Spaulding, M. (2002) 'Modelling residence-time response to freshwater input in Apalachicola Bay, Florida, USA', *Hydrological Processes*, 16(15), pp. 3051–3064. doi: 10.1002/hyp.1088.

Hutton ,P.H., Rath ,J.S., Chen ,L., Ungs ,M.J., Roy ,S.B., (2015). 'Nine Decades of Salinity Observations in the San Fransisco Bay and Delta: Modeling and Trend Evaluations'. *Journal of Water Resources Planning and Management*, vol. 142(3) : 04015069

Idier, D., Paris F., Le Cozannet G., Boulahya F., Dumas F. (2017) 'Sea-level rise impacts on the tides of the European Shelf', *Continental Shelf Research*. Elsevier Ltd, 137(January), pp. 56–71. doi: 10.1016/j.csr.2017.01.007.

IPCC in Climate Change 2007: Climate Change Impacts, Adaptation and Vulnerability, Contribution of WG2 to AR4. M.L.Parry et al. Eds(Cambridge University Press New York, 2007). ch.1.3,pp.85-111.

IPCC, 2007: Climate Change 2007: Synthesis Report. Contribution of Working Groups I, II and III to the Fourth Assess- ment Report of the Intergovernmental Panel on Climate Change [Core Writing Team, Pachauri, R.K and Reisinger, A. (eds.)]. IPCC, Geneva, Switzerland, 104 pp.

Isobe, A. (2005) 'Ballooning of river-plume bulge and its stabilization by tidal currents', *Journal of Physical Oceanography*, 35(12), pp. 2337–2351. doi: 10.1175/JPO2837.1.

Jassby ,A.D, Kimmerer, W.J., Monismith ,S.G, Armor, C., Cloern, J.E., Powell ,T.M., Schubel, J.R., Vendlinski ,T.J., (1995).'Isohaline position as a habitat indicator for estuarine populations', *Ecological Applications*, vol. 5(1), pp. 272-289.

Jay, D. A. (1991) 'Green's law revisited: Tidal long-wave propagation in channels with strong topography', *Journal of Geophysical Research*, 96(C11), p. 20585. doi: 10.1029/91jc01633.

Jay, D. A., Musiak, J. D. (1994) 'Particle trapping in estuarine tidal flows', *Journal of Geophysical Research*, 99(C10). doi: 10.1029/94jc00971.

Jerolmack, D. J. (2009) 'Conceptual framework for assessing the response of delta channel networks to Holocene sea level rise', *Quaternary Science Reviews*. Elsevier Ltd, 28(17–18), pp. 1786–1800. doi: 10.1016/j.quascirev.2009.02.015.

Jerolmack, D. J., Swenson, J. B. (2007) 'Scaling relationships and evolution of distributary networks on wave-influenced deltas', *Geophysical Research Letters*, 34(23), pp. 1–5. doi: 10.1029/2007GL031823.

Jia, P. and Li ,M., (2012). 'Circulation dynamics and salt balance in a lagoonal estuary', Journal *of Geophysical .Research*, Vol. 117, C1003.

Jiang, L., Gerkema T., Idier D., Slangen A.B.A, Soetaert K. (2020) 'Effects of sea-level rise on tides and sediment dynamics in a Dutch tidal bay', *Ocean Science*, 16(2), pp. 307–321. doi: 10.5194/os-16-307-2020.

Jones, E. R. (2017) 'Probabilistic Source-To-Sink Analysis of the Provenance of the California Paleoriver: Implications for the Early Eocene Paleogeography of Western North America', thesis

submitted to the Faculty and Board of Trustees of the Colorado school of mines, Department of Geology and Geological Engineering.

Kaplan, D. , Carpena R.M., Wan Y., Hedgepeth M., Zheng F., Roberts R., Rossmanith R. (2010) 'Linking River, Floodplain, and Vadose Zone Hydrology to Improve Restoration of a Coastal River Affected by Saltwater Intrusion', *Journal of Environmental Quality*, 39(5), pp. 1570–1584. doi: 10.2134/jeq2009.0375.

Karim, Z., S.G. Hussain and M. Ahmed. (1990). 'Salinity problems and crop intensification in the coastal regions of Bangladesh'. Soils publication No. 33. BARC, pp.17.

Kashefipour, S. M., Sadr, M. K. and Naseri, A. A. (2012) 'Modelling drainage water salinity for agricultural lands under leaching using artificial neural networks', *Irrigation and Drainage*, 61(1), pp. 99–106. doi: 10.1002/ird.634.

Kemp, R. (1979) 'The average number of registers needed to evaluate a binary tree optimally', *Acta Informatica*, 11(4), pp. 363–372. doi: 10.1007/BF00289094.

Kesel, R.H. (1989). 'The role of the Mississippi River in wetland loss in Southeastern Louisiana, USA', *Environmental Geology and Water Sciences,* vol.13,pp.1830-193.

Khan, A. E., Ireson,A., Kovats, S., Mojumder, S.K.,Khusru, A., Rahman, A., Vineis,P. (2011) 'Drinking water salinity and maternal health in coastal Bangladesh: Implications of climate change', *Environmental Health Perspectives*, 119(9), pp. 1328–1332. doi: 10.1289/ehp.1002804.

Khanom, T. (2016) 'Effect of salinity on food security in the context of interior coast of Bangladesh', *Ocean and Coastal Management*. Elsevier Ltd, 130, pp. 205–212. doi: 10.1016/j.ocecoaman.2016.06.013.

Kimmerer, W., Monismith,S. (1993). 'An estimate of the historical 2 ppt salinity in the San Francisco Bay Estuary'. Report to San Francisco Estuary Project, 75 Hawthorne Street, San Francisco, CA.

Kirchner, J. W., Feng, X. , Neal, C. (2000) 'Frail chemistry and its implications for contaminant transport in catchments', *Nature*, 403(6769), pp. 524–527. doi: 10.1038/35000537.

Kirkby, M. J. (1976) 'Tests of the random network model, and its application to basin hydrology', *Earth Surface Processes*, 1(3), pp. 197–212. doi: 10.1002/esp.3290010302.

Kleinhans, M. G., Jagers, H.R.A., Mosselman, E., Sloff, C.J. (2008) 'Bifurcation dynamics and avulsion duration in meandering rivers by one-dimensional and three-dimensional models',*Water Resources Research,* vol. 44, W08454, pp. 1–31. doi: 10.1029/2007WR005912.

Kolker A, Bargu S. et al. (2018) 'The Impacts of the Mississippi River and its Delta on the Oceanography, Ecology and Economy of the Gulf of Mexico Large Marine Ecosystem'. Available at: http://mississippiriverdelta.org/files/2018/08/Known-Impacts-of-the-Mississippi-River.pdf.

Kondolf, G. M., Boulton, A.J., O'Daniel, S., Poole, G.C., Rahel. F.J., Stanley, E.H., Wohl, E., Bang, A., Carlstrom, J., Cristoni,C., Huber, H., Koljonen, S., Louhi, P., Nakamura, K. (2006) 'Process-based ecological river restoration: Visualizing three-dimensional connectivity and dynamic vectors to recover lost linkages', *Ecology and Society*, 11(2). doi: 10.5751/ES-01747-110205.

Kourafalou, V. H., Oey L.Y., Wang J.D., Lee T.N. (1996) 'The fate of river discharge on the continental shelf 1. Modeling the river plume and the inner shelf coastal current', *Journal of Geophysical Research C: Oceans*, 101(C2), pp. 3415–3434. doi: 10.1029/95JC03024.

Kourafalou, V. H., Lee, T. N.,Wang, J.D., (1996) 'The fate of river discharge on the continental shelf 2. Transport of coastal low-salinity waters under realistic wind and tidal forcing', *Journal of Geophysical*

Research C: Oceans, 101(C2), pp. 3435–3455. doi: 10.1029/95JC03025.

Kourafalou, V. H. (1999) 'Process studies on the Po River plume , North Adriatic Sea discharge', '*Journal of Geophysical Research: Oceans',* vol.104(12), pp. 29963-29985.

Kourafalou, V. H. (2001) 'River plume development in semi-enclosed Mediterranean regions: North Adriatic Sea and Northwestern Aegean Sea', *Journal of Marine Systems*, 30(3–4), pp. 181–205. doi: 10.1016/S0924-7963(01)00058-6.

Kovchegov, Y. , Zaliapin, I. (2017) 'Horton self-similarity of Kingman's coalescent tree', *Annales de l'institut Henri Poincare (B) Probability and Statistics*.vol.53(3),pp.1069-1107. doi: 10.1214/16-AIHP748.

Kovchegov, Y. and Zaliapin, I. (2019) 'Random Self-Similar Trees: A mathematical theory of Horton laws', *Probability Surveys',* vol.17, pp. 1–213. https://doi.org/10.1214/19-PS331.

Kranenburg, C. (1986). 'A timescale for long-term salt intrusion in well mixed estuaries'. *Journal of Physical Oceanography* , vol.16: pp.1329–1331.

Kravtsova, V. I., Mikhailov, V. N. and Kidyaeva, V. M. (2009) 'Hydrological regime, morphological features and natural territorial complexes of the Irrawaddy River Delta (Myanmar)', *Water Resources*, 36(3), pp. 243–260. doi: 10.1134/S0097807809030014.

Kumar, R., Chatterjee, C., Singh, R.D., Lohani, A. K., Kumar, S. (2007) 'Runoff estimation for an ungauged catchment using geomorphological instantaneous unit hydrograph (GIUH) models', *Hydrological Processes*, 21, pp. 1829–1840. doi: 10.1002/hyp.

Kurup, G.R, Hamilton, D.P, Patterson, J.C., (1998). 'Modelling the effect of seasonal flow variations on the position of salt wedge in a microtidal Estuary'. *Estuarine, Coastal and Shelf Science* , vol. 47, pp.191–208.

Kuo-Chuin Wong (1994) 'On the nature of transverse variability in a coastal plain estuary', *Journal of Geophysical Research*, 99(C7).

Lacy, J. R., Stacey, M. T., Burau, J. R., Monismith, S. G. (2003). 'Interaction of lateral baroclinic forcing and turbulence in an estuary'.*Journal of Geophysical Research*, vol. 108(C3), 3089. https://doi.org/10.1029/2002JC001392

Lai ,X., Huang ,Q., Zhang ,Y., Jiang, J. (2014). 'Impact of lake inflow and Yangtze River flow alterations on water levels in Poyang Lake,China', *Lake and Reservoir Management*, vol. 30:4,pp.321-330, http://dx.doi.org/10.1080/10402381.2014.928390

Lamb, M. P., Nittrouer, J.A., Mohrig,D., Shaw,J. (2012) 'Backwater and river plume controls on scour upstream of river mouths: Implications for fluvio-deltaic morphodynamics', *Journal of Geophysical Research: Earth Surface*, 117(1), pp. 1–16. doi: 10.1029/2011JF002079.

Lane, R. R., Day Jr.,J.W., Marx, B.D., Reyes, E., Hyfield,E., Day,J.N. (2007) 'The effects of riverine discharge on temperature, salinity, suspended sediment and chlorophyll a in a Mississippi delta estuary measured using a flow-through system', *Estuarine, Coastal and Shelf Science*, 74(1–2), pp. 145–154. doi: 10.1016/j.ecss.2007.04.008.

Latrubesse, E. M., Stevaux, J. C., Sinha, R. (2005) 'Tropical rivers', *Geomorphology*, 70(3-4 SPEC. ISS.), pp. 187–206. doi: 10.1016/j.geomorph.2005.02.005.

Lebo, M. E., Sharp, J. H., Cifuentes, L. A. (1994) 'Contribution of river phosphate variations to apparent reactivity estimated from phosphate-salinity diagrams', *Estuarine, Coastal and Shelf Science*, 39(6), pp. 583–594. doi: 10.1016/S0272-7714(06)80011-9.

Lee, J. , Valle-Levinson, A. (2013) 'Bathymetric effects on estuarine plume dynamics', *Journal of Geophysical Research: Oceans*, 118(4), pp. 1969–1981. doi: 10.1002/jgrc.20119.

Lee, K. T., Chen, N. C., Chung, Y. R. (2008) 'Derivation of variable IUH corresponding to time-varying rainfall intensity during storms', *Hydrological Sciences Journal*, 53(2), pp. 323–337. doi: 10.1623/hysj.53.2.323.

Leier, A. L., DeCelles, P. G., Pelletier, J. D. (2005) 'Mountains, monsoons, and megafans', *Geology*, vol. 33(4), pp. 289–292. doi: 10.1130/G21228.1.

Leonardi, N., Canestrelli, A., Sun,T., Fagherazzi, S.(2013) 'Effect of tides on mouth bar morphology and hydrodynamics', *Journal of Geophysical Research: Oceans*, 118(9), pp. 4169–4183. doi: 10.1002/jgrc.20302.

Leonardi, N., Kolker, A. S., Fagherazzi, S. (2015) 'Interplay between river discharge and tides in a delta distributary', *Advances in Water Resources*. Elsevier Ltd, 80, pp. 69–78. doi: 10.1016/j.advwatres.2015.03.005.

Lerczak, J.A., Geyer, W.R. (2004). 'Modeling the lateral circulation in straight, stratified estuaries'. *Journal of Physical Oceanography*, vol.34, pp.1410–1428

Lerczak, J. A., Geyer, W. R. and Chant, R. J. (2006) 'Mechanisms driving the time-dependent salt flux in a partially stratified estuary', *Journal of Physical Oceanography*, 36(12), pp. 2296–2311. doi: 10.1175/JPO2959.1.

Lerczak, J. A., Geyer, W. R., Ralston, D. K. (2009) 'The temporal response of the length of a partially stratified estuary to changes in river flow and tidal amplitude', *Journal of Physical Oceanography*, 39(4), pp. 915–933. doi: 10.1175/2008JPO3933.1.

Lesser, G. R., Roelvink, J. A., Van Kester, J. A. T. M. & Stelling, G. S. (2004). 'Development and validation of a three-dimensional morphological model', *Coastal Engineering*, 51(8), pp.883–915.

Levin, D.R. (1993).'Tidal inlet evolution in the Mississippi River Delta Plain',*Journal of Coastal Research,* vol.9(2),p.462-480

Lewis, R. E., Uncles, R. J. (2003) 'Factors affecting longitudinal dispersion in estuaries of different scale', *Ocean Dynamics*, 53(3), pp. 197–207. doi: 10.1007/s10236-003-0030-2.

Li,L.,He, Z., Xia, Y., Dou, X. (2018).'Dynamics of sediment transport and stratification in Changjiang River Estuary, China' , *Estuarine, Coastal and Shelf Science',* vol.213,pp.1-17. https://doi.org/10.1016/j.ecss.2018.08.002

Lie-yaw Oye (1992) 'Subtidal variability of Estuarine Outflow,Plume and Coastal Current: A model study', *Journal of Physical Oceanography*, 23(2), pp. 164–171.

Lienou, G., Mahe G., Dieulin C., Paturel J.E., Bamba F.E, Sighomnou D., Dessouassi R. (2010) 'The River Niger water availability: Facing future needs and climate change', *Global change: facing risks and threats to water resources:* Proceedings of the sixth world FRIEND conference. IAHS,publ.340.

Liu, W. C., Ming-Hsi Hsu, Kuo A.Y., Kuo J.T. (2001) 'The influence of river discharge on salinity intrusion in the Tanshui Estuary, Taiwan', *Journal of Coastal Research*, 17(3), pp. 544–552.

Liu, W. C., Wei-Bo Chen, Cheng R.T., Ming-Hsi Hsu, Kuo A.Y. (2007) 'Modeling the influence of river discharge on salt intrusion and residual circulation in Danshuei River estuary, Taiwan', *Continental Shelf Research*, 27(7), pp. 900–921. doi: 10.1016/j.csr.2006.12.005.

Liu, B., Peng S., Yeying Liao Y., Wang H. (2019) 'The characteristics and causes of increasingly severe

saltwater intrusion in Pearl River Estuary', *Estuarine, Coastal and Shelf Science*. Elsevier, 220(November 2018), pp. 54–63. doi: 10.1016/j.ecss.2019.02.041.

Liu, Y.,Chen, H., Wang, J., Yang,S., Chen, A. (2020). 'Numerical simulation for the effects of waves and grain size on deltaic processes and morphologies', *Open Geosciences,*vol. 12,pp.1286-1301.

Liu, B.,Liao, Y.,Yan, S., Yan, H. (2017) 'Dynamics characteristics of saltwater intrusion in the Pearl River Estuary, China', *Natural Hazards,* vol.89,pp. 1097-1117. doi: 10.1007/s11069-017-3010-4

Liu, B., Peng S., Yeying Liao Y., Wang H. (2019) 'The characteristics and causes of increasingly severe saltwater intrusion in Pearl River Estuary', *Estuarine, Coastal and Shelf Science*. Elsevier, 220 (November 2018), pp. 54–63. doi: 10.1016/j.ecss.2019.02.041.

Liu, Y., Chen, H., Wang, J., Yang, S., Chen, A.. (2020) 'Numerical simulation for the effects of waves and grain size on deltaic processes and morphologies', *Open Geosciences*, 12(1), pp. 1286–1301. doi: 10.1515/geo-2020-0196.

Li ,C., O'Donnell ,J., (1997).'Tidally driven residual circulation in shallow estuaries with lateral depth variation'. *Journal of Geophysical Research*, vol.102, noC13,pp. 27915-27927.

Li, C., A.Valle-Levinson, K. C. Wong, Lwiza, K.M.M. (1998). 'Separating baroclinic flow from tidally induced flow in estuaries', *Journal of Geophysical Research*, vol.103, noC5, pp. 10405–10417.

Lorenz , M., Klingbeil, K, MacCready, P., Burchard, H.(2019).' Numerical issues of the Total Exchange Flow (TEF) analysis framework for quantifying estuarine circulation'. *Ocean Sciences,* vol.15 (3), pp.601-614, https://doi.org/10.5194/os-15-601-2019.

Loucks, D.P.(2019). 'Developed river deltas: are they sustainable?', '*Environmental Research Letters'*,vol 14, https://doi.org/10.1088/1748-9326/ab4165

Lucas , L.V.(2010).'Implications of estuarine transport for water quality', Contemporary issues in estuarine physics,chapter 10 ,pp. 273-303, edited by A.Valle-Levinson. Cambridge University press.

Lu, J., Vecchi, G.A., Reichler , T. (2007). 'Expansion of the Hadley cell under global warming', *Geophysical Research Letters,* vol.34, L06805, doi:10.1029/2006GL028443

MacCready, P. (1999) ' Estuarine adjustments to changes in river flow and tidal mixing' , *Journal of Physical Oceanography,* vol.29, p. 708-726. doi:10.1175/1520-0485(1999)029,0708:EATCIR.2.0.CO;2.

MacCready, P. (2004) 'Toward a unified theory of tidally-averaged estuarine salinity structure', *Estuaries*, 27(4), pp. 561–570. doi: 10.1007/BF02907644.

MacCready, P. (2007) 'Estuarine adjustment', *Journal of Physical Oceanography*, 37(8), pp. 2133–2145. doi: 10.1175/JPO3082.1.

MacCready, P. and Geyer, W. R. (2010) 'Advances in estuarine physics', *Annual Review of Marine Science*, 2(1), pp. 35–58. doi: 10.1146/annurev-marine-120308-081015.

MacCready, P. (2011). 'Calculating estuarine exchange flow using isohaline coordinates'. *Journal of Physical Oceanography*, vol.41(6), pp.1116–1124.

Maccready, P., Geyer, W. R., Burchard, H. (2018) 'Estuarine exchange flow is related to mixing through the salinity variance budget', *Journal of Physical Oceanography*, 48(6), pp. 1375–1384. doi: 10.1175/JPO-D-17-0266.1.

MacCready, P., McCabe, R.M., Siedlecki,S.A., Lorenz,M., Giddings,S.N., Bos,J., Albertson,S., Banas,N.S., Garnier,S. (2021) 'Estuarine Circulation, Mixing, and Residence Times in the Salish Sea', *Journal of Geophysical Research: Oceans*, 126(2), pp. 1–19. doi: 10.1029/2020JC016738.

MacDonald, D. G. , Geyer, W. R. (2004) 'Turbulent energy production and entrainment at a highly stratified estuarine front', *Journal of Geophysical Research C: Oceans*, 109(5), pp. 1–17. doi: 10.1029/2003JC002094.

MacDonald, D. G., Goodman, L. , Hetland, R. D. (2007) 'Turbulent dissipation in a near-field river plume: A comparison of control volume and microstructure observations with a numerical model', *Journal of Geophysical Research: Oceans*, 112(7), pp. 1–13. doi: 10.1029/2006JC004075.

MacWilliams, M. L., Bever, A. J., Gross, E. S., Ketefian,G. S., & Kimmerer W. J. (2015). 'Three-dimensional modeling of hydrodynamics and salinity in the San Francisco estuary: An evaluation of model accuracy, X2, and the low-salinity zone', *San Francisco Estuary & Watershed Science*, vol. 13(1). doi:http://dx.doi.org/10.15447/sfews.2015v13iss1art2

Mahanta, C., Zaman, A.M., Newaz, S.M.S, Rahman,S.M.M., Mazumdar, T.K., Choudhury R., Borah,P.J., Saikia, L. (2014) 'Physical Assessment of the Brahmaputra River', Ecosystems for Life: A Bangladesh-India Initiative,IUCN,International Union for Conservation of Nature.

Maicu, F., De Pascalis, F., Ferrarin, C., Umgiesser,G/(2018) 'Hydrodynamics of the Po River-Delta-Sea System', *Journal of Geophysical Research: Oceans*, 123(9), pp. 6349–6372. doi: 10.1029/2017JC013601.

Maloney, J. M.. Bentley, S.J., Xu,K., Obelcz,J., Georgiou, I.Y., Miner,M.D. (2018) 'Mississippi River subaqueous delta is entering a stage of retrogradation', *Marine Geology*, 400(March), pp. 12–23. doi: 10.1016/j.margeo.2018.03.001.

Mariotti, G., Rowland, J.C. and Slingerland, R.L., 2015. Dynamics of river mouth deposits. Reviews of Geophysics, 53(3), pp.642-672.

Maritan, A.. Rinaldo, A., Rigon, R., Giacometti, A., Rodriguez-Iturbe,I. (1996) 'Scaling laws for river networks', *Physical Review E - Statistical Physics, Plasmas, Fluids, and Related Interdisciplinary Topics*, 53(2), pp. 1510–1515. doi: 10.1103/PhysRevE.53.1510.

Martyr-Koller R.C, Kernkamp H.W.J, van Dam A., van der Wegen M., Lucas L.V, Knowles N., Jaffe B., Fregoso T.A,. (2017). 'Application of an unstructured 3D finite volume numerical model to flows and salinity dynamics in the San Francisco Bay-Delta'. *Estuarine, Coastal and Shelf Science* vol.192, p.86-107.

Maselli, V., Trincardi, F. (2013).'Man-made deltas', *Scientific reports',* vol.3,1926. DOI: 10.1038/srep01926

Matti, B., Dahlke, H.E, Dieppois, B., Lawler, D.M., Lyon, S.W. (2017). 'Flood seasonality across Scandinavia – Evidence of a shifting hydrograph?', *Hydrological Processes*, vol.31,pp.4354-4370. DOI: 10.1002/hyp.11365

Matsoukis, C., Amoudry L.O, Bricheno L., Leonardi N. (2021) 'Investigation of Spatial and Temporal Salinity Distribution in a River Dominated Delta through Idealized Numerical Modelling'. *Estuaries and Coasts.*vol.44,pp.1790-1815.

McCabe, R. M., Hickey, B. M. , MacCready, P. (2008) 'Observational estimates of entrainment and vertical salt flux in the interior of a spreading river plume', *Journal of Geophysical Research: Oceans*, 113(8), pp. 1–12. doi: 10.1029/2007JC004361.

Merz B. et al. (2014). 'Floods and climate: emerging perspectives for flood risk assessment and management', *Natural Hazards and Earth System Sciences* , vol.14,pp. 1921-1942. doi:10.5194/nhess-14-1921-2014

Miller, G.R., Cable, J.M., McDonald, A.K., Bond, B., Franz, T.E., Wang, L., Gou, S., Tyler, A.P.,Zou, C.B., Scott, R.L., (2012). 'Understanding ecohydrological connectivity in savannas: a system dynamics modelling approach', *Ecohydrology*, vol. 5, pp.200-220. doi: 10.1002/eco.245.

Milly, P.C.D, Betancourt, J., Falkenmark, M., Hirsch, R.M, Kundzewicz, Z.W., Lettenmaier, D.P., Stouffer, R.J. (2008). 'Stationarity is Dead: Whiter Water Management?', *Science,* vol.319,pp. 573-574.

de Miranda, L.B., Andutta, F.P., Kjerfve, B., de Castro Filho, B.M.(2017). 'Fundamentals of Estuarine Physical Oceanography'. Springer Nature Singapore Ltd.

Mondal, M. K. (1997). 'Management of soil and water resources for higher productivity of the coastal saline rice lands of Bangladesh'. PhD. thesis. University of the Philippines, Los Banos, Philippines.

Monismith, S.G (2017) 'An integral model of unsteady salinity intrusion in estuaries', *Journal of Hydraulic Research*, 55(3), pp. 392–408. doi: 10.1080/00221686.2016.1274682.

Monismith, S.G, (2010). 'The dynamics of Estuarine Plume and Fronts'. *Contemporary Issues in Estuarine Physics*, pp.167-182, Cambridge University Press.

Monismith, S. G., Kimmerer W., Burau J.R., Stacey M.T. (2002) 'Structure and flow-induced variability of the subtidal salinity field in northern San Francisco Bay', *Journal of Physical Oceanography*, 32(11), pp. 3003–3019. doi: 10.1175/1520-0485(2002)032<3003:SAFIVO>2.0.CO;2.

Monismith, S. G., Burau, J. and Stacey., M. (1996) 'Stratification Dynamics and Gravitational Circulation in Northern San Francisco Bay', *San Francisco Bay: The Ecosystem. Ecosystem*, J. T. Hollibaugh, Ed., (American Association for the Advancement of Science), pp. 123–153

Monsen, N. E., Cloern, J.E., Lucas, L.V., Monismith, S. G. (2002). 'A comment on the use of flushing time, residence time, and age as transport time scales'. *Limnology and Oceanography*,vol. 47, pp.1545–1553.

Montanari, A. (2012) 'Hydrology of the Po River: Looking for changing patterns in river discharge', *Hydrology and Earth System Sciences*, 16(10), pp. 3739–3747. doi: 10.5194/hess-16-3739-2012.

Moodie, A.J.,Nittrouer, J.A.,Ma, H., Lamb, M.P.,Carlson, B., Kineke, G.C., Parker, G. (2017).'Measuring density stratification and understanding its impact on sediment transport in fine-grained rivers, based on observations from the Lower Yellow River, China', *American Geophysical Union, Fall Meeting, 2017, abstract #EP12B-07*

Moussa, R. (2009) 'Definition of new equivalent indices of Horton-Strahler ratios for the derivation of the Geomorphological Instantaneous Unit Hydrograph', *Water Resources Research*, 45(9), pp. 1–24. doi: 10.1029/2008WR007330.

Murray, A. B. (2002) 'Seeking explanation affects numerical modeling strategies', *Eos*, 83(38), pp. 418–419. doi: 10.1029/2002EO000304.

Murray, A.B. (2003) 'Contrasting the goals, strategies and predictions associated with simplified numerical models and detailed simulations', *Geophysical Monograph Series*, Prediciton in Geomorphology. DOI: 10.1029/135GM11

Narayanan, C., Garvine, R. W. (2002) 'Large scale buoyancy driven circulation on the continental shelf', *Dynamics of Atmospheres and Oceans*, 36(1–3), pp. 125–152. doi: 10.1016/S0377-0265(02)00028-3.

Nardin, W., Marrioti, G., Edmonds, D.A., Guercio, R., Fagherazzi, S. (2013) 'Growth of river mouth bars in sheltered bays in the presence of frontal waves', *Journal of Geophysical Research: Earth*

Surface, 118(2), pp. 872–886. doi: 10.1002/jgrf.20057.

Nardin, W., Fagherazzi, S. (2012) 'The effect of wind waves on the development of river mouth bars', *Geophysical Research Letters*, 39(12), pp. 1–6. doi: 10.1029/2012GL051788.

Nebel ,M.E. (2000). 'On the Horton-Strahler number for combinatorial trees'. *Theoretical Informatics and Applications*, vol.34,pp.279-296.

Nelson , B.W.(1970) 'Hydrography, sediment dispersal, and recent historical development of the Po River Delta, Italy', *The Society of economic paleontologists and mineralogists (SEPM),Delta sedimentation,modern and ancient (SP15),*special publication

Nemec, W. (2009) 'Deltas-Remarks on Terminology and Classification', *Coarse-Grained Deltas*, (April 2009), pp. 3–12. doi: 10.1002/9781444303858.ch1.

Nowacki,D.J., Ogston, A.S., Nittrouer,C.A., Fricke, A.T.,van Pham, D. T. (2015) 'Sediment dynamics in the lower Mekong River: Transition from tidal river estuary', *Journal of Geophysical Research: Oceans*, pp. 6363–6383. doi: 10.1002/2015JC010754.Received.

Nguyen, H.N. (2016) 'Tidal regime deformation by sea level rise along the coast of the Mekong Delta', *Estuarine, Coastal and Shelf Science*. Elsevier Ltd, 183, pp. 382–391. doi: 10.1016/j.ecss.2016.07.004.

Nguyen, A. D. , Savenije, H. H. G. (2006) 'Hydrology and Earth System Sciences Salt intrusion in multi-channel estuaries: a case study in the Mekong Delta, Vietnam', *Hydrol. Earth Syst. Sci*, 10, pp. 743–754. Available at: www.hydrol-earth-syst-sci.net/10/743/2006/.

Nguyen, A. D., Savenije H.H.G., Pham D.N.,Thang Tang D.T. (2008) 'Using salt intrusion measurements to determine the freshwater discharge distribution over the branches of a multi-channel estuary: The Mekong Delta case', *Estuarine, Coastal and Shelf Science*, 77(3), pp. 433–445. doi: 10.1016/j.ecss.2007.10.010.

Nguyen, T. V. , Tanaka, H. (2007) 'Study on the effect of morphology change on salinity distribution in the Dinh an estuary, lower mekong river of Vietnam', *Journal of Coastal Research*, (SPEC. ISSUE 50), pp. 268–272.

Nicholls, R. J., Hutton C.W., Adger W.N., Hanson S.C., Rahman M.M , Salehin M. (2018) *Ecosystem services for well-being in deltas: Integrated assessment for policy analysis*, *Ecosystem Services for Well-Being in Deltas: Integrated Assessment for Policy Analysis*. doi: 10.1007/978-3-319-71093-8.

Nienhuis, J. H., Ashton, A.D., Edmonds,D.A., Hoitnik, A.J.F., Kettner, A.J., Rowland, J.C.,Tornqvist, T.E. (2020) 'Global-scale human impact on delta morphology has led to net land area gain', *Nature*. Springer US, 577(7791), pp. 514–518. doi: 10.1038/s41586-019-1905-9.

Nienhuis, J. H., Hoitink, A. J. F., Törnqvist, T. E. (2018) 'Future Change to Tide-Influenced Deltas', *Geophysical Research Letters*, 45(8), pp. 3499–3507. doi: 10.1029/2018GL077638.

de Nijs, M. A. J., Pietrzak, J. D. (2012) 'Saltwater intrusion and ETM dynamics in a tidally-energetic stratified estuary', *Ocean Modelling*. Elsevier Ltd, 49–50, pp. 60–85. doi: 10.1016/j.ocemod.2012.03.004.

Nittrouer, J. A., Mohrig, D. , Allison, M. (2011) 'Punctuated sand transport in the lowermost Mississippi River', *Journal of Geophysical Research: Earth Surface*, 116(4), pp. 1–24. doi: 10.1029/2011JF002026.

Nobi, N. , Das Gupta, A. (1997) 'Simulation of Regional Flow and Salinity Intrusion in an Integrated Stream-Aquifer System in Coastal Region: Southwest Region of Bangladesh', *Ground Water*, 35(5), pp. 786–796. doi: 10.1111/j.1745-6584.1997.tb00147.x.

Nunes , R.A., Simpson, J.H. (1985). 'Axial convergence in a well-mixed estuary'. *Estuarine and Coastal Shelf Science,* vol. 20, pp.637–649

O'Donnell, J. (1990) 'The formation and fate of a river plume: a numerical model', *J. Physical Oceanography*, pp. 551–569. doi: 10.1175/1520-0485(1990)020<0551:TFAFOA>2.0.CO;2.

Olariu, C. ,Bhattacharya, J. P. (2006) 'Terminal Distributary Channels and Delta Front Architecture of River-Dominated Delta Systems', *Journal of Sedimentary Research*, 76(2), pp. 212–233. doi: 10.2110/jsr.2006.026.

Orton, G. J., Reading, H. G. (1993) 'Variability of deltaic processes in terms of sediment supply, with particular emphasis on grain size', *Sedimentology*, 40(3), pp. 475–512. doi: 10.1111/j.1365-3091.1993.tb01347.x.

Paerl , H.W., Hall , N.S., Peierls , B.N., Rossignol , K.L., Joyner , A.R. (2014)'Hydrologic Variability and its control of phytoplankton community structure and function in two shallow, coastal, lagoonal ecosystems: The Neuse and New River Estuaries,North Carolina, USA' , *Estuaries and Coasts* , vol.37 (Suppl 1),S31-S45, DOI 10.1007/s12237-013-9686-0.

Paola, C., R. Twilley, D. A. Edmonds, W. Kim, D. Mohrig, G. Parker, E.Viparelli, Voller,V. (2011). 'Natural processes in delta restoration: Application to the Mississippi Delta', *Annual Review of Marine Sciences*, vol.3, pp.67–91.

Passalacqua, P., Hiatt,M. (2015) 'Hydrological connectivity in river deltas: The first-order importance of channel-island exchange', *Water Resources Research*, 51(3), pp. 2264–2282. doi: 10.1111/j.1752-1688.1969.tb04897.x.

Passalacqua, P., Lanzoni, S., Paola, C., Rinaldo, A. (2013) 'Geomorphic signatures of deltaic processes and vegetation: The Ganges-Brahmaputra-Jamuna case study', *Journal of Geophysical Research: Earth Surface*, 118(3), pp. 1838–1849. doi: 10.1002/jgrf.20128.

Passalacqua, P. (2017) 'The Delta Connectome: A network-based framework for studying connectivity in river deltas', *Geomorphology*. Elsevier B.V., 277, pp. 50–62. doi: 10.1016/j.geomorph.2016.04.001.

Pelling, H. E., Uehara, K. , Green, J. A. M. (2013) 'The impact of rapid coastline changes and sea level rise on the tides in the Bohai Sea, China', *Journal of Geophysical Research: Oceans*, 118(7), pp. 3462–3472. doi: 10.1002/jgrc.20258.

Penland, S., Boyd, R., Suter, J.R., (1988) 'Transgressive depositional systems of the Mississippi Deltas Plain: a model for barrier shoreline and shelf sand development'. *Journal of Sedimentary Research* vol.58(6), pp.932–949.

Pereira L.S, Cordery I., Iacovides I. (2009). 'Coping with water scarcity Addressing the challenges ', UNESCO, IHP-VI-Technical Documents in Hydrology- publication No. 58. ch.3.4, p.39-43.

Phan, T. D., Smart J.C.R., Sahin O., Capon S.J., Hadwen W.L. (2018) 'Assessment of the vulnerability of a coastal freshwater system to climatic and non-climatic changes: A system dynamics approach', *Journal of Cleaner Production*. Elsevier Ltd, 183, pp. 940–955. doi: 10.1016/j.jclepro.2018.02.169.

Phillip,J.R.(1994). 'Some exact solutions of the convection-diffusion and diffusion equations', *Water Resources Research*, vol.30, no12, pp.3545-3551.

Phillips, J.D., (2016). 'Vanishing point: Scale independence in geomorphological hierarchies', *Geomorphology*, vol.266, pp.66-74.

Pickering, M. D., Horsburgh K.J., Blundell J.R., Hirschi J.J.M., Nicholls R., Verlaan M. (2017) 'The impact of future sea-level rise on the global tides', *Continental Shelf Research*. Elsevier Ltd, 142(September 2016), pp. 50–68. doi: 10.1016/j.csr.2017.02.004.

Pilson, M. E. Q , (1985). 'On the residence time of water in Narragansett Bay', *Estuaries* Vol. 8, pp.2–14.

Pitlick, J., Cress, R. (2000) 'Longitudinal trends in channel characteristics of the Colorado river and implications for food-web dynamics' Department of Geography University of Colorado', (January 2000).

Plink-Björklund, P. (2015) 'Morphodynamics of rivers strongly affected by monsoon precipitation: Review of depositional style and forcing factors', *Sedimentary Geolog*y. Elsevier B.V., 323, pp. 110–147. doi: 10.1016/j.sedgeo.2015.04.004.

Polonskii, V. F. , Solodovnikova, T. Y. (2009) 'Estimation of transformation of flood runoff hydrographs and water stages in the Lower Volga and its delta', *Russian Meteorology and Hydrology*, 34(9), pp. 618–627. doi: 10.3103/S1068373909090076.

Poggioli, A. R., Horner-Devine, A. R. (2018) 'Two-layer hydraulics at the river-ocean interface', *Journal of Fluid Mechanics*, 856, pp. 633–672. doi: 10.1017/jfm.2018.688.

Prandle, D. (2004) 'Saline intrusion in partially mixed estuaries', *Estuarine, Coastal and Shelf Science*, vol. 59(3), pp. 385–397. doi: 10.1016/j.ecss.2003.10.001.

Pries ,A.R, Secomb ,T.W (2008). 'Blood Flow in Microvascular networks', *Handbook of Physiology, Microcirculation*, Academic Press, chpt.1, pp.3-36

Pritchard (1956) 'The Dynamic Structure of a Coastal Plain Estuary', *Journal of Marine Research*, (15), pp. 33–42.

Prosdocimi, I., Kjeldsen, T.R., Miller, J.D. (2015).'Detection and attribution of urbanization effect on flood extremes using nonstationary flood-frequency models', *Water Resources Research*, vol.51,pp.4244-4262. doi:10.1002/2015WR017065.

Pullen J.D., Allen J.S., (2000). 'Modelling studies of the coastal circulation off Northern California: shelf response to a major Eel river flood event'. *Continental Shelf Research*, vol.20, pp2213-2238.

Qiu, C. , Zhu, J. (2015) 'Assessing the Influence of Sea Level Rise on Salt Transport Processes and Estuarine Circulation in the Changjiang River Estuary', *Journal of Coastal Research*, 31(3), pp. 661–670. doi: 10.2112/JCOASTRES-D-13-00138.1.

Raff ,D.A, Smith ,J.L, Trlica ,M.J (2003). 'Statistical descriptions of channel networks and their shapes on non-vegetated hillslopes in Kemmerer, Wyoming'. *Hydrological Processes*, vol.17, pp. 1887-1897, doi:10.1002/hyp.1216.

Rahman ,Md. M., Mustafi ,M.A.A., Islam A,.F.M.T, Mohammad ,N.,(2015). 'The Effect of Rainfall, temperature and humidity on saline in the southern area of Bangladesh', *International Journal of Environmental and Pollution Research*, Vol. 3, No. 1, pp.48-53

Rahman, M.M,Dustegir, M., Karim , R., Hauqe, A., Nicholls, R.J., Darby, S.E.,Nakagawa, H.,Hossain, M., Dunn, F.E., Akter,M. (2018). 'Recent sediment-flux to the Ganges-Brahmaputra-Megna delta

system',*Science of the Total Environment'*,vol.643,pp.1054-1064.

Rahman, M. M., Penny G., Mondal M.S., Zaman M.H., Kryston A., Salehin M., Nahar Q., M.S. Islam M.S., Bolsterb D., J.L. Tank J.L., Müller M.F.. (2019) 'Salinization in large river deltas: Drivers, impacts and socio-hydrological feedbacks', *Water Security*. Elsevier, 6(October 2018), p. 100024. doi: 10.1016/j.wasec.2019.100024.

Ralston, D. K., & Stacey, M. T. (2005). 'Longitudinal dispersion and lateral circulation in the intertidal zone'. *Journal of Geophysical Research*,vol.110, C07015. https://doi.org/10.1029/2005JC002888

Ralston, D. K., Geyer, W. R., Lerczak, J. A. (2008) 'Subtidal salinity and velocity in the Hudson River estuary: Observations and modeling', *Journal of Physical Oceanography*, 38(4), pp. 753–770. doi: 10.1175/2007JPO3808.1.

Ralston, D. K., Geyer, W. R. , Lerczak, J. A. (2010) 'Structure, variability, and salt flux in a strongly forced salt wedge estuary', *Journal of Geophysical Research: Oceans*, 115(6), pp. 1–21. doi: 10.1029/2009JC005806.

Ranalli G., Scheidegger A.E (1968) 'Topological Significance of stream labelling methods', *Hydrological Sciences Journal,* vol13(4), pp.77-85, doi:10.1080/02626666809493628.

Reis ,A.H, (2006). 'Constructal view of scaling laws of river basins', *Geomorphology* , vol.78, pp.201-206, doi:10.1016/j.geomorph.2006.01.015.

Restrepo, J. D. and Cantera, J. R. (2013) 'Discharge diversion in the Patía River delta, the Colombian Pacific: Geomorphic and ecological consequences for mangrove ecosystems', *Journal of South American Earth Sciences*. Elsevier Ltd, vol. 46, pp. 183–198. doi: 10.1016/j.jsames.2011.04.006.

Rice, C. (2019). 'Models don't decompose that way: A holistic view of idealized models', *The British Journal for the philosophy of science,* vol.70, pp.179-208. doi:10.1093/bjps/axx045

Rinaldo, A., Vogel G.K., Rigon R., Rodriguez-Iturbe I. (1995) 'Can One Gauge the Shape of a Basin?', *Water Resources Research*, 31(4), pp. 1119–1127. doi: 10.1029/94WR03290.

Rinaldo, A., Marani, A. , Rigon, R. (1991) 'Geomorphological dispersion', *Water Resources Research*, 27(4), pp. 513–525. doi: 10.1029/90WR02501.

Rippeth, T. P., Fisher, N. R. ,Simpson, J. H. (2001) 'The cycle of turbulent dissipation in the presence of tidal straining', *Journal of Physical Oceanography*, 31(8 PART 2), pp. 2458–2471. doi: 10.1175/1520-0485(2001)031<2458:tcotdi>2.0.co;2.

Roberts, H. H., Weimer, P. , Slatt, R. M. (2012) *River deltas*, *Regional Geology and Tectonics*. Elsevier B.V. doi: 10.1016/B978-0-444-53042-4.00017-0.

Rodriguez, F., Cudennec, C. , Andrieu, H. (2005) 'Application of morphological approaches to determine unit hydrographs of urban catchments', *Hydrological Processes*, 19(5), pp. 1021–1035. doi: 10.1002/hyp.5643.

Rodriguez-Iturbe, I.,Rinaldo A.(1997). 'Fractal River Basins, Chance and shelf-organization'.p.15-28. Cambridge University Press.

Ronald Shreve (1969) 'Stream Lenghts and Basin areas in topologically random channel networks', *Journal of Geology*, 77(2), pp. 397–414.

Rong ,Z., Hetland ,R.D., Zhang ,W., Zhang ,X., (2014). 'Current Wave-interaction in the Mississippi Atchafalaya river plume on the Texas-Louisiana shelf'. *Ocean Modelling*, vol.84, pp.67-83. http://dx.doi.org/10.1016/j.ocemod.2014.09.008

Rosen, B.H., Loftin, K.A., Graham, J.L., Stahlhut, K.N., Riley, J.M., Johnston, B.D., and Senegal, S. (2018) 'Understanding the effect of salinity tolerance on cyanobacteria associated with a harmful algal bloom in Lake Okeechobee, Florida: U.S. Geological Survey Scientific Investigations Report 2018–5092, 32 p., https://doi.org/10.3133/sir20185092.

Rosso, R. (1984) 'Nash Model Relation to Horton Order Ratios', *Water Resources Research*, 20(7), pp. 914–920. doi: 10.1029/WR020i007p00914.

Sámano, M. L., Barcena, J.F, Garcia, A., Gomez, A.G., Alvarez, C., Revilla, J.A. (2012) 'Flushing time as a descriptor for heavily modified water bodies classification and management: Application to the Huelva Harbour', *Journal of Environmental Management*. Elsevier Ltd, 107, pp. 37–44. doi: 10.1016/j.jenvman.2012.04.022.

Sarwar, M. G. M. (2005) 'Impacts of Sea Level Rise on the Coastal Zone of Bangladesh', *Response*, p. 45.

Sassi, M. G., Hoitnik, A.J.F., de Brye, B., Deleersnijder, E. . (2012) 'Downstream hydraulic geometry of a tidally influenced river delta', *Journal of Geophysical Research F: Earth Surface*, 117(4), pp. 1–13. doi: 10.1029/2012JF002448.

Savenije, H. H. G. (1993) 'Predictive model for salt intrusion in estuaries', *Journal of Hydrology*, vol. 148(1–4), pp. 203–218. doi: 10.1016/0022-1694(93)90260-G.

Savenije , H.H.G (2005) 'Salinity and Tides in Alluvial Estuaries',ch.1, pp.8. Delft University of Technology

Schiller, R. V., Kourafalou V.H., Hogan P., Walker N.D. (2011) 'The dynamics of the Mississippi River plume: Impact of topography, wind and offshore forcing on the fate of plume waters', *Journal of Geophysical Research: Oceans*, 116(6), pp. 1–22. doi: 10.1029/2010JC006883.

Schiller, R. V. , Kourafalou, V. H. (2010) 'Modeling river plume dynamics with the HYbrid Coordinate Ocean Model', *Ocean Modelling*. Elsevier Ltd, 33(1–2), pp. 101–117. doi: 10.1016/j.ocemod.2009.12.005.

Schloen, J., Stanev, E. V. , Grashorn, S. (2017) 'Wave-current interactions in the southern North Sea: The impact on salinity', *Ocean Modelling*. Elsevier Ltd, 111, pp. 19–37. doi: 10.1016/j.ocemod.2017.01.003.

Schubel, J. R. (1992) *San Francisco Estuary Project*. doi: 10.4135/9781452231389.n24.

Schulz, E., Schuttelaars, H. M., Gräwe, U., Burchard, H. (2015).'Impact of the depth-to-width ratio of periodically stratified tidal channels on the estuarine circulation'. *Journal of Physical Oceanography*, vol. 45(8), pp.2048–2069. https://doi.org/10.1175/jpo-d-14-0084.1

Scully, M.E., Friedrichs, C.T. (2003).'The influence of asymmetries in overlying stratification on near-bed turbulence and sediment suspension in a partially mixed estuary', *Ocean Dynamics*, vol.53, pp. 208-219.

Scully, M.E, Friedrichs C.T., Brubaker J.M. (2005). 'Control of estuarine stratification and mixing by wind-induced straining of the estuarine density field'. *Estuaries*, vol.28, pp.321-326.

Scully, M.E., Geyer , W.R., Lerczak, J.A. (2009). 'The influence of lateral advection on the residual estuarine circulation:a numerical modeling study of the Hudson River estuary'. *Journal of Physical Oceanography*, vol. 39, pp.107–124

Scully, M. E., Geyer, W. R. (2012). 'The role of advection, straining, and mixing on the tidal variability of estuarine stratification'. *Journal of Physical Oceanography*, vol.42(5), pp.855–868.

Seal, L. , Baten, M. A. (2012) 'Salinity Intrusion in Interior Coast: A New Challenge to Agriculture in South Central part of Bangladesh', *Unnayan Onneshan-The Innovators*, pp. 1–47.

Sendrowski A., Passalacua, P. (2017) 'Process connectivity in a naturally prograding river delta', *Water Resources Research*, 53(3), pp. 1841–1863. doi: 10.1111/j.1752-1688.1969.tb04897.x.

Shaha, D. C., Yang-Ki Cho, Tae-Wan Kim , Valle-Levinson A. (2012) 'Spatio-Temporal variation of flushing time in the Sumjin River Estuary', *Terrestrial, Atmospheric and Oceanic Sciences*, vol. 23(1), pp. 119–130. doi: 10.3319/TAO.2011.08.22.01(Hy).

Shaw, J. B., Mohrig, D. , Whitman, S. K. (2013) 'The morphology and evolution of channels on the Wax Lake Delta, Louisiana, USA', *Journal of Geophysical Research: Earth Surface*, 118(3), pp. 1562–1584. doi: 10.1002/jgrf.20123.

Sheldon, J. E., Alber, M. (2002) 'A Comparison of Residence Time Calculations Using Simple Compartment Models', *Coastal and Estuarine Research Federation, Part B: Dedicated Issue: Freshwater Inflow: Science, Policy, Management: Symposium Papers from the 16th Biennial Estuarine Research Federation Conference (Dec., 2002)*, 25(6), pp. 1304–1317.

Sheldon, J. E., Alber, M. (2006) 'The Calculation of Estuarine Turnover Times Using Freshwater Fraction and Tidal Prism Models: A Critical Evaluation', *Estuaries and Coasts*, 29(1), pp. 133–146. Available at: papers2://publication/uuid/EAA85AF4-CF76-4A4B-9308-4AC95399485F.

Shen, Y., Jia , H., Li, C., Tang, J. (2018).'Numerical simulation of saltwater intrusion and storm surge effects of reclamation in Pearl River Estuary, China', *Applied Ocean Research,* vol.79,pp.101-112. https://doi.org/10.1016/j.apor.2018.07.013

Sherin, V. R. , Durand F., Papa F., Saiful Islam AKM, Gopalakrishna V.V., Khaki M., Suneel V. (2020) 'Recent salinity intrusion in the Bengal delta: Observations and possible causes', *Continental Shelf Research*. Elsevier Ltd, 202(January), p. 104142. doi: 10.1016/j.csr.2020.104142.

Simpson, J.H., (1981). 'The shelf-sea fronts: implications of their existence and behaviour'. *Philosophical Transactions of the Royal Society London Series A,* vol.302, pp.531-546.

Simpson, J. H., Brown J., Matthews J., Allen G. (1990) 'Tidal straining, density currents, and stirring in the control of estuarine stratification', *Estuaries*, 13(2), pp. 125–132. doi: 10.2307/1351581.

Smart, J. S. (1968) 'Statistical Properties of Stream Lengths', *Water Resources Research*, 4(5), pp. 1001–1014. doi: 10.1029/WR004i005p01001.

Smedema, L. K. , Shiati, K. (2002) 'Irrigation and salinity: A perspective review of the salinity hazards of irrigation development in the arid zone', *Irrigation and Drainage Systems*, 16(2), pp. 161–174. doi: 10.1023/A:1016008417327.

Smith, R. (1977) 'Long term dispersion of contaminants in small estuaries'. Journal of Fluid Mechanics, vol. 82, pp.129–146.

Snell, J. D. , Sivapalan, M. (1994) 'On geomorphological dispersion in natural catchments and the unit hydrograph', *Water Resources Research*, 30(7), pp. 2311–2323.

Sridevi, B., Sarma V. V.S.S.,Murty T. V.R., Sadhuram Y.,Reddy N. P.C., Vijayakumar K.,Raju N. S.N., Jawahar Kumar C. H., Raju Y. S.N., Luis R., Kumar M. D., Prasad K. V.S.R. (2015) 'Variability in stratification and flushing times of the Gautami–Godavari estuary, India', *Journal of Earth System Science*, vol. 124(5), pp. 993–1003. doi: 10.1007/s12040-015-0594-5.

Stacey, M. T. , Ralston, D. K. (2005) 'The scaling and structure of the estuarine bottom boundary layer', *Journal of Physical Oceanography*, 35(1), pp. 55–71. doi: 10.1175/JPO-2672.1.

Strahler A. (1952) 'Hypsometric (Area-Altitude) analysis of Erosional Topography', *Bulletin of the Geological Society of America*, 63(1), pp. 1117–1142. doi: 10.16309/j.cnki.issn.1007-1776.2003.03.004.

Stelling, G. S. and J. J. Leendertse, 1992. "Approximation of Convective Processes by Cyclic AOI methods." In M. L. Spaulding, K. Bedford and A. Blumberg, eds., *Estuarine and coastal modeling*, Proceedings 2nd Conference on Estuarine and Coastal Modelling, ASCE, pages 771–782. Tampa. 90,280,286,291.

Stephens ,R., Imberger, J., (1996). 'Dynamics of the Swan River Estuary: the Seasonal Variability', *Marine Freshwater Research*., Vol .47, pp.517-29.

Sun, J., Liu, L., Lin, J., Lin, B., Zhao, H. (2020).'Vertical water renewal in a large estuary and implications for water quality', *Science of the Total Environment',*vol.710, pp. 1-12. https://doi.org/10.1016/j.scitotenv.2019.135593

Sutherland, B.R., Barrett, K.J., Gingras, M.K. (2015). 'Clay settling in fresh and salt water', *Environmental Fluid Mechanics,* vol.15, pp.147-160. DOI 10.1007/s10652-014-9365-0

Su, N., Bethune, M., Mann, L., Heuperman, A. (2005) 'Simulating water and salt movement in tile-drained fields irrigated with saline water under a Serial Biological Concentration management scenario', *Agricultural Water Management*, 78(3), pp. 165–180. doi: 10.1016/j.agwat.2005.02.003.

Syvitski, J. P. M., Cohen S., Kettner A.J., Brakenridge G.R. (2014) 'How important and different are tropical rivers? - An overview', *Geomorphology*. Elsevier B.V., vol. 227, pp. 5–17. doi: 10.1016/j.geomorph.2014.02.029.

Syvitski, J.P.M, Kettner A.J., Overeem I.,Hutton E.W.H, Hannon M.T., Brakenridge G.R,Day J., Vorosmarty C., Saito Y., Giosan L., Nichols R.J., (2009). 'Sinking deltas due to human activities', *Nature Geoscience*., vol.2, p.681–686.

Syvitski, J. P. M., Saito, Y. (2007) 'Morphodynamics of deltas under the influence of humans', *Global and Planetary Change*, 57(3–4), pp. 261–282. doi: 10.1016/j.gloplacha.2006.12.001.

Tabarestani M.K, Fouladfar H. (2021). 'Numerical modelling of salinity changes in the desalination stage of a coastal reservoir'. *Journal of Hydraulics*',in press.

Tarboton, D. G. (1996) 'Fractal river networks, Horton's laws and Tokunaga cyclicity', *Journal of Hydrology*, 187(1–2), pp. 105–117. doi: 10.1016/S0022-1694(96)03089-2.

Tarboton, D. G., Bras, R. L. , Rodriguez-iturbe, I. (1988) 'David g. tarboton, rafael l. bras, and ignacio rodriguez-iturbe', 24(8), pp. 1317–1322.

Tessler, Z. D., Vorosmarty,C.J.,Grossber, M. , Gladkova, I., Aizenman, H., Syvitski, J.P.M, Foufoula-Georgiou, E. (2015) 'Profiling risk and sustainability in coastal deltas of the world', *Science*, 349(6248), pp. 638–643. doi: 10.1126/science.aab3574.

Thyng, K.M., C.A. Greene, R.D. Hetland, H.M. Zimmerle, DiMarco. , S.F. (2016). 'True colors of oceanography: Guidelines for effective and accurate colormap selection'. *Oceanography* vol. 29(3):pp.9–13. http://dx.doi.org/10.5670/oceanog.2016.66

Toan, T. Q. (2014) 'Climate Change and Sea Level Rise in the Mekong Delta: Flood, Tidal Inundation, Salinity Intrusion, and Irrigation Adaptation Methods',chapter 9 in *Coastal Disasters and Climate Change in Vietnam: Engineering and Planning Perspectives*. Elsevier Inc. doi: 10.1016/B978-0-12-

800007-6.00009-5.

Tokunaga, E. (1978) 'Consideration on the composition of drainage networks and their evolution.', *Tokyo Metropolitan University, Geographical Report*, 13, pp. 1–28.

Traykovski, P., Geyer, R. ,Sommerfield, C. (2004) 'Rapid sediment deposition and fine-scale strata formation in the Hudson estuary', *Journal of Geophysical Research: Earth Surface*, 109(F2), p. n/a-n/a. doi: 10.1029/2003jf000096.

Trieu, T. T. N., Phong, N. T. (2015) 'The impact of climate change on salinity intrusion and Pangasius (Pangasianodon Hypophthalmus) farming in the Mekong Delta, Vietnam', *Aquaculture International*, 23(2), pp. 523–534. doi: 10.1007/s10499-014-9833-z.

Turcotte, D. L., Pelletier, J. D. , Newman, W. I. (1998) 'Networks with side branching in biology', *Journal of Theoretical Biology*, 193(4), pp. 577–592. doi: 10.1006/jtbi.1998.0723.

Turrell, W. R., Brown, J., Simpson, J. H. (1996) 'Salt intrusion and secondary flow in a shallow, well-mixed estuary', *Estuarine, Coastal and Shelf Science*, 42(2), pp. 153–169. doi: 10.1006/ecss.1996.0012.

Tuttle , M.L.W,Charpentier R.R., Brownfield , M.E. (1999). ' The Niger Delta petroleum system: Niger Delta Province, Nigeria, Cameroon, and Equatorial Guinea, Africa: U.S. Geological Survey Open File Report 99-501',pp.4

Uddin, M. , Haque, A. (2010) 'Salinity Response in Southwest Coastal Region of Bangladesh due to Hydraulic and Hydrologic Parameters', *International Journal of Sustainable Agricultural Technology*, 6(3), pp. 1–7.

Uncles , R.J, (2002). 'Estuarine Physical Processes Research: Some Recent Studies and Progress'. *Estuarine, Coastal and Shelf Science*, vol.55 ,pp.829-856.doi: 10.1006/ecss.2002.1032.

Uncles, R. J. and Stephens, J. A. (1996) 'Salt intrusion in the Tweed Estuary', *Estuarine, Coastal and Shelf Science*, 43(3), pp. 271–293. doi: 10.1006/ecss.1996.0070.

UNESCO, 1(981)a. Background papers and supporting data on the international equation of state 1980. Tech. Rep. 38, UNESCO.

Van der Wegen, M. & Roelvink, J. A. (2008) 'Long-term morphodynamic evolution of a tidal embayment using a two-dimensional, process-based model', *Journal of Geophysical Research*, vol.113, pp. 1–23.

Valle-Levinson, A. , Wilson, R. E. (1994) 'Effects of sill processes and tidal forcing on exchange in eastern Long Island Sound', *Journal of Geophysical Research*, 99(C6). doi: 10.1029/94jc00721.

Valle-Levinson, A., O'Donnell, J. (1996). 'Tidal interaction with buoyancy-driven flow in a coastal plain estuary. Buoyancy Effects on Coastal and Estuarine Dynamics'. *Coastal and Estuarine Studies,* vol. 53, edited by D.C. Aubrey and C.T.Friedrichs , pp.265-281, AGU, Washington, D.C.

Valle-Levinson, A., Wong, K. C., Lwiza, K. M. M. (2000) 'Fortnightly variability in the transverse dynamics of a coastal plain estuary', *Journal of Geophysical Research: Oceans*, 105(C2), pp. 3413–3424. doi: 10.1029/1999jc900307.

Viglione, A., Merz, B., Dung, N.V., Parajka, J., Nester, T., Bloschl, G. (2016).'Attribution of regional flood changes based on scaling fingerprints', *Water Resources Research*, vol.52, pp.5322-5340. doi:10.1002/2016WR019036.

Vineis, P., Chan, Q. , Khan, A. (2011) 'Climate change impacts on water salinity and health', *Journal of*

Epidemiology and Global Health. Ministry of Health, Saudi Arabia, 1(1), pp. 5–10. doi: 10.1016/j.jegh.2011.09.001.

Visser, J. M., Day J.W, Battaglia L.L., Shaffer G.P.,Hester M.W. (2012) 'Mississippi river delta wetlands', *Wetland Habitats of North America: Ecology and Conservation Concerns*, (April 2014), pp. 63–74. doi: 10.1525/9780520951419-007.

Vogel, R.M., Yaindl, C.,Walter, M.(2011).'Nonstationarity: flood magnification and recurrence reduction factors in the United States', *Journal of the American Water Resources Association*, vo.47,no3, pp. 464-474. DOI: 10.1111/j.1752-1688.2011.00541.x

de Vos ,A., Bruning, B., van Straten, G., Oosterba,n R., Rozema, J., van Bodegom ,P., (2016). 'Crop salt tolerance under controlled field conditions in the Netherlands, based on trials conducted at Salt Farm Texel'. Salt Farm Texel, www.saltfarmtexel.com

Wang, C. F., Hsu, M. H., Kuo, A. Y. (2004) 'Residence time of the Danshuei River estuary, Taiwan', *Estuarine, Coastal and Shelf Science*, 60(3), pp. 381–393. doi: 10.1016/j.ecss.2004.01.013.

Wang, T., Geyer, W. R., MacCready, P. (2017). 'Total exchange flow, entrainment, and diffusive salt flux in estuaries'. *Journal of Physical Oceanography*, vol.47(5), pp.1205–1220.

Wang ,H., Krauss ,K.W., Noe ,G.B., Stagg ,C.L., SWarzensky C,.M., Duberstein ,J.A., Conner, W.H., DeAngelis, D.L. (2020). 'Modelling Soil Porewater Salinity Response to Drought in Tidal Freshwater Forest Wetlands', *Journal of Geophysical Research: Biogeosciences*, vol.125, e2018JGR004996, https://doi.org/10.129/2018JGR004996.

Wei, X., Schramkowski, G. P. , Schuttelaars, H. M. (2016) 'Salt dynamics in well-mixed estuaries: Importance of advection by tides', *Journal of Physical Oceanography*, 46(5), pp. 1457–1475. doi: 10.1175/JPO-D-15-0045.1.

Weisberg, M. (2007) 'Three kinds of idealization', *Journal of Philosophy*, 104(12), pp. 639–659. doi: 10.5840/jphil20071041240.

Werner, B.T. (1999) 'Complexity in natural landform patterns', *Science,* vol.284, pp. 102-104.

Wescott , W.A. (1992).'Deltas as Petroleum Provinces: Past, Present, and Future', paper presented at the Offshore Technology Conference, Houston, Texas, May 1992.

Western, A.W., Bloschl, G., Grayson, R.B., (2001). 'Toward capturing hydrologically significant connectivity in spatial patterns'. *Water Resources Research*, vol.37 (1), pp.83–97.http://dx.doi.org/10.1029/2000WR900241.

White, E. D., Meselhe E., Reed D., Renfro A., Snider N.P., Wang Y. (2019) 'Mitigating the effects of sea-level rise on estuaries of the Mississippi Delta Plain using river diversions', *Water (Switzerland)*, 11(10). doi: 10.3390/w11102028.

White, E. and Kaplan, D. (2017) 'Restore or retreat? saltwater intrusion and water management in coastal wetlands', *Ecosystem Health and Sustainability*, 3(1). doi: 10.1002/ehs2.1258.

Whitehead, P. G., Sarkar, S., Jin, L., Futter, M.N., Caesar , J., Barbour, E., Butterfield, E., Sinha, R., Nicholls, R., Hutton, C., Leckie, H.D.(2015) 'Dynamic modeling of the Ganga river system: Impacts of future climate and socio-economic change on flows and nitrogen fluxes in India and Bangladesh', *Environmental Sciences: Processes and Impacts*, 17(6), pp. 1082–1097. doi: 10.1039/c4em00616j.

Whitehead, P. G., Barbour, E. ,Futter, M.N.,Sarkar, S., Rodda, H., Caesar, J.,Butterfield, D., Jin, L.,Sinha, R., Nicholls, R., Salehin, M. (2015) 'Impacts of climate change and socio-economic scenarios on flow and water quality of the Ganges, Brahmaputra and Meghna (GBM) river systems: Low flow

and flood statistics', *Environmental Sciences: Processes and Impacts*, 17(6), pp. 1057–1069. doi: 10.1039/c4em00619d.

Whitney M.M, Garvine R.W., (2005). 'Wind influence on a coastal buoyant outflow', *Journal of Geophysical Research*. Vol.110, C03014, doi:10.129/2003JC002261.

Williams, B. L. (1986) 'Flushing time calculations for the Upper Waitemata Harbour, New Zealand', *New Zealand Journal of Marine and Freshwater Research*, 20(3), pp. 455–465. doi: 10.1080/00288330.1986.9516165.

Wohl, E., Magilligan, F. J., Rathburn, S. L. (2017) 'Introduction to the special issue: Connectivity in Geomorphology', *Geomorphology*. Elsevier B.V., 277, pp. 1–5. doi: 10.1016/j.geomorph.2016.11.005.

Wolanski, E., Nhan, N. H. , Spagnol, S. (1998) 'Sediment dynamics during low flow conditions in the Mekong River estuary, Vietnam', *Journal of Coastal Research*, 14(2), pp. 472–482.

Wolff G., Gleick P.H., in 'The World's Water 2002–2003', P. H. Gleick, Ed. (Island, Washington, DC,2002), pp. 1–32.

Wong, K. C. (1995) 'On the relationship between long-term salinity variations and river discharge in the middle reach of the delaware estuary', *Journal of Geophysical Research: Oceans*, 100(C10), pp. 20,705-20,713. doi: 10.1029/95JC01406.

Wright, D. G. (1989) 'On the Alongshelf Evolution of an Idealized Density Front', *Journal of Physical Oceanography*, 19(4), pp. 532–541. doi: 10.1175/1520-0485(1989)019<0532:otaeoa>2.0.co;2.

Wright, L. D. (1977) 'Sediment transport and deposition at river mouths: A synthesis', *Bulletin of the Geological Society of America*, 88(6), pp. 857–868. doi: 10.1130/0016-7606(1977)88<857:STADAR>2.0.CO;2.

Wright, L. D. , Coleman, J. M. (1971) 'Effluent expansion and interfacial mixing in the presence of a Salt Wedge, Mississippi River Delta', *Journal of Geophysical Research*, 76(36), pp. 8649–8661. doi: 10.1029/JC076i036p08649.

Wright, L. D. , Coleman, J. M. (1974) 'Mississippi River Mouth Processes: Effluent Dynamics and Morphologic Development', *The Journal of Geology*, 82(6), pp. 751–778. doi: 10.1086/628028.

Wu ,J., David ,J.L., (2002). 'A spatially explicit hierarchical approach to modelling complex ecological systems: theory and applications', *Ecological Modelling*, vol.153, pp.7-26.

Wu, S., Cheng, H., Xu, Y.J., Li,J., Zheng, S. (2016) 'Decadal changes in bathymetry of the Yangtze River Estuary: Human impacts and potential saltwater intrusion', *Estuarine, Coastal and Shelf Science*. Elsevier Ltd, 182, pp. 158–169. doi: 10.1016/j.ecss.2016.10.002.

Yalin, M.S. (1992) 'River Mechanics'. Oxford, U.K., Pergamon Press, 220 p.

Yamamoto, K. E. N. (2017) 'Central limit theorem for the Horton - Strahler bifurcation ratio of general branch order', 1124(March 2017), pp. 1111–1124. doi: 10.1017/jpr.2017.55.

Yang ,S.L, Zhang ,J., Zhu ,J., Smith ,J.P, Dai ,S.B, Gao ,A., Li, P., (2005). 'Impact of dams on Yangtze River sediment supply to the sea and delta intertidal wetland response', *Journal of Geophysical Research*, vol.110.

Yang, Y., Endreny, T. A. , Nowak, D. J. (2015) 'Simulating double-peak hydrographs from single storms over mixed-use watersheds', *Journal of Hydrologic Engineering*, vol. 20(11), pp. 1–5. doi: 10.1061/(ASCE)HE.1943-5584.0001225.

Yang, Y. C. E, Ray P.A, Brown C.M., Khalil A.F.,Yu W.H. (2015) 'Estimation of flood damage functions for river basin planning: a case study in Bangladesh', *Natural Hazards*, vo.. 75(3), pp. 2773–2791. doi: 10.1007/s11069-014-1459-y.

Yankovsky, A. E., Hickey, B., Munchow, A.K.(2001) 'Impact of variable inflow on the dynamics of a coastal buoyant plume', *Journal of Geophysical Research,* vol.106,NOC9,pp. 19809-19824.

Yankovsky, A. E. , Chapman, D. C. (1997) 'A simple theory for the fate of buoyant coastal discharges', *Journal of Physical Oceanography*, 27(7), pp. 1386–1401. doi: 10.1175/1520-0485(1997)027<1386:ASTFTF>2.0.CO;2.

Yuan, D., Lin, B. , Falconer, R. A. (2007) 'A modelling study of residence time in a macro-tidal estuary', *Estuarine, Coastal and Shelf Science*, 71(3–4), pp. 401–411. doi: 10.1016/j.ecss.2006.08.023.

Yuan, Y., Avener, M. E., Horner-Devine, A. R. (2011) 'A two-color optical method for determining layer thickness in two interacting buoyant plumes', *Experiments in Fluids*, 50(5), pp. 1235–1245. doi: 10.1007/s00348-010-0969-y.

Yuan, Y. ,Horner-Devine, A. R. (2013) 'Laboratory investigation of the impact of lateral spreading on buoyancy flux in a river plume', *Journal of Physical Oceanography*, 43(12), pp. 2588–2610. doi: 10.1175/JPO-D-12-0117.1.

Yuan, J. Z. , Wu, C. (2020) 'Insights into the design and development of Shanghai coastal reservoirs', ch.6 in Sustainable Water Resource Development Using Coastal Reservoirs. pp.97-110. Elsevier Inc. doi: 10.1016/b978-0-12-818002-0.00006-x.

Yue ,S., Ouarda ,T.B.M.J, Bobee ,B., Legendre ,R., Bruneau, P., (2002). 'Approach for describing statistical properties of flood hydrograph', *Journal of Hydrologic Engineering*, vol. 7(2), pp.147-153.

Zaman, A. M.,Molla, M.K., Pervin, I.A., Rahman, S.M.M., Haider, A.S., Ludwig, F., Franssen, W. (2017) 'Impacts on river systems under 2 °C warming: Bangladesh Case Study', *Climate Services*. , vol.7, pp. 96–114. doi: 10.1016/j.cliser.2016.10.002.

Zevenbergen, C., Khan S.A., van Alphen J., van Scheltinga C.A., Veerbeek W. (2018) 'Adaptive delta management: a comparison between the Netherlands and Bangladesh Delta Program', *International Journal of River Basin Management*. Taylor & Francis, 16(3), pp. 299–305. doi: 10.1080/15715124.2018.1433185.

Zhang, W. , Ruan X., Zheng J., Zhu Y., Wu H. (2010) 'Long-term change in tidal dynamics and its cause in the Pearl River Delta, China', *Geomorphology*. Elsevier B.V., vol.120(3–4), pp. 209–223. doi: 10.1016/j.geomorph.2010.03.031.

Zhang, E., Savenije H.H.G, Wu H., Kong Y., Zhu J.(2011) 'Analytical solution for salt intrusion in the Yangtze Estuary, China', *Estuarine, Coastal and Shelf Science*. Elsevier Ltd, 91(4), pp. 492–501. doi: 10.1016/j.ecss.2010.11.008.

Zhang ,W.,Xu ,Y.,Foitnik ,A.J.F.,Sassi ,M.G.,Zheng ,J., Chen ,X., Zhang, C., (2015). 'Morphological change in Pearl River Delta, China', *Marine Geology*, vol.363, pp.202-219.

Zhang, Q., Gu, X., Singh, V.P., Xiao , M., Chen, X. (2015).'Evaluation of flood frequency under non-stationarity resulting from climate indices and reservoir indices in the East River Basin, China', *Journal of Hydrology,* vol. 527,pp. 565-575. http://dx.doi.org/10.1016/j.jhydrol.2015.05.029

Zhang, X., Fagherazzi, S., Leonardi, N., Li, J. (2018) 'A Positive Feedback Between Sediment Deposition and Tidal Prism May Affect the Morphodynamic Evolution of Tidal Deltas', *Journal of Geophysical Research: Earth Surface*, 123(11), pp. 2767–2783. doi: 10.1029/2018JF004639.

Zhang H., Delworth, T.L. (2018). 'Robustness of anthropogenically forced decadal precipitation changes projected for the 21st century', *Nature Communications*, DOI: 10.1038/s41467-018-03611-3

Zhong, L., Li, M. , Foreman, M. G. G. (2008) 'Resonance and sea level variability in Chesapeake Bay', *Continental Shelf Research*, 28(18), pp. 2565–2573. doi: 10.1016/j.csr.2008.07.007.

Zhou, X., Yang T., Shi P., Yu Z., Wang X., Li Z. (2017) 'Prospective scenarios of the saltwater intrusion in an estuary under climate change context using Bayesian neural networks', *Stochastic Environmental Research and Risk Assessment*. Springer Berlin Heidelberg, vol. 31(4), pp. 981–991. doi: 10.1007/s00477-017-1399-7.

Zimmerman, J. T. F. (1976) 'Mixing and flushing of tidal embayments in the western Dutch Wadden Sea part I: Distribution of salinity and calculation of mixing time scales', *Netherlands Journal of Sea Research*, 10(2), pp. 149–191. doi: 10.1016/0077-7579(76)90013-2.

Zimmerman, J. T. F. (1988). 'Estuarine Residence Times'. Hydrodynamics of Estuaries, Vol1, Estuarine Physics., Chapter 6, p75-84.

Zoppou ,C., Knight, J.H.(1999). 'Analytical solution of a spatially variable coefficient advection-diffusion equation in up to three dimensions'. *Applied Mathematical Modelling*, vol.23,pp.667-685.